Multiproxy paleoclimatic reconstruction from the sediments of high latitude regions

THESIS

SUBMITTED TO THE GOA UNIVERSITY FOR THE AWARD OF THE DEGREE OF DOCTOR OF PHILOSOPHY

IN
MARINE SCIENCES

BY

SHABNAM CHOUDHARY
M.Sc.

Under the Guidance of
Dr. N. Khare **(Guide)**
Prof. G. N. Nayak **(Co-Guide)**

School of Earth, Ocean and Atmospheric Sciences
Goa University,
Taleigao Plateau, Goa, India-403206

July, 2019

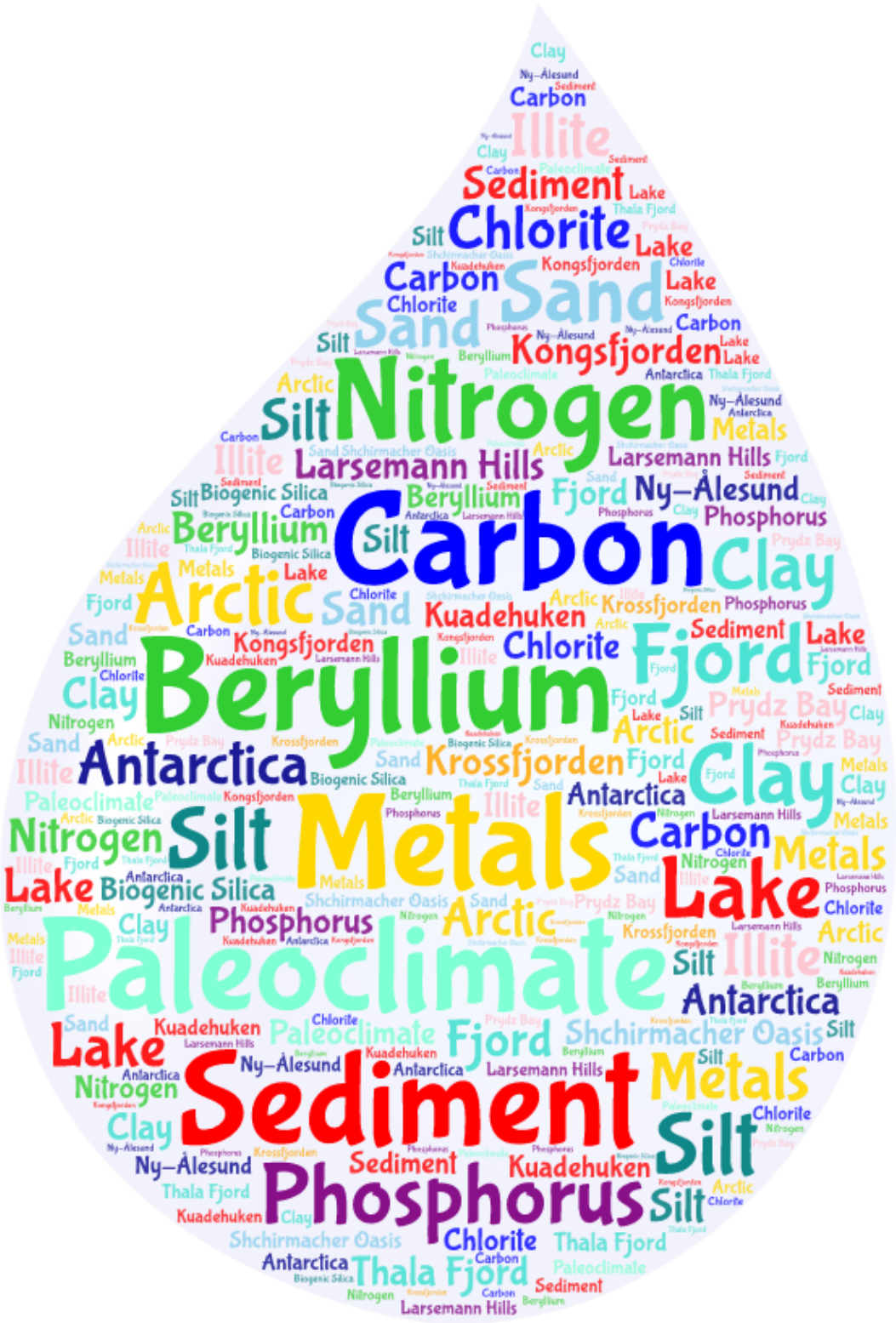
Clay
Ny−Ålesund
Sediment
Carbon
Illite
Clay
Carbon
Paleoclimate
Sediment
Sediment
Lake
Kongsfjorden
Thala Fjord
Silt
Chlorite
Prydz Bay
Lake
Shchirmacher Oasis
Kongsfjorden
Kuadehuken
Chlorite
Carbon
Sand
Lake
Chlorite
Kongsfjorden
Sand
Carbon
Phosphorus
Ny−Ålesund
Ny−Ålesund
Lake
Silt
Larsemann Hills
Nitrogen
Beryllium
Kongsfjorden
Lake
Prydz Bay
Paleoclimate
Antarctica
Thala Fjord
Arctic
Ny−Ålesund
Silt
Nitrogen
Antarctica
Metals
Carbon
Sand Shchirmacher Oasis
Arctic
Illite
Larsemann Hills
Larsemann Hills
Fjord
Sediment
Sediment
Sand
Silt
Biogenic Silica
Beryllium
Fjord
Ny−Ålesund
Clay
Ny−Ålesund
Antarctica
Larsemann Hills
Phosphorus
Carbon
Arctic
Beryllium
Silt
Carbon
Clay
Phosphorus
Illite
Thala Fjord
Biogenic Silica
Prydz Bay
Metals
Metals
Lake
Arctic
Sand
Chlorite
Shchirmacher Oasis
Arctic
Krossfjorden
Phosphorus
Fjord
Kuadehuken
Arctic
Carbon
Sediment
Lake
Sand
Kongsfjorden
Kongsfjorden
Chlorite
Fjord
Fjord
Beryllium
Kuadehuken
Larsemann Hills
Illite
Fjord
Clay
Chlorite
Beryllium
Fjord
Sediment
Clay
Prydz Bay
Nitrogen
Fjord
Lake
Silt
Clay
Arctic
Sediment
Prydz Bay
Sand
Arctic
Prydz Bay
Krossfjorden
Kuadehuken
Illite
Antarctica
Biogenic Silica
Paleoclimate
Biogenic Silica
Krossfjorden
Phosphorus
Sand
Krossfjorden
Fjord
Clay
Metals
Paleoclimate
Paleoclimate
Kongsfjorden
Thala Fjord
Sand
Lake
Clay
Antarctica
Arctic
Biogenic Silica
Beryllium
Illite
Krossfjorden
Metals
Nitrogen
Silt
Phosphorus
Nitrogen
Larsemann Hills
Carbon
Metals
Illite
Fjord
Thala Fjord
Chloride
Nitrogen
Metals
Antarctica
Sand
Illite
Phosphorus
Lake
Biogenic Silica
Metals
Lake
Chlorite
Beryllium
Antarctica
Shchirmacher Oasis
Sand
Prydz Bay
Nitrogen
Kuadehuken
Phosphorus
Clay
Arctic
Krossfjorden
Larsemann Hills
Arctic
Metals
Antarctica
Illite
Paleoclimate
Silt
Illite
Nitrogen
Fjord
Illite
Beryllium
Beryllium
Antarctica
Sand
Kuadehuken
Paleoclimate
Fjord
Shchirmacher Oasis
Silt
Lake
Chlorite
Carbon
Antarctica
Ny−Ålesund
Antarctica
Larsemann Hills
Metals
Nitrogen
Silt
Clay
Chlorite
Nitrogen
Sediment
Ny−Ålesund
Sediment
Kuadehuken
Silt
Ny−Ålesund
Phosphorus
Krossfjorden
Phosphorus
Phosphorus
Thala Fjord
Kuadehuken
Arctic
Kongsfjorden
Chlorite
Kuadehuken
Clay
Shchirmacher Oasis
Chlorite
Thala Fjord
Antarctica
Thala Fjord
Carbon
Paleoclimate
Biogenic Silica
Sediment
Nitrogen
Carbon
Beryllium
Larsemann Hills

STATEMENT

As required under the University ordinance OA-19.8 (viii), I state that the present thesis entitled "**Multiproxy paleoclimate reconstruction from the sediments of higher latitude regions**", is my original contribution and the same has not been submitted for any other degree, diploma, associate-ship, fellowship or similar titles in any universities or institutions on any previous occasion. To the best of my knowledge, the present study is the first comprehensive work of its kind from the area mentioned.

The literature related to the problem investigated has been cited. Due acknowledgements have been made wherever facilities and suggestions have been availed of.

Place: Goa University

Date: 22.7.2019 Ms. Shabnam Choudhary

CERTIFICATE

This is to certify that the thesis entitled, "**Multiproxy paleoclimate reconstruction from the sediments of high latitude regions**", submitted by Ms. Shabnam Choudhary for the award of the Degree of Doctor of Philosophy in Marine Science is based on her original studies carried out by her under our supervision. The thesis or any part thereof has not been previously submitted for any other degree, diploma, associate-ship, fellowship or similar titles in any universities or institutions. This thesis represents independent work carried out by the student.

Place: Goa
Date: 22.7. 2019

Dr. N. Khare
(Research Guide)
Scientist- G
Ministry of Earth Sciences,
New Delhi

Prof. G. N. Nayak
(Research Co-Guide)
CSIR-Emeritus Scientist
School of Earth Ocean and
Atmospheric Sciences
Goa University, Goa

ACKNOWLEDGEMENTS

First and foremost, I would like to thank my supervisor Dr. Neloy Khare and Co-Supervisor Prof. G. N. Nayak. I am indebted to them for always encouraging scientific discourse, and unfailing support. I express my sincere gratitude to both for their mentorship and their confidence to let me work in generous freedom. Their advice was instrumental throughout my degree. While I express my gratitude to Dr. Neloy Khare who introduced me to the fascinating field of polar research and motivated me to undertake research in the polar region. I feel that the mark of a great advisor is one, who ultimately cares as much, for the student's development as for the research and I am thankful to have had this in Prof. G. N. Nayak. He graciously (and patiently) offered me his time and expertise. His valuable comments and editorial advice have been critical to the completion of this thesis. I would like to thank him for the great effort he put into training me in the scientific field.

I would also like to thank the DRC members, Dr. S. Rajan, Director, NCPOR, Dr. Rajeev Saraswat, Senior Scientist, NIO, Goa and Prof. V. M. Matta, Department of Marine Sciences for their insightful comments, thought provoking questions, suggestions and encouragement.

I acknowledge the administrative help rendered by Prof. Varun Sahni, Vice-Chancellor, Goa University, Prof. Y. V. Reddy, Registrar, former Vice – Chancellor and former Registrar and their subordinates during the Ph.D. program.

I acknowledge the financial assistance provided by University Grant Commission, Maulana Azad National Fellowship and Inter University Accelerator Centre under the research project entitled "Estimation of Beryllium concentration from Polar Regions and Lake sediments (like Dal Lake, Loktak Lake, Lakes in Leh region)-Paleo-oceanographic Implications" to Prof. G. N. Nayak, Project PI during my research career.

I sincerely thank Ministry of Earth Sciences (MoES) and National Centre for Polar and Ocean research (NCPOR) for my participation in 34th Indian Scientific Expedition to Antarctica in 2015 and Summer phase, Indian Arctic Expedition, 2016. This work

would not have been possible without the help and support from the members and crew of the 34th Indian Scientific Expedition to Antarctica and Summer phase, Indian Arctic Expedition, 2016. My sincere thanks to Shri M. J. Beg, Dr. S. Saini, Dr. K. P. Krishnan from NCPOR, who were instrumental in providing all necessary logistic support for the sampling, as well as for the safe transport of samples to the laboratory. My sincere thanks also go to Dr. S. Rajan, former Director, NCPOR, for his encouragement and for providing the necessary facilities for this work.

I am grateful to Dr. M. Ravichandran, Director, NCPOR, Goa for permitting me to carry out some of the analysis at the institute. My sincere thanks go to Dr. Anoop Tiwari, Scientist, NCPOR, Goa, Dr. Waliur Rehman, Scientist, NCPOR, Goa, Ms. Lathika N Padmanabhan, Scientist, NCPOR, Goa and Dr. B. N. Nath, NIO, Goa for providing assistance in metal analysis. Further, I wish to thank Dr. Manish Tiwari, Dr. P.V. Bhaskar, Dr. K.P. Krishnan, Ms. Melena Augusta, Scientist, NCPOR, Goa for extending the instrumental facility. I also wish to thank Mr. Brijesh Dessai, Ms. Mamta Mestry, Mr. Shubham Tripathi, Mr. Siddesh Nagoji and Ms. Archana Singh, Ms. Femi Thomas, NCPOR, Goa for their help and support during the analysis.

I am thankful to the faculty of School of Earth, Ocean and Atmospheric Sciences, Goa University, Prof. V. M. Matta, Prof. C. U. Rivonkar, Prof. H. B. Menon, Dr. S. Upadhyay, and Dr. A. Can for their encouragement.

I wish to acknowledge the non-teaching staff of the department of Marine Sciences, Mr. Yeshwant Naik, Mr. Samrat Gaonkar, Mr. Shatrugan Shetgaonkar, Mr. Ratnakar Naik, Ms. Reena Tari, Mrs. Mangal for their help and support required during the course of my Ph.D.

I am indebted to Marine Geology Laboratory, Goa University for providing me the conducive environment during my Ph.D. days. The fellow lab mates were always a source of encouragement towards the work and scientific temperament. A special thanks to my seniors Dr. Cheryl Noronha D' Mello, Dr. Maria Fernandes, Dr. Maheshwar R. Nasnodkar, Dr. Shrivardhan Hulswar, Dr. Purnima Bejugam, Dr. Neelavannan Kannaiyan, Mrs. Nita Salunke and my colleagues at lab Ms. Janhavi Kangane and Ms. Priyanka Bhangle. I am also grateful to my colleagues in research

Ms. Atiba Shaikh, Mr. Partha Patil, Mr. Arjun Adhikari, Ms. Cynthia Gaonkar, Ms. Mithila Bhatt and Ms. Vijaylaxmi Parwar. My sincere gratitude to my seniors and friends from NCPOR Dr. Shridhar Jawak, Ms. Gautami Dev Samui, Dr. Mahesh Badnal, Dr. Anish Warrier, Dr. Ravi Naik, Ms. Archana Singh and Dr. Roseline Cutting Thakur who had made my life easy there. A special mention to Dr. Neelu Singh and Dr. Anoop Tiwari for standing beside me whenever I needed.

Moreover, I thank Dr. Jaya Sharma, Dr. Mira Parmekar and Dr. Shamshad Shaikh for being a constant source of inspiration and encouragement throughout my Ph.D. A deepest gratitude to my best friends Mr. Syed Mohammad Saalim, Ms. Prabha M. Pillai and Ms. Sankrita Gaonkar for their many years of unfailing support, constant encouragement, help and friendship.

My sincere gratitude towards Dr. M. Rajeevan, Secretary, Ministry of Earth Sciences, Delhi for allowing me to complete my thesis, while working at MoES. I express my sincere thanks to Dr. N. Khare, Adviser and Head, Paleoclimate change programme and my colleague, Dr. Debishree Khan, Scientist-C, for their continuous support and help in every possible way to complete my thesis. They made sure that I had ample time to finish some of my pending work.

My Parents are the rocks that I constantly lean on. This thesis is dedicated to my wonderful, inspirational, loving parents, for their amazing support and encouragement to always pursue my interests. Their patience, support and encouragement were in the end what made this dissertation possible.

Above all I would like to thank Lord almighty for providing strength, wisdom and good health to undertake and complete this research work successfully.

Ms. Shabnam Choudhary

TABLE OF CONTENT

LIST OF TABLES

LIST OF FIGURES

PREFACE

Lakes and fjords are essential components of high latitude regions in which sediments received from different geological and glacial units exhibit almost similar characteristics as there is an intermixing of the sediments of various units due to ice, melt-water and wind activities. Therefore, it is essential to identify the source of sediments and depositional processes. Climate change has severely impacted the terrestrial, marine and freshwater ecosystems in the polar regions. The components of sediments both inorganic and organic can act as a proxy to understand climate change.

The present study deals with lakes and fjords of high latitude regions as they are local response systems acting as high-resolution archives of local and regional change. High latitude lakes (Arctic and Antarctic) and their catchments experience persistent low temperature, intense seasonality and severe freeze-thaw cycles and these characteristics are likely to increase their sensitiveness to landscape and environmental change. An attempt has been made to understand the source, sedimentary environment, depositional processes and change in climate in different environments of polar regions such as lakes and fjords as they play a crucial role in biogeochemical and global carbon cycle.

The thesis includes four chapters. The ***First Chapter*** *emphasizes the rationale behind the research. It includes the "introduction" and strength of proxies. The chapter highlights the importance of lakes and fjords occurring in the Polar Regions to understand the sedimentary processes, depositional environment and change in climate. The studies on the application of sedimentological (grain size and clay minerals) and geochemical (C, N, P, BSi, major and trace metals) proxies from Arctic and Antarctic region were thoroughly reviewed and briefly outlined in this chapter along with a brief background of the study area and the objectives addressed through the present study. The sample collection and processing, and detailed methodology is discussed in* ***Second Chapter****. It includes the methods of sampling adopted for collection and storage of samples in the field and detailed procedure for different parameters analysed in the laboratory. The* ***Third Chapter*** *consists of Results and Discussion. It includes the data obtained for each parameter analysed and its detailed*

interpretations and major inferences and are presented in four major sections i.e. sediment components, organic components, major and trace elements and Be estimation. Each major section is divided in two subsections of surface and subsurface sediment samples (cores). ***Chapter Four,*** *summary and "conclusions" includes conclusions drawn from the study. The references cited in the thesis are arranged in alphabetical order at the end.*

1.1 Introduction

Polar regions are characterised by a variety of glacial landforms out of which lakes and fjords have great potential to unravel sedimentary processes, depositional environment and climate change. Despite the occurrence of numerous lakes and fjords along the coastlines of high latitude regions (Hjelstuen et al., 2009) and their potential to provide understanding of sedimentary and depositional processes, these landforms have received less attention. Lakes and fjords are local response systems which act as high-resolution archives of local and regional change. They help in understanding the source of sediment and their depositional environment. The lakes integrate the processes of their surrounding catchments and therefore they are highly sensitive to changes in landscape. Depending upon their topographic settings these lakes are classified as proglacial lakes, landlocked and epishelf lakes (Fig.1.1) (Ravindra et al., 2001; Phartiyal et al., 2011). High latitude lakes have many similar characteristics with those of temperate latitude and are subjected to similar landscape controls. These lakes are modern day analogs of paraglacial and periglacial lakes that were common during glacial periods in temperate latitudes (Phartiyal et al., 2011). The changes in the lakes and their catchments during the past are well archived in the form of sedimentary record. Sediment column of a modern lake indicates that the sediment deposited at its bottom consists of relatively older sediments than the surface and therefore, a sediment column represents the deposition of sediments in a span of time. These lakes have gained importance in recent years as they are a source for paleo-archives (Mahesh et al., 2015), present pristine conditions, and are easily accessible in ice-free areas. In general, lake sediments are ideal repositories of aeolian and fluvial materials. Lakes preserve catchment area soil, which is a product of weathering and are used to track past climatic and environmental changes (Peck et al., 2004). Their study on lakes along with fjords gained importance in the recent years as the climate change has severely impacted the terrestrial, marine and freshwater ecosystems in the polar regions (IPCC, 2014).

High latitude lakes (Arctic and Antarctic) and their catchments experience persistent low temperature, intense seasonality and severe freeze-thaw cycles and these characteristics are likely to increase their sensitiveness to landscape and

environmental change. When these lakes were compared with fresh water lakes of other areas it was found that these lakes are subjected to different physical, chemical, and biological processes because of longer duration of polar days and nights, and are ice free for only 3 to 4 months in a year.

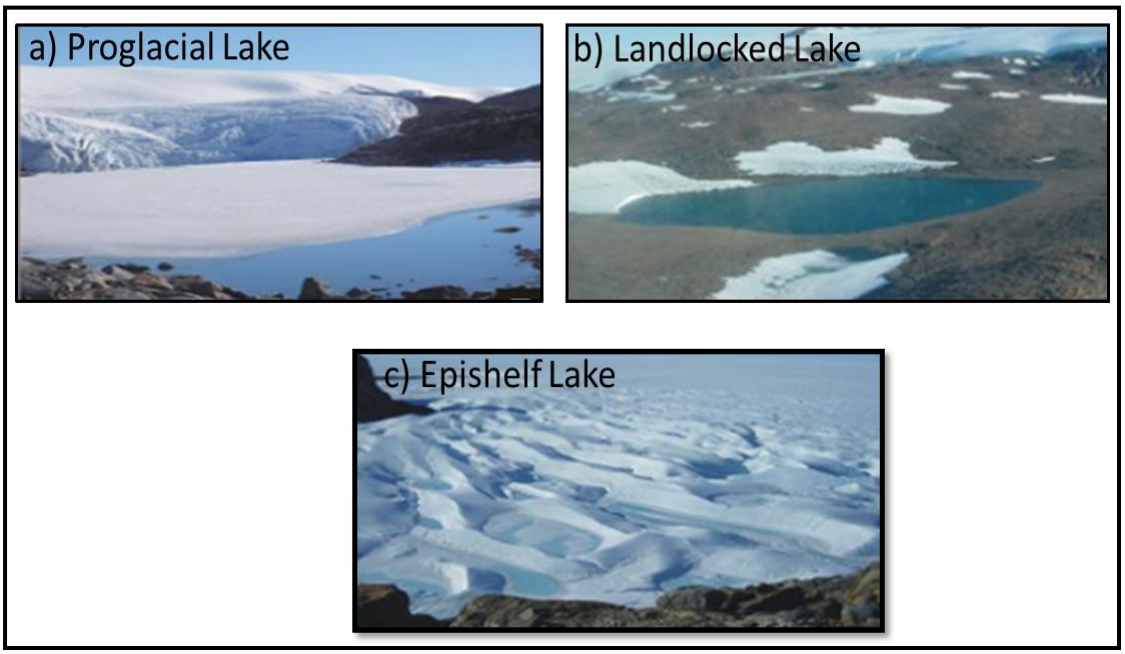

Fig. 1.1 Showing a) Proglacial Lake b) Landlocked lake and c) Epishelf Lake (Ravindra et al., 2001; Phartiyal et al., 2011)

During this period lakes are exposed to the atmosphere which influences the biogeochemistry of its ecosystem. Therefore, the extent and thickness of ice cover in the catchment area greatly influence the biogeochemistry of Arctic and Antarctic lakes (Wharton et al., 1993; Fritsen and Priscu, 1999). Conversely, in lower latitudes, terrestrial inputs through river discharge, saline water influence, plenty of vegetation and considerable anthropogenic impacts play an important role in regulating the ecosystem of the lakes (Padma and Periakali, 1999; Jeelani and Shah, 2006; Chakraborty et al., 2015; Nazneen and Raju, 2017).

The sedimentation in high latitude lakes is primarily a product of sediment input through glacial meltwater and biological productivity. The biological productivity in the Antarctic lakes is confined primarily to algae and cyanobacteria (Yoon et al., 2006; Smith et al., 2006; Hodgson et al., 2009a, b). It has been observed that the lake sedimentation is predominant during the austral summer (Simmons et al., 1986);

hence, meltwater seems to play an important role in transferring the detrital matter from the Antarctic landmass to its lakes.

Fjord is a U-shaped glacial valley formed by the glacier advance and retreat (Fig.1.2) and are located in high latitude regions from 40° N to 40° S. They act as a nexus between the terrestrial (source) and the oceanic domain (sink), providing a potential for continuous exchange between the fjord and the coastal waters on the adjacent shelf (Cottier et al., 2005). These landforms did not receive much attention of Sedimentologists despite their great potential in unravelling the character of different sedimentary processes and mechanisms responsible for the abrupt and long-term changes in sedimentary processes.

One such fjord system studied in Arctic region is Krossfjord-Kongsfjord system situated on the west coast of the Svalbard Archipelago, equilibrates Atlantic, Arctic, brine and freshwater input, which are the indicators of environmental changes (Nilsen et al., 2008). This fjord system is mainly affected by the Western Spitsbergen Current (WSC) which brings in warm and saline Atlantic water at one side and from the other side, it is affected by extensive glacial runoff from different tidewater glaciers. The Thala fjord is situated along the Prydz Bay, east Antarctica which exhibits the largest shelf on the eastern margin of Antarctica (Harris et al., 1998). It receives sediments supplied by the Lambert Glacier/Amery Ice Shelf, draining approximately 10% of the total Antarctic ice volume (Forsberg et al., 2008). Rapid sedimentation in fjord system has resulted in sedimentary record of high resolution (Griffith and Anderson, 1989) which can be used as tool to reconstruct past environmental changes. Factors like sea floor topography, oceanographic conditions, the availability of sea ice, size of the drainage area, proximity to the source of sediment and climate has controlled the sedimentation in fjords (Munoz and Wellner, 2016). In addition to these factors, glaciers have also contributed by eroding and transporting lot of terrigenous influx to the fjords. Therefore, glacial fjord system has been regarded as a natural laboratory for the study of environmental change in the high latitude regions (Fendeng et al., 2018).

Warm saline water and glacier run off is composed of terrestrial and marine particulates which on mixing of these waters, facilitate suspended material to deposit

on the sediment surface (Howe et al., 2010). The influx of particulate metals into the fjord and their transport through the marine circulation and sedimentation processes determine their distribution along the water column and in the sediments (Grotti et al., 2017). Metals occur in different forms such as dissolved species, free ions or forming organic complexes (Noronha-D' Mello and Nayak, 2015). The carbonates, oxy-hydroxides, sulfides and clay minerals can adsorb or co-precipitate particulate metals (Spencer and MacLeod, 2002). Metals cannot be degraded, either they may accumulate locally (Marchand et al., 2006) or remobilized in an aqueous environment. Fjords as compared to the freshwater lakes where pH is the controlling factor, has salinity as the key variable responsible for partitioning of metals between the sediment and overlying or interstitial waters.

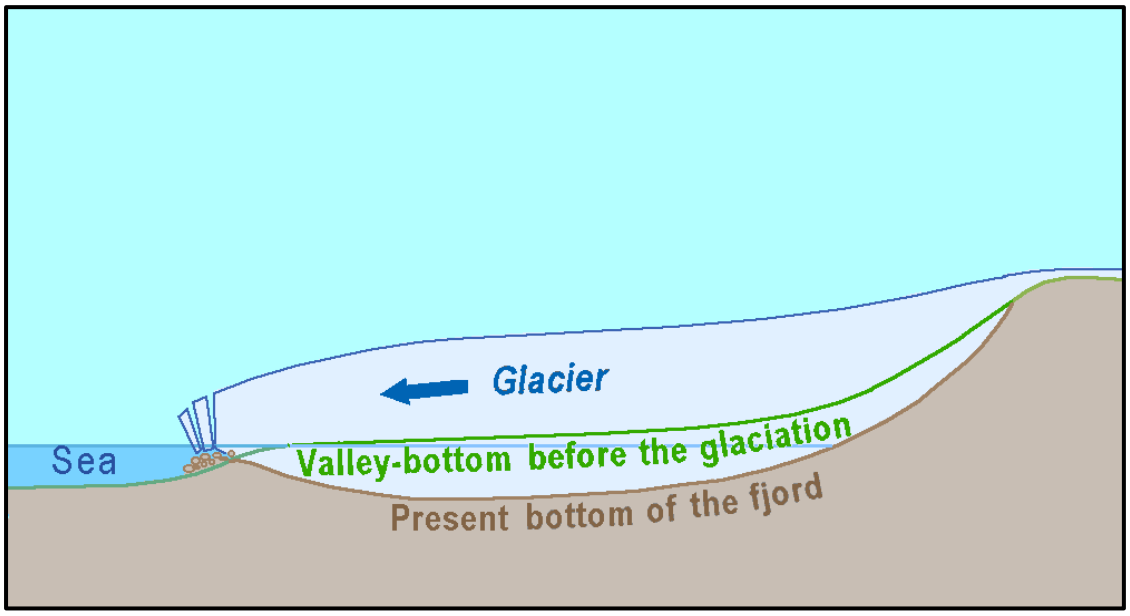

Fig. 1.2 showing formation of a fjord (https://commons.wikimedia .org)

The sediment characteristics like grain size, total organic carbon (TOC) and Biogenic silica (BSi) were used earlier as proxies to elucidate the paleo-processes that occurred within a lake system. The studies were more focussed to understand the biogeochemistry, productivity and environmental behavior of the lakes including its catchment area, fjords and surrounding ocean (Mortlock and Froelich, 1989; Muller and Schneider, 1993; Colman et al., 1995; Kamatani and Oku, 2000; Kaplan et al., 2002; Smith et al., 2006; Yoon et al., 2006). The paleoclimatic record from polar regions has

been presented by many researchers. However, geochemical aspects, from these studies on provenance and sedimentary processes in polar lakes and fjords are rare.

Proxies like grain size and clay minerals are used to understand the source, transportation, and depositional processes. Tang and You (1988) studied clay mineralogy by X-ray diffraction and reported the presence of kaolinite in surface sediments of Don Juan Pond and illite-montmorillonite in Bonney Lake. Mineralogical and geochemical studies were carried out by Sinha and Chatterjee (2000) in sediment cores of Priyadarshini Lake to study depositional and post depositional changes within the lake system. Sinha and Chatterjee (2000) analysed clay minerals in cores and varve sediments from Schirmacher Oasis suggesting hydrolysed depositional environment in high latitude regions. Grain size and elemental composition in sediments were studied by Sun et al. (2002) and determined the evolutionary history of lake environment since 4600 B.P. in the Fildes Peninsula.

Organic proxies like organic carbon, nitrogen, phosphorus, their ratios and biogenic silica are used to identify the source and helps to understand the biogeochemistry of the environment. Lyons et al. (1985) studied Total Dissolved solids (TDS), Calcium carbonate ($CaCO_3$), Total organic carbon (TOC), biogenic silica (BSi), Total nitrogen and phosphorus to establish the climatic history of Wright Valley. TOC, dissolved organic carbon (DOC), and organic constituents of particulate matter and sediment of Lake Vanda were analysed by Matsumoto et al. (1989) to study the lake water stratification and microbial distribution. Seasonal variation of nutrients was studied by Ohyama et al. (1992) at different depths of Lake O-ike and reported that ammonium and nitrate has increased in the bottom and middle layers. Lake Moutonnee were studied for sedimentological and geochemical parameters by Smith et al. (2006) and concluded that lakes were nutrient limited and phytoplankton deficient.

Vertical profiles of major and trace metals provide information on weathering, depositional and post-depositional processes and mobilization of metals. In order to understand the source and processes responsible, geochemical analysis was carried out by Masuda et al. (1982) in surface sediments of lake Vanda and concluded that the source of Cu in this lake was airborne particles carried by glacial melt water.

Isotopic studies were carried out by Tanaka et al. (1982). They investigated two sediment cores from near Antarctica in the pacific sector to study the concentration profiles of ^{9}Be, ^{10}Be and ^{230}Th and concluded that variation in concentration of ^{9}Be is greater than ^{10}Be and their ratio is controlled by ^{9}Be which is mainly derived from the continents. Minor and trace metal distribution were studied by Mentasti et al. (1988) in water, soil, sediment and algae from different lakes and concluded their source to be lithogenic in nature derived from the weathering of rocks available in the catchment area. Sheppard et al. (1997) studied the concentration of metals in Scott Base and concluded that source of metals is natural in origin as they have been derived from the regional lithology. Also, the mechanical and chemical processes have affected the distribution of different metals. Gasparon and Burgess (2000) analysed major and trace metals in Larsemann Hills and suggested that sea-spray input dominated the lake water chemistry along with geographical factors like distance from the shore, direction of winds, shallow and groundwater level. Webster et al. (2003) analysed the concentration of Pb, Zn, Ag, Cd, Cu, Ni, Co and phosphate in water and sediments of Lake Vanda and concluded that metals have low level of contamination which will not affect the quality of lake water or the growth of cyanobacteria. Baseline values of trace metals were analysed by Gasparon and Matschullat (2006) in surface sediments, moss and algae from lakes of Larsemann Hills to understand the extent of pollution in the region. The authors concluded that anthropogenic activities have negligible contribution. Andrade et al. (2012) analysed bulk concentration of mercury (Hg) and solid phase speciation of Hg in Antarctic soils and concluded that overall Hg concentrations are very low. To understand the biogeochemistry of Hg in Antarctic lakes we need to further study the relation of Hg with organic matter. Detailed literature review of recent sedimentological and geochemical studies in Arctic and Antarctic region is given below.

1.2 Literature review

Authors	Area	Inference/major findings
Shrivastava et al., 2012	Schirmacher Oasis, East Antarctica	Detrital quartz grains collected from the ESL-1 and ESL-2 lakes of Schirmacher Oasis, East Antarctica were studied with the help of SEM to understand the provenance of sediments, type of weathering, transportation history and the depositional environment. The results revealed that various types of physical weathering, chemical precipitation have affected the quartz grains prior to their deposition in lake in the form of sediments. The sediments were derived from gneissic rocks and mainly transported by the saltation and suspension mode.
Srivastava et al., 2012	Schirmacher Oasis, East Antarctica	Sediment samples from different glacial environments such as lakes, ice-free lakes, continental shelf, and polar ice were studied for sedimentological characteristics. They reported that samples were fine-skewed to symmetrical, poorly to very poorly sorted and platykurtic to leptokurtic and concluded that Schirmacher Oasis is influenced by glacial processes.
Govil et al., 2012	Larsemann Hills, East Antarctica	A sediment core from L-2 lake was studied to understand the relationship between productivity and grain size. They reported that in the coarse grain sediment organic matter is poorly preserved because of the oxygen penetration in the coarser sediment leading to the decomposition of organic matter. In addition, BSi showed a significant positive correlation with sand and Al/SiO_2 ratio suggesting that low concentration of dissolved silica is either due to the low solubility of silica in cold environments or due to the replacement of Si by Al in the frustules of diatoms.

Authors	Area	Inference/major findings
Singh et al., 2012	Schirmacher Oasis, East Antarctica	Three sediment cores were collected from Priyadarshini lake and Lake L-6 to study the diversity of mosses and its subfossils. They reported a moss species-Pohlia nutans at a depth of 160-162 cm of sediment core from lake L-6 which corresponds to 10.65 cal ka B.P.
Huang et al., 2013	Schirmacher Oasis, East Antarctica	Water samples were collected from Lake Tawani and Lake Untersee from near the sediment-water interface to study the bacterial diversity within these lakes. They reported thirteen phyla and one hundred and twelve genera of bacteria.
Srivastava et al., 2013	Schirmacher Oasis, East Antarctica	Sediment samples from different glacial environments such as lakes, ice-free lakes, continental shelf, and polar ice were studied for mineralogical and sedimentological characteristics. These samples predominantly composed of quartz and feldspar and various heavy minerals. Clay minerals accounted for a very small fraction. They concluded that these sediment samples collected from different glacial units showed similar mineralogical and geochemical composition.
Asthana et al., 2013	Schirmacher Oasis and Larsemann Hills, East Antarctica	Surface sediment samples from Schirmacher Oasis and Larsemann Hills were collected to investigate the sedimentary and glacial processes occurring in these two areas and concluded that these periglacial environments are influenced by a variety of glacial and sedimentological processes. In this study, comparison of sedimentary processes of two different periglacial environments was made which revealed that sedimentary processes vary in magnitude in both the regions due to the different physiographic settings in two geographically separated locations.

Authors	Area	Inference/major findings
Asthana et al., 2013	Fisher island and Broknes Peninsula	Sediment and water samples collected from different lakes of two locations were analysed for cation, anions and Quartz grain microtexture to study hydrochemistry and characteristics of sediments from periglacial lakes of polar regions. The authors concluded that there is a considerable difference in processes like atmospheric precipitation, evaporation and weathering in both the locations. Lithology has also influenced the sedimentary characteristics of the area.
Mazumder and Govil, 2013	Vestfold Hills, East Antarctica	A sediment core of length 47 cm was collected from an inland lake of Vestfold Hills to understand the paleoclimate of this region using diatom as a proxy. The authors have identified a total of 13 diatom species. With the help of different diatom species during early to mid-Holocene, colder conditions were interpreted which shifted to warmer conditions during the late Holocene resulting in a high concentration of nutrients in the lakes. Availability of marine diatoms throughout the core suggested that the lake was receiving a continuous supply of marine water.
Sun et al., 2013	Prydz Bay, East Antarctica	Sixteen surface sediment samples and three sediment cores were collected from the Amery Ice shelf, continental shelf and deep ocean to understand the source of the trace metals, their geographic heterogeneity and relation between Zn and Cd. The authors concluded that there is a negligible anthropogenic impact in the region and main sources of the trace metals are biogenic and lithogenic inputs. They reported an equal amount of biogenic and lithogenic input for Zn and Cd at Amery ice shelf edge, whereas biogenic input was dominant at the continental shelf and deep ocean.

Authors	Area	Inference/major findings
Grotti et al., 2013	Kongsfjord, Svalbard	Surface sediment samples from the Kongsfjord were analyzed to understand the bioavailability of trace metals and their impacts on the fjord environment. They concluded that the trace metals have a negligible anthropogenic impact. Also, the bioavailable fraction which can be leached or extracted easily in the aquatic environment is available in a very small quantity of the total concentration.
Lu et al., 2013	Kongsfjord, Svalbard	A total of 27 surface sediment samples were collected from Kongsfjord to study the distribution of trace elements in the fjord sediments. The authors reported that metals like Pb, Cd, Zn and Hg were relatively higher as compared to the other seas of Arctic region. Enrichment factor analysis using baseline values calculated by relative cumulative frequency method suggested that Hg showed some extent of anthropogenic pollution; Cd, Pb, and Zn showed anthropogenic contamination at few stations; and Mn, Cr, Cu, Co and Ni showed negligible anthropogenic contamination in the investigated areas.
Warrier et al., 2014	Schirmacher Oasis, East Antarctica	A sediment core of length 68 cm was retrieved from the sandy lake for paleoclimate/paleoenvironment reconstruction using environmental magnetic properties of sediments. The authors concluded that the Holocene period had experienced alternate warm and cold events which are in good agreement with the sediments and ice core records of other lakes. Additionally, environmental magnetic evidence for this region is provided by this study.

Authors	Area	Inference/major findings
Phartiyal, 2014	Schirmacher Oasis, East Antarctica	Samples were collected from three sedimentary sections (SWDL, DLL, PDL) of dry lake sediment of the Schirmacher Oasis (SO) East Antarctica to analyze remanent magnetism and radiocarbon ages to study past climate conditions. The authors reported that high values of magnetic susceptibility, soft isothermal remanent magnetism and saturation isothermal remanent magnetism (SIRM) represented colder periods and lower values represented relatively warmer phases in the lakes. Low coercive minerals have high remanence preserved in them.
Martinez et al., 2014	Byers Peninsula, Livingstone Island, South Shetland Island, East Antarctica	A sediment core of 57 cm was collected from Limnopolar lake, Byers Peninsula, Livingstone islands, South Shetland islands and analyzed for elemental and mineralogical composition. The authors suggested that volcanic activity taking place in the area determines the chemical and mineralogical composition of the lake sediments spanning 600 years. The main source of the volcanic material is the volcano of deception island.
Wehrmann et al., 2014	Western Svalbard, Arctic	Surface sediment samples and pore water samples were collected from Smeerenburgfjorden, Kongsfjorden, and Van Keulenfjorden along Western Svalbard of Arctic and analyzed for solid phase iron and manganese speciation. The results obtained suggested glacier sediment show a large range of iron compositions which is regulated by the mineralogy of the bedrocks of glaciers, hydrodynamic conditions and grain size sorting. Very high accumulation rate of Fe along with low input of organic carbon in the fjord is due to the very high sedimentation rate in these fjords.

Authors	Area	Inference/major findings
Xijie et al., 2014	Prydz Bay, East Antarctica	Suspended particulate samples were collected from the Prydz Bay, Antarctica to study the distribution of suspended particulate organic carbon and its stable isotope in the sea surface and factors affecting them and processes responsible. The authors concluded that the concentration of suspended POC was high near the coastal region. POC concentration was compared with chlorophyll a concentration and sea ice coverage which ascribes the association of POC with the production of phytoplankton in the water column and their growth is affected by the sea ice coverage.
Matsumoto et al., 2014	Soya Kaigan, East Antarctica	A sediment core of 135 cm was collected from Lake Oyako-ike from the Lutzow-Holm Bay region, East Antarctica was analyzed for organic components, facies analysis and microscopic observations. The authors concluded that the continuous retreat of glaciers and isostatic uplift took place during the mid-Holocene are responsible for the isolation of this lake, however eustatic sea level has played a minor role.
Kumar et al., 2014	Krossfjord and Kongsfjord, Svalbard	Six surface sediment samples along with one core were collected from Krossfjord and Kongsfjord and analyzed for grain size, ^{10}Be and metal oxides to study the distribution and deposition pattern of ^{10}Be. The authors concluded that ^{10}Be concentration increased towards the mouth in the Krossfjord. This is meteoric ^{10}Be which was trapped into the sediment got released with meltwater into the fjord, they concluded.

Authors	Area	Inference/major findings
Mahesh et al., 2015	Schirmacher Oasis, East Antarctica	A sediment core of 50 cm was collected from the long lake and analyzed for grain size, bulk organic carbon, and its isotope. The results obtained suggested that organic carbon available in the lake is autochthonous. The lowest organic carbon was recorded during the last glacial maximum and major part of Holocene indicating colder conditions during the period.
Warrier et al., 2016	Schirmacher Oasis, East Antarctica	Thirty-five sediment samples from a core collected from sandy lake Schirmacher Oasis, East Antarctica were analyzed for grain size parameters and surface textural observations using SEM. The authors suggested that physical weathering, chemical precipitation and signatures of erosion have affected quartz grain prior to its deposition in the lake in the form of sediment. The results obtained in the study are comparable with the data obtained from the ice cores and other lake sediment records available in the study area.
Hodgson et al., 2016	Prydz Bay, East Antarctica	In this study, authors have compiled the updated regional relative sea -level data from the study area. This compiled data set extended the relative sea level curve for this area to 11,528 cal kyr B.P.
Kumar et al., 2016	Kongsfjord, Arctic	A total of eleven surface sediment samples were collected from Kongsfjord and analyzed for TOC, TN and their isotopes. The authors revealed that geochemical proxies showed a clear spatial gradient regulated largely by glacial marine contrast. Organic matter concentration increases on moving away from the glaciers and it is of mixed origin.

Authors	Area	Inference/major findings
Govil et al., 2016	Schirmacher Oasis, East Antarctica	A sediment core of 1.62 m collected from L-6 lake of Schirmacher Oasis, East Antarctica was analyzed for grain size, TOC, BSi and Mg/Ca and Mn/Fe ratios to study the climatic variability during the Holocene. The authors revealed that the productivity was higher as suggested by Mg/Ca, Mn/Fe and BSi at Pleistocene-Holocene boundary.
Wang et al., 2016	Prydz Bay, East Antarctica	Surface sediment samples were collected from the continental shelf, Prydz Bay and analyzed for grain size and heavy minerals to study sediment features and provenance. The results revealed that Prydz Bay is a glaciomarine environment affected by factors such as sea ice, iceberg, topographic settings and marine circulation. Sediments deposited on the east side of the bay is derived from Princess Elizabeth land.
Kozioroswka et al., 2016	Adventfjord and Hornsund, Svalbard	Sediment cores were collected from Adventfjord and the Hornsund, Svalbard to study the spatial variation of TOC, TN, C/N ratio and stable isotopes of carbon and nitrogen. The study revealed that the concentration of organic matter in surface samples is mainly controlled by the input of terrestrial material and marine organic matter is relatively less contributing to labile organic substances supporting benthic organisms. Elemental composition and stable isotopes of bulk organic carbon showed that the spatial distribution of terrigenous organic carbon is dependent on the proximity of the glaciers.
Mahesh et al., 2017	Schirmacher Oasis, East Antarctica	A sediment core of 68 cm was collected from the sandy lake, Schirmacher Oasis, East Antarctica was studied for grain size, C/N ratio and their isotopes. The study revealed that the organic matter available in the lake is

Authors	Area	Inference/major findings
		of mixed origin. The lower content of these proxies during the LGM suggested the provenance of organic matter to be autochthonous possibly due to long colder periods in Antarctic.
Mazumder et al., 2017	Schirmacher Oasis, East Antarctica	A sediment core of 36 cm was collected from a periglacial lake (P11) and analyzed for the morphology of quartz grain, microtexture and sand percentage for the reconstruction of paleoenvironment during the Holocene. The results obtained suggested colder and relatively warmer phases in the study area supported by relative sand percentage in the sediment.
Kozioroswka et al., 2017	Kongsfjord, Svalbard	Sediment cores and suspended particulate matter was collected from the Kongsfjord and analyzed for total carbon, organic carbon and inorganic carbon, Ca, Mg and Sr to study the distribution and source of both organic and inorganic carbon. The authors revealed that organic carbon produced in Kongsfjord is mainly in -situ along with minor input from glaciers. Also, the carbonates which are deposited closer to the glacier fronts are terrestrial in origin while which are deposited near fjord mouth are biogenic in origin.
Grotti et al., 2017	Kongsfjord, Svalbard	Surface sediment samples were collected from Kongsfjord and analyzed for grain size, TOC, TN, mineralogy and major and trace metal concentrations, lead isotopes, solid phase speciation, acid volatile sulfides, and associated metals to understand the source and bioavailability. The authors concluded that the marine environment of Kongsfjorden has the natural concentration of trace elements and anthropogenic input of metals by Atlantic waters from lower latitudes may influence the mouth region of the fjord.

Authors	Area	Inference/major findings
Lu and Kang, 2018	Arctic ocean	Surface sediment samples were collected from the Pacific sector of the Arctic ocean and analyzed for metal concentrations and their extractabilities. The study concluded that the modified BCR method is a reliable method to study mobility and bioavailability as compared to bulk concentrations. The new Analytical hierarchy process method is a reliable tool for studying the mobility, toxicity and bioavailability.
Kar et al., 2018	Ny-Alesund, Svalbard	A total of 20 sediment samples were collected from a 1 m deep trench adjacent to the Kolhamma Lagoon, NY-Alesund and analyzed for pollens and spore, magnetic susceptibility and quartz grain microtexture to study the paleoenvironmental conditions of NY-Alesund area since LGM. The study revealed that overall glacial activities prevailed in the area since the beginning of LGM. The melting of the glaciers after the LGM brought a huge amount of terrigenous influx of glacial sediments which is evident by a dominating glacial environment as shown by quartz grain microtexture.
Kumar et al., 2018	Krossfjord and Kongsfjord, Svalbard	Surface sediment samples were collected from Krossfjord and Kongsfjord and analyzed for major, trace and rare earth element (REE) along with mineralogical and textural analysis to understand the geochemistry and provenance of the sediments. The study revealed that the chemical weathering in the study area is in the initial stage and grain size reduction is mainly by mechanical weathering. The geochemistry of the samples suggested that mafic rock has negligible contribution and it showed intermediate composition between

Authors	Area	Inference/major findings
		granitic and granodioritic. In the chondrite and UCC normalized plot, all the samples showed similar REE pattern with depleted HREE suggesting a lower concentration of heavy minerals in the sediments.
Kumar et al., 2018	Kongsfjord, Svalbard	Eight surface sediment samples and a core of length 21 cm were collected from Kongsfjord and analyzed for the reconstruction of productivity changes in the last 200 years and to understand whether these changes are linked to temperature variations. The authors concluded that in the last 2 centuries changes in productivity is reflected by a sudden temperature change and a general trend of warming.
Govil et al., 2018	Schirmacher Oasis, East Antarctica	A sediment core of 102 cm was collected from L-51 and analyzed for sedimentological parameters viz. sand, silt, clay, roundness and biogenic silica to understand the role of sedimentary processes in lake of Schirmacher Oasis. The study revealed three episodes of meltwater flux which is responsible for the retreat of southern glacier boundary towards more south in Schirmacher Oasis.
Mahesh et al., 2018	Broknes peninsula, Larsemann Hills	A sediment core of 135 cm was collected from the stepped lake, Broknes peninsula of Larsemann Hills and studied for diatoms, elemental and isotopic measurements. The increase in the concentration of all these proxies suggested a change from marine to lacustrine environment indicated a change from cool-dry oceanographic state to warm wet lake conditions.
Mohan et al., 2018	Kongsfjord, Svalbard	A sediment core of 28 cm was retrieved from Kongsfjorden and analyzed for Pb dating and metal concentrations to understand the history of metal contamination in the study

Authors	Area	Inference/major findings
		area. The authors concluded that the sedimentation rate has increased in the last 20 years due to the increase in glacial meltwater. Metals showed an increasing trend towards the surface and since 1970 their deposition rate is also high suggesting the effect of industrial emission which may be a potential threat to the Arctic biota.
Yang et al., 2018	London island, Svalbard	Sediment samples were collected from a paleo-notch sediment profile and analyzed for metal oxides, TOC and TN to study the climate change from mid-to-late Holocene from London Island. The authors concluded that different weathering indices were estimated and similar weathering conditions were interpreted from all the indices. TOC and TN showed similar variations as that of weathering indices and four cold and four warm periods in the study area was demarcated. The four cold periods were marked at the same time when ice rafting event took place in the North Atlantic region and glacial activities in Iceland and Svalbard. In this study, climate dynamics during the mid-to-late Holocene period was studied with the help of new proxy dataset.
Srivastava et al., 2018	Schirmacher Oasis, East Antarctica	Surface sediments samples were collected from different geological units of Schirmacher Oasis, East Antarctica and analyzed for granulometry, heavy minerals and clay minerals. The authors concluded that the study provides a good idea about the exogenic and endogenic processes taking place in the study area. Chlorite and illite minerals are minerals of high latitude and found in cold climate. Availability of kaolinite and smectite suggested an increase in temperature in the past.

Authors	Area	Inference/major findings
Fendeng et al., 2018	Kongsfjord, Arctic	Fifty-two surface sediment samples were collected from Kongsfjord and analyzed for clay minerals to study source and transportation process. Illite is the dominant mineral available in the sediments of Kongsfjord followed by kaolinite and chlorite, and smectite is completely absent. The authors stated that the factors influencing the availability of different clay mineral assemblages are source, hydrodynamic conditions and crystal behavior.
Mahesh et al., 2019	Schirmacher Oasis, East Antarctica	A 79 cm long sediment core was collected from a peri-glacial (Zub) lake and analyzed for grain size, elemental and isotopic measurements. The results obtained are for the last 43 kyr. The study revealed that all the proxies showed a good response to the shifts (glacial-interglacial) in climate and it is in good agreement with the ice core records from the study area.
Asthana et al., 2019	Larsemann Hills and Schirmacher Oasis, East Antarctica	Water samples were collected from different lakes of Larsemann Hills and Schirmacher Oasis and analysed for physical parameters and anion, cation concentration to compare the characteristics and processes affecting the chemistry of the lakes from two different periglacial environments. The authors concluded that lithology has affected the lake water chemistry in Larsemann Hills whereas in Schirmacher Oasis possibly composition of the rocks and precipitation have affected. Major ions showed balanced concentration of ions in the lakes. Also, atmospheric precipitation has also affected the ionic concentration in these lakes.

1.3 Objectives

From the detailed literature review, it was noticed that earlier studies were mainly focussed on the characterization of sediments and paleoclimatic reconstruction using bulk carbon, nitrogen and their isotopes and magnetic susceptibility on surface sediments and lake sediment cores. It is essential to understand the provenance, depositional processes, transportation and geochemistry within the lakes by studying the distribution of nutrients and metals. A multiproxy approach was adopted to understand the depositional processes, occurring in lakes and fjord as these depositional environments act as sink for nutrients and metals. The present study has been carried out in lakes and fjords of Arctic and Antarctic region with following objectives.

1. To study sediment texture and understand the depositional processes.
2. To understand the past climatic changes through the study of trace elements in sediments.
3. To study spatial and temporal variations in Be concentration in sediment of higher latitude and understand the signatures of past climatic changes.

1.4 Study area

High latitude and Polar regions (Arctic and Antarctic) are highly sensitive and promising areas of capturing even the minute changes to the environment. The pristine environment of these regions is devoid of much anthropogenic input and adapted to or can tolerate persistent low temperature, freeze and thaw cycles, seasonal and interannual variations in energy and supply of nutrients. Ecosystems of polar regions are therefore a sensitive actuator to the intensity and magnitude of environmental changes and pre-requisites for environmental research.

1.4a Surface sediment samples

Arctic: For the present study, surface sediment samples were investigated from Krossfjord-Kongsfjord system, Svalbard, Arctic and Prydz Bay (Thala Fjord), East Antarctica. Krossfjord-Kongsfjord, a typical fjord system, located between 78°40’and

77° 30'N and 11° 3' and 13° 6' E on the north-west coast of Svalbard Archipelago (Fig.2.1). The Svalbard Archipelago is covered by the ice caps and glaciers. The ice cap front of the Svalbard-Barents Sea gradually receded to the west shore of the archipelago (Landvik et al., 1998; Lehman and Forman, 1992) and formed a series of extremely deep fjords at the entrance of the sea, thus, leading to the formation of Kongsfjord during this period (Fendeng et al., 2018). Kongsfjord, the southern arm of the fjord, is oriented spatially from south-east to north-west and Krossfjord, the northern arm of the fjord, is from north to south (Svendsen et al., 2002). The fjord consists of two submarine channels, which converge to a deep glacial basin, the Kongsfjorddrenna. Kongsfjord is 20 km long and 4-10 km wide while the Krossfjord is relatively longer (~30 km) but narrower (3-6 km) as compared to Kongsfjord (Svendsen et al., 2002).

The West Spitsbergen Current (WSC), a northern extension of the North Atlantic Current modified the climate of Svalbard as it brings heat and highly saline water to the region (Svendsen et al., 2002; Saraswat et al., 2018). In recent years, Kongsfjord is influenced by a strong inflow of Atlantic water, which has affected the winter situation in Kongsfjorden, strongly reducing the sea-ice formation in the fjord (Cottier et al., 2005). The seawater temperature, wind direction and freshwater supply in Kongsfjorden and Krossfjorden system vary seasonally (Farmer and Freeland, 1983; Saraswat et al., 2018).

Kongsfjord-Krossfjord system is a part of the major tectonic boundary between the Northwestern Basement Province of Svalbard to the north-east and Tertiary fold-thrust belt of western Spitsbergen to the south-west (Bergh et al., 2000; Svendsen et al., 2002). The bedrock north of Kongsfjorden and on the islands in the fjord consists of medium-grade metamorphic rocks of Middle-Proterozoic age, mainly marbles, mica schists, and a minor amount of Quartzites (Svendsen et al., 2002). While on the south of Kongsfjord, structurally above the basal tertiary thrust, sedimentary rocks of Late Paleozoic and tertiary age occur, although some Proterozoic, low and medium-grade metamorphic rocks (mica-schists, marbles, phyllites, Quartzites) occur in south-eastern part (Svendsen et al., 2002). The coastal part of the fjord system constitutes unconsolidated deposits of Quaternary age which includes moraines, marine shore

and fluvial deposits (Kumar et al., 2014; Choudhary et al., 2018). Different glacial processes are responsible for shaping and modifying the landforms in this region.

Antarctica: Prydz Bay is an embayment along the Antarctic margin between 66° E and 79° E (Sun et al., 2013) (Fig. 2.2). On the southern side, it is surrounded by Amery Ice Shelf (AIS) and spreads to the edge of the continental shelf northwards at about 67°S. The Amery Depression dominates the inner continental shelf, which is mostly 600–700m deep. The depression is bordered by two shallow banks (< 200 m): Fram Bank to the northwest and Four Ladies Bank to the northeast, forming a spatial barrier to exchange water with the outer oceanic water (Smith and Treguer, 1994). Prydz Bay is characterized by a clockwise gyre in front of the Amery Ice Shelf (Smith et al., 1984; Passchier et al., 2003) covering almost the entire bay. It is covered by sea ice for almost whole year except few days in summers. Icebergs are also observed on the eastern side of the bay, which have originated from the West Ice Shelf and brought southward by the coastal current under the influence of cyclonic winds (Smith et al., 1984). In the bay, most of the icebergs and floating ice mass are found near the outlet glaciers. The glaciers entering the bay primarily come from the Ingrid Christensen Coast, including the Sorsdale Glacier which flows south of the Vestfold Hills and the glaciers that contribute to the Publication Ice Shelf. Four Antarctic research stations are located on the shore of Prydz Bay, the Indian station Bharati (69.4077° S, 76.1872° E), Chinese station Zhongshan (69.378° S, 76.388° E), the Russian station Progress (69.388° S, 76.388° E) and the Romanian station Law Racovita (69.398° S, 76.388° E).

Geologically, Prydz Bay is part of the Pan-African Prydz Belt, which is recognized as a result of tectonic processes initiating in the Archean (Wilson et al., 1997; Boger et al., 2001; Liu et al., 2006) and comprises of three Archean cratonic blocks, a Grenvillian granulite terrane and a Pan-African high-grade belt (Liu et al., 2006). The Archean blocks, exposed in the southern Prince Charles Mountains, Vestfold Hills and Rauer Islands, comprise primarily of orthogneiss; while the Grenvillian granulite is mainly exposed in the northern Prince Charles Mountains and consists of a metamorphic complex including felsic orthogneiss, gneiss, mafic granulite and charnockite (Li, 2006). The Pan-African high-grade belt mainly distributes along the

Prydz Bay coastline and consists of mafic-felsic composite orthogneisses and migmatitic paragneisses (Fitzsimons and Harley, 1991; Dirks and Wilson, 1995; Liu et al., 2006).

1.4b Sediment cores

Arctic: Svalbard is considered as a glacial environment of high-latitude (76-81°N) (Pelto et al., 1990). Ny-Alesund is situated on the Spitsbergen island of Svalbard archipelago, a northernmost permanent settlement of the earth. It is located on the Brogger peninsula, west coast of Spitsbergen at Kongsfjord. The important significance of the area is that it displays the rocks of all the ages right from Precambrian to Tertiary (Dallman, 1999). It consists of numerous lakes and variety of fjord environments. The lowest temperature of the area is -14°C during the month of February and 5°C during the month of July (Kar et al., 2018).

For the present study sediment cores have been investigated from lake LA (78° 56 ′ 117"; 11° 48 ′ 055"), L-1(78° 58′ 04.6";11° 24 ′ 42.1"), L-2 (78° 58′ 11.2"; 11° 26 ′ 53.2") and L-3 (78° 57 ′ 26.37";11° 27′ 16") (Fig. 2.3). These are landlocked lakes and are dependent on the seasonal snow.

The lake L-A is an oval-shaped basin situated at an altitude of 46.95 m above MSL. The maximum water depth is about 4 m, the surface area is 0.00578 km^2, and the catchment area is 0.014 km^2. Algal mats were noted on the surface of the lake and the catchment area of the lake is covered with Tundra vegetation and moss campion. The bedrock in the catchment area of the lake is sedimentary rocks and conglomerates. The pH of the lake water ranges from 7.28 to 8.72, at 0°C temperature suggesting neutral to slightly alkaline conditions of the lake during the sampling period.

The lake L-1 is a closed lake situated 1 km away from the coast on a strandflat as it is a common feature near the coast of Svalbard. It is situated at an altitude of 4 m above MSL. The maximum water depth is 3.5 m, the surface area is 0.0675 km^2 and the catchment area is 0.029 km^2.The cliffs of low metamorphosed carbonates are available in the catchment area of the lake. The pH of the lake water ranges from 7.92 to 8.59, at 0°C indicating neutral to slightly alkaline conditions of the lake during the sampling period.

Lake L-2 is situated 2 km away from the coast on a strandflat. It is situated at an altitude of 4.5 m above MSL. The maximum water depth is 3m, the surface area is 0.0968 km^2 and the catchment area is 0.0125 km^2 as it is divided by other adjacent lakes. The pH of the lake water ranges from 7.63-8.05, at 0°C indicating neutral to slightly alkaline conditions of the lake during the sampling period. There is less vegetation around the lake.

Lake L-3 is situated 7 km away from the coast on a strandflat. It is situated at an altitude of ~9m above MSL. The maximum water depth is 3 m, the surface area is 0.0495 km^2 and the catchment area is 0.789 km^2. The catchment area has flourished tundra vegetation and the area is surrounded by the moraines and cliffs of weathered, low or weakly metamorphosed carbonates. The pH of the lake water ranges from 7.35-8.25 at 0°C during the sampling period.

Antarctica: There are numerous lakes in the ice-free regions of Antarctica such as Vestfold Hills, McMurdo dry valleys, Larsemann Hills, and Schirmacher Oasis, which occupies about 2% of Antarctic landmass. The present study is focussed on the lakes of coastal Antarctica i.e. Larsemann Hills and Schirmacher Oasis.

The Larsemann Hills (69° 20′ S to 69° 30′ S latitude: 75° 55′ E to 76° 30′ E longitude), an ice-free area of approximately 50 km^2, located on the Ingrid Christensen Coast of Princess Elizabeth Land in East Antarctica (Fig.2.4), have a low, gentle, and rolling topography merging with the polar ice cap in the south southeast and surrounded by sea in other three directions, punctuated with small islands in north and northeast. The study focuses on the Grovnes peninsula (69° 24′ 36″ S 76° 12′ 16″ E) area which is dotted with small, perennial lakes. A total of 12 lakes were identified, out of which 7 lakes north of latitude 69° 25′ 00″ are inland lakes having small catchments and are dependent on seasonal snow. Whereas lakes south of latitude 69° 25′ 00″ are pro-glacial lakes. These lakes are formed by the exposure of basins after the retreat of the continental ice cap or after isolation due to isostatic uplift following deglaciation (Priscu and Foreman, 2009). The lakes located in rocky depressions formed as a result of glacial erosion are generally small (5000–3000 m^2) and shallow (maximum depth 2–5 m (Gasparon and Burgess, 2000). The periglacial process is the

main factor determining the local modern geomorphology (Feng et al., 2008) and hosts a repository of sedimentary depositional features of agencies like a glacier, seasonally active streams, and wind under a periglacial environment that have been active in the geological past (Asthana et al., 2013). A major feature of the climate of the Larsemann Hills is the existence of persistent, strong katabatic winds that blow from ENE or NE most summer days and its continental Antarctic climate which is colder and drier than the maritime Antarctic.

For the present study, sediment cores were investigated from Murk water Lake, L-8 (69° 24′ 58.00″ S 76° 12′ 53.00″ E), L-10 (69° 25′ 17.80″ S 76° 11′ 34.20″ E), and L-12 (69° 25′24.24″ S 76° 11′ 47.40″ E) lakes (Fig 2.5). These are proglacial lakes fed by the polar ice with thick sediment accumulation. The lake L-8 is an oval-shaped basin situated at an altitude of 8 m above MSL. The maximum water depth is about 4 m, the surface area is 0.00574 km^2, and the catchment area is 0.012 km^2. The important geomorphic features noted in the catchment area are glacially carved ridges, glacially abraded flat-topped hills, and depressions with a negligible amount of glacial drift. Windblown fine sediment resulting in supraglacial sediment pockets is a characteristic sediment feature of the region. Additionally, algal mats were noted on the surface of the lake. The pH of the lake water ranges from 7.1 to 7.25, at 0°C temperature suggesting neutral to slightly alkaline conditions of the lake during the sampling period.

The lake L-10 lies at an elevation of about 95 m above MSL. The water depth of the lake is about 1.25 m. This lake is comparatively small in size with an area of about 0.00173 km^2. The catchment area of the lake is 0.00675 km^2. The lake is situated at a higher elevation, and the morphological features associated are glacially eroded ridges and valleys giving rise to undulatory topography and various other landforms such as exposed ridges devoid of sediment cover (Asthana et al., 2013). During sample collection in the field, growth of lichens and mosses were observed adjacent to the lake water body. The pH of the water in the lake ranges from 7 to 7.2 at 0.6°C indicating it to be neutral to slightly alkaline in nature.

The lake L-12 has an oval-shaped basin, covering an area of 0.00263 km^2 situated at an elevation of about 95 m above MSL, and has a water depth of about 3 m. The catchment area of the lake is almost 0.0330 km^2 having geomorphic features such as glacial striations, roche moutonnees, sparse morainic sediments, and erratics. Algal mats were observed on the surface of the lake. The pH of the lake water ranges from 7.1 to 7.3 at 0.6°C suggesting neutral to slightly alkaline pH conditions of the lake during the sampling period.

The Schirmacher Oasis situated in Queen Maud Land, East Antarctica, is a 35 km^2 ice-free area, located about 100 m above mean sea level (MSL), situated between the margins of continental ice sheet and ice–shelf (Fig.2.6b). The oasis consists of several hills of low elevation of ∼200 m (Srivastava and Khare, 2009) and interspersed with around 120 freshwater glacial lakes. These glacial lakes originated during the late Pleistocene retreat of glaciers and their morphological and genetic behavior enabled their classification as epishelf, proglacial and land locked lakes (Ravindra and Laluraj, 2012) depending upon their geomorphic evolution. The region is marked with debris cover and valley systems having lakes which are either in glacially eroded bedrock or dammed by moraines or ice (Bormann and Fritzsche, 1995). In general, Schirmacher Oasis experiences milder climate as compared to other areas of Antarctica.

For the present study, sediment cores were investigated from GL-1 lake (70° 46’ 07.2’’ S; 11° 44’ 04’’ E), V-1 lake (70° 47’ 27’’ S; 11° 37’ 46.6’’ E) and L-6 lake (70° 45’ 16.6’’ S; 11° 36’ 03’’ E) situated ∼0.25 km, 4 km and 6 km, respectively from Indian research station Maitri (Fig. 2.6c). These are land locked lakes and are dependent on seasonal snow.

The lake GL-1 is situated at an altitude of 115 m above MSL. The maximum water depth is about 4 m, the surface area is 0.005 km^2 and the catchment area is 0.023 km^2. This lake is surrounded by the adjacent smaller lakes and also by Priyadarshani or Zub Lake. The important geomorphic features noted in the catchment area are structural hills, glacial valleys and roche moutonees which are left open by the receding continental ice (GSI, 2006). Growth of lichens and mosses were observed adjacent to the lake water body. Additionally, algal mats were noted on the surface of

the lake. The pH of the lake water ranges from 6.1-7.4 suggesting acidic to neutral pH conditions of the lake during the sampling period.

The Vetehiya (V-1) Lake lies at an elevation of about 400 m above MSL. The water depth of the lake is about 2.5 m. This lake is comparatively small in size with an area of about 0.003 km^2. The catchment area of Vetehiya Lake is 0.017 Km^2. As the lake is situated at a higher elevation, the morphological features associated are structural hill and typical development of roche moutonees having steep cut walls in the catchment area (GSI, 2006). During sample collection in the field presence of algal mats were observed on the surface of the lake water. The pH of the water in the lake ranges from 6.78-7.0 indicating it to be slightly acidic to neutral in nature.

L-6 Lake has an oval shaped basin, covering an area of 0.007 km^2 situated at an elevation of 70 m above MSL, and has a water depth of about 4-4.5 m. Catchment area of the lake is almost 0.128 km^2 having geomorphic features such as glacial striations, roche moutonees, elementary development of surface channels and patterned ground formed mostly through subsurface flow regime (GSI, 2006). According to Govil et al. (2016), earlier the lake basin was partially closed therefore it did not receive much clastic as well as biogenic sediments from the barren catchment area. Lower sand deposition in the lake supports a low-energy depositional environment of the basin. Further, the surface channels flowing through the large catchment area have low flow velocity due to low elevation gradient, facilitating deposition of relatively finer particles to the lake. The pH of the lake water ranges from 6.71 – 7.75 suggesting acidic to neutral pH conditions of the lake during the sampling period.

2.1 Introduction

A sample is a representative of particular environment or an area and can help in understanding the source, processes operating and prevailing hydrodynamic conditions. Based on the aims and objectives of the study, sampling location and characteristics of the sample, relevant sampling techniques and devices are used. The sampling procedure have been chosen in such a way that it should reduce the contamination and avoid alterations. Care should be taken that the collected sample should maintain its natural physical, chemical and biological integrity.

2.2 Field study and Sample collection

2.2a Surface sediment samples

For the present study, a total of thirteen surface sediment samples were collected from Arctic region at various water depths from Krossfjord and Kongsfjord as part of the Indian Arctic program (summer phase) during August 2016 (Fig. 2.1, Table 2.1). Surface sediment samples were collected using stainless steel Van Veen grab sampler using the workboat "MS Teisten". Further, seven surface sediment samples were collected at different water depths from Prydz Bay, East Antarctica (Fig. 2.2, Table 2.2) during 34th Indian Scientific Expedition to Antarctica.

Table 2.1. Details of surface samples collected from Krossfjord and Kongsfjord, Arctic

Sample name	Water Depth (m)	Latitude (°N)	Longitude (°E)
Kr-1	285.00	79° 4′ 3"	11° 13′ 9.48"
Kr-2	130.00	79° 8′ 4.56"	11° 47′ 3.48"
Kr-3	180.00	79° 9′ 12.6"	11° 39′ 0.36"
Kr-4	189.00	79° 11′ 58.2"	11° 41′ 34.08"
Kr-5	265.00	79° 14′ 1.32"	11° 41′ 21.84"
Ko-1	332.00	79° 2′ 11.4"	11°17′ 43.8"
Ko-2	180.00	79° 0′ 29.16"	11° 36′ 29.88"
Ko-3	283.00	79°.0′ 31.32"	11°.47′ 19.32"
Ko-4	235.00	78° 57′ 3.6"	11° 49′ 40.08"
Ko-5	41.70	79° 0′ 26.28"	12° 10′ 46.92"
Ko-6	302.00	78° 56′ 25.08"	11° 57′ 43.92"
Ko-7	90.00	78° 58′ 21"	12° 19′ 51.24"
Ko-8	70.10	78° 54′ 16.2"	12°13′ 48"

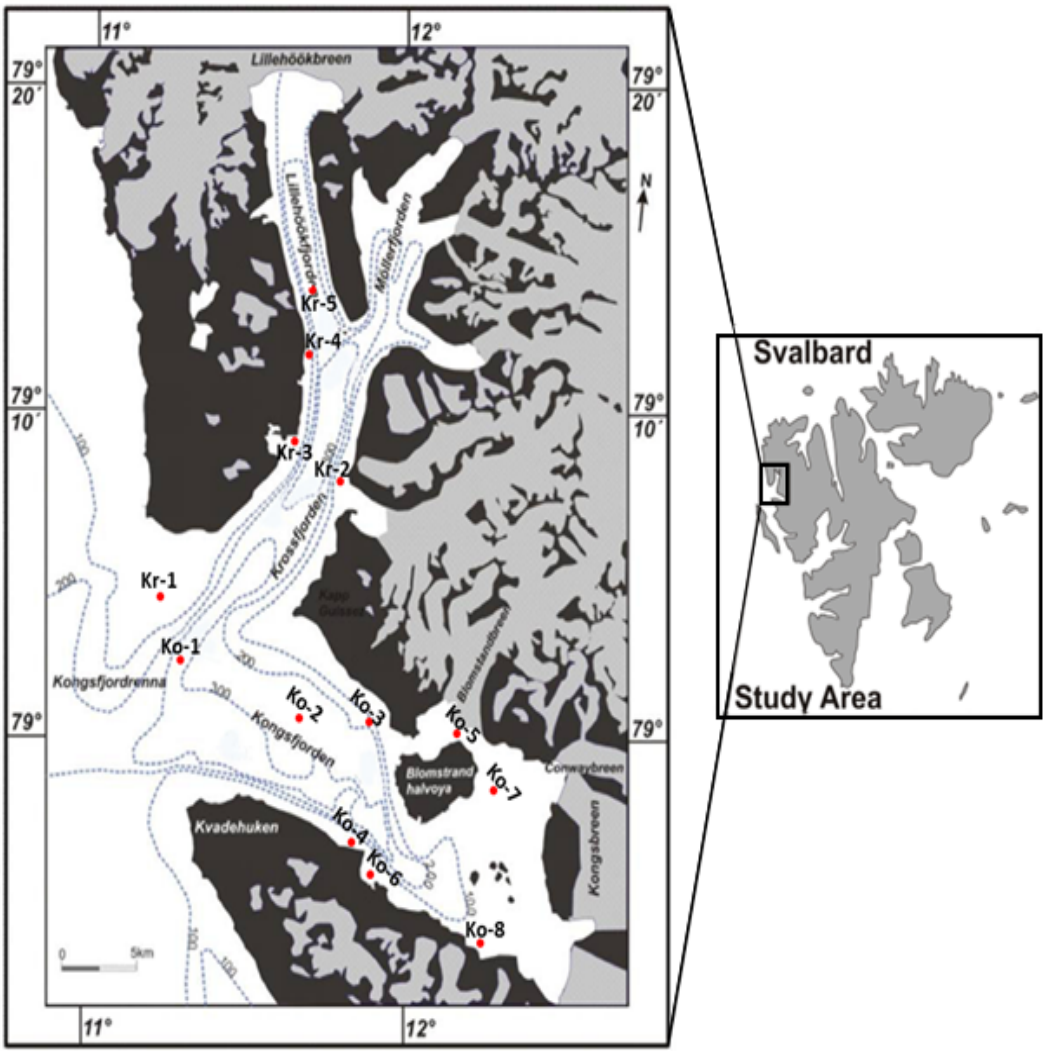

Fig 2.1. Map showing the study area (modified after Svendsen et al., 2002)

Table 2.2. Details of surface samples collected from Prydz Bay, East Antarctica

Sample name	Depth (m)	Latitude (°N)	Longitude (°E)
P1	31	69° 24′ 14.472"	76° 11′ 1.896"
P 2	40	69° 24′ 21.384"	76° 10 ′ 25.824"
P 3	50	69° 24 ′ 52.308"	76° 10 ′ 26.112"
P 4	60	69° 31′ 12"	76° 11′ 18.996"
P 5	98	69° 26 ′ 8.016"	76° 18′ 2.016"
P 6	120	69° 27′ 19.008"	76° 12′ 10.008"
P7	140	69° 31′ 54.012"	76° 21′ 47.988"

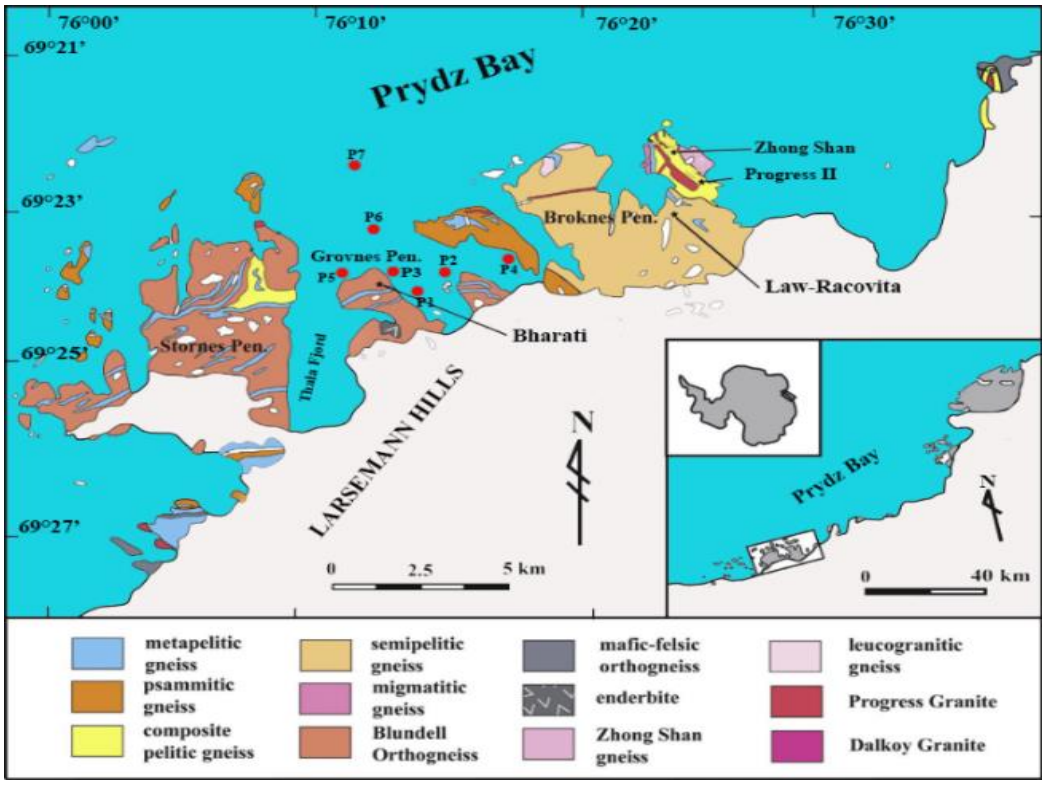

Fig. 2.2. Geological map of the Larsemann Hills, Prydz Bay, East Antarctica showing the locations of the surface samples (modified after Tong et al., 2017).

2.2b Sediment cores

In order to achieve the objectives of the present study, four sediment cores from the lakes around Ny-Alesund region and one core from the mouth of Kongsfjord, Arctic have been collected. The cores from lakes were retrieved manually from near the periphery of the lake when the lakes were ice-free and from the Kongsfjord region the core was collected with the help of a multicorer (Fig. 2.3, Table 2.3).

Table 2.3. Details of sediment cores and sampling locations from the Arctic

Cores	Sampling Area	Latitude (°N)	Longitude (°E)	Core length (cm)
Lake near Bayelva river	Ny-Alesund	78° 56 ′ 117"	11° 48 ′ 055"	28
Lake near the coast	Kuadehuken	78° 58 ′ 04.6"	11° 24 ′ 42.1"	34
1 Km away from the coast	Kuadehuken	78° 58 ′ 11.2"	11° 26 ′ 53.2"	18
2 km away from the coast	Kuadehuken	78° 57 ′ 26.37"	11° 27 ′ 16"	20
Mouth of the Krosssfjorden	Krosssfjorden	79° 2 ′ 46"	11° 20 ′ 34"	24


a
79°2.46'N, 11°20.3'E


b
K-1
78°58.11'N, 11°26.5'E
78°58.04'N, 11°24.4'E
78°57.28'N, 11°28.14'E

Fig. 2.3. Locations of the cores collected from the fjord and different lakes of Svalbard

From the Antarctic region, three sediment cores from Larsemann Hills during 34th Indian scientific expedition to Antarctica (ISEA), February, 2015 (Fig 2.4, Table 2.4), and three sediment cores from Schirmacher Oasis during the 31st Indian Scientific Expedition to Antarctica (ISEA), January 2012 (Fig. 2.5, Table 2.4) were retrieved manually from near the periphery of the lake (Fig. 2.6) when the lakes were ice-free.

Table 2.4. Details of sediment cores and sampling locations from East Antarctica

Sample name	Sampling Area	Latitude (°S)	Longitude (°E)	Core length (cm)
GL-1	Schirmacher Oasis	70° 46 ′ 07.2"	11° 44 ′ 04"	40
V-1	Schirmacher Oasis	70° 47 ′ 27 "	11° 37′ 46.6"	32
L-6	Schirmacher Oasis	70° 45 ′ 16.6"	11° 36 ′ 03"	58
L-8	Larsemann Hills	69° 24′ 58.00"	76° 12′ 53.00"	32
L-10	Larsemann Hills	69° 25′ 17.80"	76° 11′ 34.20"	30
L-12	Larsemann Hills	69° 25′ 24.24"	76° 11′ 47.40"	30

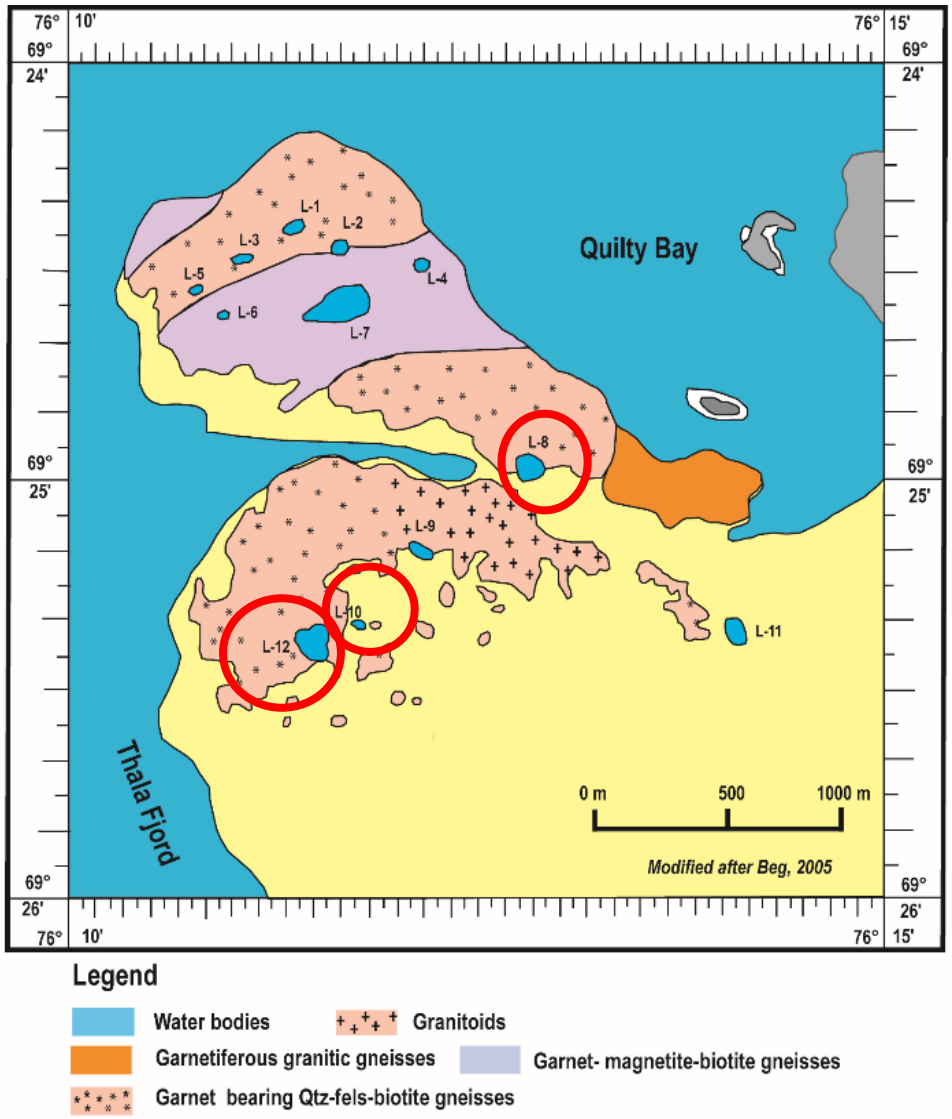

Fig. 2.4. Map of Larsemann Hills, East Antarctica (modified after Beg, 2005) showing the sampling locations in the study area

Fig. 2.5. Field photographs showing the location of cores a) L-8 b) L-10 c) L-12 from Larsemann Hills, East Antarctica

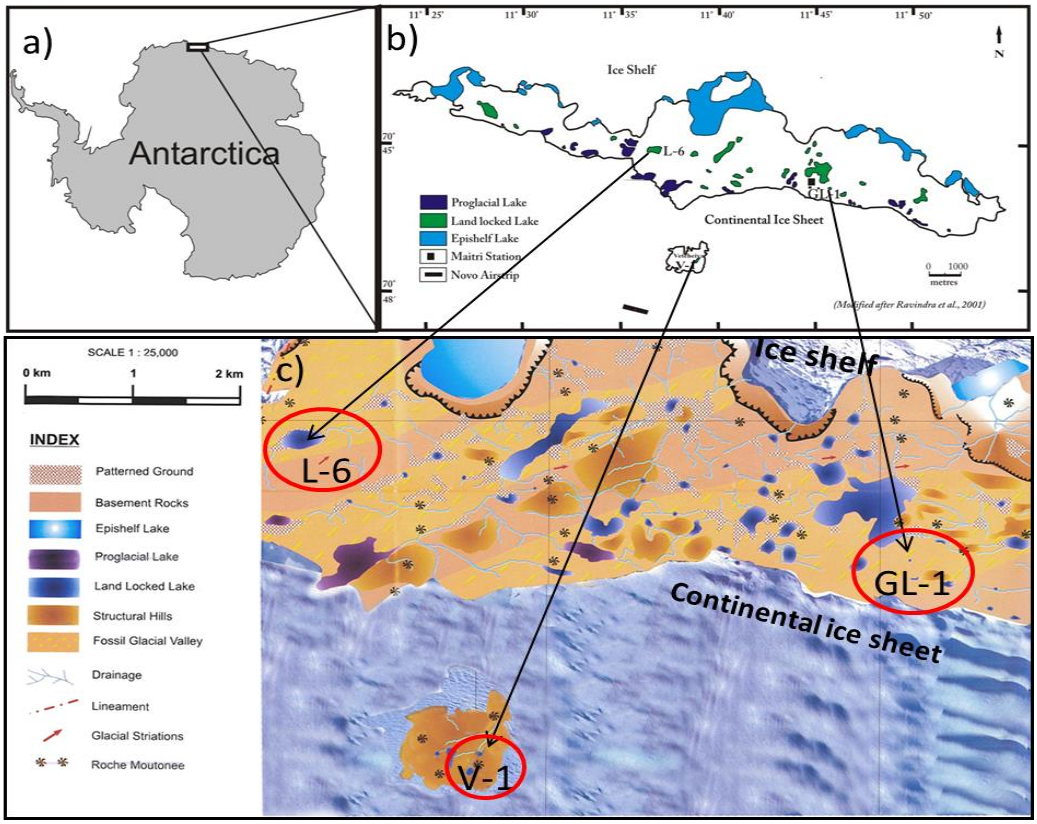

Fig.2.6. a) Map of Antarctica showing the location of Schirmacher Oasis b) Map of Schirmacher Oasis (modified after Ravindra et al., 2001) showing the sampling locations in the study area and c) Geomorphological map (modified after Geological survey of India, 2006)

2.2.1 Sediment sub-sampling

Fig. 2.7. Photograph showing sediment core collection

To collect a sediment core, a PVC handheld corer was inserted by hammering manually into the lake sediment bed and then retrieved (Fig. 2.7). Further, the cores were labeled, packed and stored in a deep freeze at <4°C. The cores were transported to the laboratory. In the laboratory, cores were subsampled at 2 cm interval with the help of a plastic knife and later on dried at 60° C. For grain size and clay mineral analysis, a small portion of the bulk sediment was utilized while remaining portion was ground in an agate mortar and pestle to a fine powder and used for analysing Biogenic Silica (BSi), Calcium carbonate ($CaCO_3$), Total Organic Carbon (TOC), Total Nitrogen (TN), Total Phosphorus (TP), major and trace metals viz. Al, Fe, Ti, Mn, Cr, Co, Zn, Pb, Ni, Cd and Ba and estimation of Be concentration .

A synoptic view of the methodology used in the study carried out is described with the help of flowchart in figure 2.8.

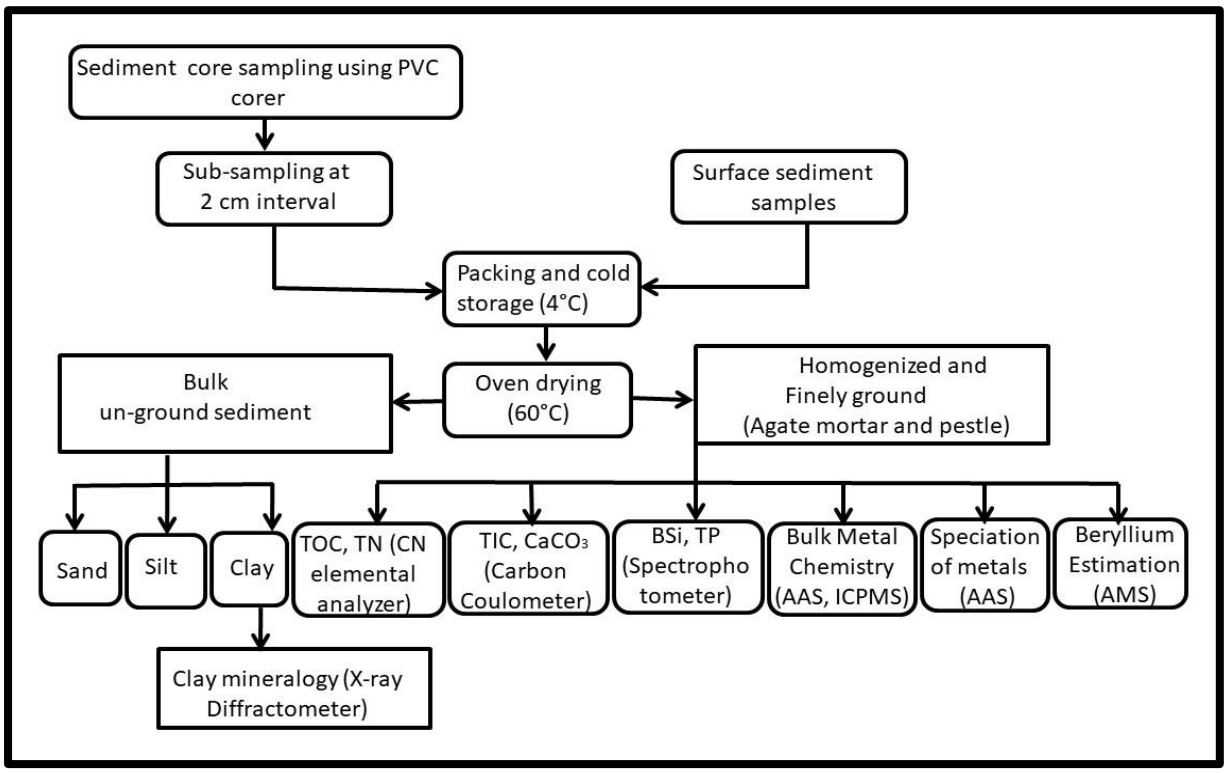

Fig. 2.8. Flowchart showing the methodology followed for the processing of sediment samples and their analysis

2.3 Laboratory analysis

2.3.1 Grain size

Sediment components (sand: silt: clay) of the subsamples were analyzed by the pipette method (Folk, 1974). The particles of sand, silt and clay fractions ranges in diameter from 2000 to 62.5 µm, 62.5 to 39.1 µm and <39.1 µm respectively. Around 10 g of oven dried (60°C) subsample was transferred to a 1000 ml beaker with distilled water. After stirring properly, sediments were left undisturbed to settle overnight. The water was decanted after 24 hours using decantation pipe, and distilled water was filled again. This step was followed repeatedly until the salinity from the sediments is removed entirely which was tested using a silver nitrate (Conc. $AgNO_3$) solution. The removal of salinity is essential as the presence of salts allows faster settling of sediment particles thereby affecting the results of analysis. After last decantation, 10 ml of 10 % sodium hexametaphosphate (Calgon solution) was added to dissociate clay particles. Most clay particles have unbalanced electrostatic charges that cause the clay particles to aggregate or flocculate in suspensions, therefore, the dispersant is added to prevent flocculation. Next day, to break and oxidize the organic matter, 5 ml of 30% hydrogen peroxide (H_2O_2) was added. The chemically treated sample was then wet sieved using 63-micron (230 mesh) sieve to separate the sand and mud (silt-clay) fractions and the filtrate was collected in 1000 ml cylinder. The sand fraction over the sieve was collected in a pre-weighed (100 ml) beaker and dried in an oven. The filtrate collected in the cylinder was used for pipette analysis. It was homogenized by using stirrer and left undisturbed to settle for a specific time period at specific room temperature. The time interval was taken corresponding to size 8Ø for pipetting out the sediments from the cylinder and the stirring time was noted (Table 2.5).

Table 2.5. Time schedule with respect to the room temperature used for pipette analysis

Size Ø	Depth up to which pipette has to be inserted (cm)	Time interval after which suspension has to be pipetted out (Hours: Minutes: seconds)				
		28°C	29°C	30°C	31°C	32°C
4	20	00:00:48	00:00:46	00:00:46	00:00:44	00:00:44
5	10	00:01:36	00:01:34	00:01:32	00:01:29	00:01:28
6	10	00:06:25	00:06:15	00:06:06	00:06:57	00:05:52
7	10	00:25:40	00:25:02	00:24:25	00:24:29	00:23:27
8	10	01:42:45	01:40:13	01:37:42	01:37:15	01:33:51
9	10	06:30:00	06:40:40	06:32:50	06:32:10	06:11:30
10	10	27:06:00	26:30:00	-	-	-

A 25 ml of suspension was pipetted out from the measuring cylinder at 10 cm depth with the help of pipette. Further, the solution pipetted was poured into pre-weighed beaker and dried in an oven (60°C) completely. The oven dried beakers consisting of sand and clay were weighed and sand, silt and clay percentage was calculated using the given formulae:

$$Sand\ \% = \left(\frac{weight\ of\ sandfraction}{Weight\ of\ sediment\ taken\ for\ analysis}\right) * 100$$

$$Clay\ \% = \left(\left(\frac{weight\ of\ Clay}{25} * 1000\right) - 1\right) = x$$

$$= \frac{x * 100}{Weight\ of\ sediment}$$

$$Silt\ \% = 100 - (sand\ \% + Clay\ \%)$$

2.3.2 Clay minerals

Clay minerals were analyzed using the methodology proposed by Rao and Rao (1995). The procedure for separation of clay fraction from the bulk sediment is the same as that used for pipette analysis. The suspension of clay was pipetted out at

depth of 10 cm to 500 ml beaker at size 9Ø from the cylinder containing the suspension of mud. To this suspension, 5 ml of hydrogen peroxide (30%) and 5 ml of glacial acetic acid was added for the elimination of organic matter and carbonates. After stirring well, the solution was left undisturbed and allowed to settle overnight. On the following day, after settling of the clay, the clear water was decanted and distilled water was filled again. Similar step was followed till the odour of glacial acetic acid persisted and clay was free from the excessive reagents. Once the clay suspension was ready, 1 ml of the concentrated clay suspension was pipetted out and spread uniformly across the pre-numbered glass slide to avoid size sorting. The slides were then left undisturbed and air dried for 24 hours. To protect from dust and moisture, slides were preserved in a box until further analysis. The slides were then processed for analysis by X-ray diffractometer exposing them to ethylene glycol vapours at 60°C for 24 hours in a glass desiccator.

Later, the slides were scanned between 3° to 30° 2θ on X-Ray diffractometer (Rigaku Altima IV apparatus) at 1.2°2θ/min with nickel-filtered CuKα radiation at CSIR-National Institute of Oceanography (NIO), Goa. The clay minerals were then identified and quantified by measuring the areas of first order reflections above the baseline from the glycolated X-ray diffractograms (Biscaye, 1965). The width (Δ2θ) of the diffraction peak of illite at half the peak height is known as crystallinity (Biscaye, 1965). The ratio of the area of 5 and 10 A° peak of illite is used for the estimation of illite chemistry (Esquevin, 1969). Different classes of clay mineral crystallinities and the illite crystallinities are available on the basis of width of the diffraction peak (Bejugam and Nayak, 2017).

2.3.3 Total carbon (TC), Total nitrogen (TN), Total inorganic carbon (TIC) and Total organic carbon (TOC)

A small quantity of the total sediment sample was ground finely in an agate pestle and mortar for estimation of the total carbon and total nitrogen concentration which was determined using an Elemental Analyser (Elementar, Vario Isotope Cube) at the Marine Stable Isotope Lab (MASTIL) of *National Centre for Antarctic & Ocean Research*, Goa, India. Around <10 mg of the ground sediment sample was packed in

a tin cup which was pre-weighed. The tin cup containing the sample in it was shaped to little round ball as the shape is relevant for a good 'Flash Combustion'. The tin cup was then dropped in a tube where in the presence of external oxygen, flash combustion occurs at a temperature of 1800° C. The gaseous combustion products N_2, NO_x, O_2 and CO_2 are carried by the helium as carrier gas through a column filled with copper oxide and from there to a Cu-column where nitrogen oxides are reduced to elementary nitrogen, and O_2 to CuO. Water was absorbed in another column and the remaining gases are introduced into a TPD (Temperature Programmed Desorption) column where N_2 is passing through it and the other gases are bound to the column. Further, with a programmed temperature rise in the column, the gases are released separately. They flow along a thermal conductivity detector (TCD) which produces an electrical signal proportional to the concentration of nitrogen and carbon. This whole process takes about 5-8 minutes for every single sample.

A UIC carbon coulometer (model no. 5015, UIC Inc., USA) was used to measure Total inorganic carbon (TIC). The total mass of Carbon di oxide emitted from acidification was measured by the coulometer based on the concept of Faraday's law.

Into the sample flask, around 10 mg of ground sediment sample was taken. Then, the CO_2-free carrier gas was introduced in the system to eliminate atmospheric carbon dioxide. Further, a small amount of acid into the sample flask was added through the acid dispenser and the analysis is initiated resulting in the release of CO_2 as inorganic carbon. The inorganic carbon is removed by the magnetic stirrer and built-in heater. Within the coulometer, reaction products are shifted to the reaction cell by the CO_2-free carrier gas and the CO_2 released at the end is measured precisely. Recovery obtained by running Magnesium carbonate ($MgCO_3$) as a standard after every ten sediment samples was 96 %.

The analytical precision for TN and TC is ±0.31 % and ±0.30 % (1σ standard deviation) obtained by repeatedly running Sulfanilamide as the standard. TIC was subtracted from TC to obtain TOC values. Calcium carbonate was calculated by multiplying a factor of 8.33 (estimated from the atomic masses of Ca, C and O) with TIC values.

2.3.4 Total Phosphorus

For total phosphorus analysis, a sediment sample was digested using a concentrated solution of HF-HNO_3-$HClO_4$ in a ratio of 7:3:1 according to the methodology followed by Yu et al. (2013). Further, in the digested sample the phosphorus concentration was analysed using the methodology provided by Murphy and Riley (1962), in which at a wavelength 880 nm phosphomolybdenum blue complex intensity was measured on visible spectrophotometer (UV-1800-Shimadzu). The reagents used for phosphorus analysis were prepared a fresh and the procedure is given below:

To the 75 ml distilled water, 25 ml H_2SO_4 (concentrated) was added slowly and carefully, to prepare 9 N H_2SO_4 solution. 7 g of ascorbic acid powder was added to 100 ml distilled water to prepare Ascorbic acid solution. 9.5 g of ammonium heptamolybdate tetrahydrate $(NH_4)_6Mo_7O_{24}$ was dissolved in 100 ml of distilled water and 3.25 g of potassium antimony tartrate was dissolved in 100 ml of distilled water to prepare Ammonium molybdate solution. By mixing 100 ml 9N H_2SO_4, 2.5 ml potassium antimony tartrate solution and 22.5 ml of ammonium molybdate solution together, a mixed reagent was prepared.

After the preparation of all the reagents required, 5 ml of the digested sediment sample was taken in a 50 ml graduated tube and made up to 50 ml with distilled water. To this solution, 1 ml ascorbic acid followed by 1 ml of mixed reagent (ammonium molybdate solution + H_2SO_4 + Potassium antimony tartrate) was added and after the addition of each reagent the solution was agitated properly. After 30 minutes, the sample solution was taken in a cuvette of 1 cm and the blue colour intensity was measured at 880 nm in the spectrophotometer against a reagent blank. A calibration curve was constructed with phosphate stock solution which is prepared using standard potassium dihydrogen phosphate known as the working solution A. The phosphorus concentration was determined from this calibration curve. To test the accuracy for phosphorus analysis, along with the samples a digested sample of certified standard JLK-1 was run and recovery obtained was 98%.

2.3.5 Biogenic silica (BSi)

Biogenic silica concentration in the sediment was measured by the wet alkaline extraction method, modified by Mortlock and Froelich (1989) and Muller and Schneider (1993) where the blue silicon-molybdenum complex intensity was measured using visible spectrophotometer (UV-1800 Shimadzu) at 810 nm. The reagents used for the determination of biogenic silica were prepared using the following procedures:

The sulphuric acid solution was prepared by adding slowly and continuously while stirring 250 ml concentrated sulphuric acid to 750 ml Milli-Q water. 38 g ammonium heptamolybdate tetrahydrate $(NH_4)_6Mo_7O_{24}$ was dissolved in 300 ml of Milli-Q water and this solution was added to 300 ml sulphuric acid solution to prepare ammonium molybdate solution. 10 g of oxalic acid was dissolved in 100 ml Milli-Q water. 2.8 g of ascorbic acid powder was added to 100 ml Milli-Q water to prepare an ascorbic acid solution.

After the preparation of all the reagents required, 0.2 g of the sediment sample was weighed accurately and transferred to a 50 ml polypropylene centrifuge tube with 25 ml of 1% Sodium Carbonate (Na_2CO_3) solution as the alkaline treatment (Na_2CO_3) has a high BSi extraction efficiency (Liu et al., 2014). The sample was then placed in a preheated water bath at 85°C for five hours along with the blank to extract the biogenic silica from the sediment. Then, the sample was centrifuged to remove the suspended matter and 1 ml of supernatant was removed in 100 ml volumetric flask containing 35 ml of Milli-Q water. To this solution, 4 drops of 1:100 HCl was added to bring the pH 7-8 i.e. close to the pH of sea water. Subsequently, 1 ml of mixed reagent was added and kept for half an hour for the formation of the yellow silicomolybdate complex. 1 ml of oxalic acid was added to the solution immediately (to decompose silicomolybdate complex) followed by 1 ml of ascorbic acid which reduces the acid complex to a blue coloured complex. Then, the solution was allowed to cool at room temperature for the reaction to complete and the whole content was made up to 100 ml using Milli-Q water. After a wait of 30 minutes, the sample solution was taken in cuvette of 1 cm and against a reagent blank at a wavelength of 810 nm the blue colour intensity was measured using the spectrophotometer. Using a

standard Sodium Hexafluorosilicate, stock solution was prepared known as working solution which is utilised for the preparation of calibration curve. The biogenic silica concentration was estimated from this calibration curve. Duplicate measurements were conducted on each sample and relative error was noted to be less than 3%.

2.3.6 Bulk metal analysis in sediments

For estimating the total/bulk concentration of elements the finely ground sediment sample was digested using the total decomposition method proposed by Jarvis and Jarvis (1985). 0.2 g of homogenised sediment sample was weighed and put in Teflon beakers which were pre- cleaned acid washed and dried. 10 ml of HF–$HClO_4$–HNO_3 acid mixture was added to this in 7:3:1 ratio slowly. The solution was heated on a hot plate at 150° C and dried completely. Again, after it gets completely dried, 5 ml of this acid mixture was added and heated on the hot plate for an hour until complete dryness. Further, 2 ml of HCl (concentrated) was added until it dries completely. The final residue was dissolved in 10 ml of 1:1 HNO_3 and heated for 15 min. The digestion steps were repeated if any particle persisted in the solution until a clear solution was obtained. Then, the clear solution was removed into 50 ml acid washed volumetric flask and diluted with distilled water up to the indicated level. This solution was transferred to pre-cleaned 50 ml polypropylene plastic bottle for further analysis and preserved in a cool and dark place. The digested sediment sample was then analysed using an Atomic Absorption Spectrophotometer (AAS). Sediment standard reference JLK-1 obtained from Geological Survey of Japan was digested following the similar procedure.

2.3.7 Speciation/ fractionation of metals

The sequential extraction protocol modified after Tessier et al. (1979) was adopted for the fractionation of metals in five geochemical phases: F1- Exchangeable, F2- Carbonate, F3-Fe-Mn oxide (Reducible), F4-organic matter/ sulfide bound (oxidizable) and F5-Residual. Fractionation of metals in sediments provide an understanding of source of metals, depositional processes, occurrence, mobility and availability of metals for uptake of biota (potential bioavailability).

(a) Exchangeable fraction (F1): 1g of powdered sediment sample was weighed and transferred into 50 ml centrifuge tubes. To this, 8 ml of magnesium chloride solution (1M, $MgCl_2$, pH 7) was added at room temperature with frequent agitation for 1hr. This solution was then centrifuged for 10 minutes at 8000 rpm and the supernatant was collected in polypropylene bottles for metal analysis.

(b) Carbonate fraction (F2): Metals in the residue from the first fraction were leached with 8 ml of 1M Sodium Acetate (NaOAc) (pH 5 adjusted with acetic acid) and then agitated continuously on an orbital shaker for 5 hours at ambient temperature. The suspension was then centrifuged for 10 minutes at 8000 rpm and the supernatant was removed and collected for analysis of metals. Then, the residue was washed with Milli-Q water.

(c) Fe-Mn oxide fraction (F3): Metals in the residue from second fraction were leached with 20 ml of 0.04 M Hydroxylamine hydrochloride in 25 % (v/v) acetic acid at 96 ±3°C with occasional agitation for 5 hours. The suspension was then centrifuged for 10 minutes at 8000 rpm and the supernatant was collected for metal analysis. The residue was then washed with Milli-Q water.

(d) Organic matter/ Sulfide fraction (F4): Metals in the residue from third fraction were leached by adding 3 ml of 0.02 M HNO_3 and 5 ml of 30% H_2O_2 (pH 2 adjusted with HNO_3) were added and the mixture was heated in water bath at 85±2°C for 2 hours with occasional agitation. Again, 3 ml of 30% H_2O_2 (adjusted to pH 2 with HNO_3) was added and heated to 65±2°C for 3 hours with intermittent agitation. Then, after cooling, 5 ml of 3.2 M ammonium acetate (NH_4OAc) in 20% (v/v) HNO_3, was added and the sample was diluted up to 20 ml and shaken well for 30 minutes continuously. The ammonium acetate was added to avoid adsorption of metals extracted on to the oxidized sediment. The suspension was then centrifuged for 10 minutes at 8000 rpm and the supernatant was collected in pre-cleaned polypropylene bottles for analysis of metals. The residue was washed with Mill-Q water.

(e) Residual phase (F5): In the residual fraction, metals are resistant as they are bound to primary and secondary minerals in the crystal lattice with the silicate matrix. Therefore, strong acids, such as HF, $HClO_4$, HCl and HNO_3 are used for

their digestion. The residue from fourth fraction was transferred into the Teflon beakers from the centrifuge tubes and dried at 60°C in an oven. After drying, the residue was digested using acid mixture HF-HNO_3-$HClO_4$ following the procedure used for bulk metal analysis.

The extracts derived from these five fractions are used for analysis of metals. The first two fractions are known as the labile fractions and the first four fractions together are known as the bioavailable fractions.

2.3.8 Atomic Absorption Spectrophotometry

The digested bulk sediment and sediment fractions were analysed using atomic absorption spectrophotometer (Thermo Scientific-SOLAAR M6 AAS model). The metals Fe, Mn, Al, Co, Cu and Zn were analysed using flame atomic absorption spectrophotometer and Cd, Pb and Cr using graphite furnace atomic absorption spectrophotometer. An air/ acetylene flame was used for Fe, Mn, Zn, Cr, Co, Cu, Pb and nitrous oxide-acetylene flame was utilized for Al at specific wavelengths. Ba and Ti were analysed using an Agilent 7700x Inductively coupled plasma Mass Spectrometry (ICP-MS). Together with the samples, certified reference standard JLK-1 from the Geological Survey of Japan was analysed and to determine the analytical accuracy of the method. The average recoveries were 94% for Ba and Ti, 95 % for Mn and Co, 96% for Fe, Cu, Ni, and Al, and 99% for Zn and Pb. Internal chemical standards obtained from Merck were used to calibrate the instrument and recalibration checks were performed at regular intervals.

In the Atomic Absorption Spectrophotometer, the digested sample which has to be analysed for metal concentration after atomisation gets mixed with fuel-gas air mixture. At a specific controlled rate, it is introduced into the burner. In the flame AAS, the sample gets disintegrated into the atoms after the solvent evaporates and flame behaves as a conduit for transporting atoms of the elements to be studied. For a particular element being investigated, external source requires a beam of resonance radiation which is provided by respective hollow cathode lamp. This beam after passing from the flame enters the spectrophotometer assembly. The photomultiplier and amplifier measure the entering light and is noted in a scale convenient to the

instrument. Graphite AAS works almost on the similar procedure as that of flame spectrophotometry. Only difference is the flame which is replaced by a closed graphite tube in Graphite AAS. This tube is heated electrically and have transparent windows at the end. A cloud of atoms is formed inside the tube and get exposed to the light from the hollow cathode lamp. Due to the increase in density of atoms and their longer residence time in the tube, results in its lower detection limit.

2.3.9 Beryllium estimation

Sediment sample was chemically processed for Be analysis at Inter University Accelerator Centre (IUAC), New Delhi. Fe-Mn oxide fraction was extracted following the sequential extraction procedure for the speciation of trace metals (Tessier et al., 1979) as this method have been found efficient to extract ^{10}Be (meteoric) as compared to other methods. A portion of each subsample was powdered and homogenized in an agate pestle and mortar. 1 g of sediment sample was taken in a centrifuge tube and treated with 20 ml 0.04 M hydroxylamine hydrochloride ($NH_2OH.HCl$) in 25% (v/v) acetic acid (HOAc) mixture for 6 hrs. at 90ºC, 400 rpm with continuous agitation (Tessier et al.,1979). The supernatant was removed after centrifugation, and dried completely on the hot plate. Then, the dried extract was dissolved in 10 ml of 1N HCl (Non-Calibrated). 1 ml of this solution was removed and kept for ^{9} Be analysis by ICPMS. Remaining 9 ml of solution was spiked with (.2 ml) ^{9}Be carrier solution (NIST SRM-3105a) and dried on the hot plate. Further, the extract was dissolved in 1 ml 6 N HCl and passed through Anion column and the residue was collected in Teflon beakers and dried completely. Further, it was dissolved in 0.2 M H_2SO_4 + 2% H_2O_2 and passed through cation column. This residue was collected and mixed with 5-8 drops of 8 M HNO_3 and dried completely and precipitated with the help of NH_3. The supernatant was removed with the help of centrifugation and precipitate (BeOH) was collected in quartz vials. The quartz vials containing BeOH precipitate were kept in a furnace with step heating up to 900°C to convert precipitate BeOH to BeO. After drying, the BeO powder was loaded to the cathode tube mixed with Nb powder in a ratio of 1:3 and will be analysed for $^{10}Be/^{9}Be$ ratio using an Accelerator Mass Spectrometry (AMS).

In AMS, the ratio between radioisotope and stable isotope was measured and the calibration was done with a known standard sample. For ^{10}Be measurement, 40 cathode MC-SNICS source is being utilised. During the standardization, seven standards (SRM 4325) and six blanks (SRM 3105a) were run after precipitating them as $Be(OH)_2$. Further, these samples are combusted in furnace at 900° C to BeO in AMS chemistry lab at IUAC, Delhi. This BeO powder was mixed with Nb in a ratio of 1:3 and targets are prepared by pressing in NEC copper target holder. Then $^{10}Be^{16}O^-$ (mass 26) and $^{9}Be^{16}O^-$ (mass 25) were injected sequentially into accelerator (Sharma et al., 2019). Analyser magnet was used to select Be^+ ions. Measurement of ^{10}Be was carried out at 550 kV terminal potential and transmission of 70% was obtained for ^{9}Be. $^{9}Be^+$ current measured in off axis faraday cup was 1.6μA. Depending on their atomic number, $^{10}Be^+$ and $^{10}B^+$ ions loses energy when beam passed through 75 nm foil. ~10% of incoming beam lose their electrons and get converted to 2^+. High energy Electrostatic Analyser (HE ESA) and 45° bending magnet was tuned for charge state 2^+. Both of these isobars get separated in detector depending on the difference in energy losses in foil.

2.4 Data Processing

2.4.1Ternary diagram, Isocon diagram and Statistical analysis

To understand the depositional environment and hydrodynamic conditions in which the sediments have been deposited, the data was plotted on a ternary diagram proposed by Shepard (1954) and Pejrup (1988). Isocon diagram (Grant, 1986) was used for comparison of sediment components and metal concentrations between two environments/areas. Pearson's correlation ($p<0.05$), paired sample t-test (two-tailed) and factor analysis were conducted on sediment components and metals to determine the inter-relationship between metals and sediment components to identify possible sources or sinks by using software STATISTICA-9 and Grapher 8, Adobe illustrator 10 along with Microsoft Excel was used in computation to make figures and illustrations.

2.4.2 Lithogenic Vs Biogenic components

The trace elements, after entering into the aquatic environment follow two different paths, some get involves in biological processes and are deposited as faecal matter representing a source of biogenic input and remaining participates through

physicochemical processes and gets deposited in sediments, constituting a lithogenic source.

Based on the crustal composition ([M/Al] $_{crust}$), the proportion of the lithogenic input of trace metal (M $_{lith}$) can be estimated (Tribovillard et al., 2011) as follows:

$$M_{lith} = Al_{sample} * (M/Al)_{crust}$$

Where Al $_{sample}$ and Al $_{crust}$ were the concentration of the element Al in the sample and in the continental crust respectively. Al was used as a normalizer, since; it is a conservative element and has no significant anthropogenic source.

The biogenic trace metal (M $_{bio}$) was obtained by subtracting the metal concentration of the sample from the Lithogenic input.

$$M_{bio} = M - M_{lith}$$

Section 1: Sediment components

3.1.A. Surface sediment samples

Surface sediment samples collected from the Krossfjord-Kongsfjord system, Arctic and the Prydz Bay (Thala Fjord), East Antarctica were studied to understand the source and processes. The study of surface sediment samples helps in understanding of modern sedimentary environments and processes occurring therein and further, provides a geological basis for the reconstruction of past environmental records.

3.1.A.a Krossfjord- Kongsfjord, Arctic

A total of thirteen surface sediment samples were collected from the Krossfjord-Kongsfjord. Sand, silt and clay in the Krossfjord varied in the range from 5.70 to 21.24%, 43.15 to 61.04% and 20.00 to 48.27% respectively, with the average value of 10.46%, 52.95% and 36.59% respectively. Among sediment components silt was predominant. Sand was highest at station Kr-2 due to its close proximity to the D'Arodesbreen glacier, silt showed a decreasing trend from station Kr-5 to Kr-1 except at Kr-2 while clay exhibited an increasing trend from station Kr-5 to Kr-1 except at Kr-2. Along the Kongsfjord, sand, silt and clay varied from 5.66 to 33.78%, 29.69 to 53.35% and 32.27 to 50.67% respectively, with the average value of 18.21%, 42.22% and 39.57% respectively. Silt was dominant amongst the sediment components with considerable clay content. Station Ko-8, Ko-6 and Ko-5 showed a high concentration of sand as compared to the other stations due to their glacial fed and proximal location to the coast while station Ko-7, Ko-3, Ko-2, Ko-1 and Ko-4 showed comparatively lower concentration as they are located away from the glacier. However, station Ko-1 showed higher sand as compared to the station Ko-7, Ko-3 and Ko-2 possibly due to the presence of Ice-rafted debris (IRD). Clay exhibited fluctuating and an overall increasing trend from station Ko-8 to Ko-1. The coarse fraction is higher in Kongsfjord (average 18.21%) as compared to Krossfjord (average 10.46%) as it is largely influenced by the presence of many tidewater glaciers like Kronebreen and Kongsvegen at the head and Conwaybreen and Blomstrandbreen on the northern coast debouching in the Kongsfjord. In the Krossfjord, however, glacial outlets are relatively far from the main channel (Saraswat et al., 2018).

In general, sand in Kongsfjord and silt in Krossfjord showed higher values towards the head (inner part of the fjord) (Fig. 3.1.1) indicating that the coarser grains are

deposited close to the glacier front which corresponds to glacial deposition due to the retreat of glaciers in the study area. This suggested warm conditions in the region due to which coarse-grained particles have been transported to the fjord through physical (glacial) weathering of rocks present in the catchment area. While the finer fractions (clay) are transported by the surface waters to the central and outer part of the fjord (Fig.3.1.1). Overall, sediment grain size showed the dominance of fine-grained sediment (silt and clay) in both the fjords suggesting sediment deposition from suspension mode (Choudhary et al., 2018).

Further, an attempt has been made to infer the hydrodynamic conditions of the depositional environment using sediment components. For this purpose, a ternary diagram (Fig.3.1.2) proposed by Pejrup (1988) was used.

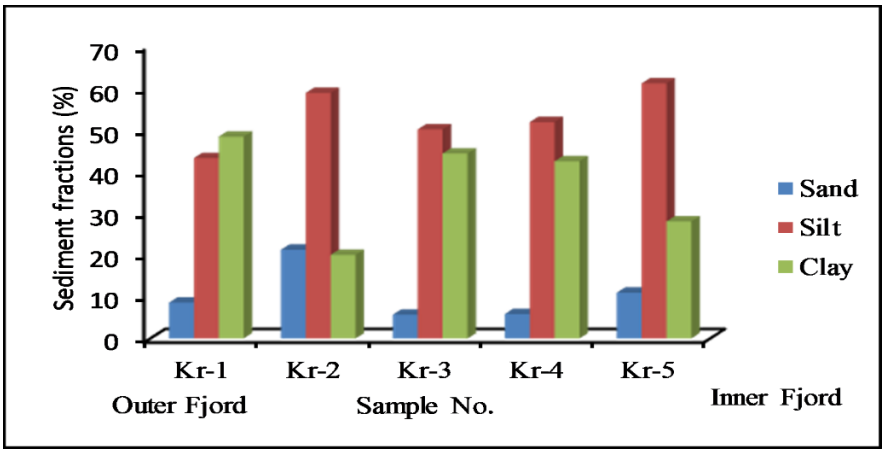

a)

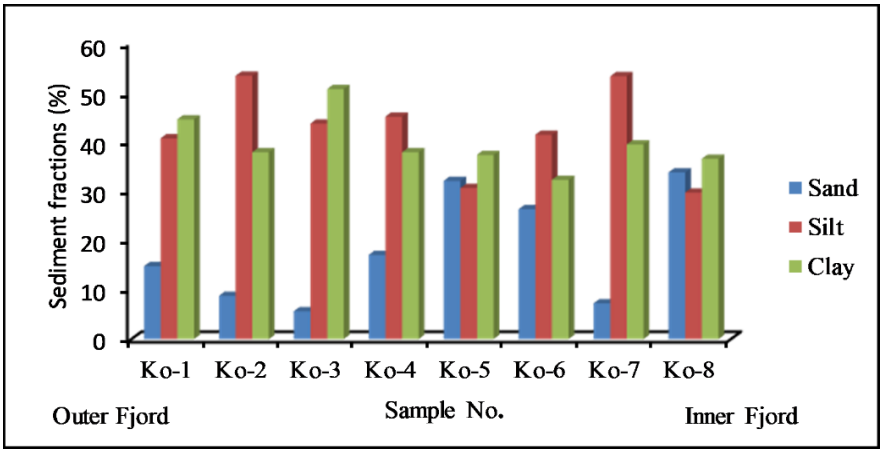

b)

Fig.3.1.1 Distribution of sediment components along (a) Krossfjord and (b) Kongsfjord

When the data was plotted on the hydrodynamic diagram, surface sediments collected from Krossfjord mostly falls between section III(C) and III(D) with a single point being part of II(D) and in the Kongsfjord, all the data points lie between section II(C), II(D), III(C) and III(D) indicating less calm to less violent conditions prevailed facilitating deposition of finer sediments. Therefore, less varying hydrodynamic conditions prevailed in the fjord system was responsible for the deposition of relatively finer grained sediments towards the outer fjord. In addition, factors like glacier outflow and aggregation of fine particles due to the temperature and salinity stratification must have contributed in the distribution of sediments as they ascribe the offshore transportation of fine-grained material (Zaborska et al., 2006).

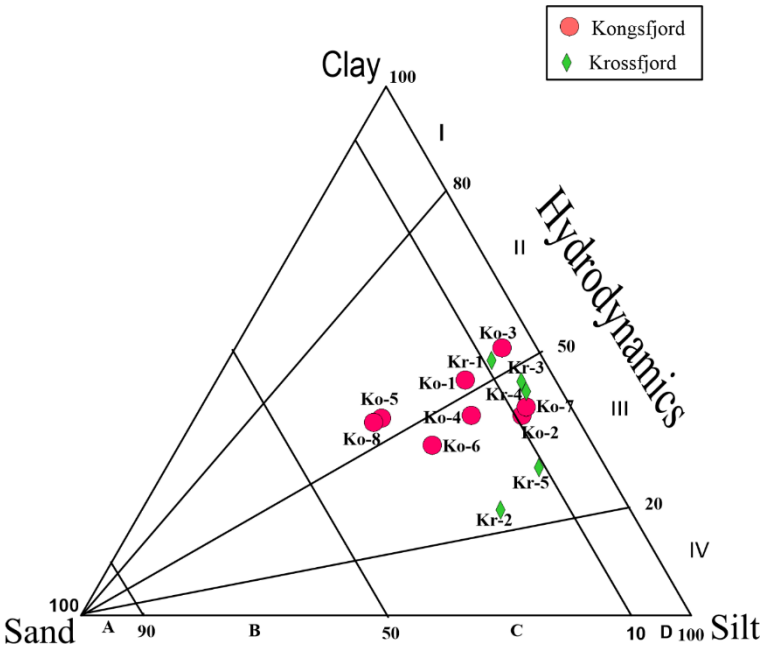

Fig.3.1.2 Triangular diagram for classification of hydrodynamic conditions of Kongsfjord and Krossfjord (after Pejrup, 1988)

3.1.A.b Prydz Bay (Thala Fjord), East Antarctica

The surface sediment samples collected from the Prydz Bay (Thala Fjord) were studied to understand the depositional processes of the area. Sand, silt and clay fraction of the studied samples ranged from 4.64 to 24.58%, 49.88 to 82.16% and 13.20 to 34.80% respectively, with the average of 15.27%, 63.71% and 21.01% respectively. Among the sediment components, silt was predominant. Sand was highest at station P1, silt showed highest values at station P3 and P5 and clay was

highest at station P4. The data on sediment components of surface sediments from Prydz Bay is presented in Fig. 3.1.3. Grain size analysis of surface sediments (P1-P7) has indicated an overall decrease in sediment size with increasing water depth (31-140 m) away from the coast. The sediment components showed the dominance of clayey silt (21.01% clay, 63.71% silt).

Textural analysis has been used to infer the hydrodynamic conditions of the depositional environment. For this purpose, a ternary diagram (Fig. 3.1.4) proposed by Pejrup (1988) has been used. When the data of surface sediments collected from Prydz Bay was plotted, points mostly fell in section III (C), with single point been part of IV (D) indicating less violent to violent conditions prevailed facilitating deposition of sediments. Relatively higher sand content in the shallower areas of the Bay (station P1 and station P2) corresponds to the glaciomarine input that may be due to the combined effect of coastal currents and iceberg scouring. The study area remains covered largely by sea ice and floating ice in winter, with scattered occurrences of icebergs in the Prydz Bay (Passchier et al., 2003). When these icebergs calve from the ice-shelves and outlet-glaciers, they gradually melt and release coarse material debris into the sea. The sediment deposited are redistributed by the coastal currents. Sediment supply to the Prydz Bay is mainly by glacio-fluvial meltwater, however, supply due to intense wind (katabatic winds) that helps in transporting terrigenous material derived from erosion and weathering of the catchment rocks, which gets deposited on ice and percolates through cracks in the ice and get deposited in the Bay (Spaulding et al., 1997) cannot be ruled out. Therefore, the removal of fine-grained material leaving behind the coarser and its subsequent transport into the shallow marine environment also corresponds to the aeolian deposition of sediment in the inshore environment (Franklin, 1997). At shallower depths, high energy environment must have facilitated deposition of coarse grain sediments and its winnowing effects transported the finer fraction of sediments away from the coast. The high energy environment, water depth and topography together play an important role in regulating the sedimentation processes of the area (Wang et al., 2016).

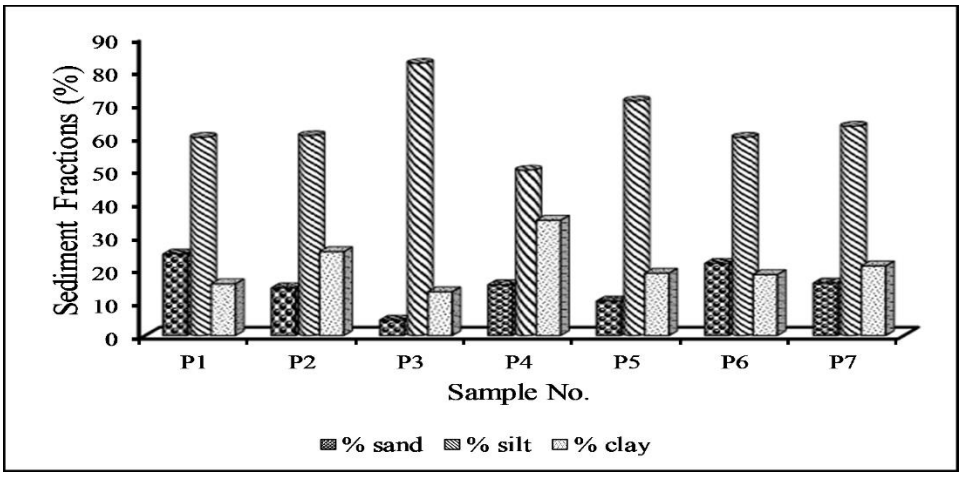

Fig.3.1.3**.** Histogram showing percentage of sediment components along the Prydz Bay

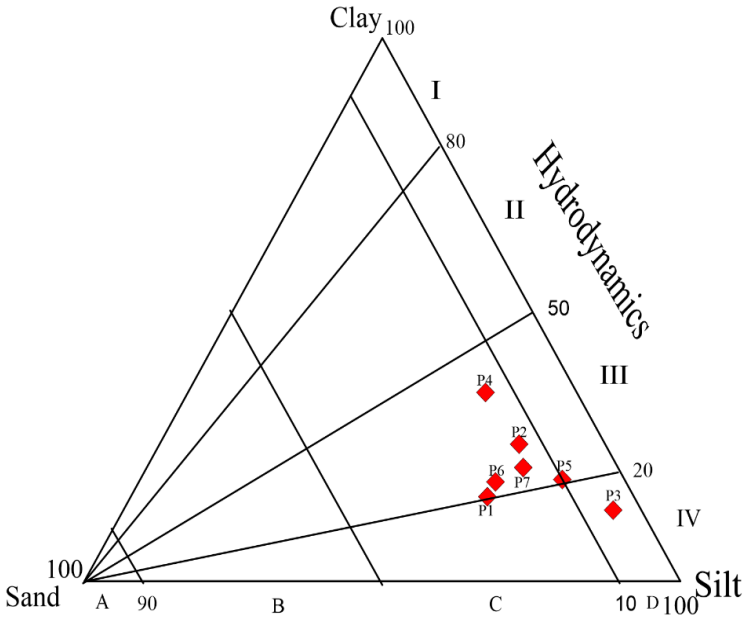

Fig.3.1.4. Triangular diagram for the classification of hydrodynamic conditions of Prydz Bay (after Pejrup, 1988)

3.1.B. Sediment cores

Along with the surface sediment samples, sediment cores were collected from the different lakes of Arctic and Antarctic region. In the modern sedimentary environment, it is known that the sediment column indicates deposition of sediments in a time span and bottom layer indicates the sediment deposited relatively earlier that is older sediments than the surface. Therefore, variation in different sub-samples along the sediment column is used to understand the sedimentary characteristics and depositional processes with depth.

3.1.B.a. Arctic Fjord

A sediment core K-1 was collected to study the depositional processes with time from the mouth of the Krossfjord. The range and average values of the sediment components are presented in Table 3.1.1. The silt and clay concentration was higher with the average values of 54.50% and 42.00% respectively. Sand concentration was found to be lower (average 3.50%) in this core. Depth wise distribution of sediment components is given in Fig.3.1.5.

In the lower portion of the core from 24 cm to 14 cm depth, sand showed lower than the average values with overall decreasing trend while silt showed higher than the average values indicating deposition of fine-grained sediment through suspension mode. In the middle section of the core from 14 cm to 6 cm depth, sand showed higher than the average value which is attributed to the warming conditions in the region leading to the melting of the icebergs. This released coarse-grained material deposited at the bottom of the icebergs (Dowdeswell and Forsberg, 1992) must have transported to the fjord as it is the main mechanism transporting coarse-grained material to the deeper waters (Dowdeswell et al., 1998). Further, in the upper portion from 6 cm to the surface sand showed lower than average values with the increasing trend towards the surface while clay showed higher than the average values with decreasing towards the surface. Higher concentration of clay in the upper portion as compared to the lower sections may be due to the temperature-salinity stratification resulting in aggregation of finer particles and/or due to the hydrodynamic conditions responsible for transportation of fine-grained sediments from offshore as suggested by Zaborska et al. (2006).

When the sediment components were plotted on a ternary diagram (Fig. 3.1.6), it was found that sediments are composed of mainly clayey silt with two points being part of silty clay throughout the core suggesting that sediments from the outer part of the fjord (mouth) showed consistent distribution indicating uniform sedimentation condition in the study area (Zaborska et al., 2006).

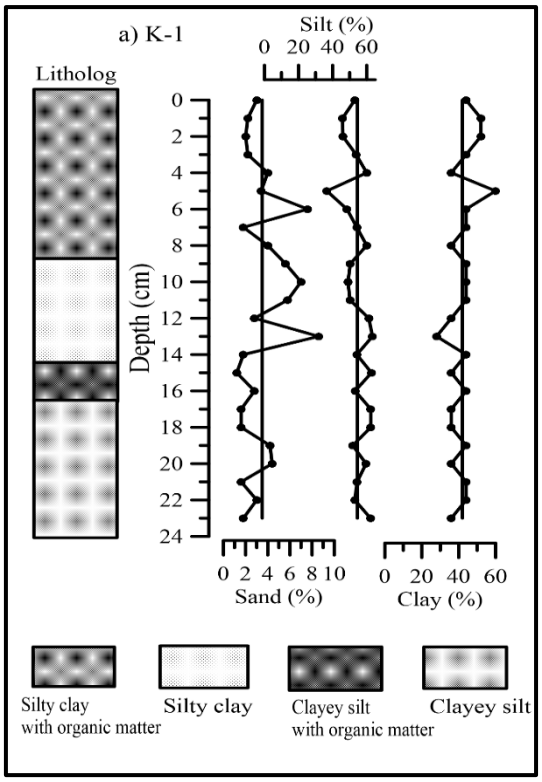

Fig.3.1.5 Depth wise distribution of sediment components of core K-1

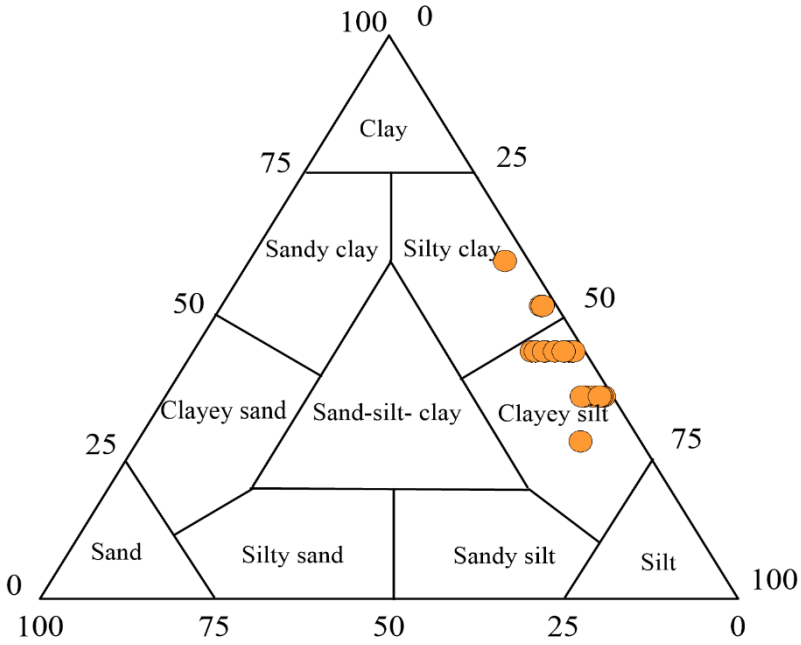

Fig.3.1.6. Ternary diagram (Shepard, 1954) of sand-silt-clay percentages of sediment for core K-1

3.1.B.b. Arctic Lakes

A total of four cores were collected from lake LA from NY-Alesund and lake L-1, L-2 and L-3 from Kuadehuken region of Svalbard. The range and average values of sediment components are presented in Table 3.1.1. The sand was predominant in core L-1 (avg. 57.03%), in core L-3 (avg. 50.42%) and in core LA (avg. 49.94%) as compared to core L-2 (avg. 44.29%). Silt was high in core L-2 (avg. 49.39%) and low in core LA (avg. 17.09%) and clay was high in core LA (avg.32.97%), in core L-3 (avg. 31.47%) and low in core L-2 (avg. 6.32%). Depth-wise distribution of sediment components is provided in Fig. 3.1.7 a, b, c and d.

Table 3.1.1 Range and average values for sediment components of cores from the mouth of Krossfjord and lakes from NY-Alesund and Kuadehuken region

Cores	Sand (%)			Silt (%)			Clay (%)		
	Min	Max	Avg	Min	Max	Avg	Min	Max	Avg
K-1	1.20	8.60	3.50	36.60	63.40	54.50	28.00	60.00	42.00
L-A	23.64	63.64	49.94	5.62	42.92	17.09	8.00	56.00	32.97
L-1	23.34	67.02	57.03	12.58	29.80	19.82	11.20	50.40	23.15
L-2	36.54	57.24	44.29	34.80	61.86	49.39	0.80	20.00	6.32
L-3	38.08	66.90	50.42	6.78	41.52	18.12	14.40	44.00	31.47

The upper portion of all the four cores (Fig.3.1.7) consists of higher than the average values of sand suggesting the dominance of mechanical (glacial) weathering / frost weathering processes (Jiang et al., 2011) releasing coarse-grained material to the lake basin in the recent years. The sand grains exhibited angular to sub-angular and rounded to sub-rounded shape supporting their mechanical origin as also observed by Kar et al. (2018). Along with the glacial activity, aeolian processes must have also played an important role in supplying finer sediments to the lake basin. Due to the warming conditions in the region, glaciers retreated and the area was with less ice allowing intense winds to rework the sediments (Kar et al., 2018). The lower portion of core LA and L-1, lower and middle portion of core L-2 and middle portion of core

L-3 consist of silt higher than the average value which is attributed to the deposition of finer sediments by snowmelt water. All these lakes, as observed in the field are mostly fed by ice meltwater, meltwater from snow drift and precipitation taking place in the area. Lake L-2 is composed of a relatively higher concentration of silt as compared to the sand may be due to the low elevation gradient, flat topography and presence of vegetation in the catchment area of this lake.

When the sediment components are plotted on a ternary diagram (Fig. 3.1.8), it was seen that core LA, L-1 and L-3 is composed of mostly clayey sand along with some silty sand fractions while core L-2 is composed of silty sand and sandy silt suggesting different conditions prevailed during the deposition of sediments at core L-2. The sediments of three cores L-1, L-3 and LA displayed a dominance of sand with less percentage of silt and clay while core L-2 exhibited a high percentage of silt with a low percentage of sand and clay indicating a difference in terrain morphology of this lake.

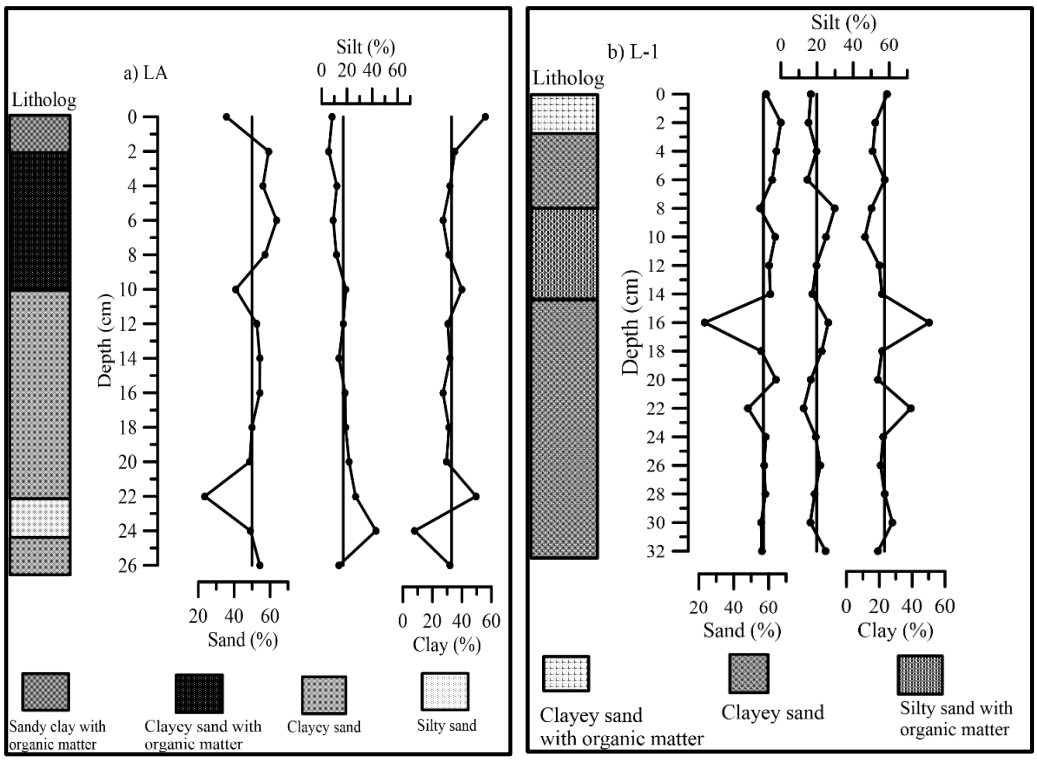

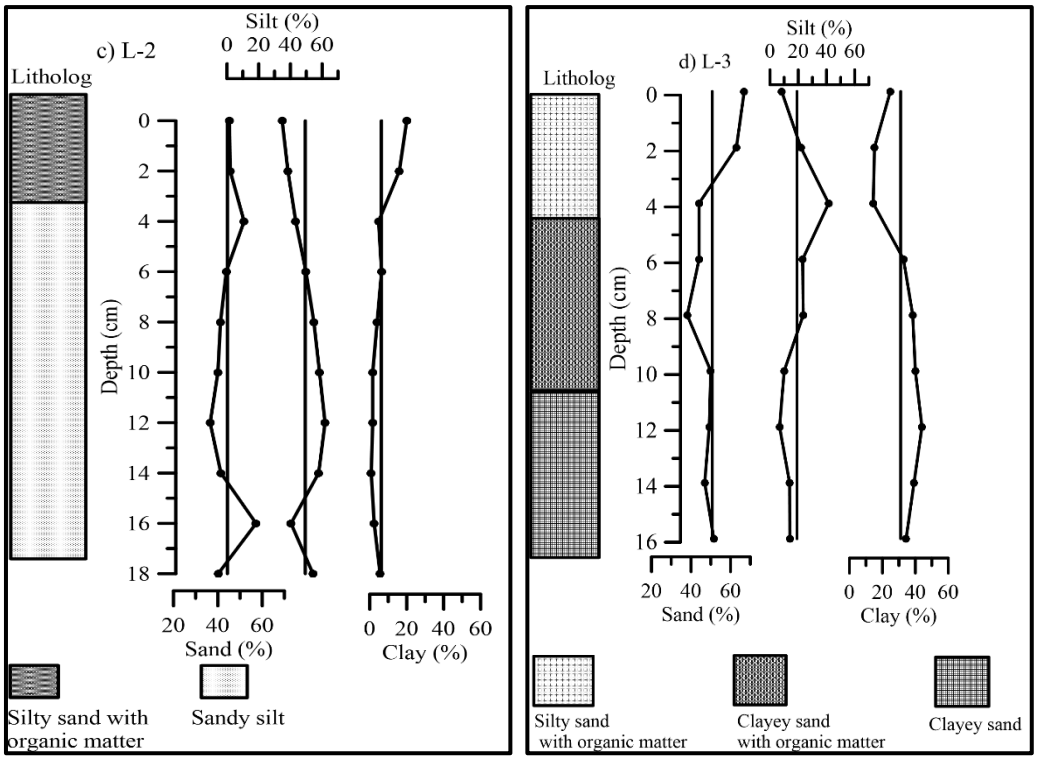

Fig. 3.1.7. Depth wise distribution of sediment components of core a) LA b) L-1 c) L-2 d) L-3.

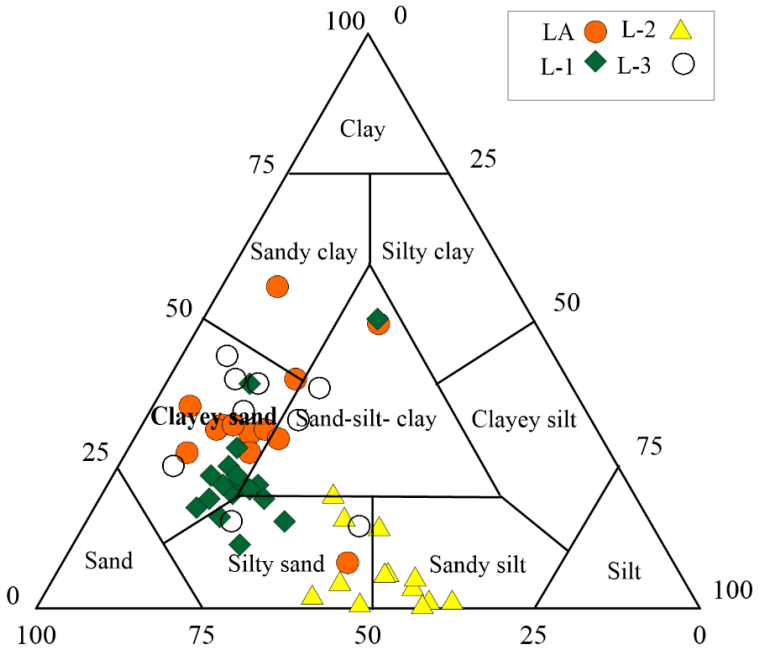

Fig. 3.1.8. Ternary diagram (Shepard, 1954) of sand-silt-clay percentages of sediment for core LA, L-2, L-1 and L-3

3.1.B.c. Antarctic lakes (Larsemann Hills, East Antarctica)

Three sediment cores were collected one each from lake L-8, L-10, and L-12 of Larsemann Hills to study the source and depositional processes with depth. The concentrations of sediment components of the cores are presented in Table 3.1.2. The sand was noted to be higher in core L-10 (avg. 90.41%) and in core L-12 (avg. 72.17%) as compared to core L-8 (avg. 63.77%). Silt was high in core L-8 (avg. 17.90%) and low in core L-10 (avg. 4.52%) and clay was high in core L-8 (avg. 18.33%) and in core L-12 (avg. 18.22%) and low in core L-10 (avg. 5.07%). Depth wise distribution of sediment components is provided in Figs. 3.1.9a, b, and c.

The sediments of core L-10 and core L-12 showed the presence of pebbles and granules along with sand indicating a difference in mode and distance of transportation as compared to lake L-8. The coarse-grained sands with angular to subangular shape must have been released after mechanical weathering. Further, the sediments of all the three cores exhibited more than 60% sand with less percentage of silt and clay which suggested that the physical and mechanical weathering played an important role in releasing coarse-grained particles from the rocks in the catchment area. When the distribution of sediment components is considered with the depth, the lower section from 30 to 22 cm and the upper section around 4 cm in core L-8 (Fig. 3.1.9a) consist of sand higher than the average value which was compensated by silt. In core L-10 (Fig. 3.1.9b), a major section of the core from 26 to 4 cm depth consists of sand higher than the average value (90.41%) due to its smaller catchment area providing a shorter distance of transportation to the sediments resulting in deposition of higher concentration of sand particles in to the lake basin. In the upper section from 4 cm depth to the surface, sand content decreased. Silt compensated sand from the bottom to the surface in this core, while the lower sand peak at 12 cm was compensated by positive clay peak. In core L-12, the middle section from 22 to 10 cm and at 4 cm sand content was noted to be higher than average (Fig. 3.1.9c). Sand was compensated by clay and to some extent silt from bottom to the surface of the core.

In general, in Antarctic lakes, sediment deposition is mostly by glacio-fluvial meltwater delivery of sediments during austral summer (Spaulding et al., 1997) and movement of glaciers which transports rock fragments and soils that are lying underneath them. The lower and upper sections of core L-8, a major section of core L-10, and middle section of core L-12 consist of sand higher than the average value with

a low percentage of silt and clay. Higher sand corresponds to glaciofluvial deposition due to the retreat of glaciers in the study area, suggesting warmer conditions in the region. The coarse-grained particles were transported from the catchment area into the lake basin by glacial meltwater during warmer conditions. Relatively, higher clay from 18 to 10 cm and upper 6 cm in core L-8, around 12 cm and upper 2 cm in core L-10, and 28 to 24 cm and from 10 cm to the surface in core L-12 indicated deposition of fine-grained sediments in the lake due to the supply of ice meltwater. In addition, sediments in these lakes are redistributed over the coring site within the lake due to the processes of freezing and thawing. Hodgson et al. (2001), Verleyen et al. (2004), and Cremer et al. (2007) have reported significant differences in sedimentation rates in several lakes in this region. Available sedimentation rate cannot be adopted for the studied lakes as in general, the rate of sedimentation varies considerably from one lake to the other.

The sediments of lake L-10 are composed of only sand, whereas in lake L-8, sediments are composed of sand along with clayey sand and silty sand while sediments of lake L-12 are composed of sand and clayey sand as seen from the ternary diagram (Shepard, 1954) (Fig. 3.1.10).

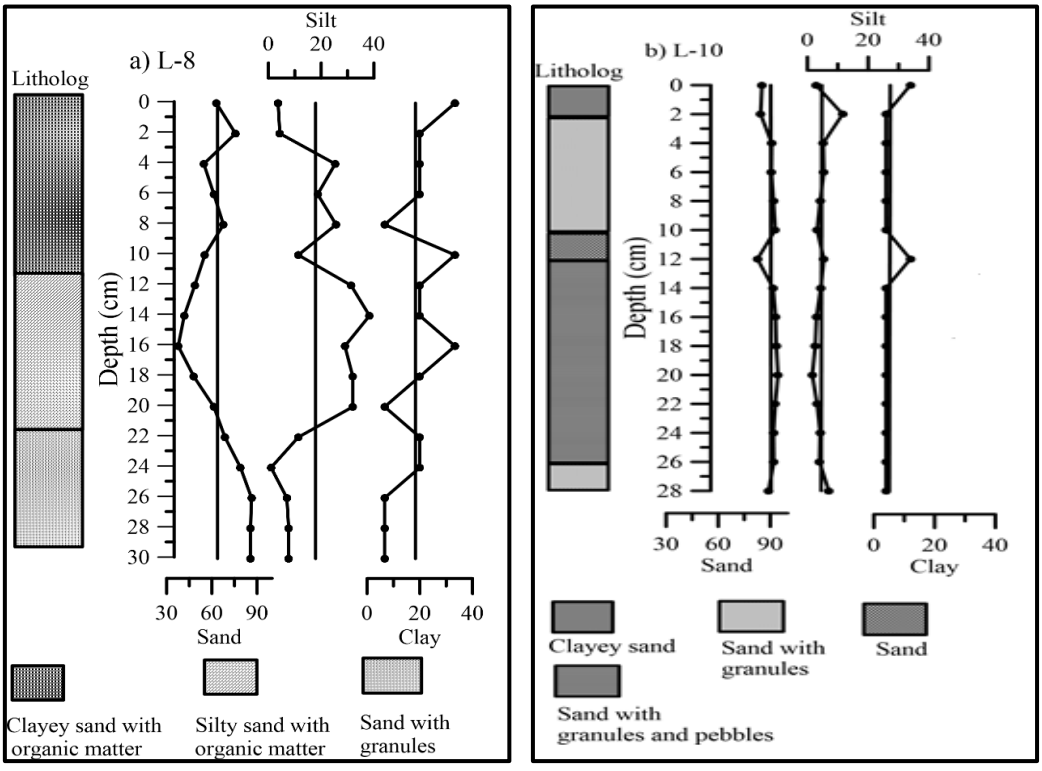

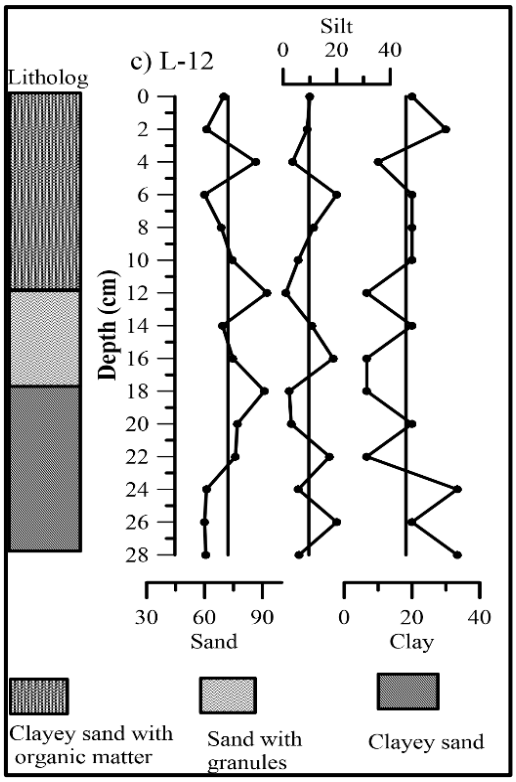

Fig.3.1.9. Depth wise distribution of sediment components of cores a) L-8 b) L-10 and c) L-12

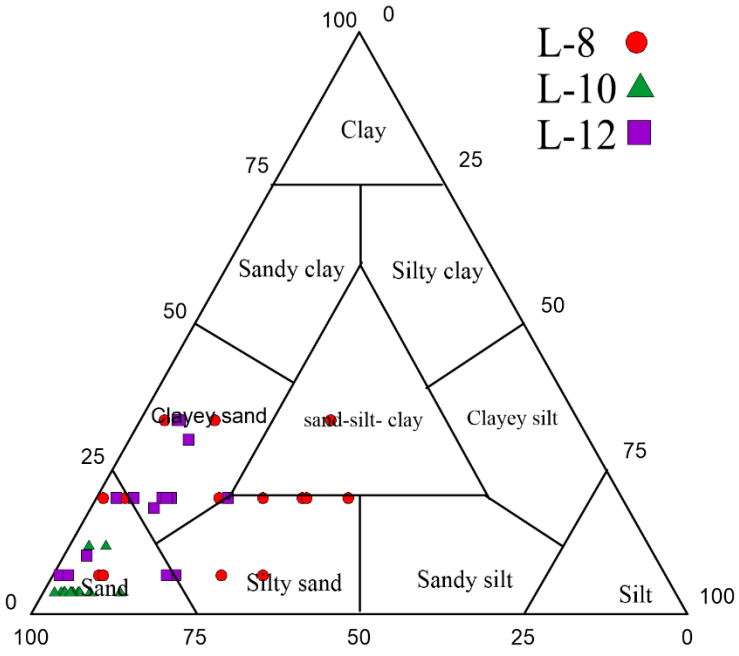

Fig.3.1.10. Ternary diagram (Shepard, 1954) of sand-silt-clay percentages of sediment for cores L-8, L-10 and L-12

Table 3.1.2. Range and average values for sediment components of cores from Larsemann Hills and Schirmacher Oasis, East Antarctica

Cores	Sand (%)			Silt (%)			Clay (%)		
	Min	Max	Avg	Min	Max	Avg	Min	Max	Avg
L-8	37.67	86.33	63.77	1.00	38.33	17.90	6.67	33.33	18.33
L-10	82.60	94.40	90.41	1.60	11.60	4.52	4.00	12.00	5.07
L-12	60.00	92.33	72.17	1.00	20.00	9.61	6.67	33.33	18.22
GL-1	62.50	95.80	80.87	0.20	18.60	7.46	4.00	30.00	11.67
V-1	62.00	90.00	80.48	2.00	26.00	10.03	2.40	20.00	9.50
L-6	32.51	53.32	42.02	4.72	23.16	17.21	29.27	53.20	40.76

3.1.B.d. Antarctic lakes (Schirmacher Oasis, East Antarctica)

Further, three sediment cores were collected one each from lake GL-1, V-1 and L-6 from Schirmacher Oasis. The range and average values of sediment components are presented in Table 3.1.2. The sand was predominant in core GL-1 (avg. 80.87%) and in core V-1 (avg. 80.48%) as compared to core L-6 (avg. 42.02%). Silt was high in core L-6 (avg.17.21%) and low in core GL-1 (avg.7.46%) and clay was high in core L-6 (avg.40.76%) and low in core V-1 (avg. 9.50%). Depth-wise distribution of sediment components is provided in Fig. 3.1.11 a, b, c.

The high average percentage of sand in bottom and top sections of core GL-1, major portion of core V-1 and middle section of core L-6 (Fig. 3.1.11a, b, c) indicated deposition of sediments associated with fluvio-glacial input (Govil et al., 2011) suggesting warmer conditions in the region due to which coarse-grained particles are transported from the catchment area into the lake-basin by glacial melt water as also reported by Tatur et al. (2004) and Yoon et al. (2006). In addition to this, Doran et al. (2002) suggested that Katabatic winds which can move sediments up to sand size must have also contributed to the deposition of coarse-grained particles to the lake. Therefore, sediment supply to the Antarctic lakes is mainly by glacio-fluvial melt water and intense wind (Katabatic winds) that helps in transporting coarse particles,

which gets deposited on lake-ice and percolates through cracks in the lake-ice and get deposited on the lake-floor (Spaulding et al., 1997). While, higher clay from 20 cm to 12 cm and upper 4 cm in core GL-1, from 8 cm to the surface in core V-1 and the bottom section of core L-6 from 56 cm to 36 cm indicated the influx of finer material to the lakes by ice melt water suggesting lower melting in the region. In core L-6, relatively lower sand compensated by higher clay suggested a difference in terrain morphology as compared to other lakes as observed from the larger catchment area and low elevation gradient. In core GL-1 and V-1, larger input of coarser material was probably due to short transportation processes and smaller surface area.

When the sediment components namely sand, silt and clay were plotted on a ternary diagram (Fig. 3.1.12), three cores showed different classes of sediment indicating different conditions of deposition of sediments. The sediments of all the three cores displayed a dominance of sand with less percentage of silt and clay, which indicated that the intensity of mechanical weathering dominated the area releasing coarse-grained material from the rocks in the catchment area (Reynolds and King, 1995; Santos et al., 2007).

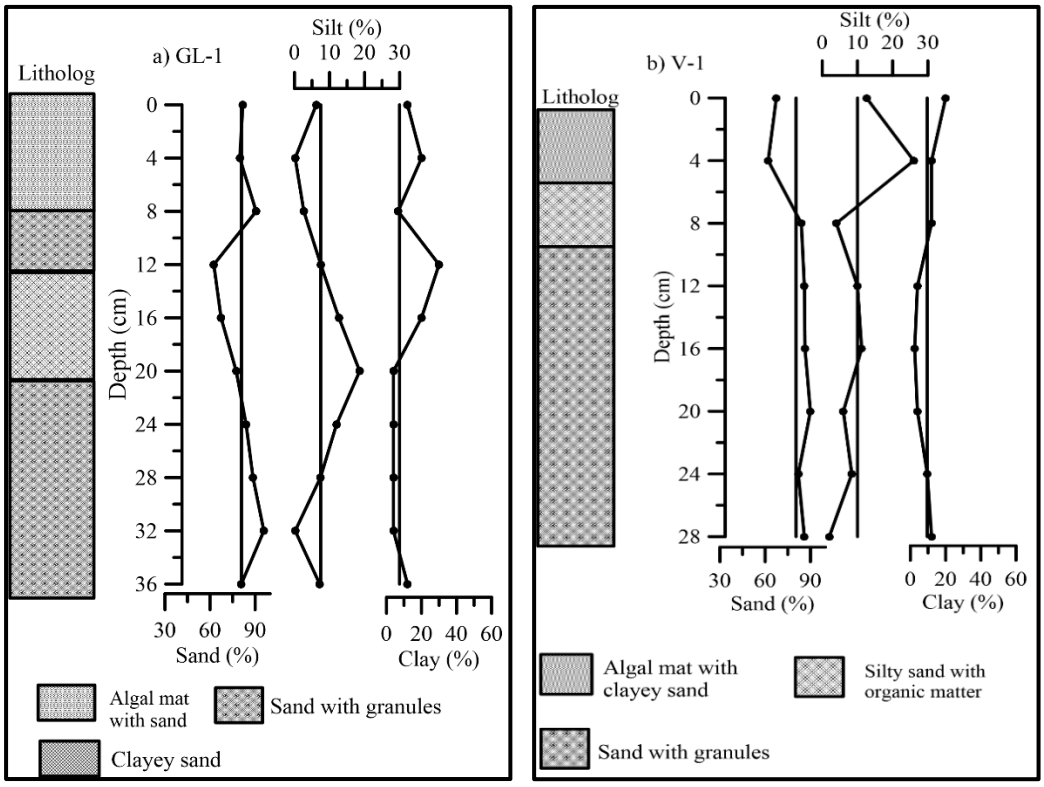

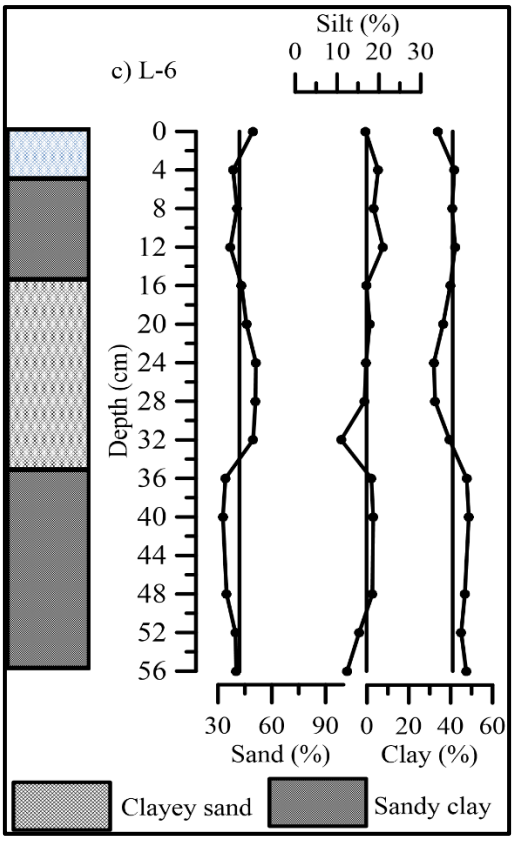

Fig.3.1.11. Depth wise distribution of sediment components of cores a) GL-1 b) V-1 and c) L-6

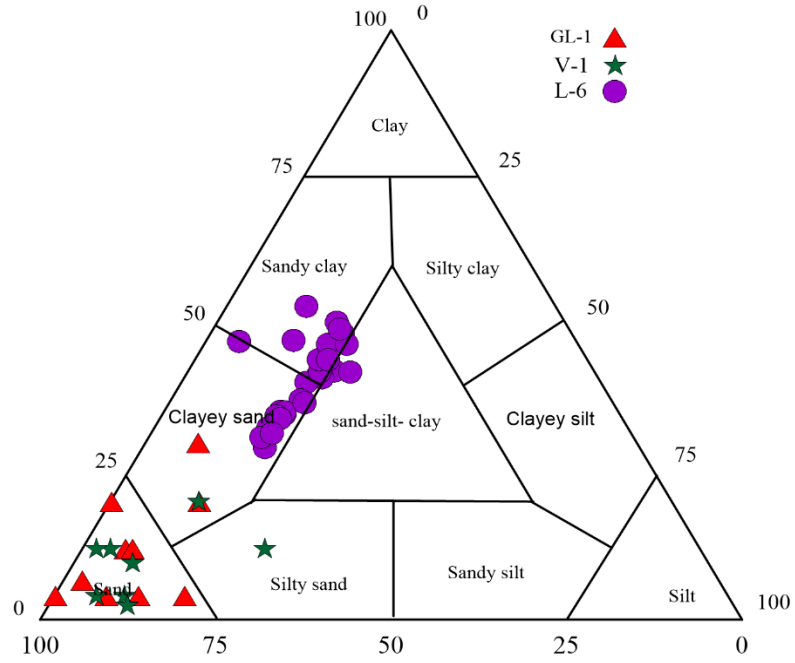

Fig.3.1.12. Ternary diagram (Shepard, 1954) of sand-silt-clay percentages of sediment for cores GL-1, V-1 and L-6

Section 2: Organic components

3.2.A Surface sediment samples

3.2.A.a Krossfjord-Kongsfjord, Arctic

The total organic carbon (TOC) and total nitrogen (TN) concentration varied within a range from 0.04% to 1.70% and 0.04 % to 0.17% respectively along the Krossfjord**.** Highest TOC (1.70%) and TN (0.17%) at station Kr-1 while least concentration of TOC (0.04%) at station Kr-4 and TN (0.04%) at station Kr-4 and Kr-5 was noted (Fig.3.2.1a). Total phosphorus (TP) varied from 0.019 to 0.023 %. High concentration of TP was noted at station Kr-1 while least concentration was at station Kr-2 and Kr-5. Biogenic Silica (BSi) varied from 2.74% to 4.19%. High concentration of BSi was at station Kr-1 and least concentration noted at Kr-5 (Fig. 3.2.1a). Calcium Carbonate ($CaCO_3$) varied within a range from 4.32% to 13.79% along the Krossfjord. $CaCO_3$ (13.79%) was highest at station Kr-5 while least concentration (4.32%) at station Kr-3. In general, the carbonate content of the surface sediments is relatively low, most of the values are lower than 15%.

Along the Kongsfjord, TOC and TN varied from 0.20% to 1.74% and 0.03% to 0.17% respectively**.** Highest TOC (1.74%) and TN (0.17%) was at station Ko-1 and least concentration of TOC (0.20%) and TN (0.03%) was noted at station Ko-7. TP varied from 0.017% to 0.061%. Ko-5 showed high concentration of TP while Ko-7 the lowest concentration (Fig.3.2.1b). BSi varied from 1.42% to 4.03%. High concentration of BSi was observed at station Ko-1 and least concentration at station Ko-8 (Fig 3.2.1b**).** Along the Kongsfjord, $CaCO_3$ varied from 4.81% to 15.56%. Ko-5 station exhibited a high concentration of $CaCO_3$ while least concentration was exhibited by station Ko-3.

Organic carbon content in the surface sediments showed an overall increasing trend towards the mouth of the Krossfjord and Kongsfjord (Fig. 3.2.1a and b) except for maintaining higher value at head region. The total nitrogen concentration in surface sediments followed an increasing trend. TOC and TN in surface sediments of both the fjords showed a clear spatial gradient with higher values towards the outer fjord and lower values in the glacier-dominated inner fjord.

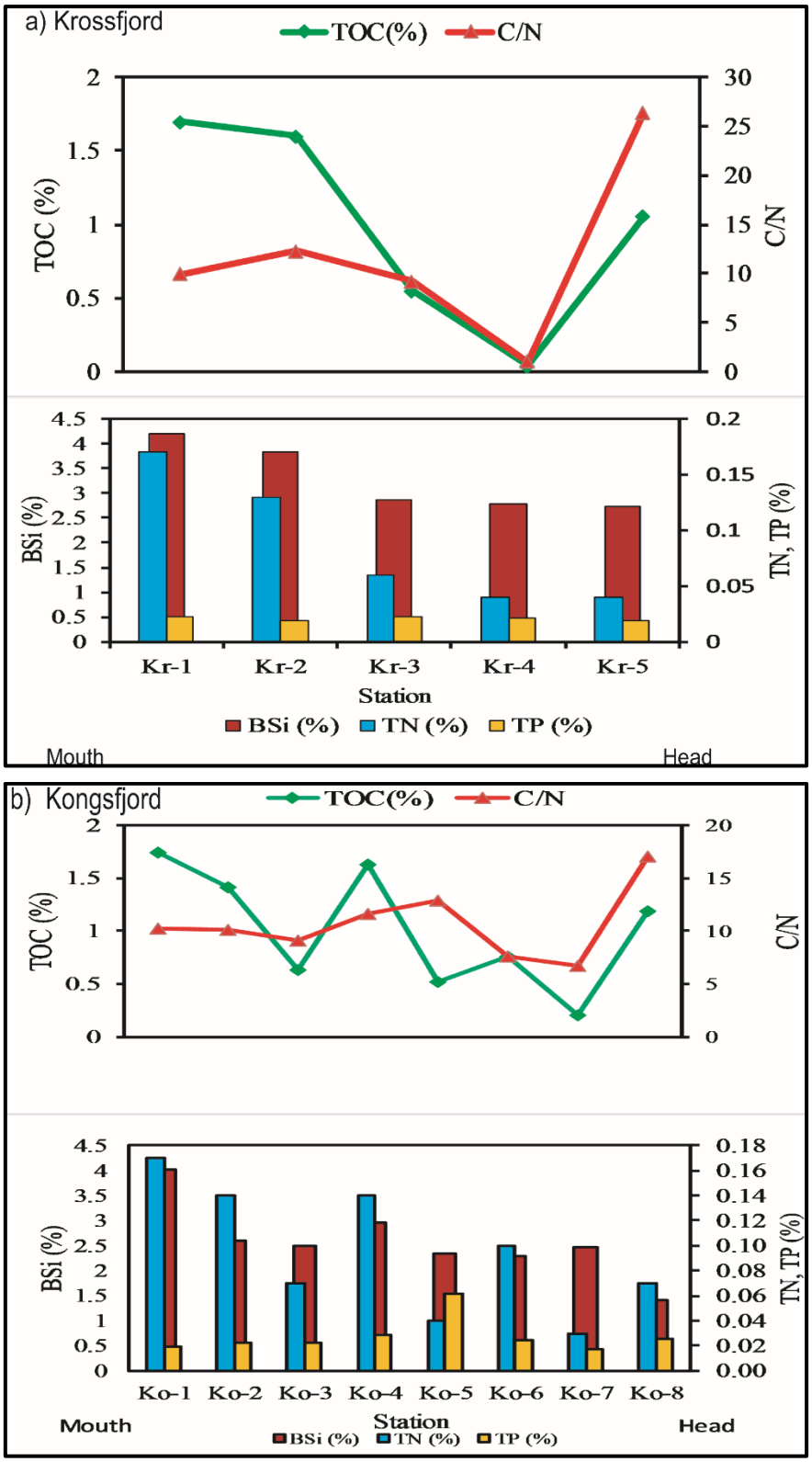

Fig. 3.2.1. Distribution of total organic carbon (TOC), total nitrogen (TN), total phosphorus (TP), biogenic silica (BSi) and C/N ratio in surface sediments of a) Krossfjord (Kr) b) Kongsfjord (Ko).

Shetye et al. (2011) reported that due to the high turbidity towards the fjord head, inner fjord has a shallow photic zone close to the glacier fronts Consequently, algae become light limited and Eilertson et al. (1989) suggested that during the summer, algal biomass decreased due to increased grazing in the inner part of the fjord. High input of sediment-loaded glacial meltwater deteriorates growth of phytoplanktons during summer (Svendsen et al., 2002), therefore, low organic matter in the inner part of the fjord resulted in lower primary productivity. The distribution of sediment size from inner fjord to the outer fjord may also have played a role in the distribution of organic matter. Increase in organic carbon along with finer sediments in the outer fjord is justified as the finer particles of the sediments provide, large surface area, thus having high adsorption capacity (Siraswar and Nayak, 2012; Fernandes and Nayak, 2017).

Further, a strong correlation between TOC and TN exists in the surface sediments of Krossfjord (r^2=0.69) and Kongsfjord (r^2=0.84) suggesting that the availability of inorganic nitrogen is negligible in the total nitrogen pool in Krossfjord-Kongsfjord system (Kim et al., 2011). TP fluctuates without any particular trend in both the fjords. TOC and TN showed poor association with TP indicating a differential pathway for phosphorus. BSi shows an increasing trend from inner fjord towards the outer fjord indicating high productivity towards the outer fjord. The nutrient (C, N, P and Si) concentrations in the inner fjord are low may be due to less concentration of organic matter, possibly because of the proximity of glacier as glacial meltwater is low in nutrient concentrations and also diluted possibly by the presence of coarse-grained sediments. All geochemical proxies TN, TOC and BSi showed similar variations from inner fjord to outer fjord indicating their common source. The close relationship between BSi and other nutrient parameters could confirm that sedimentary organic matter was predominantly derived from the natural source and anthropogenic input did not significantly influence the organic matter.

The C: N ratio is used oftenly for tracing the sources of organic matter (marine vs. terrestrial) in Arctic environments (Stein and Macdonald, 2004). Organic matter derived from higher plants exhibits higher C:N ratio (>20; Meyers and Ishiwatari,1993) as compared to the organic matter derived from marine organisms (6-9; Muller, 1977) as terrestrial organic matter contains a high percentage of non-proteinaceous material (cellulose and lignin). According to Bordowskiy (1965) and Hedges et al. (1986), C: N ratio of marine organic matter is around 6 whereas terrigenous organic matter has C: N

ratios of >15. Increasing marine influence is observed towards the fjord mouth. Along the Krossfjord, the C: N ratio in sediments varied from 1.01 to 26.37 and along the Kongsfjord the C: N ratio varied from 6.67 to 17.00 suggesting the mixed source of organic matter derived from terrestrial as well as marine source. Variation in C:N ratio between stations is regulated by quantity of TOC supply from terrestrial and marine origin. The meltwater discharge and glacial erosion processes are responsible for supplying terrestrial organic matter (TOM). The contribution of organic matter from the vegetation cover seems to play a minor role since the area is glaciated and small areas provide favorable ground for plant growth. Hop et al. (2002) stated that higher proportion of marine organic matter (MOM) towards the mouth of the fjord reflects the dominant influence of nutrient-rich Atlantic water inflow which is indicated by a high temporal variability in annual primary productivity (4-180 gC m^{-2} yr^{-1}). Both the fjords showed higher C: N values in shallower regions because of the presence of high amount of terrestrial material and their association with coarse-grained sediment suggested grain size to be a dominant factor regulating the distribution of organic matter. C/N ratio is lowest at station Kr-4 in Krossfjord and station Ko-7 in Kongsfjord as they are located away from the glacier resulting in high concentration of marine organic matter. Inorganic nitrogen can affect C: N values in marine surface sediments can be affected by a contribution of inorganic nitrogen. Winkelmann and Kneis (2005) reported inorganic nitrogen up to 70% of the total nitrogen content off Spitsbergen. This resulted in relatively low C: N values due to the high amount of inorganic nitrogen present. However, in the present study, TOC shows a strong correlation with TN indicating that most of the nitrogen was associated with organic carbon and it can be considered as a measure of organic nitrogen suggesting a negligible contribution of inorganic nitrogen to the total nitrogen pool as also reported earlier by Kim et al. (2011).

Variations in carbonate content are mainly controlled by dissolution during its journey through the water column, dilution by the non-carbonate fraction and terrigenous matter and/or productivity changes (Stein et al.,1994). In general, in polar regions, CO_2 dissolution is high which leads to increase in carbonic acid concentration which in turn explains the low $CaCO_3$ content. The $CaCO_3$ concentration is associated with coarse grain size and therefore with increasing sand fraction towards the head of the fjord calcium carbonate increases. While the $CaCO_3$ content was low towards the mouth of the fjord due to increased clay loads which must have caused dilution of carbonates. Association of carbonate with coarse-grained sediment in the surface sediments of the fjord indicates

that it is of detrital origin derived from the weathering of rocks present in the catchment area of the fjord (Midproterozoic and Proterozoic metamorphic rocks, mainly marble towards north and south of Kongsfjord respectively).

3.2.A.b Prydz Bay (Thala Fjord), East Antarctica

TOC and TN concentration varied within a range from 1.49 to 3.40% and 0.23 to 0.59% respectively. TOC (3.40%) and TN (0.59%) were highest at station P4 at 60 m at water depth while least concentration of TOC (1.49%) and TN (0.23%) concentration was observed at water depth of 31 m at station P1. TOC and TN showed good correlation with each other (Fig. 3.2.2) as with high organic carbon, the nitrogen concentration increased indicating that most of the TN was associated with TOC and therefore it indicates the amount of organic nitrogen (Kurian et al., 2013). TP in the Prydz bay varied from 0.013 to 0.036 %. High concentration was at station P4 at 60 m water depth while least concentration was at station P7 at 140 m.

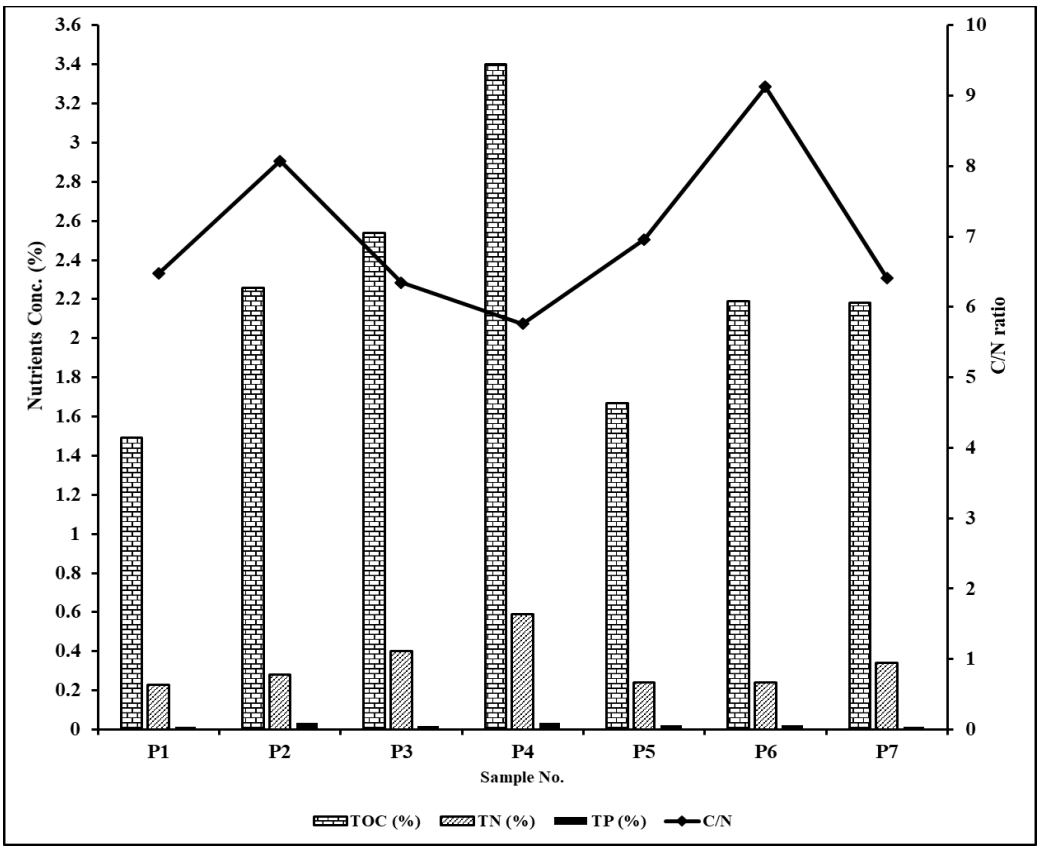

Fig. 3.2.2. Distribution of total organic carbon (TOC), total nitrogen (TN) total phosphorus (TP) and C/N ratio in surface sediments along the Prydz Bay

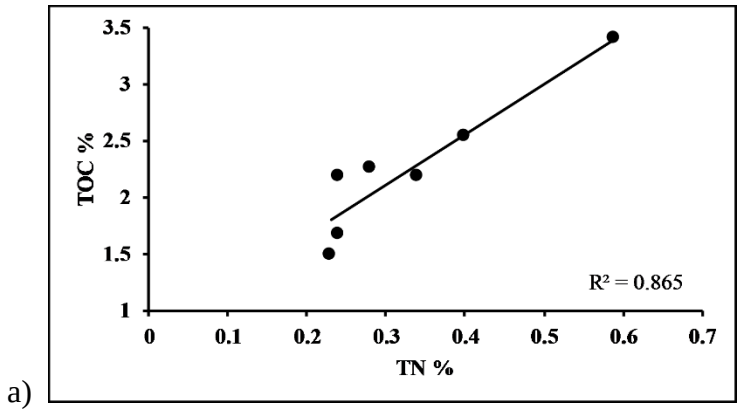

a)

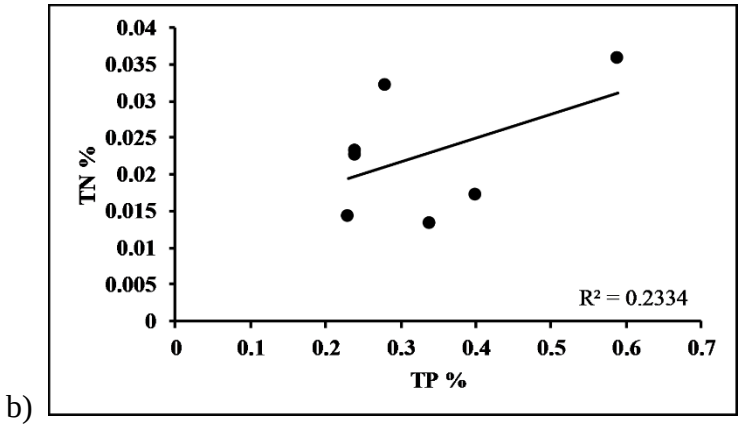

b)

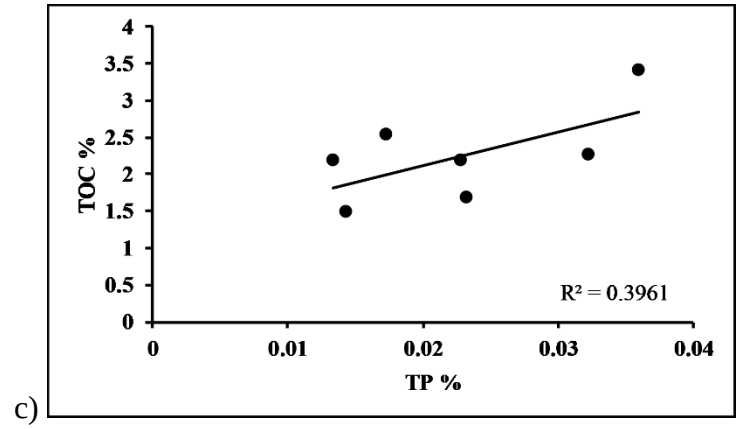

c)

Fig.3.2.3. Scatter plots between a) - total organic carbon and total nitrogen b) total organic carbon and total phosphorus c) total nitrogen and total phosphorus

In Prydz Bay, the C/N ratio varied between 5.76 and 9.13 (Fig.3.2.2) indicating the marine source (in situ). The values obtained can be classified following Meyers (1994) as exclusively derived from algae (C/N <10). C/N ratio was found to be low for the coastal area may be because of the dissolution of organic matter by the bacterial action and either C or N is diagenetically affected, lowering the C/N ratio.

N/P (molar) ratios were low and varied between 3.93 and 11.53 indicating nitrogen deficiency which must have limited primary productivity. C/P (molar) ratios varied from 27.20 to 63.39, with the lowest ratio at station P2 at 40 m water depth and the highest ratio was observed in station P7 at 140 m water depth. $CaCO_3$ content in Prydz Bay varied from 0.83 to 3.50% (Fig. 3.2.2) except for stations P2 and P6 which showed the exceptionally high $CaCO_3$ content of 28.74 and 48.56% respectively possibly due to high inorganic carbon content. High $CaCO_3$ in the nearshore sediments may be due to glacial meltwater and terrigenous sediments which bring nutrients along with them facilitating high productivity. However, higher values were obtained only for two stations. Scatter plots (Fig. 3.2.3a, b and c) of TOC and TN with TP revealed a poor association with each other indicating a differential pathway for phosphorus or the possible influence of diagenesis on phosphorus.

The biogenic opal or biogenic silica concentration in the Southern Ocean is ascribed to the siliceous diatom productivity (Chase et al., 2003; Bradtmiller et al., 2006). BSi concentration varied from 16.42 to 35.41% in the surface sediments of Prydz Bay. BSi showed significant correlation with TOC (r=0.79) and TN (r=0.76) indicating that the content of BSi was controlled by the amount of algae (Shan et al., 2011) along with other phytoplanktons. The close relationship between BSi and other geochemical parameters confirmed that sedimentary organic matter was predominantly derived from the ocean. Increase in BSi concentration is accompanied by a decrease in carbonate content suggesting that when diatom dominates the surface waters, coccolithophore production declines and vice-versa (Manoj and Thamban, 2015). This relationship suggested the influence of nutrients on the survival and proliferation of the two major producers of the ocean, hence affecting overall productivity.

Further, $CaCO_3$ content is generally controlled by surface water productivity, the rate of carbonate dissolution and dilution by the non-carbonate fraction. The low values of $CaCO_3$ in all the stations of the Prydz Bay (except station P2 and P6) can be attributed to the decreased carbonate productivity and/or increased dissolution. The increase of TOC is accompanied with the decrease of $CaCO_3$ indicating that the CO_2 produced by the decomposition of organic carbon and production of organic acids reduces the pH of anoxic pore waters enough to dissolve $CaCO_3$ that reaches the sediment-water interface (Nioti et al., 2013). $CaCO_3$ and TOC are inversely related implying different origin.

3.2.B Sediment cores

3.2.B.a. Arctic Fjord

TOC concentration in core K-1 from the fjord varied from 0.83% to 4.22 %. TN concentration was found to be low and varied from 0.04% to 0.44% and TP concentration varied from 0.016% to 0.061%. BSi concentration varied from 1.11% to 2.82%. $CaCO_3$ concentration is higher in the fjord and fluctuated from 5.62% to 20.47%.

Depth wise distribution of the organic elements are presented in Fig.3.2.4. TOC fluctuated around the average line throughout the core. TOC showed negative peaks at depth 22 cm and 4 cm similar to that of silt and clay respectively and a positive peak at 15 cm similar to that of silt indicating that these sediment components regulated the distribution of organic matter at these depths. Further, TOC showed an increasing trend from 4 cm to the surface similar to that of clay towards the surface suggesting increased primary productivity. Fluctuating trend with depth indicates changing rate of supply of organic matter through changing processes. Organic matter concentration in the sediments of fjord mainly depends on the location of sampling. Whether the location of sampling lies in the proximity of high primary production areas or the glaciers are available in the vicinity, supplying land derived material. High concentration of land derived material causes high turbidity resulting in shallow photic zone. Regions receiving high amount of fresh water discharge from glaciers and rivers fed by glaciers, generally, have low primary production due to the high turbidity (Gorlich et al., 1987; Zajączkowski and Włodarska-Kowalczuk, 2007). The marine organic matter gets diluted with suspended material discharged by glaciers. Therefore, glaciers play an important role in regulating the distribution of organic matter in the fjord system.

TN and TP showed higher concentration in the lower depth range from 23 cm to 17 cm and increasing trend towards the surface in the upper portion. TN showed a positive peak at 14 cm similar to that of clay and TP at 9 cm similar to that of TOC. TN does not show similarity with TOC in its distribution throughout the core indicating their different source. The nitrogen content in the sediments of other

locations around Spitsbergen are reported less and only few reports are available. Schubert and Calvert (2001); Kneis et al. (2007); Kozioroswka et al. (2016) and Kumar et al. (2016) have reported nitrogen concentration ranged from 0.04% to 0.31%. Thus, the range of nitrogen concentration obtained as a part of this study is within the reported range.

C/N ratio is commonly used as an indicator of provenance of organic matter in marine sediments. Terrestrial organic matter typically has C/N ratio higher than 15 while C/N ratio around 6 suggested animal tissues as the main source of organic matter (Stein, 2008). The marine organisms have C/N ratio (Redfield, 1934; Takahashi et al.,1985) ranged between 6.5 and 8.7 (C: N:P = 122 (±18):16:1). Terrestrial organic matter is mainly composed of nitrogen poor compounds such as cellulose, lignin etc. Therefore, terrestrial organic matter has higher C/N value varied between 20 and 100 (Meyers, 2003). The C/N ratio of core K-1 varied from 5.60 to 84.03 (average 28.52) indicating a mixed source of organic matter derived from marine as well as terrestrial. C/N ratio showed lower than average values in the lower depth range from 23 cm to 14 cm while at 13 cm C/N ratio was found to be high similar to that of sand indicating ice-free conditions and increased glacial melt water which must have delivered terrestrial organic matter to the fjord. The high primary production may lead to nitrogen limitation in the surface water. Also, the nitrogen loss in sediments can be possible due to diagenesis which must have resulted in relatively large range of C/N ratio. Further, it decreased up to 4 cm and then increased towards the surface.

BSi showed a slightly increasing trend towards the surface. High concentration of TOC, TN, TP and BSi along with clay indicated high productivity during the recent years. BSi showed positive correlation with clay ($r=0.46$, $n= 24$) indicating the role of finer sediments in regulating its distribution.

The $CaCO_3$ concentration varied from 5.62% to 20.47% (average 8.80%) in core K-1. It showed an overall fluctuating trend (Fig. 3.2.4) which is attributed to the varying deposition of carbonates in the sediments and/ or the soluble bicarbonates formation using CO_2 which has originated during the mineralization of organic matter. $CaCO_3$

showed a positive peak opposite to that of TOC at a depth of 4 cm and negative correlation (r=-0.41, n=24) with TOC. In this fjord, primary production and the activities of benthic organisms are very limited due to the presence of glaciers in the proximity (Gorlich et al., 1987; Stein and Macdonald, 2004; Włodarska-Kowalczuk et al., 2007). Therefore, the source of calcium carbonate is considered to be allochthonous i.e. from the weathering of rocks available in the catchment area mainly limestone (Trusel et al., 2010).

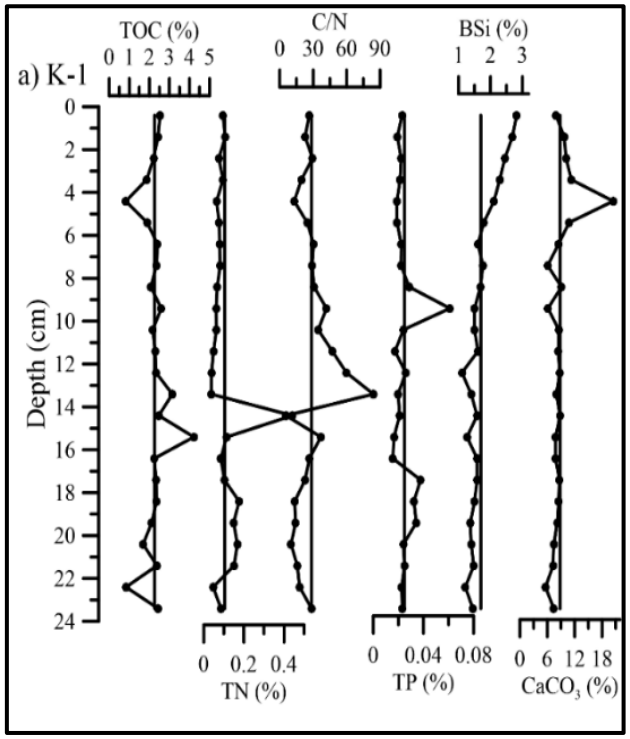

Fig.3.2.4 Depth wise distribution of organic components of cores a) K-1

3.2.B.b. Arctic Lakes

The TOC was higher in core L-2 (avg. 2.17%) and lowest in LA (avg. 1.27%). TN was high in core L-3 (avg. 0.34%) and low in core LA (0.07%) and TP was also high in core L-3 (0.027%) and low in core L-1 (0.011%). BSi was higher in core L-1 (6.35%) and low in core L-3 (2.59 %). $CaCO_3$ was higher in core L-3 (22.06%) than in core L-1 (6.65%) and LA (8.94%) (Table 3.2.1).

Vertical distribution of organic elements is presented in Fig. 3.2.5 a, b, c and d. In core LA, TOC showed lower than the average values in the lower depths range from

26 to 20 cm and higher than the average values in the upper portion from 8 to 6 cm and at 2 cm with an overall increasing trend towards the surface. TN and TP showed uniform distribution throughout the core. In core L-1, TOC and TN showed a similar fluctuating trend up to 8 cm and further increased towards the surface. TOC showed decreasing trend from bottom to 6 cm and further increased towards the surface in core L-2 and TN showed an overall increasing trend towards the surface with almost similar values in the lower depths range from 18 to 10 cm. High concentration of TOC and TN in core L-1, L-2 and L-3 towards the surface along with clay and silt indicated high productivity due to the increased ice melt water influx in the recent years. TP showed an increasing trend in the upper portion from 4 cm to the surface in core L-1 and L-3 similar to that of silt and sand. In core L-3, TOC showed an overall increasing trend up to 6 cm and slightly lower values at the surface. Lower than the average values in the lower depths range from 16 cm to 8 cm and higher than the average values in the upper portion up to 6 cm was noted in this core. TOC and TN showed similar trend in the lower portion from 16 to 6 cm depth, further TOC decreased up to 2cm followed by an increase towards the surface while TN continues to increase towards the surface.

TOC showed strong correlation with TN in core LA (r=0.70), L-1 (r=0.71) and L-2 (r=0.59) indicating that most of the nitrogen was associated with TOC suggesting that the contribution of inorganic nitrogen to the total nitrogen pool is negligible in these lakes while in core L-3 it showed poor correlation indicating different source of nitrogen in this lake. In core L-3, TN showed good correlation with TP (r=0.91, n=9) and sand (r=0.79, n=9) indicating the source of nitrogen and phosphorus to be terrestrial in this core. In core L-1, TP showed good correlation with TN (r=0.91, n=17) indicating that they have been derived from the similar source.

The C/N ratio is a widely used proxy for identifying the source of organic matter into the lacustrine sediments (Talbot and Johannessen, 1992). High latitude lakes vary largely from that of the terrestrial lakes of the low latitudes mainly in terms of their source of organic matter. Terrestrial vegetation forms a significant component of the organic matter along with in-situ production by aquatic–organisms. Benthic cyanobacteria and diatoms dominate lake biomass and aquatic mosses form the

highest forms of plants (Hodgson et al., 2003). Therefore, majority of organic matter is contributed through the production of aquatic organisms such as algae and cyanobacteria (Yoon et al., 2006; Hodgson et al., 2009 a, b). As per the classification of Meyers (1994) algae and cyanobacteria typically have atomic C/N ratio between 4 and 10, whereas vascular land plants have C/N ratios of 20 and greater. C/N ratio of 5-6 is exhibited by freshwater and marine phytoplanktons (Prahl et al., 1994; Meyers, 1997) whereas the C/N ratio of 12-14 is found in terrestrial plants which are poor in nitrogen (Hedges et al., 1986; Prahl et al., 1994; Lamb et al., 2006). According to Talbot and Johannessen (1992) autochthonous lacustrine organic matter is characterized by relatively low C/N ratios, typically <10 as it is N-rich due to their high protein and lipid content. Lignin and cellulose, which are dominant components of terrestrial higher plants, are nitrogen poor and thus allochthonous organic matter has C/N ratios which are normally higher than 20 and may be >200.

C/N ratio varied from 15.50 to 38.32 in all the four cores indicating the source of organic matter to be of mixed origin as per the classification of Meyers (1994, 2003) and Meyers and Terranes (2001). In core LA, C/N ratio fluctuated around the average line up to a depth of 6 cm and further it showed lower than the average values suggesting the source of organic matter to be autochthonous. In core L-1, from 20 cm to 14 cm C/N ratio was found to be higher (>20) indicating the source of organic matter to be of terrestrial origin at these depths. In core L-2, C/N ratio showed a decreasing trend from 18 cm to 10 cm depth and then showed higher values from 10 cm to 6 cm followed by a decrease towards the surface. While in core L-3, C/N ratio showed higher than the average values in the lower portion from 16 cm to 8 cm and further showed lower than the average values towards the surface (Fig. 3.2.5d). Thus, in all the cores there is a mixed source of organic matter at some intervals having terrestrial origin.

Overall, BSi concentration was found low (average 2.59 to 6.35%) (Table 3.2.1) in lake LA, L-1, L-2 and L-3 suggesting low concentration of siliceous microfossils in these lakes. Increased concentration of biogenic silica from 6 cm to the surface along with clay in core LA and L-2 indicated high productivity. In core L-1, BSi was found to be high in the middle portion of the core from 22 cm to 6 cm along with TOC and

clay suggested deposition of finer particles from suspension facilitating high productivity.

$CaCO_3$ content fluctuated from 6.65% to 22.06% in these lakes. Increased concentration of $CaCO_3$ in the Arctic lakes is due to the weathering of rocks present in the catchment area viz. limestone. With increasing TOC, $CaCO_3$ concentration decreased in almost all the cores except lake L-2 (Fig. 3.2.5c) due to the reduction of pH resulting in dissolution of $CaCO_3$.

Table 3.2.1. Range and average values for organic components of cores from the mouth of Krossfjord and lakes from NY-Alesund and Kuadehuken region

Cores	TOC (%)		TN (%)		C/N		TP (%)		BSi (%)		$CaCO_3$ (%)	
	Range	Avg	Range	Avg	Range	Avg	Range	Avg	Range	Avg.	Range	Avg.
K-1	0.83-4.22	2.26	0.04-0.44	0.10	5.60-84.03	28.52	0.016-0.061	0.025	1.11-2.82	1.70	5.62-20.47	8.80
L-A	0.55-2.58	1.27	0.04-0.11	0.07	10.47-26.89	17.87	0.014-0.021	0.017	2.90-7.35	4.64	0.31-35.30	8.94
L-1	1.09-3.04	1.85	0.05-0.44	0.14	6.88-26.48	15.50	0.008-0.020	0.011	0.82-15.49	6.35	2.03-11.12	6.65
L-2	0.85-2.79	2.17	0.02-0.30	0.09	8.97-88.00	38.32	0.013-0.024	0.018	1.79-6.56	2.96	5.49-33.63	17.96
L-3	0.71-2.53	1.37	0.02-1.15	0.34	1.36-34.85	18.19	0.022-0.038	0.027	1.95-3.77	2.59	15.93-25.23	22.06

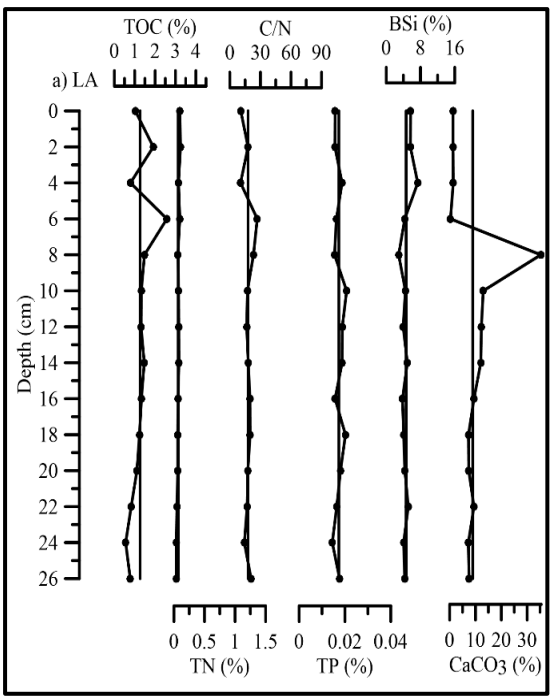

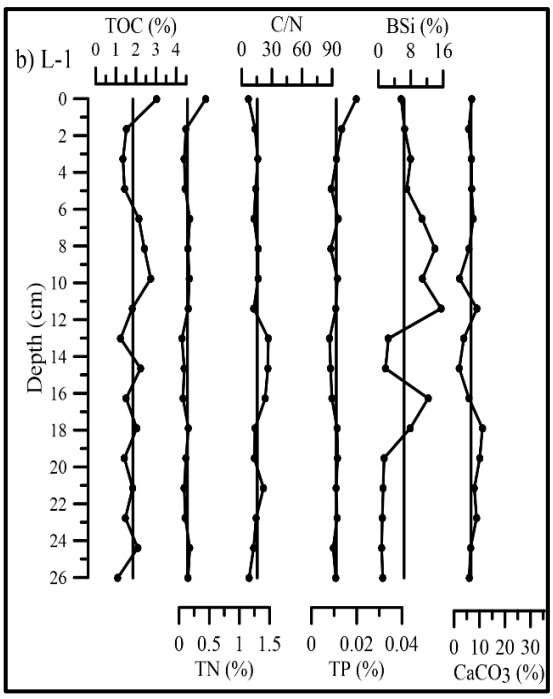

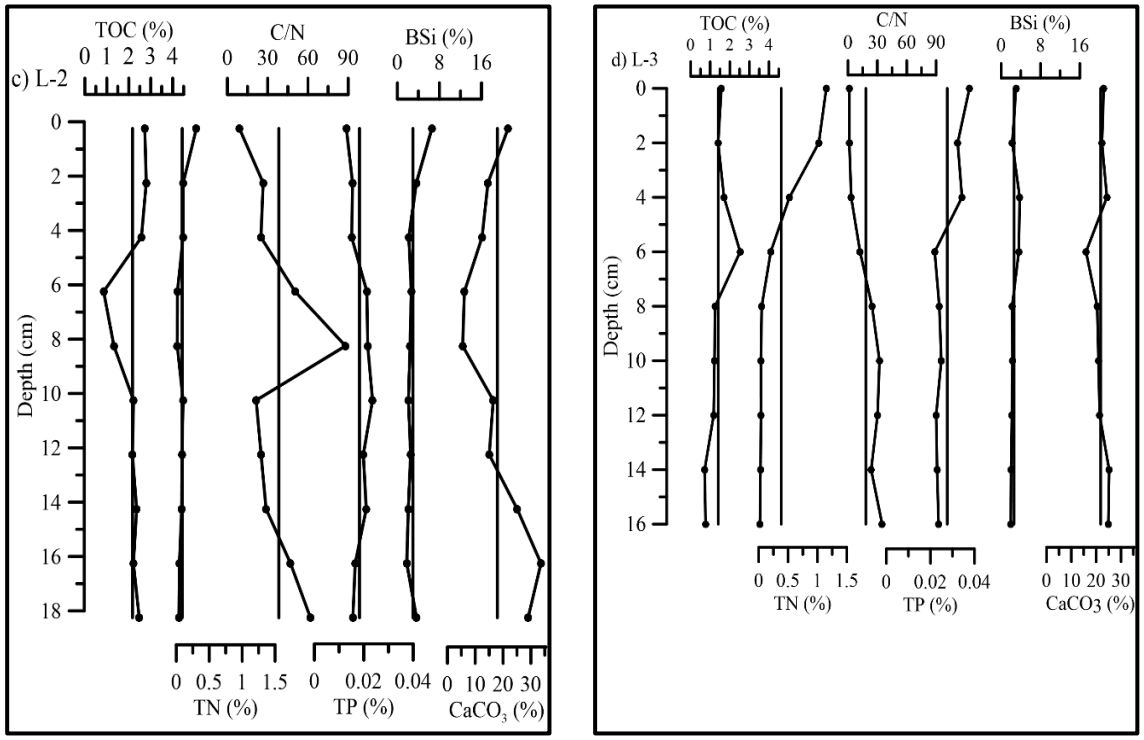

Fig. 3.2.5 Depth wise distribution of organic components of cores a) LA b) L-1 c) L-2 and d) L-3

3.2.B.c. Antarctic lakes (Larsemann Hills, East Antarctica)

The TOC was higher in core L-8 (avg. 0.76%) and lowest in L-12 (avg. 0.10%); TN was high in both the cores L-8 and L-10 (avg. 0.16% and 0.10%) and low in core L-12 (0.08%) and TP was high in core L-8 (0.06 %) and L-10 (0.05 %) and low in core L-12 (0.02%). BSi was higher in core L-8 (5.64%) and low in core L-12 (0.94 %). $CaCO_3$ was higher in core L-12 (6.36%) than in core L-8 (4.55%) and L-10 (4.72%) (Table 3.2.2).

Vertical distribution of organic elements is presented in Fig. 3.2.6a, b and c. In core L-10 and L-12, TOC consistently showed lower concentration from bottom to 6 cm and further increased towards the surface while in core L-8, it showed lower values in the lower section of the core up to 20 cm and further it showed higher values in the upper section. TOC distribution was similar to that of silt and clay indicating the association of organic matter with the finer sediments as they provide a large surface

area for the adsorption of organic matter. High TOC along with high clay in the upper section of all the three cores indicated deposition of finer particles from the suspension facilitating high primary productivity due to exposure of the lakes to the ice–meltwater influx. In core L-8, TOC and TN showed similar variation suggesting that most of the TN was associated with TOC and it is considered as a measure of organic nitrogen (Kurian et al., 2013) while in core L-10 and L-12 they showed different variation indicating their different source. TP fluctuated around the average line in all the three cores. Pearson's correlation of TOC and TN with TP in all the three cores revealed a poor association with each other indicating a differential pathway for phosphorus.

The C/N ratio of core L-8, L-10 and L-12 varied from 1.22 to 4.08 (Table 3.2.2) indicating that the source of organic matter as in-situ. The C/N ratio obtained for the three cores namely L-8, L-10 and L-12 must have been derived exclusively from algae (C/N <10) as in Antarctica terrestrial vegetation is less and there is an absence of vascular plants. C/N ratio was found to be relatively higher in the upper section of core L-10 and L-12 (Fig.3.2.6b and 3.2.6c) due to the presence of algae and cyanobacteria as lakes are exposed to the atmosphere because of the ice-free conditions of the lake. In core L-8, C/N ratio was found to be low in the lower section of the core up to 20 cm (Fig.3.2.6a). Low C/N ratio may be because either C or N is diagenetically affected and bacterial action might have caused dissolution of organic matter. Further, in the upper section of the core from 18 cm to the surface, C/N ratio was found to be higher may be due to the loss of N from the sediments during remobilization (Choudhary et al., 2018). Further, a wide range of C/N ratio in this lake may be due to nitrogen limitation in the water column as reported by Hawes (1983) in Lakes on Signy Island, Antarctica.

Biogenic silica or biogenic opal is attributed to siliceous diatom productivity (Chase et al., 2003; Bradtmiller et al., 2006). Average BSi concentration varies from 0.94% to 5.64% in all the three cores indicating a low concentration of siliceous microfossils in these lakes. From the vertical distribution, biogenic silica concentration was found

to be relatively higher in the middle section of core L-8, from 18 cm to 12 cm along with organic carbon, silt and clay (Fig. 3.2.6a) indicating relatively higher primary productivity due to exposure of the lakes to ice-melt water influx during the warm period. In core L-10, it showed fluctuation around the average line while in core L-12, BSi showed similar variation as that of TOC (Fig.3.2.6b and 3.2.6c) from bottom to top of the core indicating that the content of BSi in this lake was mainly controlled by the amount of lake algae.

The average concentration of $CaCO_3$ concentration varied from 4.55% to 6.36% in all the three cores (Table 3.2.2). Overall, low concentration of $CaCO_3$ indicated the presence of low calcareous materials. $CaCO_3$ is precipitated from suspension as a result of algal CO_2 fixation as observed by Lawrence and Hendy (1985), in Lake Fryxell, Taylor Valley, Antarctica. It showed decreasing concentration with increasing TOC in all the three cores (Fig. 3.2.6a, 3.2.6b, 3.2.6c). Increase in TOC accompanied by a decrease of $CaCO_3$ indicated that the CO_2 produced by the decomposition of organic carbon along with the production of organic acid reduces the pH of anoxic pore waters which is enough to dissolve $CaCO_3$.

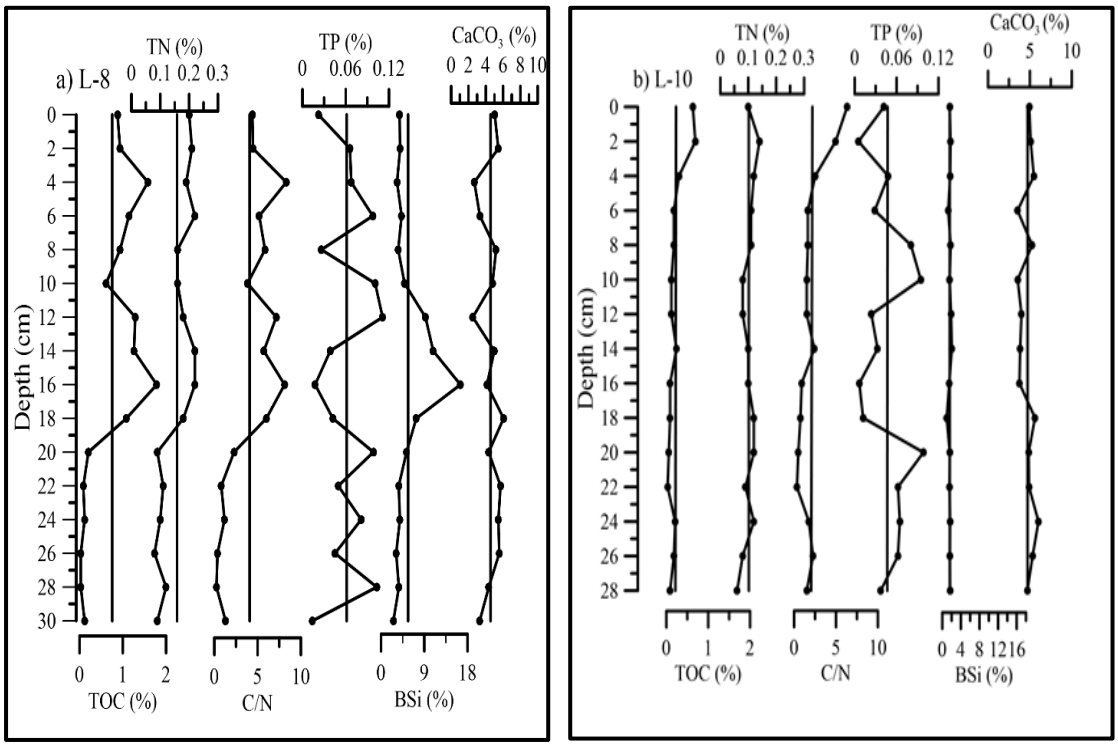

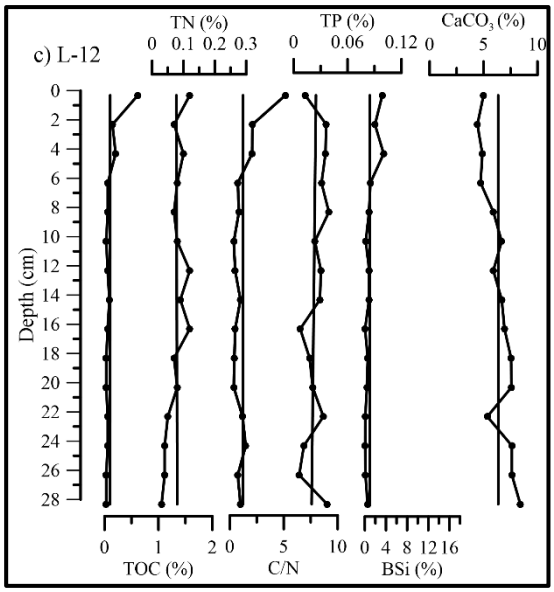

Fig. 3.2.6. Depth wise distribution of organic components of cores a) L-8 b) L-10 and c) L-12

3.2.B.d. Antarctic lakes (Schirmacher Oasis, East Antarctica)

TOC was highest in core V-1 (avg. 1.05%) and lowest in L-6 (avg. 0.24%); TN was high in both the cores V-1 and L-6 (avg. 0.15% and 0.17%) and low in core GL-1 (0.08%). TP was high in core L-6 (0.05 %) and low in core V-1 (0.03%). BSi was high in cores GL-1 (1.56%) and V-1 (1.48%) and low in core L-6 (0.1%). $CaCO_3$ was higher in core V-1 (6.50%) than in core GL-1 (4.65%) and L-6 (4.45%) (Table 3.2.2)

Vertical distribution of TOC, TN, TP, BSi and $CaCO_3$ in the three cores namely GL-1, V-1 and L-6 are presented in Fig. 3.2.7a, b and c respectively. High TOC along with high clay in the upper section of core GL-1 and V-1 indicated the development of algal mat during ice free conditions in these lakes. The presence of microbial mats, formed as thick, cohesive and highly pigmented mats is well documented in Schirmacher Oasis lakes (Vincent, 1988). The association of organic matter in sediment and its accumulation seem to be strongly influenced by temperature and availability of oxygen (Ingole and Dhargalkar, 1998). Low TOC in the lower section of core GL-1 and V-1 indicated that the algal mat might have been decayed with time and buried in the sediments. However, Yoon et al. (2006) in King Georges Island, West Antarctica, attributed low TOC values to the existence of grounded glaciers at the sampling site before the formation of post-glacial lake environment. In cores V-1

and L-6, all along the length of the core, TOC showed similar distribution as that of clay. It is well established that the organic carbon is largely associated with finer sediments due to surface area / volume ratio of sediment grains (Choudhary et al., 2018; Muzuka and Shaghude, 2000). In core GL-1, TN showed similar distribution with that of sand in its lower section up to a depth of 16 cm and similar to clay in upper section from 16 cm to the surface (Fig. 3.2.7a) indicating nitrogen addition through weathering of rocks (Choudhary et al., 2018; Holloway and Dahlgren, 1999). In core V-1, higher TN from 4 cm to the surface must be due to the ability of cyanobacteria to fix nitrogen from the atmosphere during the ice-free conditions of the lake. In core GL-1, TP showed an overall increasing trend towards the surface with lower than the average values in the lower depths range from 36 cm to 24 cm, at 12 and 4 cm in the upper portion and higher than the average values in the middle portion from 24 cm to 12 cm similar to that of sand. In core V-1, TP increased towards the surface similar to that of TOC, TN and BSi indicating high primary productivity. TP showed higher than the average values in lower depth range from 40 to 36 cm and 16 to 4 cm in the upper portion and lower than average values in the middle portion from 32 to 20 cm similar to that of clay in core L-6 indicating their similar source. Further, TOC and TN showed good correlation (r^2=0.88) in core V-1 indicating their similar source and poor correlation between them in core GL-1 (r^2=0.064) and L-6 (r^2=0.0048) indicated their different source.

Analysis of sediments of core GL-1, V-1 and L-6 gave average C/N values between 2.72 and 8.52 indicating the source of organic matter from aquatic source (in-situ). The results obtained are in good agreement with those obtained from sediment of Long Lake located in Schirmacher Oasis (Mahesh et al., 2015). The results obtained from C/N ratio have helped in distinguishing between organic matters of aquatic from terrestrial origin. The C/N ratio for all the three cores was less than 10 for the entire core length which suggested that organic matter was mainly autochthonous (in-situ). However, the high C/N ratio in core GL-1 at a depth of 16 cm and also on the surface indicated prolonged ice-free conditions and increased melt water which must have delivered terrestrial organic matter to the lake possibly from lichens and mosses. Also, the loss of N from the sediments during diagenesis or nitrogen limitation in the surface water due to high primary production must have resulted in the relatively

large range of C/N ratio. The low C/N ratio (2.72) in core L-6 may be due to the absorption of ammonia by clay particles derived from decomposition of organic matter accompanied by the remineralization and release of carbon.

BSi documents direct measure of biological production from the siliceous algae and diatoms (Conley, 1998; Kaplan et al., 2002). Biological productivity in lake sediment is largely characterized by the diatom production (Birnie, 1990; Roberts et al., 2001). Average values of BSi in the three cores varied between 0.1 and 1.56%, which indicated presence of very low silicate microfossils in these lakes. From the vertical distribution it was noted that relatively higher BSi along with high TOC associated with high clay from 12 cm to the surface in core GL-1 and V-1 indicating relatively high primary productivity due to the exposure of the lakes to the ice-melt water influx. In core L-6, BSi was very less but found to be relatively high from 36 cm to 24 cm showing a similar pattern as that of sand. BSi showed positive correlation with TOC in core GL-1($r=0.52$, $n=10$) and V-1($r=0.79$, $n= 8$) indicating that the content of BSi in these lakes was mainly controlled by the amount of algae in the lakes. In these lakes BSi is well associated with TOC suggesting that it has originated from biogenic source. The average concentration of $CaCO_3$ concentration varied from 4.45% to 6.50% in all the three cores (Table 3.2.2). Overall, low concentration of $CaCO_3$ indicated the presence of low calcareous materials in these lakes.

Table 3.2.2. Range and average values for organic components of cores from Larsemann Hills and Schirmacher Oasis, East Antarctica

	Core L-8		Core L-10		Core L-12		Core GL-1		CoreV-1		Core L-6	
	Range	Avg.	Range	Avg.	Range	Avg.	Range	Avg.	Range	Avg.	Range	Avg.
TOC (%)	0.03-1.79	0.76	0.03-0.69	0.22	0.03-0.62	0.10	0.06-1.80	0.60	0.06-3.06	1.05	0.17-0.30	0.24
TN (%)	0.08-0.22	0.16	0.06--0.14	0.10	0.03-0.12	0.08	0.05-0.12	0.08	0.04-0.32	0.15	0.06-1.07	0.17
C/N	0.24-8.32	4.08	0.34-6.33	2.04	0.37-5.15	1.22	0.97-35.94	8.52	0.65-10.66	6.00	1.37-4.65	2.72
TP (%)	0.01-0.11	0.06	0.01-0.10	0.05	0.01-0.04	0.02	0.01-0.09	0.04	0.01-0.04	0.03	0.01-0.10	0.05
BSi (%)	2.57-16.51	5.64	0.95-2.05	1.62	0.04-3.56	0.94	0.50-2.09	1.56	0.28-2.74	1.48	0.03-0.28	0.10
$CaCO_3$ (%)	2.50-6.06	4.55	3.52-6.02	4.72	4.43-8.41	6.36	3.53-6.02	4.65	4.73-7.58	6.50	2.50-6.06	4.45

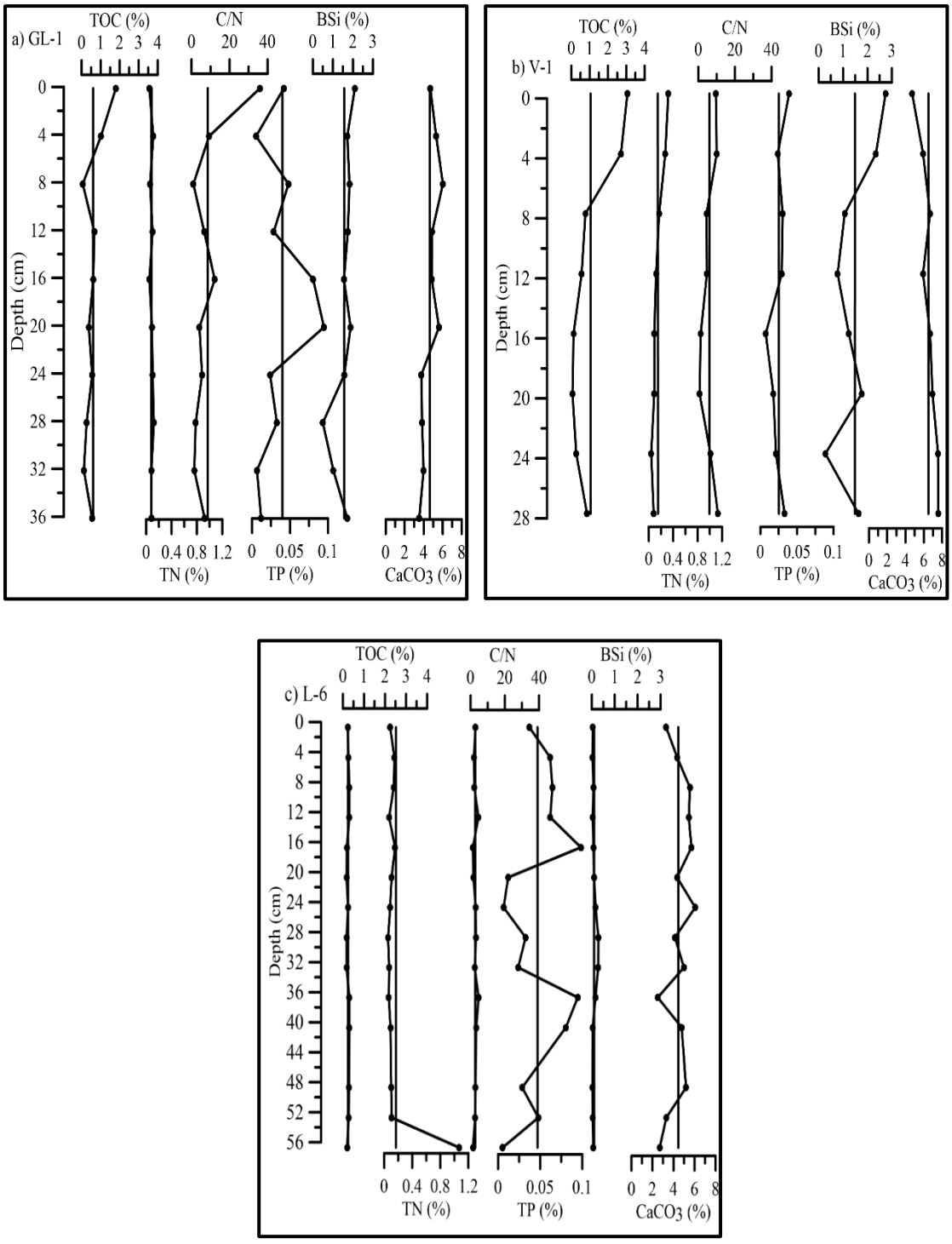

Fig. 3.2.7. Depth wise distribution of organic components of cores a) GL-1 b) V-1 and c) L-6

Section 3: Major and Trace Elements

3.3.A Surface sediment samples

3.3.A.a Krossfjord- Kongsfjord, Arctic

Along the Krossfjord (Fig. 3.3.1a), Al content fluctuated in a range between 3.49% at station Kr-1 and 5.01% at station Kr-5. Ti varied within a small range of 0.20% in sample Kr-1 and 0.29% in sample Kr-5. Fe and Mn content were largely consistent from shallow to deeper water regions and varied from 4.22% and 0.04% respectively at station Kr-4 to 5.44% and 0.08% at station Kr-1. Mg ranged between 1.56% at station Kr-1 and 2.32% at station Kr-5. Ca decreased from inner fjord to the outer fjord and ranged between 0.37% at station Kr-1 and 1.19% at station Kr-3. Along the Kongsfjord (Fig.3.3.1b), Al content varied from 5.11% to 7.96% from outer fjord to inner fjord. Ti showed relatively higher values along the Kongsfjord and varied from 0.36% to 0.58%. Fe fluctuated without any particular trend with a minimum value of 3.89% at station Ko-1 and a maximum value of 5.84% at station Ko-7. Mn fluctuated from the outer fjord to inner fjord with a minimum value of 0.05% at station Ko-1, Ko-7 and Ko-4 maximum value of 0.08% at Ko-6. Mg showed an overall increasing trend from the outer fjord towards the inner fjord with a minimum value of 1.14% at station Ko-1 and 4.50% at station Ko-8. Ca ranged from 0.45% to 3.11% with an overall increasing trend towards the inner fjord.

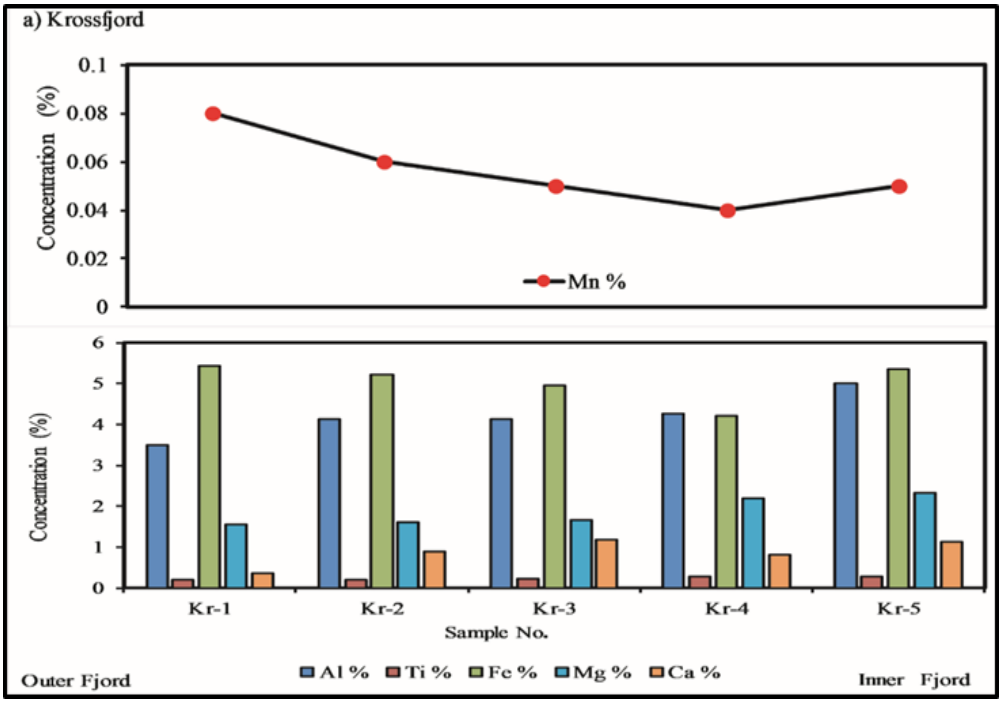

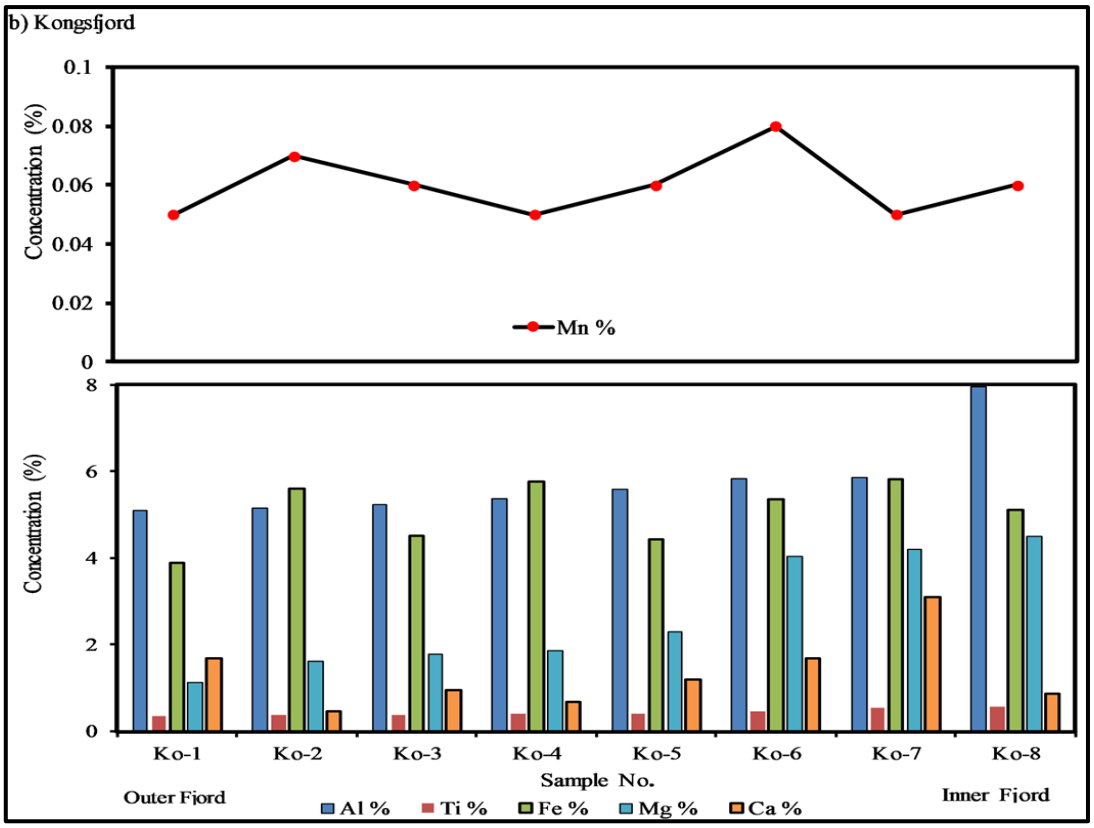

Fig. 3.3.1 Distribution of major elements in the surface sediments along the a) Krossfjord and b) Kongsfjord.

Along the Krossfjord (Fig.3.3.2a), trace elements like Cr varied from 12.44 ppm at station Kr-5 to 20.18 ppm at station Kr-1. Co varied from 12.44 ppm in the inner fjord at station Kr-5 to a maximum of 17.28 ppm at station Kr-2. Cu content varied from 18.50 ppm at station Kr-2 to 24.36 ppm at station Kr-4 and Kr-5. Pb and Ba showed similar variations with their minimum concentrations at station Kr-2 (9.25 ppm and 366.72 ppm respectively) and maximum (14.61 ppm and 567.52 ppm respectively) in the inner fjord at station Kr-5. Cd showed decreasing trend with a minimum of 0.20 ppm and a maximum of 0.65 ppm while Ni showed an increasing trend with a minimum of 17.50 ppm and a maximum of 26.83 ppm from the outer fjord towards the inner fjord. Zn content varied from 50.28 ppm at station Kr-4 to a maximum of 82.91 ppm at station Kr-5. Along the Kongsfjord (Fig. 3.3.2b), trace elements like Cr varied from 15.69 ppm at station Ko-5 to 20.56 ppm at station Ko-4. Co varied from 14.43 ppm in the inner fjord at station Ko-5 to a maximum of 20.18 ppm at station Ko-2. Cu content varied from 19.38 ppm at station Ko-7 to 29.46 ppm at station Ko-1. Pb and Ba showed similar variations with their minimum concentrations at station

Ko-1 (7.26 ppm and 324.30 ppm respectively) and maximum (18.96 ppm and 683.26 ppm respectively) in the inner fjord at station Ko-6. Cd showed decreasing trend with a minimum of 0.12 ppm at station Ko-7 and a maximum of 0.20 ppm at station Ko-1 while Ni showed an increasing trend with a minimum of 27.50 ppm at station Ko-1 and a maximum of 32.55 ppm at station Ko-8 from the outer fjord towards the inner fjord. Zn content varied from 58.24 ppm at station Ko-4 to a maximum of 107.01 ppm at station Ko-8. Elemental concentrations are relatively higher in Kongsfjord as compared to the Krossfjord.

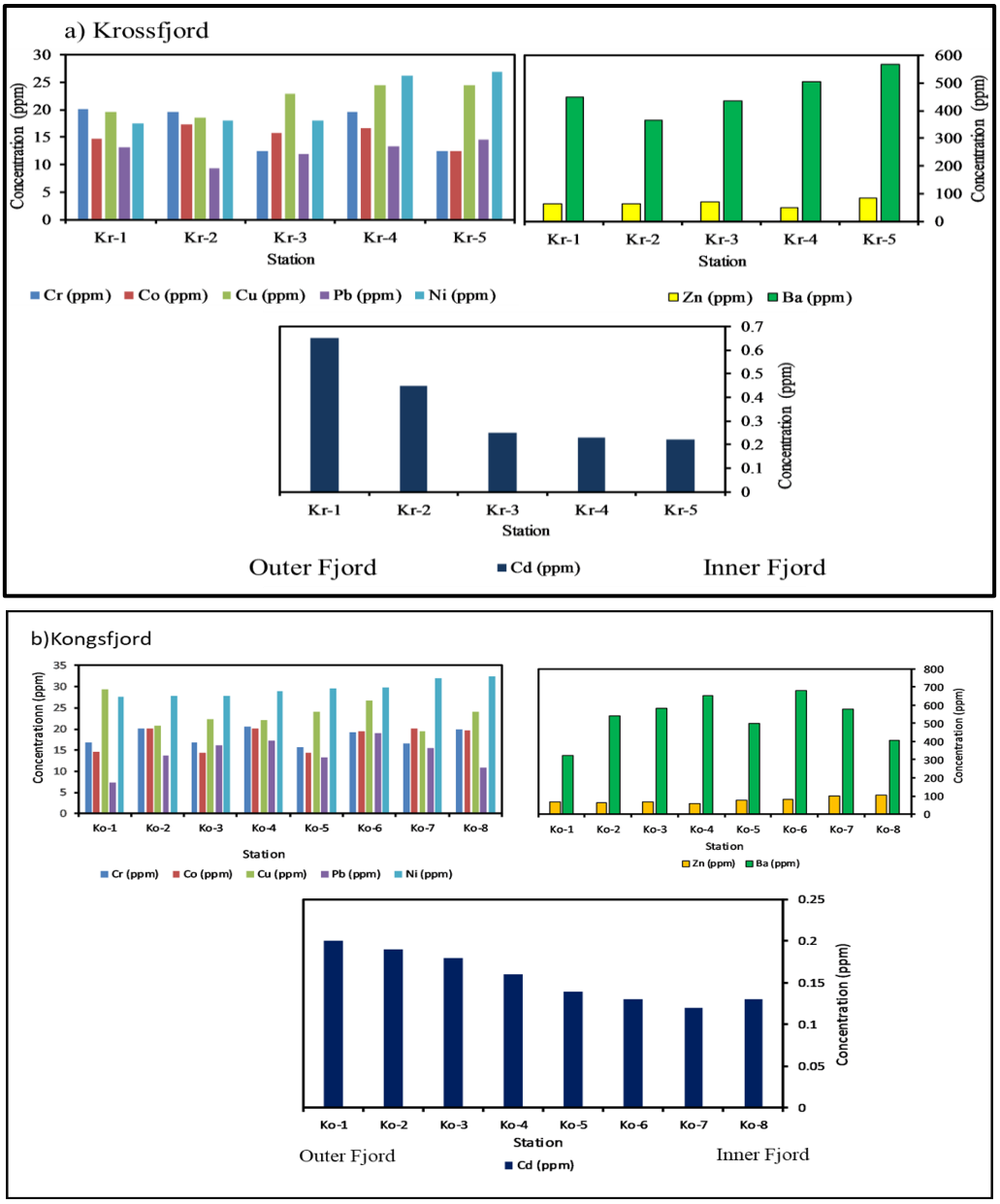

Fig. 3.3.2 Distribution of trace elements in the surface sediments along the a) Krossfjord and b) Kongsfjord.

Element distribution exhibited considerable spatial variations in both the fjords on moving away from the glacier outlets. Major elements like Al and Ti showed an overall decreasing trend from the inner fjord towards the outer region in both the fjords (Fig. 3.3.1a and b) indicating their lithogenic nature. However, average concentration 0.31% and 0.40% in Krossfjord and Kongsfjord respectively of Ti is low indicating felsic source rocks. Al and Ti are dominant components of sediments derived from the catchment rocks (Taylor and McLennan, 1985) and are good indicators of the degree of deposition of the lithogenic material (Murray and Leinen, 1996). Elements like Mg and Ca showed a similar distribution to that of Al and Ti suggesting their source to be lithogenic in nature.

Trace elements like Ni, Ba and Pb showed higher concentration in the glacier-dominated inner fjord (Fig. 3.3.2a and b) similar to that of major elements indicating their similar source and post-depositional processes. High Ba and Pb content in surface samples along the Krossfjord and Kongsfjord supports that sediment was mainly derived from felsic rocks. Ba and Pb are usually accommodated in rocks rich in feldspars (Prinz, 1967; Sensarma et al., 2016) such as gneisses and granites. Pb is higher in most of the samples along the Krossfjord and Kongsfjord where illite is also high. The higher Pb concentration in the sediments is attributed to the tendency of illite to adsorb Pb more easily into its structure (Serrano et al., 2005). Due to the similarity in ionic radii (Wedepohl, 1995), Ba replaces K in the lattice structure (Pais and Jones, 1997) and perhaps gets enhanced in micas and K-feldspars. Illite is formed by Weathering of rocks having higher content of micas and potash feldspars resulted in the formation of illite supporting the higher concentration of Ba in the surface samples of Krossfjord and Kongsfjord. Ba is found to be higher at deeper water depths at station Kr-1 and Kr-5 along the Krossfjord and at station Ko-3, Ko-4 and Ko-6 in Kongsfjord as in the water column the formation of barytes takes place below the photic zone and requires adequate water depth for its preservation (Schoepfer et al., 2015). Cd exhibited an increasing trend towards the outer fjord similar to that of finer sediments and organic carbon suggesting that Cd is biologically active and

behaves as nutrients, therefore, its distribution is regulated by the organic matter. In addition, Cd is a redox sensitive element and may have been enriched in anoxic sediments by Cadmium sulphide precipitation (Grotti et al., 2017).

3.3.A.a. i Clay mineralogy

Clay mineral assemblage of the Krossfjord-Kongsfjord system comprised of kaolinite, chlorite and illite. Illite is the predominant clay mineral in the study area followed by kaolinite and chlorite. Along the Krossfjord (Fig. 3.3.3a), illite varied within a range of 69.90% at station Kr-1 to 79.53% at station Kr-4 while along the Kongsfjord (Fig.3.3.3b) it varied from 72.55% at station Ko-1 and 80.00% at station Ko-7. Illite showed a decreasing trend on moving away from the glacial outlets in both the fjords similar to that of sand suggesting its source to be terrigenous originated from glacial weathering of the source rocks. The bedrock north of Kongsfjorden consists of mid-Proterozoic metamorphic rocks, mainly mica-schists and phyllites which act as the major source for illite in the study area. Abundant illite concentration in the study area supports its major supply from Northern Greenland and from Svalbard into the Arctic Ocean (Stein et al., 1994). Illite formation in high latitude region from muscovite is quite common. Generally, illite is considered as a detrital clay derived from acidic crystalline rock (Biscaye, 1965; Griffin et al., 1968; Windom, 1976). Illite may have also been formed by alteration of Potassium Feldspars supplied by pre-Devonian igneous rocks (gneisses) transporting through streams draining this region. The decreasing illite concentration towards the outer fjord indicates dilution by other minerals brought by Arctic and Atlantic water mass. Kaolinite content fluctuated from 9.30% at station Kr-4 to 18.06% at station Kr-1along the Krossfjord while along the Kongsfjord, it varied from 7.80% at station Ko-7 and 18.30% at station Ko-6. An appreciable amount of kaolinite in this region might have been formed either in an interval of warmer and colder conditions resulting in chemical weathering of Quartzites or possibly it is of detrital nature, transported from a distant source, probably located underneath the ice (Srivastava et al., 2011). Hjelle (1993) suggested that the Kaolinite present in the fjord system originated from the fluvial facies dominated by reddish

sandstone and conglomerate in the middle Carboniferous. Smectite concentrations are particularly absent in Svalbard areas. Among the clay minerals, chlorite content was low having average concentration 10.96% along the Krossfjord and 10.69% along the Kongsfjord which may be due to the highly unstable nature of chlorite. The minimum concentration 9.30% along the Krossfjord at station Kr-4 and 8.45% of chlorite is at station Ko-6 along the Kongsfjord and the maximum 12.04% at station Kr-1 along the Krossfjord and 14.04% is at station Ko-8 along the Kongsfjord. The chlorite in the study area mainly comes from low-grade Proterozoic metamorphic phyllite and mica schists that surround Kongsfjord (Fendeng et al., 2018).

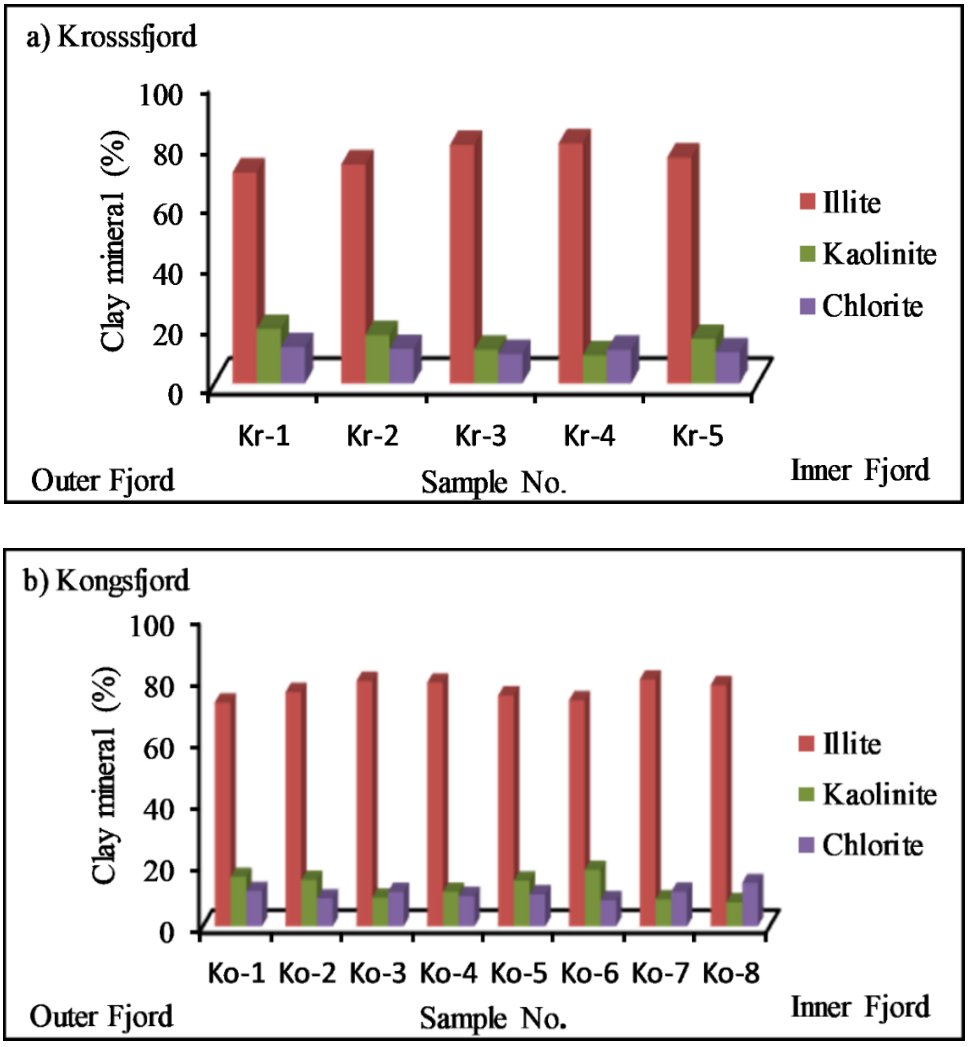

Fig. 3.3.3 Distribution clay minerals in the surface sediments along the a) Krossfjord and b) Kongsfjord.

Illite crystallinity and illite chemistry were computed to understand the degree of weathering and source for clay minerals. Crystallinity defines the extent of "opening" present in the clay minerals and is considered to be the index of hydrolyzation in the study area (Chamley, 1989; Bejugam and Nayak, 2017). A larger opening (poor crystallinity) suggests enhanced rainfall and temperature conditions resulting in hydrolyzation of clay minerals (Thamban et al., 2002). The illite crystallinity in all the sediment samples studied was noted <0.4 $\Delta 2\theta$ suggesting the availability of very well crystalline illite (Ehrmann et al., 2005) in the region derived from physical weathering. Illite chemistry showed values <0.5 indicating strong physical weathering of mica schists present in the north of Kongsfjorden supplying Fe, Mg-rich illites (Gingele, 1996). This is also supported by lower Chemical Index of alteration (CIA) ranging between 39-47% reported by Kumar et al. (2014) suggesting least degree of chemical alteration of the sediments in the study area.

Further, interpretation made on the source of elements input in sediments of the Krossfjord and Kongsfjord are supported by R–mode factor analysis. The factor loadings are presented in Table 3.3.1a. For the surface samples collected from Krossfjord, four factors could be extracted contributing to about 52.86, 22.34, 16.20 and 8.59 percent of the variance respectively which account for a cumulative percentage of 100.00 with Eigen value >1. For the first factor, TOC, TN, BSi, Mn, Cd are observed to be positively loaded, thus indicating their association with organic matter. Elements like Al, Ti, Mg, Ca, Cu, Ni and Ba are found to be negatively loaded indicating their common lithogenic nature. Factor 2, 3 and 4 are less significant and does not represent any major association of elements. Along the Kongsfjord, four factors could be extracted contributing to about 38.85, 20.98, 15.50 and 18.26 percent of the variance respectively which account for a cumulative percentage of 86.97 with Eigen value >1 (Table 3.3.1b). For the first factor, BSi and Cd are observed to be negatively loaded, thus indicating their similar source. Elements like Al, Ti, Mg, Ni and Zn are found to be positively loaded indicating their common lithogenic nature. For, the second factor silt, Fe and Ba are observed to be positively loaded indicating their similar source.

Table 3.3.1a Factor loadings of the surface sediments of Krossfjord

	Factor1	Factor2	Factor3	Factor4
% of total Variance	52.86	22.34	16.20	8.59
Cumulative % of total variance	52.86	75.20	91.40	100.00
Sand	0.38	**0.86**	-0.28	-0.20
Silt	-0.54	**0.81**	-0.21	-0.12
Clay	0.12	**-0.94**	0.27	0.18
TOC	**0.73**	0.54	0.41	-0.12
TN	**0.97**	0.08	0.18	-0.13
TP	0.39	**-0.87**	0.15	0.27
BSi	**0.96**	0.11	0.13	-0.21
Al	**-0.88**	0.47	0.06	-0.06
Ti	**-0.98**	-0.06	-0.04	-0.18
Fe	0.45	0.56	0.68	0.13
Mn	**0.86**	0.05	0.50	-0.09
Mg	**-0.89**	0.01	0.07	-0.44
Ca	**-0.71**	0.39	-0.18	0.56
Cr	0.64	-0.22	-0.37	-0.63
Co	0.39	-0.15	**-0.91**	0.06
Cu	**-0.94**	-0.33	0.09	0.03
Pb	-0.57	-0.42	0.66	-0.26
Cd	**0.94**	-0.02	0.26	-0.22
Ni	**-0.86**	-0.04	0.04	-0.51
Ba	**-0.78**	-0.18	0.50	-0.33
Zn	-0.34	0.52	**0.70**	0.35
Explored variance	11.10	4.69	3.40	1.80
Proportion Total	0.53	0.22	0.16	0.09

Extraction: Principal components (marked loadings are significant >0.7

Table 3.3.1b Factor loadings of the surface sediments of Kongsfjord

	Factor1	Factor 2	Factor 3	Factor 4
% of total variance	38.85	20.98	15.50	18.26
Cumulative % of total variance	38.85	59.84	75.34	86.97
Sand	0.47	-0.59	-0.53	-0.32
Silt	-0.21	**0.84**	0.34	0.29
Clay	-0.61	-0.14	0.52	0.19
TOC	-0.56	0.05	**-0.74**	**0.34**
TN	-0.70	0.23	-0.59	0.26
TP	0.08	-0.47	-0.01	**-0.73**
BSi	**-0.84**	0.04	0.13	0.26
Al	**0.76**	-0.38	-0.35	0.26
Ti	**0.93**	-0.12	0.02	0.33
Fe	0.55	**0.79**	-0.11	0.09
Mn	0.23	0.21	-0.35	-0.51
Mg	**0.96**	-0.04	0.01	0.14
Ca	0.34	-0.05	0.67	0.37
Cr	0.20	0.52	**-0.80**	0.13
Co	0.56	0.65	-0.39	0.29
Cu	-0.34	-0.58	-0.37	0.02
Pb	0.35	0.68	0.15	-0.53
Cd	**-0.94**	0.07	-0.14	0.13
Ni	**0.94**	-0.18	0.03	0.25
Ba	0.28	**0.75**	0.13	-0.50
Zn	**0.85**	-0.33	0.10	0.35
Explored variance	8.16	4.41	3.26	2.44
Proportion Total	0.39	0.21	0.16	0.12

Extraction: Principal components (marked loadings are significant >0.7)

Pearson's correlation was also carried out. Although the number of samples were very less, it showed significant correlations. Clay displayed good correlation with TP and TOC showed good correlation with Fe indicating the association of Fe with organic matter in Krossfjord. TN showed significant correlation with BSi, Mn and Cd. Ti showed good correlation with Mg, Cu and Ni. Mn showed good correlation with Cd. Mg showed good correlation with Ni and Ba and Pb with Ba. Along the Kongsfjord, TOC showed good correlation with TN indicating their similar source. TN showed good correlation with Cd. Al showed good correlation with Ti, Mg, Ni and Zn. Fe showed good correlation with Co. Mg showed good correlation with Ni and Zn. Cr showed good correlation with Co and Pb showed good correlation with Ba. Elements like Cr and Cu does not show similarity with any of the trace elements indicating their different source (Table 3.3.2a and b) or post-depositional remobilization. Further, to understand the source and post-depositional remobilization of these elements fractionation of these elements have been carried out.

Table 3.3.2: Pearson's correlation between major and trace elements of a) Krossfjord and b) Kongsfjord

a) Krossfjord

	Sand	Silt	Clay	TOC	TN	TP	BSi	Al	Ti	Fe	Mn	Mg	Ca	Cr	Co	Cu	Pb	Cd	Ni	Zn	Ba
Sand	1.00																				
Silt	0.57	1.00																			
Clay	-0.87	**-0.90**	1.00																		
TOC	0.65	-0.02	-0.34	1.00																	
TN	0.42	-0.48	0.06	0.84	1.00																
TP	-0.69	**-0.97**	**0.95**	-0.16	0.30	1.00															
BSi	0.47	-0.43	0.01	0.84	**1.00**	0.25	1.00														
Al	0.06	0.85	-0.54	-0.35	-0.80	-0.76	-0.77	1.00													
Ti	-0.38	0.51	-0.10	-0.74	**-0.94**	-0.38	**-0.92**	0.84	1.00												
Fe	0.44	0.06	-0.27	**0.89**	0.58	-0.17	0.55	-0.09	-0.52	1.00											
Mn	0.25	-0.52	0.17	0.87	**0.94**	0.35	**0.92**	-0.70	-0.85	0.74	1.00										
Mg	-0.27	0.53	-0.17	-0.56	-0.80	-0.46	-0.76	0.82	**0.95**	-0.40	-0.69	1.00									
Ca	0.00	0.67	-0.40	-0.45	-0.77	-0.50	-0.78	0.77	0.58	-0.15	-0.73	0.38	1.00								
Cr	0.28	-0.38	0.07	0.27	0.63	0.22	0.68	-0.66	-0.49	-0.17	0.41	-0.33	-0.83	1.00							
Co	0.26	-0.15	-0.05	-0.17	0.20	0.16	0.23	-0.47	-0.36	-0.52	-0.13	-0.45	-0.14	0.58	1.00						
Cu	-0.67	0.22	0.23	-0.82	**-0.93**	-0.06	**-0.93**	0.67	**0.93**	-0.54	-0.78	0.83	0.54	-0.59	-0.41	1.00					
Pb	-0.71	-0.14	0.46	-0.34	-0.43	0.17	-0.45	0.35	0.60	-0.07	-0.16	0.67	-0.02	-0.35	-0.78	0.72	1.00				
Cd	0.31	-0.55	0.17	0.80	**0.99**	0.37	**0.98**	-0.81	**-0.89**	0.56	**0.96**	-0.72	-0.85	0.65	0.12	-0.86	-0.29	1.00			
Ni	-0.27	0.48	-0.14	-0.57	-0.76	-0.43	-0.72	0.77	**0.94**	-0.45	-0.68	**1.00**	0.31	-0.24	-0.40	0.81	0.66	-0.68	1.00		
Zn	0.05	0.41	-0.27	0.28	-0.21	-0.38	-0.25	0.56	0.21	0.67	0.06	0.20	0.51	-0.82	-0.82	0.22	0.35	-0.22	0.12	1.00	
Ba	-0.53	0.21	0.15	-0.42	-0.64	-0.16	-0.64	0.65	0.82	-0.16	-0.41	**0.88**	0.21	-0.44	-0.75	0.83	**0.93**	-0.53	0.87	0.40	1.00

Bold values represent correlation significant at P =<0.05, N=5

b) Kongsfjord

	Sand	Silt	Clay	TOC	TN	TP	BSi	Al	Ti	Fe	Mn	Mg	Ca	Cr	Co	Cu	Pb	Cd	Ni	Zn	Ba
Sand	1.00																				
Silt	**-0.87**	1.00																			
Clay	-0.62	0.15	1.00																		
TOC	0.01	-0.02	0.01	1.00																	
TN	-0.20	0.22	0.06	**0.92**	1.00																
TP	0.61	-0.61	-0.25	-0.24	-0.37	1.00															
BSi	-0.47	0.34	0.41	0.48	0.67	-0.22	1.00														
Al	0.63	-0.56	-0.38	-0.10	-0.40	0.00	**-0.75**	1.00													
Ti	0.40	-0.20	-0.47	-0.43	-0.59	-0.13	-0.69	**0.84**	1.00												
Fe	-0.16	0.55	-0.54	-0.13	-0.13	-0.28	-0.40	0.16	0.44	1.00											
Mn	0.27	-0.04	-0.46	-0.15	0.00	0.05	-0.41	0.07	0.00	0.16	1.00										
Mg	0.42	-0.19	-0.55	-0.52	-0.61	-0.10	**-0.74**	**0.77**	**0.96**	0.46	0.25	1.00									
Ca	-0.20	0.27	-0.03	-0.57	-0.42	-0.25	0.13	-0.01	0.46	0.09	-0.26	0.46	1.00								
Cr	0.14	0.14	-0.50	0.56	0.45	-0.32	-0.28	0.32	0.16	0.62	0.31	0.17	-0.52	1.00							
Co	0.01	0.40	-0.65	0.11	0.06	-0.40	-0.39	0.36	0.53	**0.92**	0.21	0.53	0.04	**0.79**	1.00						
Cu	0.44	-0.53	-0.03	0.40	0.45	0.06	0.40	0.00	-0.22	-0.69	0.14	-0.17	-0.03	-0.14	-0.45	1.00					
Pb	-0.13	0.34	-0.28	-0.43	-0.28	0.00	-0.34	-0.17	0.09	0.63	0.42	0.27	0.03	0.26	0.39	-0.45	1.00				
Cd	-0.51	0.26	0.60	0.65	**0.74**	-0.24	0.70	-0.61	**-0.86**	-0.46	-0.13	**-0.90**	-0.47	-0.02	-0.41	0.25	-0.41	1.00			
Ni	0.47	-0.28	-0.50	-0.45	-0.65	0.03	**-0.71**	**0.84**	**0.99**	0.41	-0.05	**0.93**	0.43	0.11	0.49	-0.25	0.08	**-0.89**	1.00		
Zn	0.40	-0.30	-0.33	-0.48	-0.65	-0.08	-0.67	**0.85**	**0.95**	0.20	0.02	**0.90**	0.48	-0.04	0.31	-0.12	-0.12	**-0.76**	**0.93**	1.00	
Ba	-0.20	0.42	-0.28	-0.37	-0.20	-0.03	-0.25	-0.25	0.03	0.67	0.38	0.20	0.03	0.29	0.43	-0.46	**0.99**	-0.35	0.01	-0.19	1.00

Bold values represent correlation significant at P =<0.05, N=8

3.3.A.a. ii Fractionation of metals and potential bioavailability

In the aquatic system, bulk metal concentrations are used oftenly to evaluate the level of input of metals. However, it can overestimate the risk associated as it does not take the factors such as bioavailability, mobility and toxicity which depends on the chemical form (Cuong and Obbard, 2006; Nemati et al., 2011) into consideration. Thus, the assessment of different chemical forms of metals in the sediment is essential. Speciation of an element in any geochemical environment gives a comprehensive understanding of various phases of metal.

The potential bioavailability of the metals for the fjord system has been assessed by the metal fractionation approach. The fractionation of the metals was carried out in the five geochemical phases namely exchangeable (F1), Carbonate (F2), Fe-Mn oxide (Reducible-F3), organic matter/ sulfide bound (oxidizable-F4) and Residual (F5) for the surface samples of Krossfjord and Kongsfjord. A sum of the first four fractions (F1+F2+F3+F4) is considered as the potential bioavailability. The most extractable fractions among these fractions significantly affect the aquatic ecosystems. The residual fraction (F5) is of detrital or primary mineral origin which is an indicator of the natural source (Salomons and Forstner, 1980).

In the surface sediments of Krossfjord and Kongsfjord, Fe concentrations varied in the order of F5>F3>F2>F4>F1. Iron was concentrated in substantial amount in the residual fraction at all the stations along the Krossfjord and Kongsfjord (Fig. 3.3.4). High concentration of Fe (>80%) in the residual phase indicated an input of terrigenous material from weathering of rocks available in the catchment area. In the residual fraction, Fe is immobile due to its bonding with primary and secondary minerals and therefore it is unavailable for uptake of organisms (Tessier et al., 1979). Among the bioavailable phses, Fe was concentrated in the Fe-Mn oxide phase at all the stations in both the fjords. The concentration of Fe in the organic/ sulfide bound phase is attributed to the formation of iron sulfides. It is known that Fe prefers oxide phase in oxic conditions and sulphides in anoxic environments.

Chester and Jickells (2012) suggested that Mn is a redox-sensitive element similar to that of Fe which exhibits active biogeochemical behavior in the aqueous environment and transforms easily from dissolved phase to the particulate phase and vice-versa due to the physicochemical changes. Further, various parameters like redox conditions, pH and

presence of carbonate ions regulates the geochemical association of Mn in the form of oxides, carbonates, organo-metallic complexes or sulfides (Farias et al., 2007). Residual phase consists of relatively lower concentration of Mn in the sediments of the Krossfjord (average 37.73%) and Kongsfjord (average 34.05%) and was found concentrated in the Fe-Mn oxide bound phase in both the fjords (average 42.16% in Krossfjord and 43.33% in Kongsfjord) due to the formation of oxides (Fig. 3.3.4). Carbonate fraction is a loosely bound phase. Considerable quantity of Mn (average 10.90% in Krossfjord and 11.34% Kongsfjord) is concentrated in carbonate fraction. Similar ionic radii of Mn as that of Ca enables Mn to replace Ca in the carbonate fraction (Noronha-D' Mello and Nayak, 2015; Grotti et al., 2017). Loosely bound exchangeable and carbonate Mn can be released from surface sediments to water and preferentially bioavailable to the biota living in sediments and water. Manganese is relatively low (4.96% in Krossfjord and 5.98% in Kongsfjord) in the organic/sulfide phase due to low organic affinity of Mn (Bendell young and Harvey, 1992). Chromium was largely associated with the residual phase in the sediments of Krossfjord (average 85.80%) and Kongsfjord (average 83.92%) as it mainly gets transported to the sediment within the residual phase (Noronha-D' Mello and Nayak, 2015). Among bioavailable phases a considerable quantity of Cr was found associated with organic/ sulfide bound fraction. Tribovillard et al. (2008) stated that because of structural and electronic incompatibilities with pyrite, Cr (III) uptake by authigenic Fe-sulfides is very limited. Therefore Cr, is preferably associated with organic matter as compared to sulfides. Additionally, Cr does not form an insoluble sulfide (Huerta-Diaz and Morse, 1992; Tribovillard et al., 2008). The concentration of Cr in the Exchangeable and Carbonate bound fraction was very less compared to the other two bioavailable fractions (Fig.3.3.4). Cobalt was predominantly bound to the residual fraction both in Kongsfjord (average 39.55%) and Krossfjord (average 35.05%) indicating its preferential association with silicates and aluminosilicates (Grotti et al., 2017). Higher Co concentration in Fe-Mn Oxide (average 34.00 %) fraction in the Krossfjord explains the adsorption of Co on the surface of Fe-Mn colloids as observed by Nasnodkar and Nayak (2017) in the sediments of the tropical estuaries. Fe-Mn colloids have played an important role in controlling the mobility of Co in the fjord environment due to their ability of scavenging Co in sediments (Kaasalainen and Yli-Halla, 2003). Considerable percentage of Co was available in reducible fraction (average 33.01%) in Kongsfjord. Lower amount of Co was found in the oxidizable (12.20%) and exchangeable (10.18%) fraction in both the fjords. Average 50% of Cu was found associated with the residual fraction and the remaining 50% was found distributed in the bioavailable fractions in both the fjords

indicating their availability to the sediment-associated biota. Among bioavailable phases, Cu in oxidizable (organic/sulfide) fraction was appreciable (average 27.11% in Krossfjord and 24.49% in Kongsfjord) suggesting its partial association with the refractory organic matter as humic substances or sulfides (Grotti et al., 2017). Thus, grain size, Fe-Mn oxy-hydroxides and organic matter along with pH and Eh have affected the fractionation of metals in different geochemical phases within the sediments of Krossfjord and Kongsfjord.

The metal fractionation showed >80% average concentration of metals viz. Fe and Cr in the residual phase indicating their source to be lithogenic derived from the weathering of source rock while bio-available phases consist of the remaining <20%. Cu showed 50% average concentration in residual phases and remaining 50% was associated with bioavailable phases. However, Mn and Co showed <40% concentration in the residual phase and >60% concentration of these metals were distributed in the bioavailable phases suggesting their availability for uptake and accumulation in aquatic biota (Gambrell, 1994; Ladigbolu, 2014).

Bioavailability of metals like Mn, Co and Cu showed considerable spatial variations from inner fjord to the outer fjord. Mn showed an increasing trend from station Kr-1 to station Kr-5 while in the Kongsfjord Mn decreased from station Ko-1 to Ko-8 with an overall decreasing trend towards the inner fjord. In the Kongsfjord, bioavailability of Co increased station Kr-1 to station Kr-5 with highest concentration at station Kr-3 and Kr-4 whereas in the Kongsfjord, Co fluctuated from one station to the other with an overall decreasing trend from station Ko-1 to station Ko-8. Higher bioavailability was noted at station Ko-1, Ko-3, Ko-5 and station Ko-7 while lower bioavailability was at station Ko-2, Ko-4, Ko-6 and Ko-8. Further, Cu showed an increasing trend from station Kr-1 to station Kr-5 with the highest bioavailability percentage at station Kr-3 in Krossfjord. In the Kongsfjord, bioavailability of Cu showed an increasing trend from station Ko-1 to Ko-8 with high percentage of bioavailability at station Ko-2 and Ko-7.

In labile fractions (F1+F2), due to weak electrostatic interaction, metals are sorbed weakly and retained on the surface of sediment and can precipitate with carbonates present in the sediments after releasing by ion exchange processes (Filgueiras et al., 2004, Nasnodkar and Nayak, 2017). In the labile fraction (F1+F2), Mn showed 15.15% average in Krossfjord and 16.64% average in Kongsfjord, Co showed 11.06% average in Krossfjord and 10.18% average in Kongsfjord posing a medium risk to the sediment associated biota. Cu showed 6.83% in Krossfjord and 4.33% average in Kongsfjord posing low risk to the

sediment-associated biota. The metals available in labile fractions can migrate easily in neutral or slightly acidic waters (Alvarez-Valero et al., 2009) causing a potential ecological risk to the sediment-associated biota.

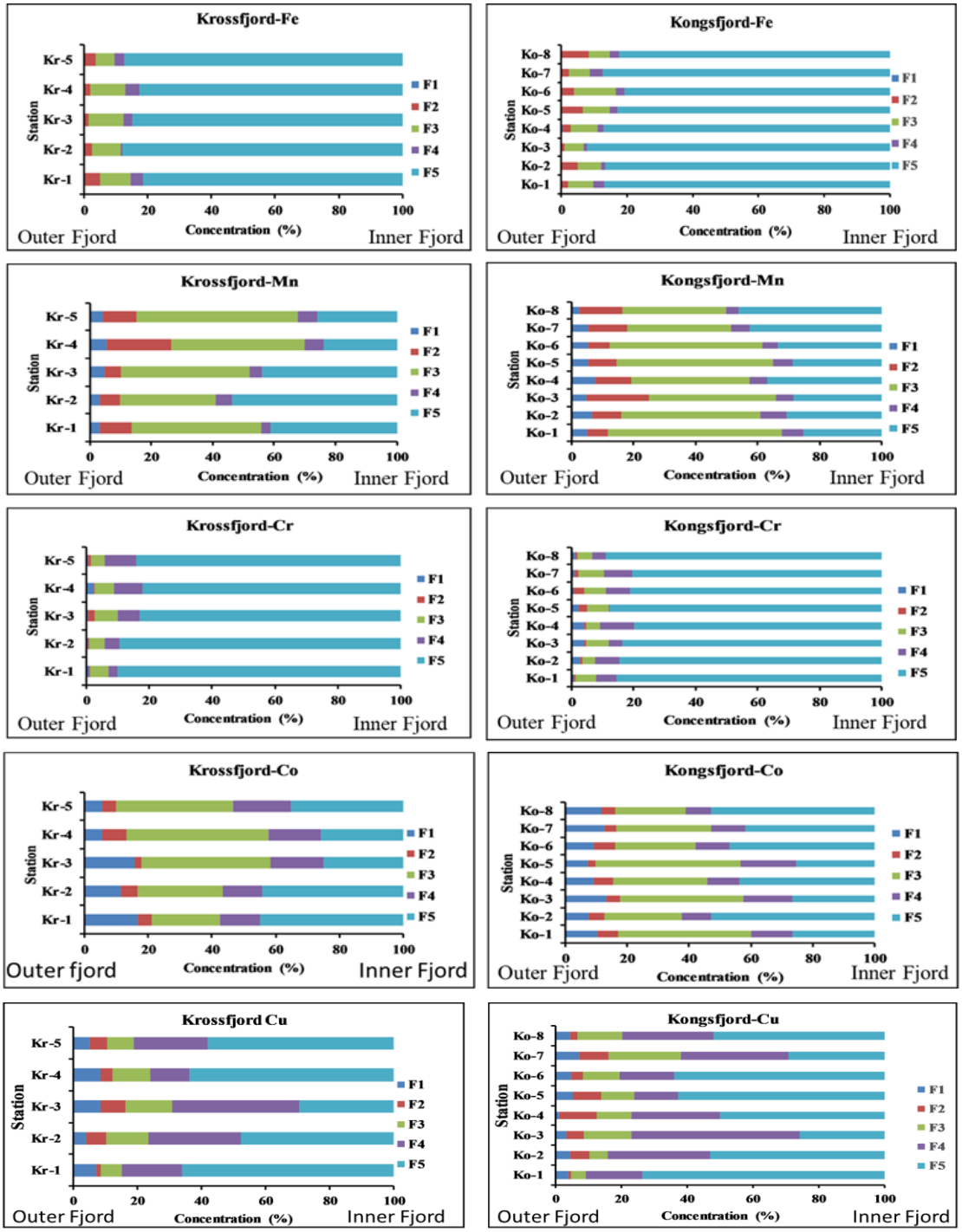

Fig. 3.3.4. Speciation of metals Fe, Mn, Cr, Co and Cu in Krossfjord and Kongsfjord where F1 exchangeable, F2 carbonate bound, F3 Fe–Mn oxide, F4 organic/sulphide bound, F5 residual fractions.

3.3.A.b. Prydz Bay (Thala Fjord), East Antarctica

Along the Prydz Bay (Fig. 3.3.5) Al content fluctuated in a range between 0.23% at station P2 and 1.74% at station P1. Ti varied within a small range of 0.05% in sample P2 and 0.21% in sample P5. Fe and Mn content were largely consistent from shallow to deeper water regions and varied from 0.47% and 0.010% respectively at station P2 to 2.50% and 0.033% at station P5 and P7 respectively. Mg ranged between 0.13% at station P4 and 0.42% at station P1. Ca ranged between 1.36% at station P7 and 26.77% at station P2 with exceptionally high content 26.77% and 16.38% at station P2 and P6 respectively.

Trace elements like Cr varied from 44.50 ppm at station P3 to 124.00 ppm at station P7 (Fig.3.3.5) along the Prydz Bay. Co varied from 4.72 ppm at station P1 to a maximum of 27.11 ppm at station P4. Cu content varied from 72.78 ppm at station P1 to 315.73 ppm at station P4. Pb and Ba showed minimum concentrations at station P4 and P1 respectively (0.80 ppm and 154.08 ppm respectively) and showed similar variations with their maximum concentrations at (2.51 ppm and 331.13 ppm respectively) at station P7. Cd and Ni showed similar variations with a minimum concentration of 4.86 ppm and 87.68 ppm respectively at P1 and a maximum of 9.25 ppm and 159.60 ppm respectively at P4. Zn content varied from 13.25 ppm at station P1 to a maximum of 36.15 ppm at station P4.

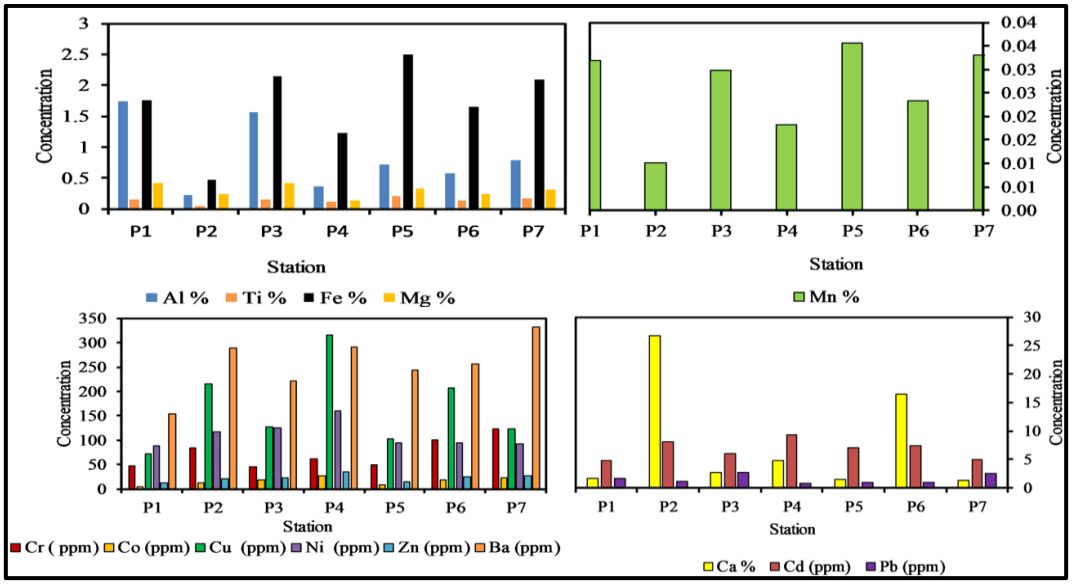

Fig. 3.3.5. Distribution of major and trace elements in the surface sediments along the Prydz Bay

The major elements in the study area are in the order of Fe>Al>Mg>Ti>Mn (Fig. 3.3.6). Bulk concentration of elements like Al, Ti, Fe, Mn and Mg in the marine sediments generally reflects the concentration of terrigenous aluminosilicate phases (Shimmield and Mowbray, 1991). Variations in these elements are predominantly controlled by a varying supply of detrital material. In Prydz bay, most of these elements reveal similar variability indicating their similar lithogenic source and common depositional processes. Elements like Al and Mg exhibited strong correlation (r=0.87) indicating their terrigenous source and common post-depositional behavior. The Al content in marine sediments is an indicator of lithogenous input as the average concentration of Al in different rocks varies by only 10% from an average crustal value (Turekian and Wedepohl, 1961). Ti showed strong correlation with Fe (r=0.97) and Mn (r=0.95). These elements thus support their lithogenic nature derived from the weathering of rocks such as gneisses present in the catchment area, thus, these elements are classified as terrigenous elements. The supply of terrigenous material to the Prydz bay is mainly due to either by glaciomarine input (glaciogenic) or by erosion and weathering of the catchment rocks, transported to the sea by rafting of iceberg, melting and roll over at the margin of the bay or by strong katabatic winds (aeolian).

Among the trace elements Ba was the most abundant element in the study area, followed by Cu and Ni. In general, the overall abundance of elemental concentrations in the sediments follows the order: Ba>Cu> Ni>Zn>Co>Cd>Pb (Fig.3.3.5). Cu showed good correlation with Cd, Ni and Zn. The enrichment of trace elements along with carbonate, TOC and opal in marine sediments has been used as Palaeo- productivity indicators (Collier and Edmond, 1984; Shimmield and Pedersen, 1990). Metals like Co (r=0.85), Cu (r=0.85) and Zn (r=0.93) showed strong correlation with TOC (Table 3.3.4) and Ni exhibited significant correlation with TOC (r=0.93), TN (r=0.91) along with BSi (r=0.81) indicating their biogenic source. Cd showed a positive correlation with TOC (r=0.65) and strong correlation with phosphorus (r=0.97) while Zn showed a positive correlation with BSi (r=0.61) and strong correlation with TOC (r=0.93) and TN (r=0.83) indicating that these elements are derived biogenically and are classified as biogenic and organic associated element. Elements absorbed and assimilated by marine organisms are released back into the water column as biological material, forming biogenically sourced material in the sediments. In the Prydz Bay, the average bulk content of

Cd, Co, Cu, Ni and Zn were 6.82 ppm, 16.57 ppm, 166.56 ppm, 110.29 ppm and 22.91 ppm respectively and their respective biogenic proportion was 6.81 ppm, 15.45 ppm, 165.19 ppm, 108.50 ppm and 17.91 ppm respectively suggesting that ~99.85%, 93.24%, 99.18%, 98.38% and 78.18% of these elements respectively was derived from biogenic input. While the remaining portion 0.15%, 6.76%, 0.82%, 1.62% and 21.82% of these elements were associated with silicates. However, Pb (avg. 1.56 ppm) and Ba (255.31 ppm) was found to be of lithogenic origin as biogenic input is negligible. Lithogenic sources probably have made less contribution in this region may be because most of the lithogenic fraction are used up by phytoplankton resulting in high values of the biogenic fraction. In the absence of fluvial input and lack of soil (Gasparon and Matschullat, 2006) around the bay trace elements in the sediments originated from lithogenic inputs and marine biogenic deposition. High biogenic input on the continental shelf was evidenced by the high content of BSi and TOC suggesting extensive biological processes in the area which is supported by the observation of Isla et al. (2004) that the biogenic deposition is high on the continental shelf than that in the deep ocean. Anthropogenic activities at the research stations must have contributed negligible levels (lower than natural variability) of trace metals to the Prydz Bay (Choudhary et al., 2018).

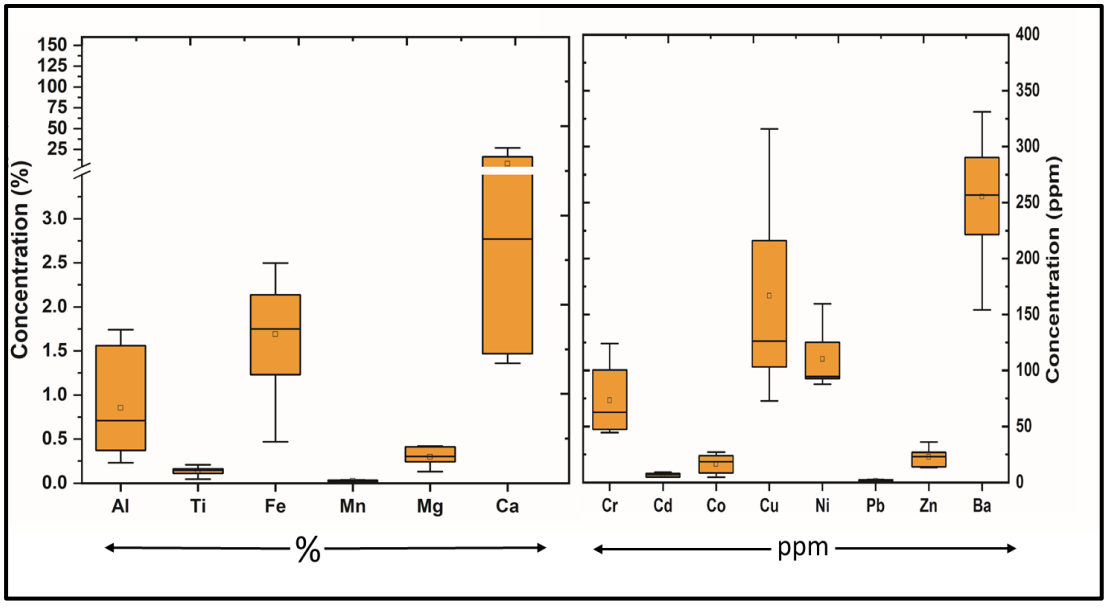

Fig.3.3.6**.** Box and Whisker plots of element concentrations in surface sediments along the Prydz Bay (The horizontal bar in the box displays the mean value, the ends of the Whiskers to the maximum and minimum values. The top and bottom of the boxes include half the data points between the average and the extremes of the range).

To support interpretation made on the source of element input in sediments of the continental shelf, Prydz Bay, R–mode factor analysis was performed. The factor loadings are presented in Table 3.3.3. For the surface samples, four factors could be extracted contributing to about 54.59, 20.92, 8.96 and 7.65 percent of the variance respectively which account for a cumulative percentage of 92.12 with Eigen value >1. For the first factor, clay, TOC, TP, Cd, Cu, Ni and Zn are observed to be negatively loaded, thus indicating their association with organic matter along with fine-grained sediments. Elements like Al, Mn and Mg are found to be positively loaded indicating their common lithogenic nature. Factor 2, 3 and 4 are less significant and does not represent any major association.

Table 3.3.3. Factor loadings of the surface sediments of Prydz Bay

	Factor 1	Factor 2	Factor 3	Factor 4
% of total Variance	57.62564	19.73373	8.96557	8.06759
Cumulative % of total variance	57.62564	77.35937	86.32495	94.39253
Sand	0.04999	**-0.727961**	0.313785	0.459341
silt	0.60384	0.491033	-0.234676	-0.507957
clay	**-0.90254**	-0.021105	0.041734	0.294224
TOC	**-0.84004**	0.486421	-0.008436	-0.010530
TN	-0.67244	0.642469	-0.050023	0.172340
BSi	-0.58414	**0.722966**	-0.236149	-0.139661
TP	**-0.88660**	-0.146064	-0.383963	0.076970
Al	**0.79694**	0.253515	-0.201999	0.034577
Ti	0.67520	0.396067	0.136808	0.495329
Fe	0.69233	0.536811	0.164985	0.299227
Mn	**0.81549**	0.393911	0.205789	0.334310
Mg	**0.93626**	0.094799	-0.181381	-0.233183
Ca	-0.48840	-0.651908	-0.094821	-0.538642
Cr	-0.24918	-0.242662	**0.902521**	-0.232156
Co	-0.66998	0.499854	0.498374	-0.048294
Cu	**-0.98092**	0.000380	-0.032569	0.083489
Pb	0.51875	0.493939	0.300563	-0.496324
Cd	**-0.87460**	-0.077548	-0.354672	0.098260
Ni	**-0.78950**	0.446500	-0.352528	0.013242
Ba	-0.63483	0.156295	0.597563	-0.228542
Zn	**-0.80707**	0.387492	0.351358	0.053356
Explored Variance	11.00216	3.995982	2.416944	1.777625
Proportion Total	0.52391	0.190285	0.115093	0.084649

Extraction: Principal components (marked loadings are significant >0.7)

Further, TOC (1.49%), TN (0.23%) and TP (0.014%), was found low near the coast at station P1 at 30 m water depth as minimum nutrient concentrations are found in oligotrophic surface waters. Further, these organic elements showed an increase with increasing water depth. Low concentrations of Cd (4.86 ppm) and Zn (13.25 ppm) at station P1 suggested their depletion, caused by its use by marine phytoplanktons. Cd showed strong positive correlation with TP and Zn exhibiting significant correlation with TOC and TN (Table 3.3.4) which indicated their similar behavior suggesting the role of trace metal along with the nutrients in controlling productivity. Cd, is generally detrimental to living organisms, however, along with Zn it has a nutrient-like profile. Its concentration is well correlated to that of TP that reveals the accumulation of Cd in the fossilized tests of marine organisms and is used as a measure of past nutrient concentrations in the sea (Sunda, 2012). Cd enhances the growth rate of some marine phytoplankton and can be used as a substitution for Zn when Zn is limited (Morel et al., 1994). High Zn concentration is usually found below the photic zone; however, thermohaline and wind-driven upwelling can bring high-nutrient and high-zinc to the surface, especially in polar regions (Sunda, 2012). The near-surface processes such as algal uptake, settling and shallow water regeneration can influence the composition of nutrients and trace metals.

Table 3.3.4 Pearson's correlation coefficients of sediment components and elements in Prydz Bay

	Sand	Silt	Clay	TOC	TN	BSi	TP	Al	Ti	Fe	Mn	Mg	Ca	Cr	Co	Cu	Pb	Cd	Ni	Zn	Ba
Sand	1.00																				
Silt	-0.71	1.00																			
Clay	0.08	**-0.76**	1.00																		
TOC	-0.31	-0.30	0.71	1.00																	
TN	-0.34	-0.26	0.68	**0.93**	1.00																
BSi	**-0.78**	0.19	0.45	**0.80**	**0.77**	1.00															
P	-0.10	-0.52	**0.83**	0.63	0.48	0.54	1.00														
Al	0.01	0.52	-0.74	-0.43	-0.21	-0.36	**-0.76**	1.00													
Ti	-0.11	0.41	-0.49	-0.45	-0.23	-0.12	-0.61	0.46	1.00												
Fe	-0.27	0.59	-0.59	-0.38	-0.19	-0.02	-0.68	0.52	**0.97**	1.00											
Mn	-0.09	0.51	-0.63	-0.53	-0.29	-0.25	**-0.80**	0.64	**0.95**	**0.96**	1.00										
Mg	-0.13	0.73	**-0.91**	-0.71	-0.55	-0.44	**-0.82**	**0.87**	0.47	0.54	0.66	1.00									
Ca	0.15	-0.27	0.24	0.09	-0.23	-0.06	0.53	-0.59	**-0.82**	**-0.81**	**-0.84**	-0.40	1.00								
Cr	0.31	-0.33	0.19	0.07	-0.11	-0.19	-0.09	-0.50	-0.22	-0.19	-0.18	-0.38	0.34	1.00							
Co	-0.20	-0.25	0.54	**0.85**	0.75	0.62	0.29	-0.44	-0.24	-0.13	-0.28	-0.65	0.00	0.50	1.00						
Cu	0.02	-0.62	**0.86**	**0.85**	0.68	0.56	**0.87**	-0.73	-0.64	-0.65	**-0.79**	**-0.93**	0.46	0.20	0.68	1.00					
Pb	-0.35	0.63	-0.56	-0.13	-0.01	-0.04	-0.75	0.63	0.21	0.39	0.46	0.66	-0.40	0.10	0.08	-0.56	1.00				
Cd	-0.14	-0.45	**0.76**	0.65	0.48	0.60	**0.97**	**-0.77**	-0.52	-0.57	-0.74	**-0.83**	0.51	-0.07	0.36	**0.88**	**-0.77**	1.00			
Ni	-0.39	-0.25	0.71	**0.93**	**0.91**	**0.81**	0.73	-0.34	-0.48	-0.44	-0.57	-0.60	0.09	-0.26	0.59	**0.79**	-0.21	0.71	1.00		
Zn	-0.09	-0.44	0.70	**0.93**	0.83	0.61	0.48	-0.49	-0.38	-0.32	-0.45	**-0.77**	0.08	0.40	**0.96**	**0.82**	-0.09	0.52	0.73	1.00	
Ba	-0.22	-0.27	0.59	0.51	0.38	0.45	0.37	**-0.78**	-0.29	-0.25	-0.35	-0.68	0.28	0.74	0.73	0.53	-0.05	0.37	0.29	0.66	1.00

Bold values represent correlation significant at P = <0.05, N=7

3.3. B Sediment cores

3.3.B.a Arctic Fjord

The minimum, maximum and average concentration of major and trace elements in core K-1 is provided in Table 3.3.5. Al concentration is low and varied from 1.19 to 7.96% (average 3.77%). Ti fluctuated from 0.07 to 0.55% (average 0.27%) and Fe content varied within a range of 1.01 to 6.62% (average 3.06%). Mn fluctuated from 0.01 to 0.17% (average 0.05%). Mg concentration varied from 0.34 to 4.21% (average 1.69%) and Ca content fluctuated within a range of 0.05 to 3.11% (average 0.75%). Among the trace metals, Cr concentration varied between 55.09 and 197.85 ppm (average 108.99 ppm) and Co varied from 1.84 to 20.49 ppm (average 8.78 ppm). Cu ranged from 5.61 to 39.34 ppm (average 22.84 ppm) and Pb fluctuated from 1.39 to 21.43 ppm (10.67 ppm). Cd varied within a range of 0.67 to 2.73 ppm (average 1.18 ppm) and Ni ranged from 8.31 to 91.21 ppm (average 35.35 ppm). Ba concentration fluctuated within a range of 107.21 to 855.03 ppm (average 358.87 ppm) and Zn concentration varied from 108.75 to 157.75 (average 136.11 ppm). The data obtained is in good agreement with those obtained from the sediments of Kongsfjord (Mohan et al., 2018). However, elements like Al, Ti, Fe, Co, Pb, Ba and Zn are lower in core K-1 as compared to the crustal average.

Depth wise distribution of these major and trace elements in core K-1 is presented in Fig.3.3.7. Among the major elements, Al, Ti and Fe showed lower than the average values in the lower depth range from 23 to 15 cm followed by an increase from 15 to 13 cm and then decrease up to 10 cm. Further, increased from 10 to 9 cm and then decreased up to 4 cm followed by an increasing trend towards the surface. Mn showed lower than average values in the lower depth range up to 14 cm and further showed almost similar to average values up to 4 cm and further increased towards the surface. Ca and Cr showed opposite trend in the lower depth range from 24 to 22 cm and in the upper portion from 4 cm to the surface wherein Ca increased and Cr decreased. While in the middle portion from 15 cm to the 4 cm they showed similar fluctuating trend with relatively higher value between 15 and 8 cm. Mg fluctuated around the average line. Co and Cu showed lower

than the average values in the lower depth range from 24 cm to the 15 cm. Further Co fluctuated with higher than average values up to 8 cm and then increased consistently towards the surface while Cu showed higher than the average values up to 4 cm and further decreased towards the surface. Pb showed lower than the average values from 24 cm to 12 cm and higher than the average values from 12 cm to the surface with an overall increasing trend. Ba and Cd showed almost similar trend from 24 cm to 2 cm further Cd decreased while Ba increased towards the surface. Ba showed similar distribution as that of Al indicating its source to be lithogenic in nature. Ni showed an overall increasing trend towards the surface while Zn fluctuated around the average line throughout the core. In Zone A from 24 cm to 15 cm all the elements are either constant or decrease. Further, in Zone B from 15 cm to 8 cm almost all the elements except Mn and Zn showed higher concentration similar to that of sand, clay and TOC suggesting these sediment components have regulated the distribution of these elements. In zone C from 8 cm to the surface elements like Ti, Cr, Cu, Pb and Cd showed a decreasing trend while other elements viz. Al, Fe, Mn, Ca, Mg, Co, Ni, Zn and Ba showed increasing trend similar to that of silt, TOC, TN, TP and BSi towards the surface due to increased influx of fresh water in recent years facilitating high concentration of elements along with the silt and organic elements.

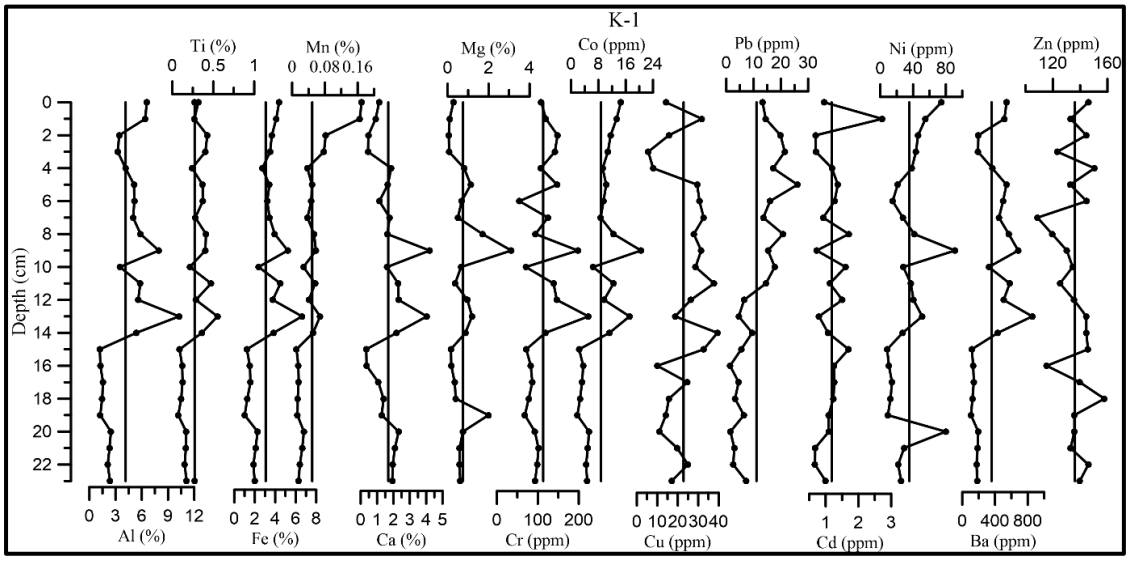

Fig.3.3.7. Distribution of elements Al, Ti, Fe, Mn, Mg, Ca, Cr, Co, Cu, Pb, Cd, Ni, Ba and Zn in sediment with depth of core K-1

Further, to determine the inter-relationship between elements and sediment components and identify possible sources or sinks, Pearson's correlation coefficient was computed and PCA was carried out. Sand displayed a significant positive correlation with Al, Ti, Fe, Ca, Mg, Co and Ba (Table 3.3.6) indicating their source to be terrigenous and they must have been derived from the weathering of rocks present in the catchment area. Clay exhibited significant correlation with BSi and Pb while BSi showed significant correlation with clay, Mn and Pb. TP showed significant correlation with Ca and Mg indicating their similar source and their association during post depositional processes. Elements like Ti, Fe, Mn, Ca, Cr, Co, Ni and Ba exhibited strong correlation with Al indicating that these elements were associated with aluminosilicate minerals suggesting their source to be lithogenic in nature. Trace metals like Cr, Co, Pb, Ni and Ba displayed significant positive correlation with major elements like Al, Ti, Fe, Mn, Mg and Ca indicating the role of aluminosilicates and Fe-Mn oxides in regulating the distribution of these trace elements.

In the principal component analysis (PCA), the three axis, axis 1 (2.36 Eigen value), axis 2 (1.44 Eigen value) and axis 3 (1.01 Eigen value) account for 33.73% , 20.58% and 14.40% of the total variation, thus making a total of 68.73% . On the biplot the length of the arrow indicates the intensity of the sediment components (Fig. 3.3.8). The major and trace elements are projected orthogonally on the sediment component arrows. The angle between the sediment component arrows suggests the correlation. Mn exhibited significant correlation with clay and Cd showed significant correlation with BSi. Most of the elements like Al, Ti, Fe, Ba, Co, Cr showed significant correlation with sand. Mg and Ca showed significant correlation with TP. Zn showed significant correlation with silt.

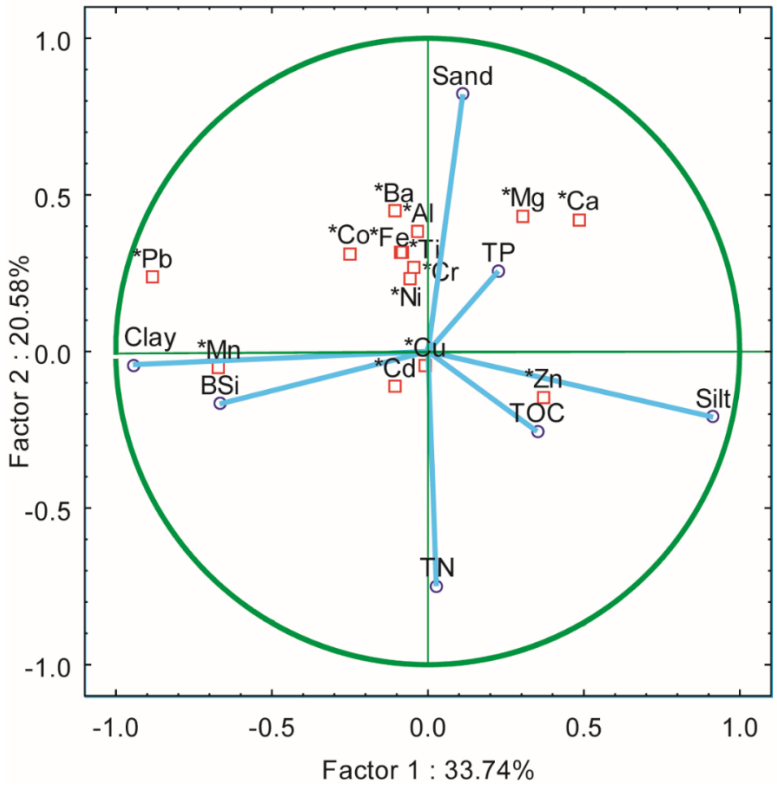

Fig:3.3.8. The principal component analysis biplot of major and trace elements and the sediment components. The red squares denote the elements and the blue circles with blue lines denote the sediment components

The vertical distribution and association of elements in the fjord suggested that mainly the sediment components regulated the distribution of elements. The distribution of trace metals is also regulated by the major elements. The elements in the sediments may be available either as silicates in the rock fragments or Fe-Mn oxides and hydroxides. Oxides/hydroxides have tendency to take up different elements either by incorporating them in to their crystal lattice or by adsorbing on the surface (Burdige, 1993). Increase in elements concentrations in the recent years as well as intermediate depths may be due to the increase in melting, releasing metals trapped beneath the ice or may be due to the increased local erosion (Mohan et al., 2018). In addition, variation in physico-chemical parameters like salinity, weathering, topography, hydrodynamic conditions and climate change may also control the distribution of metals in the fjord region.

Table 3.3.5. Concentration of major and trace elements in the sediments of a) core K-1 b) core LA c) core L-1 d) core L-2 e) core L-3

	Core K-1			Core LA			Core L-1			Core L-2			Core L-3		
	Min	Max	Average	Min	Max	Average	Min	Max	Average	Min	Max	Average	Min	Max	Average
Al (%)	1.19	7.96	3.77	1.19	2.59	1.91	1.12	2.89	1.82	1.11	2.24	1.57	1.45	3.48	2.52
Ti (%)	0.07	0.55	0.27	0.07	0.17	0.14	0.04	0.35	0.13	0.05	0.12	0.08	0.03	0.19	0.12
Fe (%)	1.01	6.62	3.06	1.01	2.38	1.78	1.49	3.96	2.69	1.06	2.94	1.72	0.32	3.18	1.56
Mn (%)	0.01	0.17	0.05	0.01	0.03	0.02	0.01	0.97	0.24	0.02	0.04	0.02	0.02	0.05	0.03
Mg (%)	0.34	4.21	1.69	0.34	2.32	1.40	0.23	4.46	1.76	2.23	4.69	3.24	0.86	3.33	1.65
Ca (%)	0.05	3.11	0.75	0.16	1.99	0.56	1.36	3.04	2.20	0.74	2.45	1.25	0.01	2.43	1.22
Cr (ppm)	55.09	197.85	108.99	68.38	101.53	86.42	16.32	85.00	42.82	31.93	55.41	43.95	10.06	49.23	29.13
Co (ppm)	1.84	20.49	8.78	1.84	6.26	4.10	0.30	19.14	5.15	11.09	14.35	12.50	10.55	21.09	15.00
Cu(ppm)	5.61	39.34	22.84	5.61	32.64	23.16	32.15	73.67	53.10	15.04	91.21	40.73	32.15	167.35	97.71
Pb(ppm)	1.39	21.43	10.67	10.79	17.51	14.39	1.14	3.76	2.11	6.46	20.49	11.20	6.46	13.90	9.73
Cd(ppm)	0.67	2.73	1.18	0.70	2.73	1.27	0.97	5.28	1.88	1.09	4.35	2.50	1.04	2.15	1.53
Ni (ppm)	8.31	91.21	35.35	8.31	79.81	25.75	3.60	80.34	32.74	10.11	18.34	13.14	16.55	85.38	31.60
Ba (ppm)	107.21	855.03	358.87	107.21	207.72	157.08	132.18	290.84	215.43	104.42	195.04	141.23	117.14	320.54	235.77
Zn (ppm)	108.75	157.75	136.11	101.55	194.74	133.74	82.00	163.00	119.91	50.28	82.91	67.01	18.53	97.68	65.03

Table 3.3.6. Pearson's correlation coefficients of sediment components and elements of core K-1

	Sand	Silt	Clay	TOC	TN	TP	BSi	Al	Ti	Fe	Mn	Mg	Ca	Cr	Co	Cu	Pb	Cd	Ni	Zn	Ba
Sand	1.00																				
Silt	-0.14	1.00																			
Clay	-0.16	**-0.95**	1.00																		
TOC	-0.03	0.21	-0.20	1.00																	
TN	-0.35	0.06	0.05	0.11	1.00																
TP	0.10	0.07	-0.10	0.03	-0.03	1.00															
BSi	-0.19	-0.40	**0.46**	-0.12	-0.04	-0.20	1.00														
Al	**0.55**	-0.16	-0.01	0.16	-0.17	0.11	0.24	1.00													
Ti	**0.49**	-0.29	0.14	0.06	-0.16	-0.04	0.32	**0.84**	1.00												
Fe	**0.48**	-0.18	0.04	0.15	-0.17	0.07	0.32	**0.97**	**0.92**	1.00											
Mn	0.04	-0.36	0.35	0.08	-0.06	-0.11	**0.84**	**0.59**	**0.50**	**0.62**	1.00										
Mg	**0.42**	-0.04	-0.09	-0.03	-0.04	**0.73**	-0.35	0.38	0.20	0.29	-0.15	1.00									
Ca	**0.52**	0.16	-0.32	-0.02	-0.05	**0.45**	-0.40	**0.62**	0.40	**0.57**	-0.07	**0.52**	**1.00**	-0.32							
Cr	0.26	-0.11	0.03	0.10	-0.21	0.20	0.13	**0.75**	**0.73**	**0.83**	0.36	0.33	**0.64**	1.00							
Co	0.43	-0.28	0.15	0.09	-0.16	0.22	**0.42**	**0.93**	**0.88**	**0.96**	**0.68**	0.38	**0.52**	**0.78**	1.00						
Cu	0.11	-0.26	0.23	0.36	0.16	0.08	-0.23	0.35	0.25	0.27	0.04	0.17	0.23	0.09	0.25	1.00					
Pb	0.19	**-0.60**	**0.54**	-0.18	-0.22	-0.03	**0.55**	0.39	**0.60**	**0.43**	**0.42**	0.12	-0.13	0.24	**0.53**	0.18	1.00				
Cd	-0.06	-0.09	0.11	0.21	-0.02	-0.21	0.16	0.05	-0.16	-0.07	0.26	-0.16	-0.31	-0.30	-0.05	0.35	0.14	1.00			
Ni	0.25	-0.06	-0.02	-0.07	-0.13	0.34	0.38	**0.60**	**0.47**	**0.65**	**0.60**	0.32	**0.49**	**0.57**	**0.72**	-0.10	0.20	-0.11	1.00		
Zn	0.02	0.23	-0.24	0.02	0.22	0.01	-0.02	-0.09	-0.17	-0.14	0.00	-0.11	0.04	-0.13	-0.13	-0.14	-0.23	-0.06	-0.07	1.00	
Ba	0.59	-0.19	0.01	0.15	-0.21	0.09	0.15	**0.98**	**0.80**	**0.91**	**0.50**	**0.42**	**0.63**	**0.67**	**0.87**	**0.44**	**0.41**	0.11	**0.51**	-0.14	1.00

Bold values represent correlation significant at P = <0.05, N=23

3.3.B.b Arctic lakes

The range and average values of the major and trace elements for cores LA, L-1, L-2 and L3 are given in Table 3.3.5. Average Al, Co, Cu and Ba were considerably higher in core L-3. Ti, Cr, Pb and Zn were higher in core LA. Fe, Mn, Ca and Ni were found higher in core L-1 while Mg and Cd were higher in core L-2. Mn concentrations were found similar in core L-2 and LA. Down core variations of elemental concentrations from lake sediments are used since many years as a proxy to monitor the level of input of major and trace metals in the environment (El Bilali et al., 2002).) Depth-wise distribution of elements is provided in Fig. 3.3.9 a, b, c and d.

In core LA (Fig.3.3.9a), zone 1 from 24 to 18 cm elements like Al, Ti, Fe, Co, Ni, Ba and Zn showed higher than the average value. Mn and Ca remained constant. Elements like Al, Ti, Fe, Cr, Co, Ni, Ba and Zn showed decrease from 20 to 18 cm. In zone 2 from 18 to 8 cm, elements like Al, Ti, Fe, Mg, Cr, Cu, Ba and Zn showed higher than the average values. Mn, Co and Cu showed almost constant trend. In this zone most of the elements showed an increase from 18 to 16 cm and further remained constant up to 10 cm followed by a decrease up to 8 cm. In zone 3 Al, Ti, Fe, Cr, Co, Cu, Ba, Ni showed an increasing trend from 8 cm to the 4 cm followed by a decreasing trend. Ca and Mg showed decreasing trend. Pb, Cd and Zn showed decreasing trend up to 4 cm and then slightly increased. Overall, Al, Ti and Fe showed similar decreasing trend towards the surface similar to that of sand indicating their association with the coarser sediments. Al is lithogenic in nature and it is a robust indicator of erosion and terrigenous input (Shi et al., 2010). Mn showed consistently similar trend with average values throughout the core. Mg showed higher than the average values from 22 cm to 10 cm depth (except at 18 cm depth) and lower than the average values from 8 cm to the surface with an overall decreasing trend. Ca showed similar decreasing trend as that of Mg except a positive peak at 8 cm. Cr, Co, Ni, Ba and Cu showed decreasing trend towards the surface similar to that of Al indicating their common source and post-depositional processes. Pb and Cd showed fluctuating trend with a decrease towards the surface. Zn showed large fluctuation around average line with increasing trend in the upper 4 cm.

In core L-1 (Fig. 3.3.9b) zone 1, from 32 to 22 cm elements like Ti, Mn, Ca, Cr, Cu, Ni, Ba and Zn showed higher than the average values while Al, Fe, Mg and Cd fluctuated around the average line. Further, Ti, Mn, Co showed increasing trend while Ca, Cu, Ni, Ba, Zn showed decreasing trend in this zone. In zone 2 from 22 to 8 cm, elements like Al, Ti, Mn, Mg, Ca, Cr and Co decreased while Ba and Zn increased. Mg and Cr along with Fe showed a positive peak at 16 cm similar to that of silt indicating their association with finer sediments. In zone 3 from 8 cm to the surface elements like Al, Fe, Mn, Ca, Cd and Zn decreased similar to that of sand indicating their association with coarser sediments while Ti, Mg, Cr, Co, Cu, Ni, Ba slightly increased towards the surface similar to that of clay suggesting that their distribution is regulated by the finer sediments due to the influx of melt water. Overall, Al and Fe fluctuated around the average line. Cu and Pb remained constant throughout the core. Cd fluctuated around the average line with an overall decreasing trend towards the surface. Ni fluctuated up to 12 cm and further increased consistently towards the surface. Zn fluctuated around the average line up to 18 cm depth and further remained almost constant. Ti, Mn, Mg, Ca, Cr, Co exhibited overall decreasing trend.

In core L-2 (Fig.3.3.9c) zone 1 from 18 to 12 cm, elements like Al, Ti, Cr, Co and Cd showed lower than the average value, while, Fe, Mg, Cu and Ba showed higher than the average values while Mn, Zn and Ni remained constant. In zone 2 from 12 to 4 cm elements like Fe, Mg, Ca, Cu and Pb showed lower than the average values. Ti, Mn, Cr, Co, Cd, Ni remained constant while Ba and Zn fluctuated around the average line. In zone 3 elements like Al, Fe, Cd and Ba showed a decreasing trend. Mg, Ca, Cu, and Zn showed increase towards the surface. Cr, Co, Pb and Ni remained constant. Overall elements like Al, Ti, Cr and Ba showed similar decreasing trend towards the surface especially in the zone 2 and 3. Fe showed higher than the average values from 18 cm to 14 cm and then decreased up to 12 cm remained constant up to a depth of 6 cm, followed by an increase up to 4 cm and then decreased towards the surface. Mg showed higher than average values from 18 cm to 16 cm and then decreased up to 14 cm. Further it decreases continuously up to a depth of 4 cm and further increased up to 2 cm and then decreased towards the surface. Ca showed an increasing trend towards the surface from 4 cm. Pb showed similar distribution as that of silt in the

lower depth range up to 12 cm, further it decreased consistently towards the surface while Cd showed an overall increasing trend in zone 1 and then maintained constant. Zn fluctuated around the average line. Ni showed similar constant trend throughout the core.

In core L-3 (Fig. 3.3.9d), zone 1 from 16 to 12 cm elements like Al, Ca, Cr, Cu, Cd and Zn showed an increasing trend after an initial decrease up to 14 cm. Ti, Mn, Mg and Ni remained constant. Fe, Co, Pb and Ni showed a decreasing tend after an initial increase. In zone 2 from 12 to 6 cm elements like Al, Ti, Fe, Cr and Ba remained constant up to 8 cm and further showed decreasing trend up to 6 cm and Co showed constant trend up to 8 cm and further increased towards the surface. Elements like Mn, Mg, Ca and Cd remained constant and Zn fluctuated around the average line. In zone 3 from 6 cm to the surface Cu, Pb, Ba and Zn showed an increasing trend towards the surface while elements like Ca, Co, Ni and Cd decreased towards the surface. Overall Al, Ca, Cr, Cu, Cd and Ba showed a decreasing trend in the lower depths range from 16 to14 cm similar to that of sand indicating their association with coarser sediments. Further, in the middle zone from 12 cm to 6 cm elements like Al, Ti, Fe, Cr and Cd showed a decreasing trend similar to that of clay indicating the role of finer sediments in their distribution at these depths. In the upper portion from 4 cm to the surface, elements like Al, Ti, Fe, Cr, Co, Cd and Ba showed decreasing trend similar to that of silt while Pb and Zn showed similar increasing trend towards the surface as that of clay suggesting that these sediment components controlled the distribution of elements at these depths.

In all the four cores studied, it is noticed that the elemental concentrations have increased towards the surface suggested either increased melt water influx in recent years or diagenetic remobilisation (Volvoikar and Nayak, 2014). Earlier studies, Davis (1984); Ali and Dzomback (1996); Tessier et al. (1996) have reported that oxides (Murray,1975) or organic ligands by forming stable complexes can scavenge elements from surface water to the sediment.

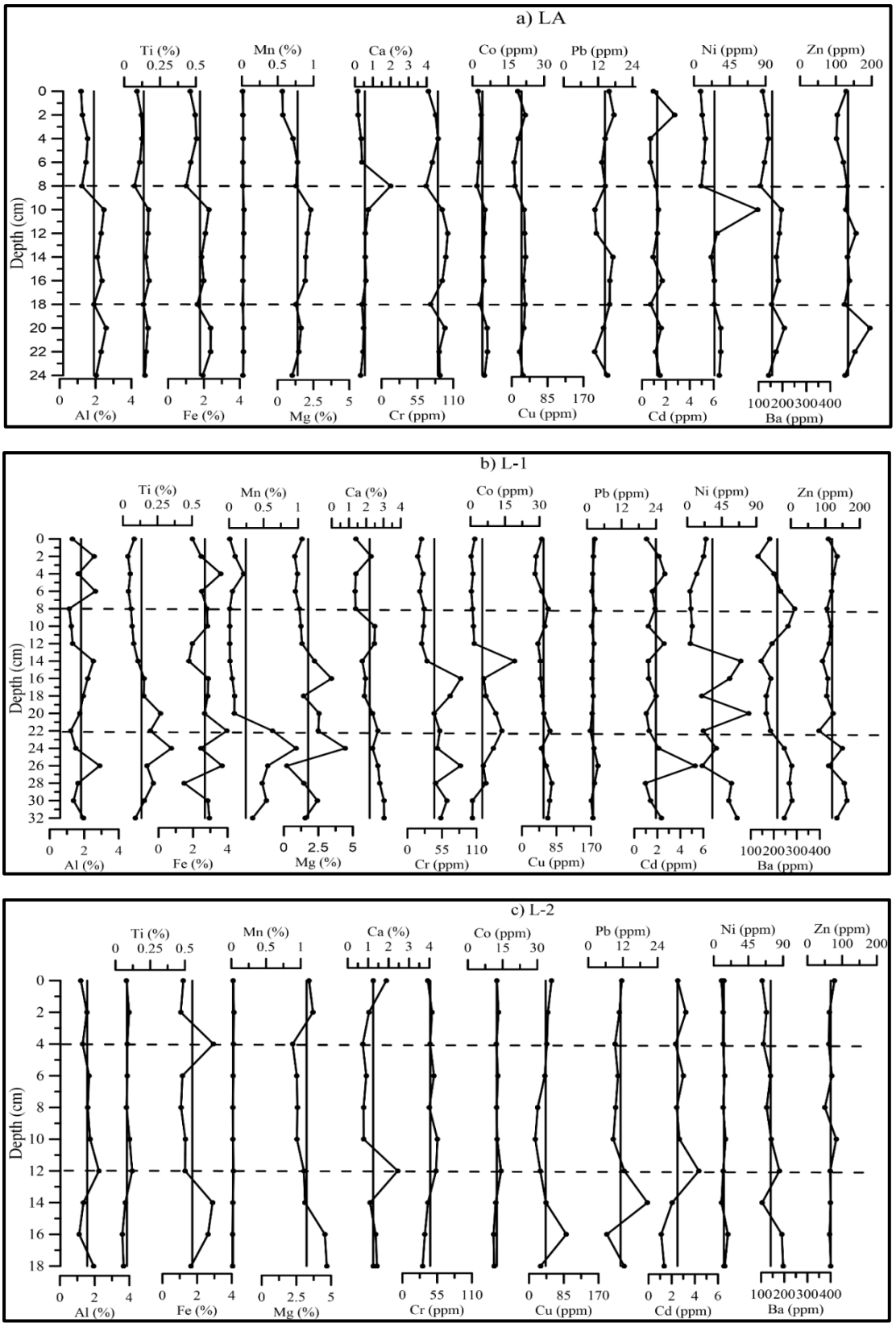
a) LA
b) L-1
c) L-2
Depth (cm)
Ti (%)
Mn (%)
Ca (%)
Co (ppm)
Pb (ppm)
Ni (ppm)
Zn (ppm)
Al (%)
Fe (%)
Mg (%)
Cr (ppm)
Cu (ppm)
Cd (ppm)
Ba (ppm)

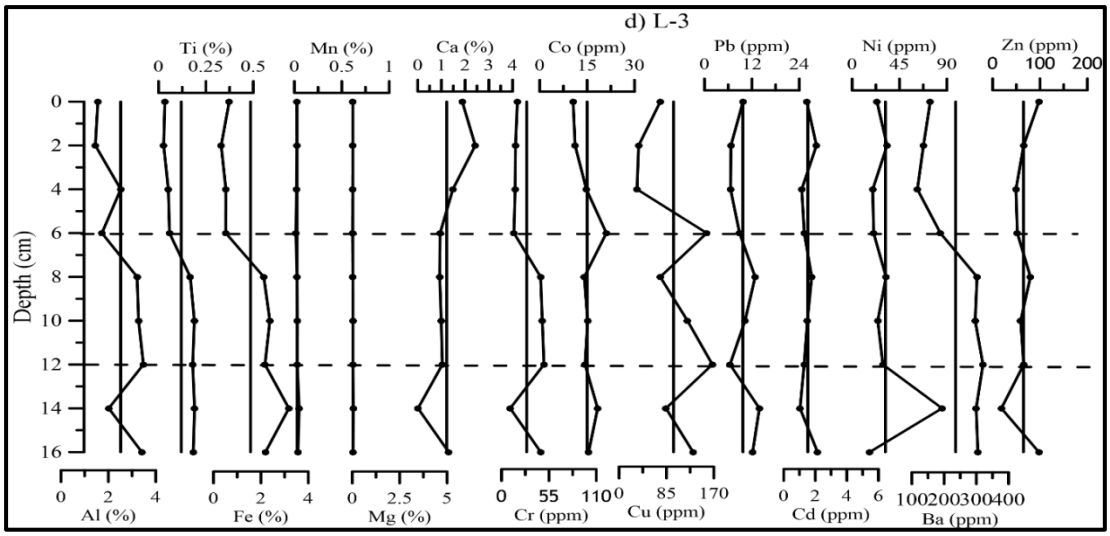

Fig. 3.3.9 Distribution of elements Al, Ti, Fe, Mn, Mg, Ca, Cr, Co, Cu, Pb, Cd, Ni, Ba and Zn in sediment with depth of a) core LA b) core L-1 c) core L-2 d) core L-3

In order to understand the relative enrichment between the four lakes studied, the data was plotted on Isocon diagram (Grant, 1986). When all the parameters of lake LA and L-1 were compared (Fig.3.3.10a), it was seen that Ti fell on the isocon line indicating minor variations between the two cores. However, core LA showed high concentration of clay, TP, Al, Pb, Cr and Zn indicating the role of clay in distribution of these elements. Whereas, sand, silt, TOC, TN, BSi, Fe, Mn, Mg, Co, Cu, Cd, Ba, Ni and Co were more enriched in core L-1 indicating the role of sediment components and organic carbon along with Fe-Mn oxide in the distribution of Cd, Cu, Ca, Mg, Cu, Ba, Co and Ni. Rasmussen et al. (1998) and Gobeil et al. (1999) reported that organic matter and oxides have regulated the distribution of elements in sediments of lake and Arctic Ocean basin. When core L-2 was compared with L-1 (Fig. 3.3.10b), it was observed that Cr fell on the Isocon line. Clay, TOC, TP, Mg, Pb, Co, Cd were highly concentrated in core L-2 indicating the role of clay and organic matter in regulating the distribution of these elements, while, sand, silt, BSi, TN, Al, Fe, Ti, Mn, Ca, Ni, Zn, Ba and Cu are enriched in core L-1 indicating the role of aluminosilicate phases, Fe-Mn oxides, sand and silt regulated the distribution of metals in this core. When data of core L-3 and L-2 was compared (Fig.3.3.10c), it was observed that Ca and Zn fell on the isocon line indicating minor variations in these elements between the two cores. Sand, silt, TN, TP, Al, Ti, Fe, Mn, Co, Cu, Ni and Ba were more pronounced in core L-3 while clay, TOC, BSi, Mg, Cr, Cd, Pb were enriched in core L-2 indicating the role of finer sediments along with organic matter in regulating these elements. When core LA and L-3 was compared (Fig.3.3.10d),

it was observed that sand fell on the isocon line and TOC, silt and clay fell very close to the isocon line indicating not much variations between the cores with respect to these parameters. BSi, Ti, Fe, Cr, Zn and Pb were enriched in core LA while, TP, TN, Al, Mg Mn, Ca, Cd, Ni, Co, Cu and Ba were more pronounced in core L-3. When core LA and L-2 was compared (Fig.3.3.10e), it was observed that clay, TOC, TN, TP, Mn, Mg, Ca, Cd, Co and Cu were enriched in core L-2 and Sand, silt, BSi, Ti, Fe, Cr, Ni, Pb, Zn and Ba were concentrated in core LA. When core L3 and L1 was compared (3.3.10f), it was observed that Mg, silt and Ni fell on the isocon line. Sand, TOC, BSi, Ti, Fe, Mn, Ca, Cr, Cd and Zn were more pronounced in core L-1 while clay, TP, TN, Al, Co, Cu, Pb and Ba were high in core L-3. From the isocon diagram, it was observed that core L-2 consists of lower concentration of elements possibly due to its relatively smaller catchment area.

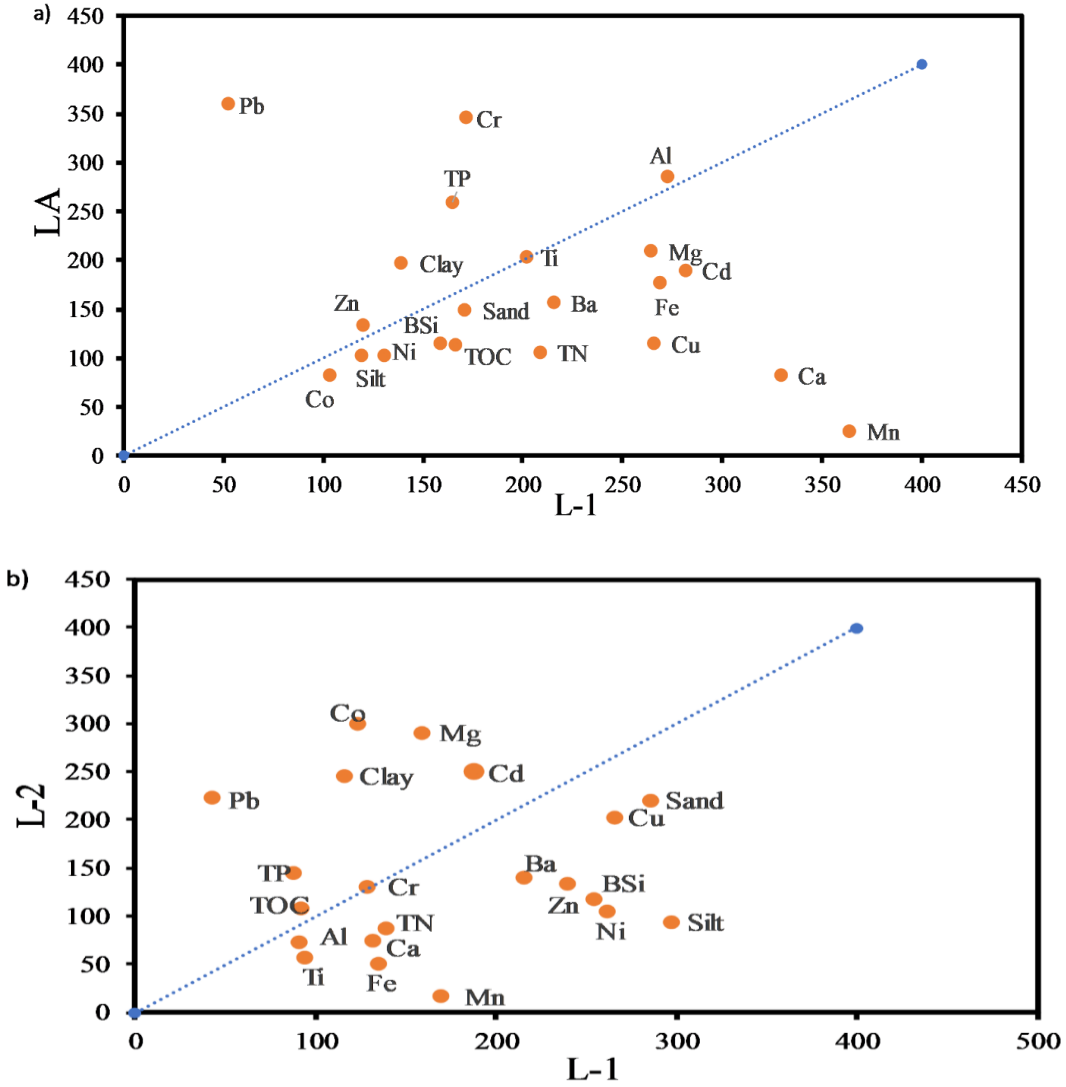

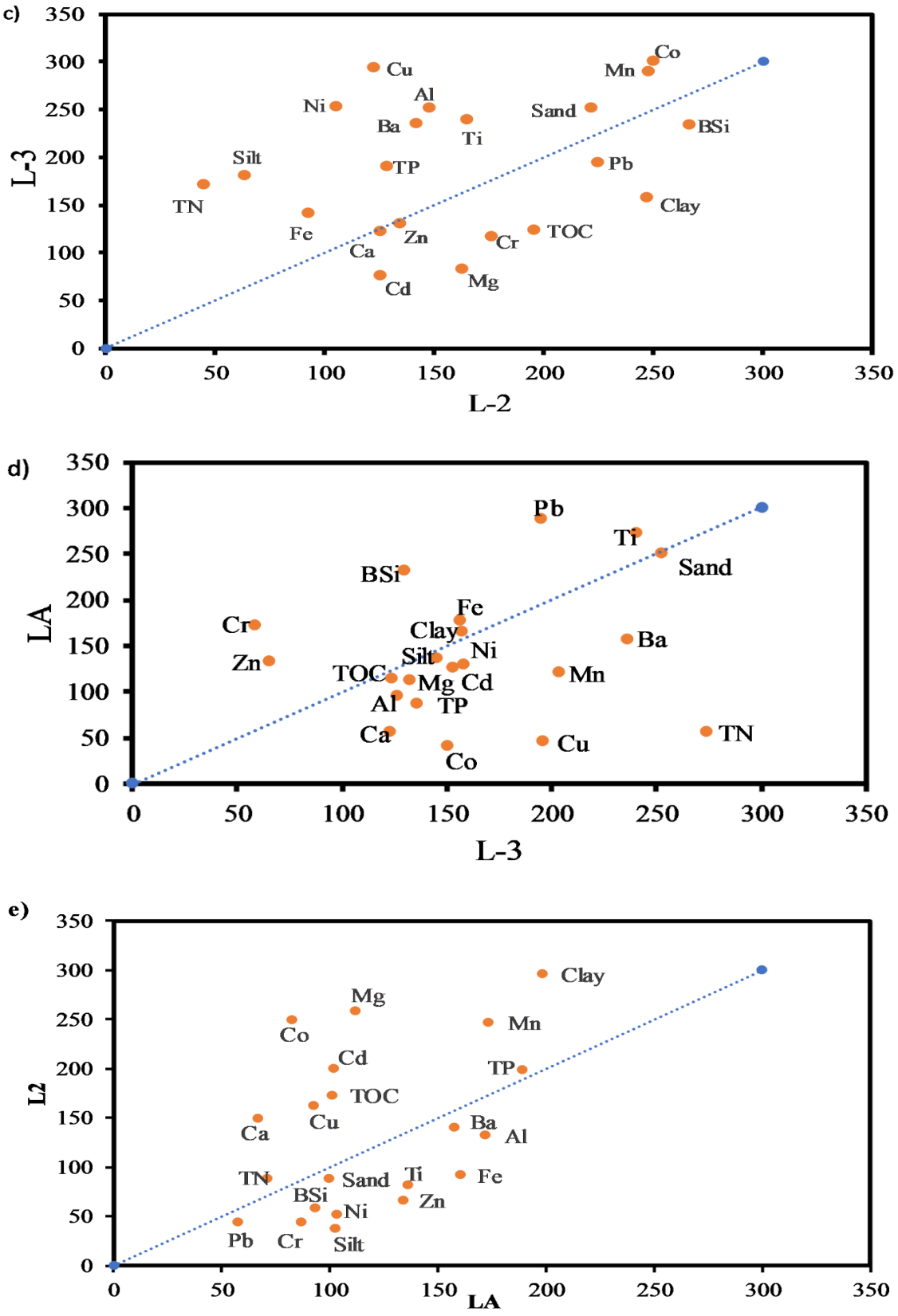
c)
L-3
L-2
Cu
Co
Mn
Al
Ni
Sand
Ba
Ti
BSi
Silt
TP
Pb
TN
Clay
Fe
Zn
Cr
TOC
Ca
Mg
Cd
d)
LA
L-3
Pb
Ti
Sand
BSi
Fe
Cr
Clay
Ba
Zn
Silt
Ni
TOC
Mn
Mg
Cd
Al
TP
Ca
Cu
TN
Co
e)
L2
LA
Clay
Mg
Co
Mn
Cd
TP
TOC
Ca
Cu
Ba
Al
TN
Sand
Ti
Fe
BSi
Zn
Ni
Pb
Cr
Silt

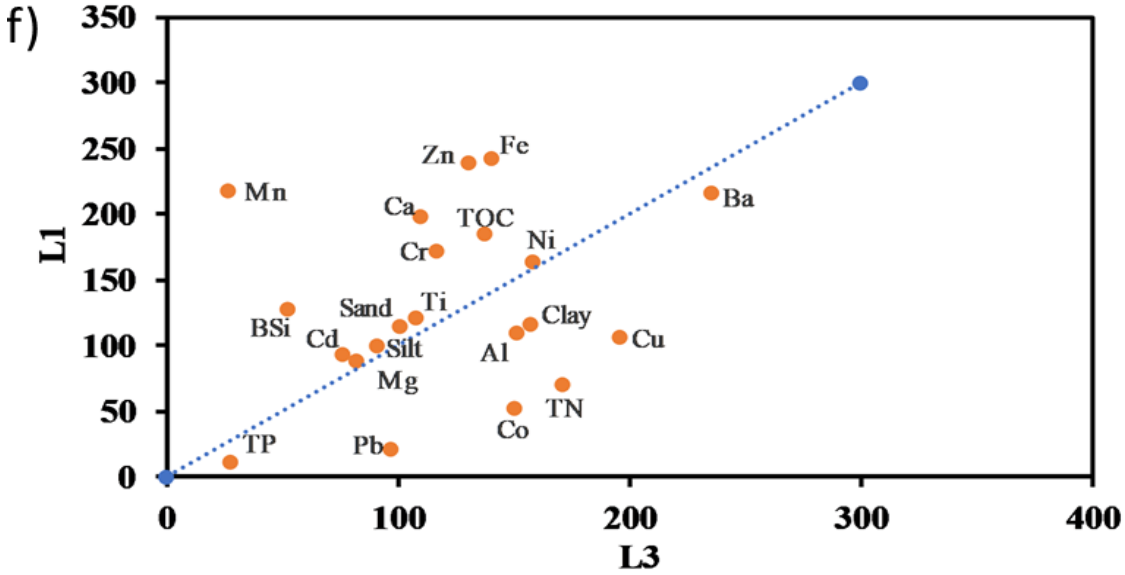

Fig.3.3.10 Isocon diagram (Grant, 1986). Individual points represent average value of sediment components and elements in each core.

Further, when the Pearson's correlation was carried out (Table 3.3.7a) for core LA, sand showed significant positive correlation with TOC. Silt exhibited significant positive correlation with Al, Fe and Co indicating their association with finer sediments. TOC showed significant positive correlation with TN indicating their similar source. TP showed significant positive correlation with Mg indicating their similar source and post depositional processes. Al exhibited significant positive correlation with elements like Ti, Fe, Mn, Mg, Cr, Co, Cu, Ni, Ba and Zn suggesting their association with aluminosilicates indicating their detrital source. Ti displayed significant positive correlation with Fe, Mn, Mg and almost all the trace metals except Pb, Cd and Zn. Fe showed significant correlation with Mn indicating their similar source and post depositional processes and trace metals like Cr, Co, Cu, Ni, Ba and Zn indicating the role of Fe-oxides in regulating the distribution of these elements. Fe and Mg show good correlation as Fe can replace Mg in mafic minerals. Mn is significantly correlated with Mg, Cr, Co, Ni and Ba suggesting that Mn oxide is controlling the distribution of these elements. Mg showed significant correlation with Cr, Ni and Ba while elements like Co, Cu and Ba are significantly correlated with Cr. Cu, Ni, Ba and Zn are significantly

correlated with Co. Cu and Ni are significantly correlated with Ba while Ba is significantly correlated with Zn indicating that similar mechanism regulated their abundance.

In core L-1 (Table 3.3.7b) sand showed negative correlation with clay and Cr. Clay showed significant positive correlation with Mg, Ca and Cr indicating their association with finer sediments. TOC showed significant positive correlation with TN; TN is positively correlated with TP indicating their similar source while TOC is negatively correlated with Al indicating its biogenic source. Ti displayed a significant positive correlation with metals like Mn, Mg, Cr, Co and Ni indicating their detrital source. Mn is correlated with Ca; Mg is significantly correlated with Co and Ni and Ca is significantly correlated with Cu. Co is significantly correlated with Ni, Cu is significantly correlated with Ba and Pb showed significant correlation with Cd suggesting that these elements have been derived from the similar source and are regulated by similar post depositional processes.

In core L-2 (Table 3.3.7c) sand and clay showed negative correlation with silt; silt showed positive correlation with TN and BSi. Al showed significant positive correlation with Ti, Fe, Cr, Co and Cd indicating their lithogenic source derived from the weathering of rocks of the catchment area. Elements like Fe, Mn, Cr, Co and Cd showed significant positive correlation with Ti indicating their common source and post depositional processes. Cr, Co and Cd showed significant correlation with Fe and Mn indicating the role of Fe-Mn oxides in their distribution. Cr exhibited significant correlation with Co and Cd. Pb showed negative correlation with Ni while Ni showed positive correlation with Ba.

In core L-3 (Table 3.3.7d) sand showed positive correlation with TN indicating its terrigenous source. Clay showed significant correlation with Ti, Fe, Mg, Cu and Ba suggesting their association with finer sediments. During diffusion and mobilization clay minerals are the main carriers of trace metals (Horowitz, 1991). Al showed significant correlation with Ti, Cr and Ba while Ti displayed

significant correlation with Fe, Mn, Mg, Cr and Ba. Fe exhibited significant correlation with Mn, Mg, Pb and Ba and Mn showed significant correlation with Mg and Ni suggesting the role of Fe-Mn oxides in the distribution of these trace metals Mg showed significant positive correlation with Pb, Ni and Ba. Cr showed significant correlation with Ba and Cd showed significant correlation with Zn.

In the four cores studied in general it can be stated that aluminosilicates and Fe-Mn oxides along with the sediment components viz. sand and clay regulated the distribution of most of the elements. Trace metals are mainly controlled by the major elements like Al, Ti, Fe and Mn suggesting their natural source and input of anthropogenic activities are negligible. In these cores, distribution of Fe and Mn is similar to that of Al at different depths corresponds to the weathered, terrestrial source rock material and/or the fraction bound to the aluminosilicate mineral (El Bilali et al., 2002). In core L-1, sand concentration is high leading to the infiltration of oxygenated water through the sand particles which may have remobilised the metals towards the surface (Ohmsen et al., 1995). Role of organic elements seems to be negligible in trace metal distribution.

Table 3.3.7 Pearson's correlation coefficients of sediment components and elements of a) core LA b) core L-1 c) core L-2 d) core L-3

a) LA

	Sand	Silt	Clay	TOC	TN	TP	BSi	Al	Ti	Fe	Mn	Mg	Ca	Cr	Co	Cu	Pb	Cd	Ni	Zn	Ba
Sand	1.00																				
silt	-0.37	1.00																			
clay	**-0.62**	-0.49	1.00																		
TOC	**0.59**	**-0.64**	-0.01	1.00																	
TN	0.37	**-0.87**	0.39	**0.68**	1.00																
TP	-0.06	-0.12	0.16	-0.04	0.05	1.00	0.13														
BSi	-0.15	-0.29	0.38	-0.21	0.36	0.13	1.00														
Al	-0.33	**0.58**	-0.18	-0.34	-0.52	0.42	-0.27	1.00													
Ti	-0.21	0.48	-0.21	-0.26	-0.33	0.37	-0.08	**0.93**	1.00												
Fe	-0.47	**0.58**	-0.05	-0.42	-0.46	0.50	-0.03	**0.94**	**0.93**	1.00											
Mn	-0.32	0.26	0.08	-0.15	-0.15	**0.55**	-0.04	**0.73**	**0.71**	**0.79**	1.00										
Mg	-0.02	0.23	-0.18	0.03	-0.29	-0.06	-0.43	**0.79**	**0.69**	**0.61**	**0.72**	1.00									
Ca	0.18	-0.09	-0.09	0.10	-0.24	0.35	**-0.60**	-0.09	-0.32	-0.27	0.03	0.18	1.00								
Cr	-0.05	0.36	-0.25	-0.22	-0.18	0.19	0.03	**0.81**	**0.89**	**0.83**	**0.76**	**0.66**	-0.25	1.00							
Co	-0.47	**0.63**	-0.09	-0.41	-0.48	0.43	-0.05	**0.89**	**0.88**	**0.98**	**0.75**	0.53	-0.26	**0.82**	1.00						
Cu	-0.05	0.28	-0.19	-0.23	-0.10	-0.31	-0.05	**0.59**	**0.73**	**0.62**	0.42	0.32	-0.33	**0.66**	**0.57**	1.00					
Pb	0.45	-0.25	-0.21	0.11	0.27	-0.36	0.13	-0.45	-0.30	-0.47	**-0.71**	-0.52	-0.17	-0.26	-0.44	0.20	1.00				
Cd	0.12	0.02	-0.13	0.10	0.17	0.55	-0.08	0.05	0.21	0.20	0.15	-0.20	-0.09	0.22	0.29	0.46	0.25	1.00			
Ni	-0.41	0.45	0.01	-0.24	-0.32	0.10	-0.18	**0.73**	**0.67**	**0.72**	**0.80**	**0.65**	0.01	0.50	**0.64**	0.44	**-0.59**	0.07	1.00		
Zn	-0.34	0.32	0.05	-0.21	-0.38	0.55	-0.40	**0.67**	0.46	**0.61**	0.42	0.45	0.12	0.46	**0.63**	0.21	-0.39	0.04	0.27	1.00	
Ba	-0.26	0.34	-0.04	-0.23	-0.28	0.42	-0.12	**0.95**	**0.94**	**0.92**	**0.77**	**0.75**	-0.17	**0.86**	**0.86**	**0.68**	-0.39	0.15	**0.69**	**0.65**	1.00

Bold values represent correlation significant at P = <0.05, N=15

b) L-1

	Sand	Silt	Clay	TOC	TN	TP	BSi	Al	Ti	Fe	Mn	Mg	Ca	Cr	Co	Cu	Pb	Cd	Ni	Zn	Ba
Sand	1.00																				
Silt	-0.35	1.00																			
Clay	**-0.88**	-0.13	1.00																		
TOC	0.17	-0.04	-0.16	1.00																	
TN	0.16	-0.16	-0.08	**0.71**	1.00																
TP	0.24	-0.26	-0.12	0.46	**0.84**	1.00															
BSi	0.35	-0.04	-0.35	0.30	0.10	-0.02	1.00														
Al	0.00	-0.13	0.06	**-0.49**	-0.42	-0.21	-0.16	1.00													
Ti	-0.18	-0.17	0.28	-0.24	-0.27	-0.17	-0.34	-0.13	1.00												
Fe	-0.22	0.11	0.18	-0.19	-0.30	-0.29	-0.14	0.01	0.01	1.00											
Mn	-0.06	-0.24	0.18	-0.29	-0.16	-0.01	**-0.58**	-0.10	**0.70**	0.29	1.00										
Mg	-0.47	-0.07	**0.53**	-0.25	-0.14	-0.19	-0.14	-0.26	**0.72**	-0.07	0.44	1.00									
Ca	-0.03	-0.09	**0.08**	-0.14	-0.21	-0.24	-0.36	-0.09	0.42	0.12	**0.56**	0.18	1.00								
Cr	**-0.66**	0.26	**0.57**	-0.26	-0.38	-0.40	**-0.63**	0.23	**0.50**	0.41	0.43	0.33	0.43	1.00							
Co	-0.14	-0.30	0.29	-0.12	-0.19	-0.14	0.24	0.13	**0.58**	-0.07	0.25	**0.51**	0.08	0.24	1.00						
Cu	-0.18	0.09	0.14	0.02	0.07	-0.12	-0.29	-0.30	0.33	0.11	0.42	0.06	**0.54**	0.38	0.11	1.00					
Pb	0.14	0.29	-0.30	0.13	0.14	0.42	-0.32	0.25	0.07	-0.13	0.14	-0.38	-0.03	0.15	-0.17	-0.01	1.00				
Cd	0.13	0.19	-0.24	-0.09	-0.23	0.00	-0.29	0.43	-0.05	0.44	0.27	-0.41	0.16	0.31	-0.20	-0.15	**0.68**	1.00			
Ni	-0.20	-0.11	0.27	-0.46	-0.17	-0.16	-0.15	0.15	**0.51**	-0.26	0.18	**0.52**	0.39	0.37	**0.51**	0.27	-0.18	-0.32	1.00		
Zn	0.24	-0.09	-0.21	-0.34	-0.11	-0.04	**-0.51**	-0.08	0.27	-0.27	0.43	0.16	0.43	0.02	-0.37	0.17	0.09	-0.04	0.30	1.00	
Ba	-0.02	0.43	-0.19	-0.02	-0.02	-0.16	-0.33	-0.26	0.11	0.16	0.41	-0.10	0.29	0.22	-0.38	**0.63**	0.30	0.26	-0.15	0.41	1.00

Bold values represent correlation significant at P = <0.05, N=18

c) L-2

	Sand	Silt	clay	TOC	TN	TP	BSi	Al	Ti	Fe	Mn	Mg	Ca	Cr	Co	Cu	Pb	Cd	Ni	Zn	Ba
Sand	1.00																				
Silt	0.13	1.00																			
clay	**-0.73**	**-0.77**	1.00																		
TOC	0.18	0.37	-0.37	1.00																	
TN	0.07	**0.70**	-0.52	0.57	1.00																
TP	-0.50	**-0.68**	**0.79**	**-0.65**	-0.51	1.00															
BSi	-0.11	**0.89**	-0.54	0.37	**0.78**	-0.63	1.00														
Al	-0.54	-0.25	0.52	-0.35	-0.10	0.59	-0.27	1.00													
Ti	-0.54	0.04	0.32	-0.01	0.19	0.32	-0.01	**0.89**	1.00												
Fe	-0.53	0.18	0.22	-0.19	0.39	0.39	0.20	**0.80**	**0.87**	1.00											
Mn	-0.06	0.46	-0.27	0.17	0.29	-0.16	0.17	0.50	**0.72**	0.56	1.00										
Mg	0.24	0.17	-0.27	0.40	-0.05	-0.51	0.23	-0.57	-0.58	**-0.69**	-0.42	1.00									
Ca	-0.26	0.17	0.06	0.28	0.38	-0.31	0.42	0.24	0.23	0.16	0.02	0.38	1.00								
Cr	-0.41	-0.13	0.35	-0.27	0.05	0.57	-0.23	**0.89**	**0.89**	**0.87**	0.61	**-0.70**	-0.03	1.00							
Co	-0.54	0.13	0.26	-0.14	0.17	0.26	0.07	**0.90**	**0.95**	**0.84**	**0.76**	-0.53	0.35	**0.82**	1.00						
Cu	**0.85**	0.22	**-0.71**	0.24	0.20	-0.55	0.09	-0.49	-0.57	-0.53	-0.13	0.51	0.15	-0.49	-0.45	1.00					
Pb	-0.49	-0.09	0.38	0.17	0.09	0.13	0.08	0.00	0.01	-0.03	-0.02	-0.01	0.18	-0.12	0.08	-0.23	1.00				
Cd	-0.54	0.13	0.26	-0.14	0.17	0.26	0.07	**0.90**	**0.95**	**0.84**	**0.76**	-0.53	0.35	**0.82**	**1.00**	-0.45	0.08	1.00			
Ni	0.44	-0.39	-0.01	-0.23	-0.49	0.15	-0.47	-0.15	-0.34	-0.38	-0.41	0.38	-0.16	-0.08	-0.41	0.35	**-0.67**	-0.41	1.00		
Zn	-0.17	0.20	-0.03	0.24	0.52	0.03	0.36	0.02	0.18	0.37	0.03	0.00	0.18	0.31	0.08	-0.06	0.04	0.08	0.08	1.00	
Ba	-0.02	-0.39	0.28	-0.09	-0.48	0.02	-0.26	-0.01	-0.18	-0.37	-0.43	0.62	0.40	-0.19	-0.17	0.12	-0.32	-0.17	**0.72**	-0.02	1.00

Bold values represent correlation significant at P = <0.05, N=10

d) L-3

	Sand	Silt	Clay	TOC	TN	TP	BSi	Al	Ti	Fe	Mn	Mg	Ca	Cr	Co	Cu	Pb	Cd	Ni	Zn	Ba
Sand	1.00																				
Silt	-0.42	1.00																			
Clay	-0.43	-0.64	1.00																		
TOC	-0.06	0.42	-0.37	1.00																	
TN	**0.79**	0.13	**-0.80**	0.32	1.00																
TP	0.65	0.28	**-0.82**	0.20	**0.91**	1.00															
BSi	-0.09	0.62	-0.55	**0.85**	0.37	0.44	1.00														
Al	-0.51	-0.18	0.61	-0.47	**-0.73**	-0.52	-0.43	1.00													
Ti	-0.48	-0.46	**0.86**	**-0.70**	**-0.86**	**-0.75**	**-0.71**	**0.79**	1.00												
Fe	-0.39	-0.50	**0.82**	**-0.77**	**-0.77**	-0.66	**-0.74**	0.61	**0.96**	1.00											
Mn	-0.06	-0.39	0.44	**-0.87**	-0.41	-0.34	**-0.71**	0.23	**0.69**	**0.83**	1.00										
Mg	-0.34	-0.44	**0.73**	**-0.74**	**-0.68**	-0.64	**-0.69**	0.38	**0.85**	**0.95**	**0.91**	1.00									
Ca	**0.69**	0.17	**-0.75**	0.27	**0.81**	**0.73**	0.21	-0.34	**-0.72**	**-0.78**	-0.57	**-0.81**	1.00								
Cr	-0.25	-0.41	0.62	-0.41	-0.55	-0.45	-0.53	**0.91**	**0.68**	0.49	0.08	0.24	-0.11	1.00							
Co	-0.66	0.14	0.42	0.26	**-0.67**	**-0.72**	0.19	0.05	0.29	0.27	0.12	0.36	**-0.73**	-0.16	1.00						
Cu	-0.23	-0.57	**0.76**	0.06	-0.61	**-0.73**	-0.18	0.45	0.50	0.37	0.01	0.28	-0.43	0.50	0.52	1.00					
Pb	-0.28	-0.28	0.51	-0.50	-0.46	-0.41	-0.48	0.18	0.58	**0.69**	0.65	**0.69**	-0.62	0.13	0.29	0.08	1.00				
Cd	0.32	-0.11	-0.16	-0.24	0.17	0.04	-0.46	0.15	-0.02	-0.12	-0.08	-0.23	0.56	0.38	-0.44	-0.10	0.08	1.00			
Ni	-0.11	-0.18	0.28	-0.47	-0.20	-0.25	-0.41	-0.23	0.34	0.57	**0.77**	**0.77**	-0.60	-0.37	0.25	-0.17	0.50	-0.40	1.00		
Zn	0.40	-0.26	-0.08	-0.04	0.30	0.29	-0.11	0.22	-0.13	-0.24	-0.33	-0.42	0.57	0.48	-0.58	0.08	-0.02	**0.68**	**-0.69**	1.00	
Ba	-0.42	-0.58	**0.93**	-0.63	**-0.83**	**-0.80**	**-0.75**	**0.74**	**0.97**	**0.92**	0.61	**0.81**	**-0.68**	**0.72**	0.28	0.61	0.58	0.05	0.30	-0.01	1.00

Bold values represent correlation significant at P=<0.05, N=9

3.3.B.c. Antarctic lakes (Larsemann Hills, East Antarctica)

The concentration of major and trace elements is provided in Table 3.3.8. Among the elements, average Al was considerably high in core L-10 than the other two cores. Fe, Mn, Ti, Mg, Cu, Co, Cd, Zn and Cr were higher in core L-8 while Ca, Ni, Ba and Pb were noted to be higher in Core L-12. Ti concentrations were found to be similar in core L-10 and L-12. However, in core L-8 elements like Cr, Cd, Ni and Zn, in core L-10 Cu along with Cr, Cd, Ni and Zn and in core L-12 Ba along with Cr, Cu, Cd and Ni are higher than the average crustal values.

In lacustrine environments, Ti and Al have been considered as good proxy elements to measure the intensity of detrital input (Whitlock et al., 2008; Armstrong-Altrin et al., 2015a, 2017, 2018). Chen et al., 2010, 2011; Hernandez-Hinojosa et al., 2018 stated that as the intensity of weathering increases, sediment becomes enriched in Al, Fe, Ti and Mn indicating increased supply of siliciclastic material to lacustrine sediments.

In core L-8 (Fig. 3.3.11a), in zone 1 from 30 to 18 cm elements like Al, Ca and Ba showed higher than the average values. Ti, Fe, Mg, Co, Cu, Cd, Ni and Zn showed increasing trend in this zone, and Mn and Pb remained constant. Elements like Fe, Pb, Cu, Ca and Ni showed similar fluctuating trend around the average line. In this zone Fe and Mg showed increasing trend similar to that of silt. Al showed increase up to 22 cm and then decreased in this section agreeing with a pattern of sand between 22 cm and 20 cm indicating its association with coarser sediments. Ba showed a decreasing trend as that of sand. Elements like Cu, Ni, Zn and Cd showed higher value at 24 cm depth in this zone similar to that of clay, TP and $CaCO_3$ indicating their association with finer sediments and organic elements. Cr however, increased up to 26 cm and then decreased up to 22 cm followed by large fluctuating increasing trend up to 8 cm and then showed slight decrease. In zone 2 from 18 to 4 cm depth, elements like Al, Ti, Fe, Mg, Ca, Ba, Zn, Co and Pb showed decreasing trend. Ni, Cd, Cu, Mn and Cr fluctuated around the average line. Mn, Co and Cr showed slight increasing trend which agreed to that of sand while Ti, Ca and Mg showed large decreasing trend similarly to that of silt indicating the role of sediment components in regulating the distribution of these elements. Cu, Ba, Zn and Cd showed a slightly decreasing trend, while Co showed higher values in the middle section. Al, Fe, Mn, Mg, Ti, Cu, Ba,

Zn, Ca, Cd, Pb and Co showed a negative peak at 12 cm coinciding with lower values of sand indicating their association with coarser sediments. In zone 3 from 0-4 cm almost all the elements showed an increasing trend towards the surface. Elements like Al, Ti, Ca, Ni, Ba, Zn, Cd, Pb and Co showed higher value at the surface similar to that of clay indicating their association with finer particles due to increase in freshwater influx in recent years. Fe, Mn, Mg and Cu maintained the highest concentration at 2 cm depth and Cr with lower peak at 2 cm largely decreased indicating their different source and/or depositional process. Overall in this core Fe, Mg and Co showed a distribution similar to that of TOC and TN indicating their association with organic elements. Al and Ca distribution largely agreed with that of sand indicating their source to be lithogenic. Ba showed opposite trend to that of TOC as it might have been dissolved when exposed to anoxic pore waters from which the sulfate has been removed by microbial activity (Van Os et al., 1991; Von Breymann et al., 1992; Paytan and Kastner, 1996; Torres et al., 1996; Schenau and De Lange, 2001). High Ba concentration in the sediments indicates the source of sediments from felsic rocks since Ba is usually hosted in rocks rich in K-feldspars and micas as Ba substitutes K, Pb, Sr and even Ca in the lattice structure due to its similar ionic radius. Cr did not show a similar distribution with any of the element indicating its source to be different from other elements.

In core L-10 (Fig.3.3.11b), in Zone 1 from 28 to 18 cm, Ca showed slightly higher than the average values while Cd showed lower than the average value. Cr and Ni showed positive peak values in this zone. Elements like Ti, Fe, Mn, Mg, Cr, Co showed decreasing trend while elements like Al and Cd showed increase in this zone. Cu, Pb, Ba and Zn fluctuated around the average line. Ti, Mg, Ca, Cu, Ni, Zn, Cd, Pb and Zn showed a positive peak at 24 cm depth in this zone similar to that of silt indicating the role of finer sediments in regulating the distribution of these elements. In zone 2 from 18 to 4cm, most of the elements like Al, Ca, Cr, Cd, Ni and Ba showed lower than the average values. Elements Fe and Cr showed a slightly decreasing trend in the middle zone. In this zone Mn, Cu, Ni, Pb and Co showed slight increasing trend and Mg, Ba, Zn and Cd exhibited an almost constant trend. All the elements showed a positive peak at 8 cm coinciding with upper higher values of sand suggesting their

association with coarser sediments. In Zone 3 from 4cm to the surface, elements like Ti, Mg, Co, Ni, Cd, Pb and Ba showed an increasing trend while elements like Fe, Mn, Ca, Cr, Cu and Zn showed a decreasing trend towards the surface. Ca and Zn exhibited almost linear decreasing trend indicating their association with finer sediments. Most of the elements associated with silt and clay suggested high runoff of the weathered material and finer sediment deposition, leading to overall increased productivity (Govil et al., 2016). Overall, Fe and Ti showed similar distribution suggesting their source to be lithogenic in nature and Mg and Cd exhibited similar distribution as that of TOC indicating their association with organic matter. Elements like Fe, Cd, Cr, Cu and Ba was found to be low in this lake possibly because the lake sediments are relatively coarse grained and therefore, unable to adsorb the metals effectively and they remained in the water column.

In core L-12 (Fig.3.3.11c), in zone 1 from 28 to 14 cm elements like Al and Ca showed higher than the average values while remaining elements showed lower than the average values in this zone. Elements Ca, Cu, Ba, Pb and to some extent Cd exhibited a decreasing trend in the lower zone of the core similar to that of clay while Ni and Cr showed an increase similar to sand distribution. Al, Ca, Cr, Cu, Ba, Pb and Zn showed a negative peak at 22 cm similar to that of clay indicating their association with clay. Elements like Cu, Cd and Zn showed a positive peak at 18 cm similar to that of sand indicating their association with coarser sediments at this depth. In zone 2 from 14 to 6 cm, elements like Al, Ti, Fe, Mn, Mg, Co showed similar increasing trend indicating their common source while Ca, Cu, Ba, Cd and Pb showed decreasing trend while Zn exhibited constant trend. Co and Cr showed increasing trend agreeing with that of TN and BSi indicating their association with organic elements. In zone 3 from 4 cm to the surface, almost all the elements except Mn showed an increasing trend towards the surface similar to that of TOC, TN, BSi along with sand and silt indicating the role of these sediment components in regulating the distribution of elements. Overall Fe, Mn, Mg, Ti, Cr and Co showed a similar distribution to that of organic carbon indicating their association with organic matter.

In all the three cores most of the elements showed an increase in top 4 cm indicating their mobilization and association with finer sediments. In the sediment samples

analysed Fe, Mn, Mg, Ca are less than the crustal average. When geology of the area is taken into account, the adjacent rocks should be rich in garnet, however, it is not revealed in sediment composition. This may be because transportation of garnet requires high energy as garnet is relatively stable during weathering and has high specific gravity. Garnet must have been transported to the shorter distance and must have deposited near the periphery of the lake and might not have reached the core location. This resulted in a low concentration of Fe, Mn, Mg and Ca in the sediment. The trace elements, after entering into the aquatic environment follow two different paths, some get involved in biological processes and are deposited as faecal matter representing a source of biogenic input and remaining participates through physicochemical processes and gets deposited in sediments, constituting a lithogenic source. Boyle et al. (1977), Chan et al. (1977) and Bruland and Franks (1983) stated that Dissolved concentration profiles of many trace elements such as Ba, Cd, Pb, Ni and Cu co-vary with those of nutrients such as nitrate, silicate and phosphate indicating that these trace elements are cycled with major biogenic phases; however, their association with the biogenic phases may be different. The enrichment of elements such as Cu, Ni, Ba, Zn, Cd, Co and Pb along with carbonate, TOC and opal in marine sediments have been used as Palaeo-productivity indicators earlier (Collier and Edmond, 1984; Shimmield and Pedersen, 1990).

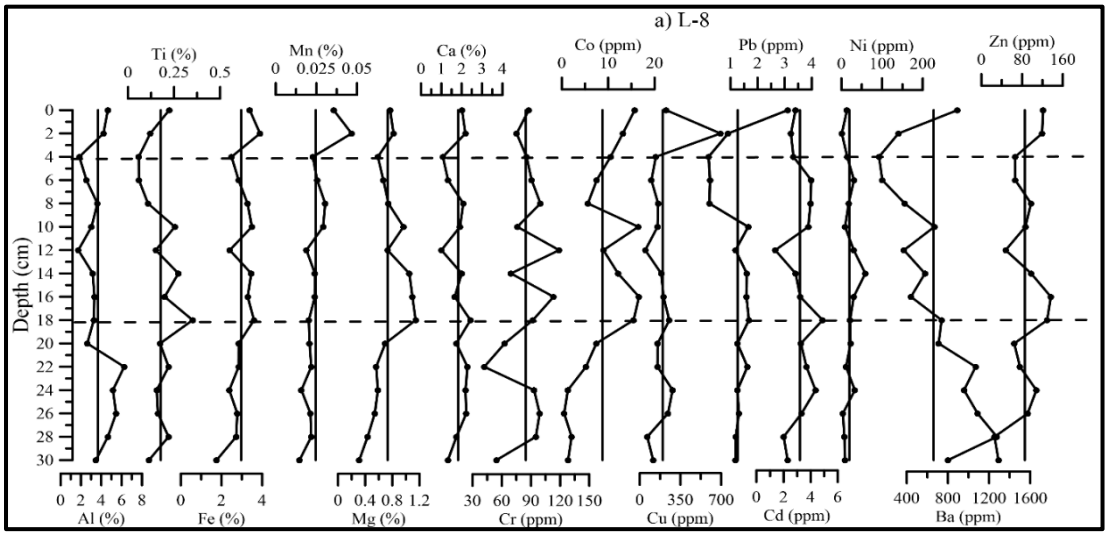

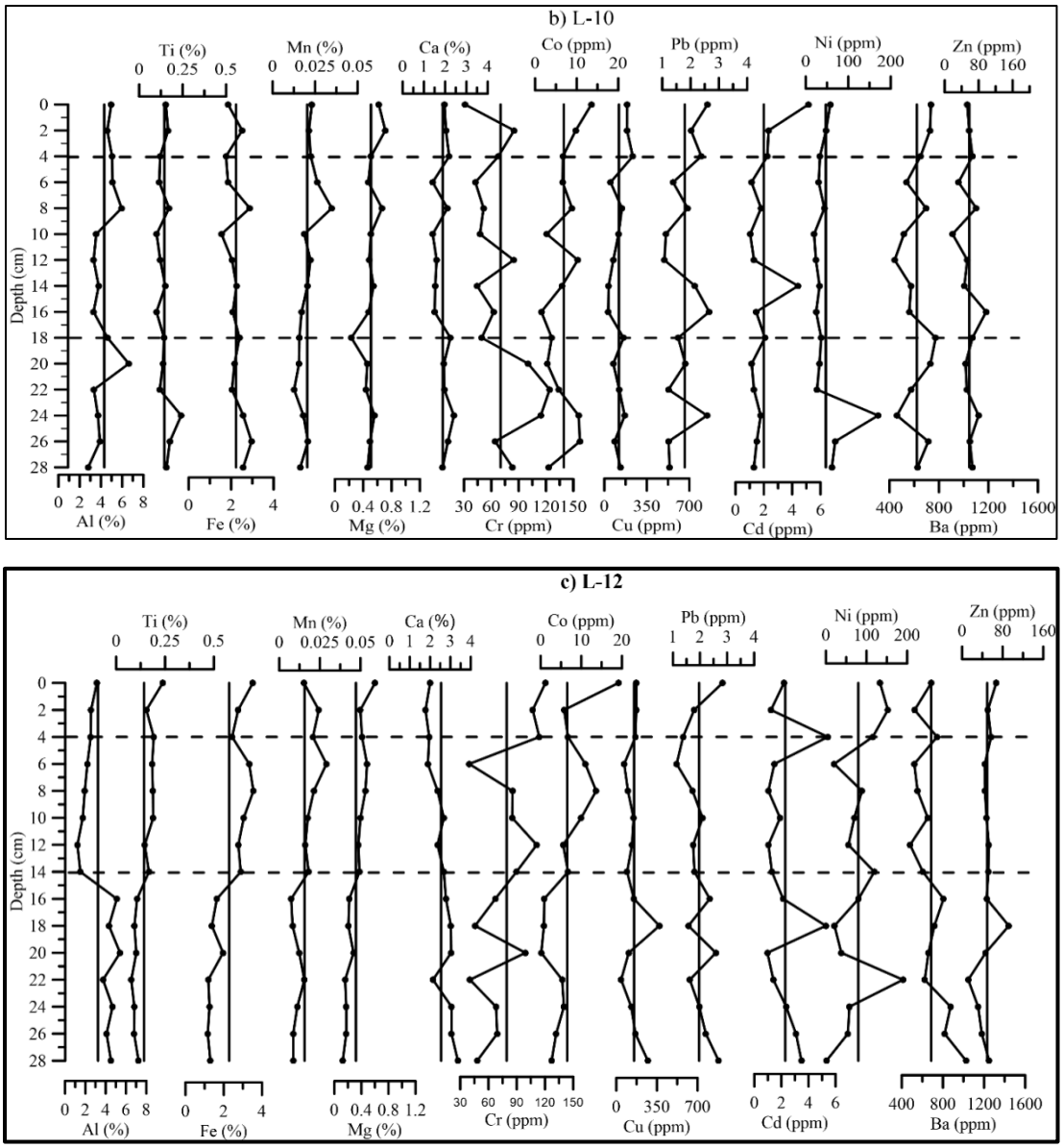

Fig.3.3.11 Distribution of elements Al, Ti, Fe, Mn, Mg, Ca, Cu, Ba, Ni, Zn, Cd, Pb, Cr and Co in sediment with depth of a) core L-8 b) core L-10 c) core L-12

Based on the crustal composition ($[M/Al]_{crust}$), the proportion of the lithogenic input of trace metal (M_{lith}) was estimated (Tribovillard et al., 2011) as follows:

$$M_{lith} = Al_{sample} \times (M/Al)_{crust}$$

Where Al_{sample} and Al_{crust} were the concentration of the element Al in the sample and in the continental crust respectively. Al was used as a normalizer, since; it is a

conservative element and has no significant anthropogenic source. M is the metal concentration in the sample.

The biogenic trace metal (M_{bio}) can be obtained by subtracting the Metal concentration of the sample from the Lithogenic input.

$$M_{bio} = M - M_{lith}$$

Metals like Cu, Zn, Ni, and Cd showed a high concentration of biogenic input when computed as compared to lithogenic source in all the three cores (Table 3.3.9). Ba showed high biogenic concentration in core L-8 and L-12 while its lithogenic concentration was found higher in core L-10. The lithogenic input of Ca was found higher in core L-8 and L-10 and biogenic input was found higher in core L-12. Pb and Co were found to be of Lithogenic origin as biogenic input is negligible in all the three cores, due to their similar distribution with that of lithogenic elements indicating that it has been derived from weathering of the rocks present in the catchment area. Zn showed higher biogenic input in all the three cores as it might have been absorbed and assimilated by the organisms and released back into the water column as biological material, ultimately deposited into the lake, forming biogenically sourced trace element in the sediment (Sun et al., 2013), however, in core L-10, lithogenic (28.92 ppm) and biogenic (29.13 ppm) input of Zn was almost similar suggesting that it was equally determined from biogenic and Lithogenic input. Elements like Ca, Co and Pb exhibited high contribution from the lithogenic input. All the three lakes are dominated by the sand fraction; therefore, dilution effect by coarse-grained particles leads to the low proportion of organic matter in the sediments. Overall, trace metals in the sediments are mainly controlled by lithogenic components (sand, silt and clay); however, some elements showed considerable biogenic inputs.

Further, to compare the three lakes, means paired samples t-test was conducted on metals of core L-8 and L-10, L-10 and L-12 and L-12 and L-8 where p values indicated statistically significant differences ($p<0.05$) between variables of the two cores. The result of paired samples t-test (p:2 tailed) indicated means of metals like

Fe, Mn, Mg, Cd, Pb, Zn, Cu and Ni showed statistically significant differences between core L-8 and L-10 (Table 3.3.10a). The negative t-values indicated higher mean values of Pb and Ni in core L-10. Comparison between these two cores, therefore, showed the significant greater addition of metals Fe, Mn, Mg, Cd, Zn, and Cu in core L-8 as compared to core L-10. Further, in core L-10 and L-12 (Table 3.3.10b), Al, Mn, Ca and Mg exhibited statistically significant difference. Ca showed negative t-value suggesting higher mean value of Ca in core L-12. On comparison of core L-10 and L-12, Al, Mn and Mg were found higher in core L-10. Furthermore, Metals like Fe, Mn, Ca, Mg, Cd, Pb, Zn and Ni showed statistically significant differences between L-12 and L-8 core (Table 3.3.10c). The negative t-values obtained for Fe, Mn, Mg, Cd and Zn indicated higher mean values of these metals in core L-8. When comparison was made between core L-12 and L-8, metals like Ca, Pb and Ni were found higher in core L-12. Therefore, the sediments exhibited differential accumulation of metals in three different lacustrine environments with depth due to varying catchment area processes and supply of sediment material.

Table 3.3.8 Concentration of major and trace elements in the sediments of a) core L-8 b) core L-10 c) core L-12

	a) Core L-8			b) Core L-10			c) Core L-12		
	Min	Max	Avg	Min	Max	Avg	Min	Max	Avg
Al (%)	1.74	6.25	3.69	2.80	6.62	4.31	1.21	5.42	3.25
Ti (%)	0.06	0.35	0.18	0.10	0.24	0.14	0.08	0.24	0.14
Fe (%)	1.76	3.89	2.97	1.55	2.96	2.23	1.16	3.55	2.28
Mn (%)	0.047	0.075	0.058	0.013	0.035	0.020	0.016	0.007	0.029
Mg (%)	0.31	1.14	0.73	0.23	0.71	0.51	0.12	0.60	0.32
Ca (%)	1.00	2.43	1.82	1.41	2.41	1.89	1.77	3.37	2.54
Cr (ppm)	42.00	119.00	84.72	31.25	124.00	70.20	39.50	120.50	79.37
Co (ppm)	0.51	16.64	8.76	1.49	13.52	6.90	0.14	19.14	6.53
Cu (ppm)	47.23	694.95	198.35	32.15	234.23	120.03	41.43	371.15	152.60
Cd (ppm)	1.39	4.88	3.21	1.04	5.15	2.00	0.97	5.43	2.29
Pb (ppm)	0.19	3.11	1.26	1.08	2.66	1.80	1.14	2.83	1.97
Ni (ppm)	1.01	58.63	19.57	19.64	170.23	47.26	1.33	189.69	79.76
Ba (ppm)	130.05	1275.78	661.28	441.70	773.35	621.28	480.95	1025.25	686.07
Zn (ppm)	25.70	136.58	85.44	18.53	97.68	58.04	12.18	92.10	49.41

3.3.9 Average values of Lithogenic and Biogenic fractions of trace elements in cores a) L-8 b) L-10 c) L-12

	Cu_{Lith}	Cu_{Bio}	Ni_{Lith}	Ni_{Bio}	Zn_{Lith}	Zn_{Bio}	Pb_{Lith}	Pb_{Bio}	Cd_{lith}	Cd_{bio}	Ba_{Lith}	Ba_{Bio}	Co_{Lith}	Co_{Bio}	Ca_{Lith}	Ca_{Bio}
L-8	6.81	**191.54**	8.86	**10.72**	24.76	**60.68**	**8.09**	-6.83	0.05	**3.16**	318.07	**343.21**	**5.52**	3.23	**14022.65**	4206.88
L-10	7.95	**112.08**	10.34	**36.92**	28.92	**29.13**	**9.45**	-7.66	0.06	**1.94**	**371.48**	249.79	**6.45**	0.45	**16377.56**	2509.78
L-12	6.00	**146.60**	7.80	**71.96**	21.80	**27.61**	**7.13**	-5.16	0.04	**2.24**	280.07	**406.00**	**4.86**	1.66	12347.27	**13100.56**

Table 3.3.10 Paired sample t test for the comparison of elements in cores a) L-8 and L-10 b) L-10 and L-12 c) L-12 and L-8

a) L-8 & L-10

Pairs of variables	t	df	P(2-tailed)
Pair 1 Al_1 - Al_2	-1.190	14	.254
Pair 2 Ti_1 - Ti_2	1.590	14	.134
Pair 3 Fe_1 - Fe_2	5.052	14	.000
Pair 4 Mn_1 - Mn_2	2.506	14	.025
Pair 5 Mg_1 – Mg_2	3.702	14	.002
Pair 6 Ca_1 - Ca_2	-.305	14	.765
Pair 7 Cr_1 - Cr_2	1.651	14	.121
Pair 8 Co_1 - Co_2	1.240	14	.235
Pair 9 Cu_1 - Cu_2	2.298	14	.037
Pair 10 Pb_1 - Pb_2	-2.399	14	.031
Pair 11 Cd1-Cd2	3.061	14	.008
Pair 12 Ni_1 - Ni_2	-2.651	14	.019
Pair 13 Ba_1 - Ba_2	.333	14	.744
Pair 14 Zn_1 - Zn_2	3.943	14	.001

b) L-10 &L-12

Pair of variables	t	df	P(2-tailed)
Pair 1 Al_1-Al_2	2.340	14	.035
Pair 2 Ti_1 - Ti_1	.139	14	.891
Pair 3 Fe_1 - Fe_2	-.172	14	.866
Pair 4 Mn_1 - Mn_2	3.489	14	.004
Pair 5 Mg_1 - Mg_2	5.830	14	.000
Pair 6 Ca_1 - Ca_2	-4.526	14	.000
Pair 7 Cr_1 - Cr_2	-.838	14	.416
Pair 8 Co_1 - Co_2	.345	14	.735
Pair 9 Cu_1 - Cu_2	-1.533	14	.147
Pair 10 Pb_1 - Pb_2	-.970	14	.349
Pair 11 Cd_1 - Cd_2	-.601	14	.557
Pair 12 Ni_1 - Ni_2	-1.816	14	.091
Pair 13 Ba_1 - Ba_2	-1.411	14	.180
Pair 14 Zn_1 - Zn_2	1.339	14	.202

c) L-12 & L-8

Pairs of Variables	t	df	P(2-tailed)
Pair 1 Al_1 - Al_2	-1.193	14	.253
Pair 2 Ti_1 - Ti_2	-1.454	14	.168
Pair 3 Fe_1 - Fe_2	-3.428	14	.004
Pair 4 Mn_1 - Mn_2	-5.364	14	.000
Pair 5 Mg_1 - Mg_2	-7.234	14	.000
Pair 6 Ca_1 - Ca_2	4.667	14	.000
Pair 7 Cr_1 - Cr_2	-.878	14	.395
Pair 8 Co_1 - Co_2	-1.518	14	.151
Pair 9 Cu_1 - Cu_2	-1.235	14	.237
Pair 10 Pb_1 - Pb_2	4.792	14	.000
Pair 11 Cd_1 - Cd_2	-2.417	14	.030
Pair 12 Ni_1 - Ni_2	7.961	14	.000
Pair 13 Ba_1 - Ba_2	.472	14	.644
Pair 14 Zn_1 - Zn_2	-4.854	14	.000

Pearson's correlation coefficient was computed using whole data set to check overall interrelationship between various parameters studied to understand the source to sink processes. In core L-8, Pearson's correlation coefficient (Table 3.3.11a) for metals like Ba and Ca showed strong association with Al indicating that these metals were associated with alumino-silicate minerals (Rubio et al., 2000; Armstrong-Altrin, 2009). Mn, Ca, Mg, Co, Zn and Cu showed significant correlation with Fe indicating the role of Fe-oxyhydroxides in regulating the distribution of these metals. Co and Cu exhibited positive correlation with Mn indicating the role of Mn-oxide in the distribution and concentration of Co and Cu. Ba, Pb, Ca and Mg displayed a strong correlation with Ti indicating sediment input from rocks namely granitoids and gneisses present in the catchment area. Zn with Cu, Cd, Co; Mg with Zn, Co; Ca with Cd, Zn, Cu, Ba showed strong correlation values which may indicate similar depositional behavior. Al and Ba showed a strong correlation with the coarser fraction of the sediment. Mg exhibited a strong correlation with silt, clay, TOC, TN, BSi while Co showed a positive correlation with clay, TOC, TN, BSi implying that organic matter aids in the trapping of Mg and Co in the finer sediments. The fine sediment fraction contains a large amount of autochthonic organic matter derived from biological production and plays an important role in the enrichment of trace metals.

In core L-10, Al was significantly correlated with Ba indicating their natural lithogenic source. Ca, Ni, Co and Fe showed significant positive correlation with Ti indicating their lithogenic source. Cu and Ni showed a positive correlation with Ca indicating their Co-precipitation with Ca. Pb exhibited significant correlation with Cd and Zn exhibited positive correlation with Pb. TOC and silt showed good association in this core (Table 3.3.11b). Clay with Co, TN with Pb, Mg, Co, Cu and Cd with TOC showed good correlation.

Further, in core L-12 Ti, Mg, Cr and Co displayed a good correlation with TOC, TN and BSi indicating the role of organic matter in governing the distribution of these elements in sediments. Increase in freshwater influx must have resulted in the accumulation of these elements with organic matter and biogenic silica. Fe and Mn showed significant correlation with each other indicating that they are derived from the same source or with similar post-depositional behavior. Mn showed significant positive association with TP, Co and Mg. Ba and Ca showed significant positive correlation with Al suggesting that they are derived from the same lithogenous source. Cr and Co showed significant correlation with Mg; Zn, Cu and Ni are significantly correlated with Cd implying their common source or a common mechanism regulated their concentration (Table 3.3.11c). From the above discussion, it is clear that the finer sediments, organic carbon, and Fe-Mn oxides regulated the abundance and distribution of elements. Therefore, it is apparent that various sedimentary and biogeochemical processes affected elemental distribution.

Table 3.3.11 Pearson's correlation coefficients of sediment components and elements of a) core L-8 b) core L-10 c) core L-12

a) Core L-8

	Sand	Silt	Clay	TOC	TN	TP	BSi	Al	Ti	Fe	Mn	Mg	Ca	Cr	Co	Cu	Pb	Cd	Ni	Ba	Zn
Sand	1.00																				
Silt	**-0.79**	1.00																			
Clay	**-0.61**	0.00	1.00																		
TOC	**-0.82**	**0.61**	**0.54**	1.00																	
TN	**-0.70**	0.39	**0.64**	**0.90**	1.00																
TP	0.04	0.00	-0.06	-0.16	-0.10	1.00															
BSi	**-0.78**	**0.63**	0.46	**0.63**	**0.51**	-0.17	1.00														
Al	**0.60**	**-0.68**	-0.10	**-0.65**	-0.47	-0.29	-0.33	1.00													
Ti	-0.33	0.19	0.30	-0.07	0.03	-0.14	0.36	0.23	1.00												
Fe	-0.41	0.17	0.45	0.38	**0.58**	-0.14	0.29	0.06	0.48	1.00											
Mn	-0.03	-0.22	0.34	0.28	**0.53**	-0.09	-0.09	0.08	-0.07	**0.75**	1.00										
Mg	**-0.81**	**0.56**	**0.61**	**0.65**	**0.67**	-0.15	**0.70**	-0.29	**0.58**	**0.79**	0.32	1.00									
Ca	0.19	-0.26	0.03	-0.36	-0.18	-0.31	-0.11	**0.72**	**0.58**	**0.58**	0.28	0.30	1.00								
Cr	-0.25	0.19	0.16	0.46	0.34	0.13	0.40	-0.28	-0.09	0.07	0.00	0.26	-0.21	1.00							
Co	**-0.78**	0.37	**0.79**	**0.71**	**0.77**	-0.12	**0.53**	-0.39	0.41	**0.73**	**0.51**	**0.85**	0.05	0.14	1.00						
Cu	0.17	-0.33	0.15	0.05	0.21	-0.18	-0.07	0.30	0.00	**0.55**	**0.69**	0.25	**0.51**	-0.10	0.25	1.00					
Pb	-0.14	-0.20	0.49	-0.15	-0.01	-0.29	0.21	0.38	**0.70**	0.27	0.09	0.29	0.40	-0.12	0.37	0.06	1.00				
Cd	-0.11	0.03	0.15	-0.06	-0.04	-0.15	-0.07	0.22	0.26	0.33	-0.05	0.36	**0.59**	-0.08	0.11	0.12	-0.02	1.00			
Ni	**-0.63**	0.63	0.20	0.44	0.40	0.01	**0.62**	-0.36	0.18	0.04	-0.30	0.45	-0.13	0.17	0.18	-0.26	0.01	0.12	1.00		
Ba	**0.54**	-0.49	-0.25	**-0.80**	**-0.70**	-0.06	-0.27	**0.76**	**0.50**	-0.18	-0.32	-0.35	**0.50**	-0.25	-0.45	-0.12	**0.55**	0.04	-0.28	1.00	
Zn	-0.39	0.06	**0.56**	0.40	0.44	-0.47	0.39	0.20	0.36	**0.72**	0.46	**0.73**	**0.61**	0.22	**0.60**	**0.60**	0.36	**0.54**	0.17	-0.15	1.00

Bold values represent correlation significant at P=<0.05, N=16

b) Core L-10

	Sand	Silt	Clay	TOC	TN	TP	BSi	Al	Ti	Fe	Mn	Mg	Ca	Cr	Co	Cu	Pb	Cd	Ni	Ba	Zn
Sand	1.00																				
Silt	**-0.61**	1.00																			
Clay	**-0.74**	-0.07	1.00																		
TOC	**-0.63**	**0.55**	0.34	1.00																	
TN	0.06	0.19	-0.23	0.45	1.00																
TP	0.46	-0.47	-0.19	-0.31	-0.15	1.00															
BSi	-0.37	0.32	0.20	0.24	-0.17	0.18	1.00														
Al	0.16	-0.17	-0.06	0.22	**0.64**	0.34	-0.13	1.00													
Ti	-0.07	0.20	-0.08	0.27	0.24	0.13	0.23	0.06	1.00												
Fe	0.06	0.24	-0.28	-0.01	0.04	-0.02	0.16	0.03	**0.72**	1.00											
Mn	-0.27	0.20	0.17	0.32	0.18	0.06	0.27	0.46	0.14	0.19	1.00										
Mg	-0.46	0.50	0.16	**0.69**	0.21	0.11	**0.70**	0.18	0.34	0.17	**0.58**	1.00									
Ca	0.08	0.04	-0.13	0.20	0.40	0.14	-0.11	0.27	**0.70**	**0.55**	-0.03	0.03	1.00								
Cr	0.06	0.12	-0.18	-0.27	0.05	0.20	0.17	-0.20	0.27	0.20	**-0.52**	-0.05	0.37	1.00							
Co	**-0.62**	0.26	**0.56**	**0.64**	0.15	-0.06	0.34	0.12	**0.56**	0.27	0.48	**0.56**	0.38	-0.07	1.00						
Cu	-0.24	0.28	0.07	**0.52**	0.36	0.05	-0.07	0.20	0.34	0.02	0.11	0.24	**0.71**	0.09	0.36	1.00					
Pb	0.01	-0.05	0.03	0.47	**0.56**	-0.19	0.15	0.25	0.30	-0.03	0.12	0.39	0.27	-0.11	0.19	0.28	1.00				
Cd	-0.32	-0.01	0.41	**0.66**	0.18	-0.25	0.27	0.12	0.20	-0.08	0.18	0.34	0.09	-0.47	0.48	0.23	**0.56**	1.00			
Ni	0.01	0.07	-0.07	0.16	0.16	0.14	0.10	-0.12	**0.90**	0.47	-0.04	0.22	0.61	0.36	0.44	0.32	0.36	0.07	1.00		
Ba	0.10	0.01	-0.13	0.36	0.35	-0.01	-0.28	**0.57**	0.11	0.34	0.07	0.00	0.47	-0.25	0.06	0.37	0.13	0.30	-0.16	1.00	
Zn	0.08	0.01	-0.10	-0.03	0.19	-0.33	0.00	-0.09	0.35	0.50	-0.01	0.03	0.47	0.23	0.02	0.14	0.57	0.00	0.38	0.11	1.00

Bold values represent correlation significant at P=<0.05, N=15

c) Core L-12

	Sand	Silt	Clay	TOC	TN	TP	BSi	Al	Ti	Fe	Mn	Mg	Ca	Cr	Co	Cu	Pb	Cd	Ni	Ba	Zn
Sand	1.00																				
silt	**-0.54**	1.00																			
clay	**-0.80**	-0.07	1.00																		
TOC	-0.01	-0.03	0.03	1.00																	
TN	**0.53**	-0.12	**-0.55**	0.48	1.00																
TP	0.05	-0.22	0.09	-0.14	-0.10	1.00															
BSi	0.15	-0.22	-0.03	**0.79**	0.47	0.25	1.00														
Al	-0.13	0.08	0.10	-0.13	-0.36	**-0.54**	-0.33	1.00													
Ti	-0.02	-0.09	0.08	**0.64**	**0.55**	0.30	**0.71**	**-0.70**	1.00												
Fe	-0.01	-0.05	0.04	0.45	**0.57**	0.38	0.51	**-0.77**	**0.92**	1.00											
Mn	-0.16	0.12	0.10	0.15	0.21	**0.63**	0.44	**-0.73**	**0.65**	**0.76**	1.00										
Mg	0.03	-0.03	-0.02	**0.64**	**0.63**	0.24	**0.69**	**-0.66**	**0.94**	**0.95**	**0.71**	1.00									
Ca	-0.06	-0.20	0.21	-0.49	-0.45	-0.43	**-0.65**	**0.59**	**-0.62**	**-0.64**	**-0.82**	**-0.71**	1.00								
Cr	0.25	-0.44	0.02	**0.55**	**0.60**	0.06	**0.64**	-0.38	**0.58**	**0.54**	0.23	**0.60**	-0.37	1.00							
Co	-0.22	0.15	0.16	**0.69**	0.29	0.16	**0.53**	**-0.58**	**0.84**	**0.78**	**0.55**	**0.82**	**-0.59**	0.35	1.00						
Cu	0.25	-0.44	0.01	0.02	-0.13	-0.17	0.09	0.31	-0.17	-0.32	-0.50	-0.28	0.42	-0.12	-0.31	1.00					
Pb	-0.23	-0.09	0.33	0.33	0.00	-0.44	-0.07	0.50	-0.07	-0.18	**-0.61**	-0.14	0.49	0.22	-0.02	0.21	1.00				
Cd	0.31	-0.27	-0.18	0.06	-0.14	-0.14	0.30	0.27	-0.11	-0.40	-0.35	-0.26	0.22	-0.16	-0.25	**0.73**	-0.11	1.00			
Ni	0.18	-0.50	0.14	0.20	-0.04	-0.15	0.29	0.24	0.04	-0.18	-0.41	-0.11	0.35	0.08	-0.16	**0.96**	0.29	**0.74**	1.00		
Ba	-0.26	-0.03	0.33	-0.07	-0.46	-0.39	-0.18	**0.69**	-0.41	**-0.68**	**-0.72**	**-0.62**	**0.69**	-0.33	-0.36	0.47	**0.52**	**0.55**	0.51	1.00	
Zn	0.42	-0.48	-0.16	0.29	0.38	-0.10	0.39	-0.05	0.30	0.21	-0.13	0.28	0.09	0.22	0.02	**0.79**	0.07	**0.53**	**0.81**	0.03	1.00

Bold values represent correlation significant at P=<0.05, N=15

3.3.B.d. Antarctic lakes (Schirmacher Oasis, East Antarctica)

The range and average values for major and trace elements are presented in Table 3.3.12. Among the elements Al, Ti, Fe and Cd were slightly higher in core V-1. Relatively, Mg, Ca, Co, Pb and Ba were higher in core GL-1 with considerable concentration of Cr, while, Mn, Cr, Cu, Ni and Zn were higher in core L-6 with considerable concentration of Co. Cd concentration ranges from 0.58 ppm to 1.23 ppm in the three cores and is slightly less than the value reported earlier (2 ppm) by Shrivastava et al. (2012).

In core GL-1 (Fig.3.3.12a), in the lower zone from 36 to 24 cm Mg and Co showed higher than the average values, Al, Cr, Pb, Ni, Cd, Zn showed lower than the average values. Ti, Fe, Mn, Ca, Cu and Ba fluctuated around the average line in this zone. Elements like Al, Mn, Ca, Cr, Ni, Ba showed an increasing trend while Ti, Mg and Co showed a decreasing trend. In the middle zone from 24 to 8 cm Al, Mg, Cd, Co, Zn and Pb showed lower than the average values while Ni showed higher than average values. Fe and Ba fluctuated around the average line. Further, Cr and Zn showed a peak similar to that of Fe and Mn at 12 cm. From 8 cm to the surface, Zn, Cd and Pb showed similar increasing distribution to that of Al, Fe and Mn indicating their similar source. Further, in the upper zone from 8 cm to the surface elements like Al, Fe, Mn, Ca, Co, Zn, Cd and Pb showed an increasing trend towards the surface coinciding with higher clay and TOC indicating association of elements with finer sediments and organic matter. The distribution pattern of all the trace elements, except Co and Ni largely agreed with the trend of Al. Co distribution largely agreed with that of Fe throughout the length of the core. Ni and Ba showed fluctuating trend with an overall increase towards the surface.

In core V-1 (Fig. 3.3.12b), in the lower portion from 28 cm to the 12 cm elements like Al, Ti, Cr, Ni, Zn showed lower than the average values while elements like Fe, Mn, Mg, Ca, Pb, Ba, Co and Zn fluctuated around the average line. Al, Ti, Cr, Pb, Cd showed an increase in their concentration from the bottom up to 12 cm while Fe, Mn, Ca, Co, Cu and Zn showed decrease in their concentration in this zone. In the middle portion from 12 to 4 cm elements like Al, Fe, Mn, Mg, Co, Ba and Zn showed a peak

at a depth of 8cm. In the upper portion from 4 cm to the surface almost all the elements except Pb showed am increasing trend towards the surface.

Overall, trace metals like Co, Cr, Ni and Zn showed a similar trend in their distribution with slight fluctuation around average line up to a depth of 12 cm and further increased towards the surface coinciding with clay and TOC. These elements therefore seem to be associated with finer sediments along with organic matter. The distribution of Ca, Co, Ba and Zn largely agreed with that of Al, Ti and Fe from bottom to the surface and distribution of Cr and Ni agreed with Fe especially in upper section from 12 cm to surface indicating the role of Fe oxide in regulating the distribution of these metals. Increase in fresh water influx in recent years must have facilitated in higher concentration of metals within the lake along with clay and TOC. The clay acts as adsorbent and plays an important role in ion exchange reactions (Matini et al., 2011) and therefore, involves in regulating distribution of metals. Cd and Pb showed different distribution trend compared to other trace metals indicating that they were from a different source.

In core L-6 (Fig. 3.3.12c), in zone 1 from 56 to 40 cm elements like Fe, Mn, Mg, Cr and Cu decreased while elements like Ca, Cd and Zn increased. Ni and Co remained constant in this zone. In zone 2 from 40 to 24 cm, almost all the elements showed fluctuating decreasing trend except Al, Mg, Ca, Cu and Pb. Elements like Mn, Co, Cu, Ni and Zn showed a peak at 24 cm similar to Al which coincided with higher values of sand. Elements like Al, Mn, Co, Ni, Cu, Ba and Zn showed decreasing trend in zone 2 from 24 to 8cm depth. Fe, Mg, Cr, Pb and Cd showed an increasing trend. In zone 4 from 8 cm to the surface, elements like Al, Mn, Ba, Cd showed a similar increasing trend. Ti, Mg and Pb displayed decreasing trend towards surface. The trend of Co largely fluctuated but with a steadily decreasing trend from the bottom to the surface which largely agreed to that of Fe, Mn as Mn decreased from 56 to 54 cm, 40 to 20 cm and 12 to 8 cm with value at the bottom (2089.75 ppm) and at the top (1974.75 ppm), and in the lower section agreed to that of clay suggesting their association with Fe, Mn oxide and clay. In the middle section of the core, elements

Mn, Co, Cu, Ni and Zn showed a peak at 24 cm similar to Al which coincided with higher values of sand. The elements Al, Fe, Mn, Cu, Ni, Zn and Co therefore seem to have a common lithogenic origin. These elements therefore seemed to have been derived from weathering of rocks namely gneisses and charnockites present in the catchment area. In the upper section from 12 cm to the surface, elements like Al, Mn, Ba, Ni, Cd showed a similar increasing trend. In the upper section Co and Pb distribution was regulated by Fe-oxide. From the figure (Fig. 3.3.12c) it is noted that Cr decreased from 56 to 54 cm and 40 to 28 cm, Ni showed a decrease from 40 to 20 cm and increased from 8 cm to surface, Ba decreased from 56 to 54 cm and from 42 to 24 cm and Cd increased from 8 cm to the surface similar to that of Mn indicating the role of Mn-oxide in the diagenetic remobilization of elements. In addition, sediment components namely sand and clay played a significant role in the distribution of elements in this core.

It is clear from the distribution of trace metals in the three studied cores, that the finer sediments, organic carbon, rock type present in the catchment area and Fe-Mn oxides regulate the abundance and distribution of metals. However, in addition to these factors, type of weathering, hydraulic sorting during transport to the lake basin, topographic setting and climatic conditions may play a role in regulating distribution of trace elements (Wronkiewicz and Condie, 1989; McLennan et al., 1990, 1993).

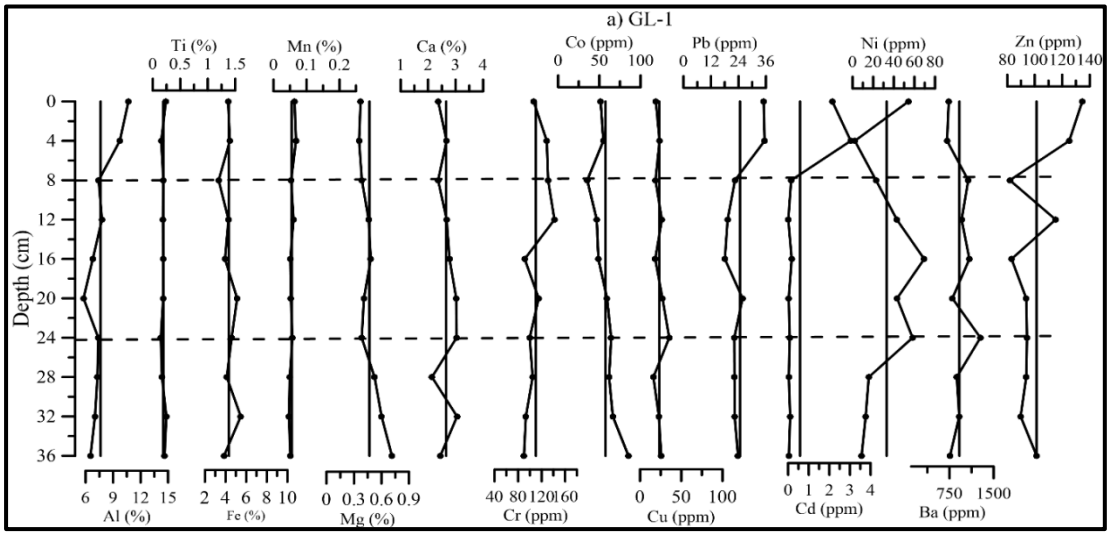

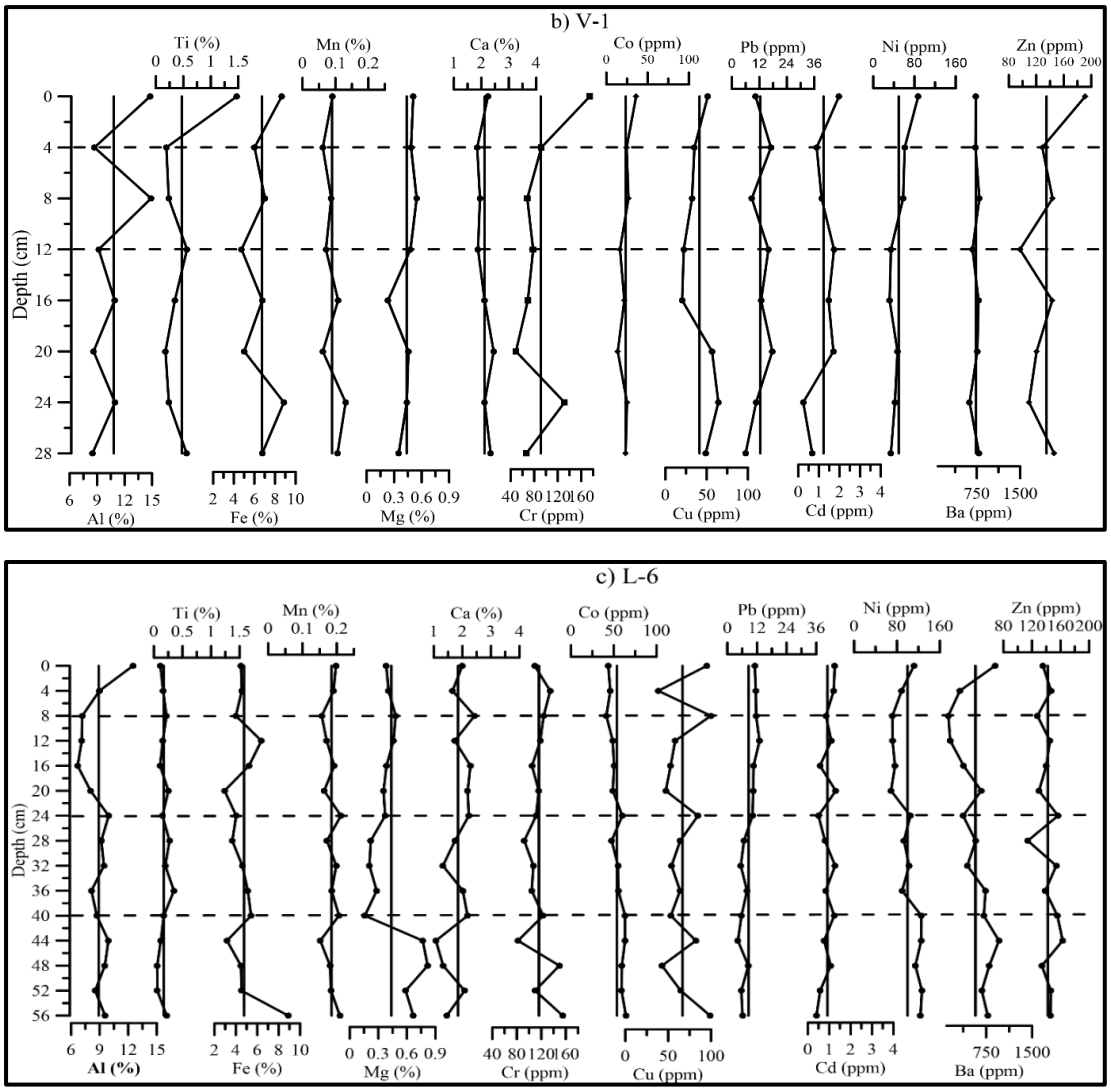

Fig. 3.3.12 Distribution of elements Al, Ti, Fe, Mn, Mg, Ca, Cr, Co, Cu, Pb, Cd, Ni, Ba and Zn, in sediment with depth of a) core GL-1 b) core V-1 and c) core L-6

Further, elemental associations signify that each paired element has an identical element source or common sink in sediments (Singh et al., 2002; Nyangababo et al., 2005). Pearson's correlation coefficient was computed for all the three cores. In core GL-1 (Table 3.3.13a), silt displayed a significant positive correlation with Ni. Organic carbon exhibited a significant positive correlation with elements Al, Mn, Cd, Pb and Zn. It is well established that organic carbon is an important factor in the distribution and concentration of trace metals (Rubio et al., 2000). Positive correlation of organic carbon with metals infer that organic carbon present in sediments provides active sites for sorption of these metals as it has high complexation ability with trace metals (Mantoura et al., 1978; Boszke et al., 2004). Pearson's correlation coefficients for

metals namely Mn, Zn, Cd and Pb showed strong correlation with Al indicating that these metals were associated with aluminosilicate minerals (Rubio et al., 2000; Algarasamy and Zhang, 2008) suggesting their lithogenic nature. The strong association of these metals with Al rich phases demonstrated the role of sediment transport and mineral sorting in influencing the distribution of metal abundances (Dalai et al., 2004). Mn with Zn, Pb and Cd also exhibited strong positive correlation values which may indicate the role of Mn-oxide in the distribution and concentration of Zn, Pb and Cd. Mg with Co and Ca with Cu showed significant correlation. Among the trace metals Pb with Cd and Zn, Cd with Zn exhibited significant correlation.

In core V-1 (Table 3.3.13b), clay showed significant correlation with TOC, TP, Zn, Cr, Ni, and Co. Sand showed negative correlation with silt, TOC, TN and with Ni. Ni and Co displayed a significant positive correlation with TOC indicating the role of TOC in governing distribution of elements in sediments. TN exhibited strong correlation with Ni. Al significantly correlated with Co and Ti with Cr and Zn indicating its lithogenic source. Ni showed significant positive correlation with Co indicating its co-precipitation with Co. Fe and Mn showed significant correlation with each other indicating that they are derived from similar source or with similar post depositional behavior. Fe showed significant positive correlation with Cr and Co. Cr exhibited significant correlation with Co while Co showed significant correlation with Zn and Ni. Majority of the trace metals except Cd and Pb were associated with clay and TOC indicating the role of finer sediments and TOC in regulating the distribution of metals in addition to Fe-Mn oxides.

In core L-6 (Table 3.3.13c), TOC, silt and clay showed a good association. BSi exhibited significant correlation with sand, Ti and Pb. Further, TP displayed good correlation with Fe. Ni and Ba showed significant positive correlation with Al suggesting that they are from the same lithogenous source. Ca with Pb; Co with Cd, Ni and Zn; Ni with Ba; Cd with Zn exhibited significant positive correlations implying that a common mechanism regulated their concentration. Cd and Pb, however, did not show any significant correlation with the lithogenous elements in core V-1 and L-6 indicating an alternative source for these elements. The input of Cd

and Pb in the sediments may be through anthropogenic activities like use of leaded gasoline in vehicles used for logistic operations.

When the three cores studied were compared (Table 3.3.12), it was observed that Lake L-6, has higher concentration of metals. This is possibly due to the surface channels flowing through the catchment area of this lake (GSI, 2006) having low flow velocity due to low elevation gradient facilitating transportation of relatively finer particles to the lake leaving behind coarser particles in the channel. In the lake GL-1 and V-1, presence of high concentration of coarse-grained particles must have diluted the concentration of metals.

Table 3.3.12. Concentration of major and trace elements in the sediments of a) core GL-1 b) core V-1 c) core L-6

	Core GL-1			Core V-1			Core L-6		
	Min	Max	Average	Min	Max	Average	Min	Max	Average
Al (%)	5.77	10.67	7.64	8.49	14.89	10.81	6.68	12.49	8.89
Ti (%)	0.15	0.25	0.19	0.18	1.47	0.47	0.06	0.35	0.17
Fe (%)	3.33	5.48	4.34	4.75	8.86	6.73	2.94	8.88	4.76
Mn(%)	0.05	0.07	0.06	0.06	0.13	0.09	0.15	0.21	0.18
Mg (%)	0.36	0.71	0.47	0.23	0.55	0.44	0.16	0.82	0.44
Ca (%)	2.14	3.06	2.66	1.85	2.45	2.12	1.07	2.43	1.85
Cr (ppm)	90.00	141.75	110	49.00	174.50	91.22	82.00	155.50	116
Co(ppm)	35.25	85.25	57.38	13.75	36.00	23.44	41.38	64.25	53.78
Cu (ppm)	16.24	35.45	23.42	20.24	64.15	41.30	38.53	99.90	66.69
Cd (ppm)	0.01	3.04	0.58	0.24	1.97	1.23	0.40	1.30	0.92
Pb (ppm)	18.05	35.40	24.65	5.98	17.65	12.37	4.25	13.01	8.58
Ni (ppm)	2.25	69.50	33.05	31.75	87.25	49.44	68.88	126.63	100
Ba (ppm)	709.85	1275.78	919.10	625.6	795.05	736.20	130.05	957.00	573.14
Zn (ppm)	81.90	134.58	101	96.25	191.25	135	114.13	163.00	142

Table 3.3.13. Pearson's correlation coefficients of sediment components and elements of a) core GL-1 b) core V-1 c) core L-6

a) Core GL-1

	Sand	silt	clay	TOC	TN	TP	BSi	Al	Ti	Fe	Mn	Mg	Ca	Cr	Co	Cu	Pb	Cd	Ni	Zn	Ba
Sand	1.00																				
silt	-0.46	1.00																			
clay	**-0.82**	-0.12	1.00																		
TOC	-0.33	-0.04	0.39	1.00																	
TN	0.05	-0.03	-0.04	-0.25	1.00																
TP	-0.37	0.77	-0.08	-0.06	-0.40	1.00															
BSi	-0.42	0.18	0.35	0.52	-0.50	0.27	1.00														
Al	0.01	-0.51	0.32	**0.82**	-0.10	1.00	0.30	1.00													
Ti	0.26	-0.26	-0.12	0.15	-0.61	-0.37	0.12	0.07	1.00												
Fe	0.17	0.13	-0.27	-0.06	0.29	-0.04	-0.20	-0.14	0.21	1.00											
Mn	-0.35	-0.21	0.53	**0.76**	0.12	-0.06	0.57	**0.81**	-0.31	-0.13	1.00										
Mg	0.14	-0.11	-0.09	-0.37	0.02	-0.22	-0.42	-0.50	0.44	0.04	**-0.65**	1.00									
Ca	-0.11	0.32	-0.08	-0.19	0.03	-0.31	0.14	-0.35	-0.04	**0.74**	-0.10	-0.09	1.00								
Cr	-0.29	-0.20	0.46	0.05	0.27	0.13	0.34	0.30	-0.34	-0.20	0.57	-0.57	-0.16	1.00							
Co	0.22	0.10	-0.31	-0.08	0.31	0.00	-0.28	-0.31	0.16	0.34	-0.32	**0.73**	0.14	**-0.66**	1.00						
Cu	-0.15	0.34	-0.05	-0.04	0.34	-0.39	0.28	-0.22	-0.34	0.40	0.19	-0.08	**0.67**	0.01	0.37	1.00					
Pb	0.19	-0.31	-0.01	**0.72**	0.01	-0.18	0.39	**0.77**	0.09	0.11	**0.71**	-0.42	-0.18	0.18	0.01	-0.08	1.00				
Cd	0.00	-0.44	0.28	**0.75**	-0.01	-0.22	0.35	**0.87**	-0.04	-0.01	**0.81**	-0.48	-0.17	0.25	-0.17	-0.16	**0.91**	1.00			
Ni	-0.52	**0.67**	0.16	0.30	-0.45	-0.28	0.34	-0.03	-0.07	-0.01	0.06	-0.39	0.30	-0.14	-0.34	0.18	-0.26	-0.19	1.00		
Zn	-0.26	-0.26	0.46	**0.87**	0.10	0.63	0.41	**0.83**	0.09	0.06	**0.84**	-0.30	-0.23	0.33	-0.01	0.04	**0.77**	**0.78**	-0.06	1.00	-
Ba	-0.02	0.24	-0.13	-0.42	-0.10	-0.35	-0.13	-0.35	-0.37	-0.14	-0.27	-0.18	0.33	-0.10	-0.27	0.33	**-0.67**	-0.54	0.52	-0.61	1.00

Bold values represent correlation significant at P=<0.05, N=10

b) Core V-1

	Sand	Silt	clay	TOC	TN	TP	BSi	Al	Ti	Fe	Mn	Mg	Ca	Cr	Co	Cu	Pb	Cd	Ni	Zn	Ba
Sand	1.00																				
Silt	**-0.82**	1.00																			
Clay	-0.69	0.15	1.00																		
TOC	**-0.94**	0.64	**0.81**	1.00																	
TN	**-0.86**	0.61	0.71	**0.94**	1.00																
TP	-0.36	-0.13	**0.79**	0.58	0.52	1.00															
BSi	-0.65	0.45	0.56	**0.79**	**0.80**	0.35	1.00														
Al	-0.22	-0.15	0.56	0.30	0.45	0.37	0.10	1.00													
Ti	-0.38	0.01	0.64	0.60	0.58	0.65	0.53	0.48	1.00												
Fe	-0.33	-0.07	0.64	0.29	0.16	0.25	0.00	0.63	0.41	1.00											
Mn	0.22	-0.39	0.11	-0.29	-0.45	-0.10	-0.48	0.25	0.08	**0.76**	1.00										
Mg	-0.38	0.13	0.50	0.44	0.51	0.64	0.17	0.37	0.16	0.01	-0.46	1.00									
Ca	0.38	-0.54	0.02	-0.23	-0.29	-0.03	0.23	-0.12	0.20	0.13	0.19	-0.30	1.00								
Cr	-0.63	0.30	**0.72**	0.64	0.53	0.46	0.28	0.53	**0.72**	**0.77**	0.34	0.30	-0.04	1.00							
Co	-0.65	0.19	**0.89**	**0.71**	0.66	0.55	0.42	**0.75**	0.66	**0.82**	0.36	0.25	-0.09	**0.80**	1.00						
Cu	-0.05	-0.24	0.39	0.05	-0.12	0.23	0.08	-0.01	0.11	0.48	0.29	0.23	0.63	0.39	0.19	1.00					
Pb	-0.13	0.57	-0.50	0.00	0.12	-0.44	0.13	-0.45	-0.30	-0.65	**-0.71**	0.14	-0.22	-0.22	-0.56	-0.21	1.00				
Cd	0.01	0.05	-0.08	0.19	0.42	0.10	0.45	0.23	0.51	-0.37	-0.56	0.13	0.12	0.03	-0.05	-0.35	0.40	1.00			
Ni	**-0.74**	0.36	**0.82**	**0.83**	**0.88**	0.57	0.70	0.64	0.61	0.43	-0.25	0.64	-0.02	0.68	**0.75**	0.27	-0.03	0.33	1.00		
Zn	-0.43	0.01	**0.72**	0.61	0.63	0.42	0.70	0.63	**0.71**	0.54	0.13	0.01	0.32	0.49	**0.80**	0.11	-0.48	0.31	0.69	1.00	
Ba	0.16	-0.26	0.05	0.01	0.15	-0.01	0.43	0.15	0.00	-0.22	-0.23	-0.24	0.29	-0.49	0.03	-0.30	-0.27	0.28	0.06	0.52	1.00

Bold values represent correlation significant at P=<0.05, N=8

c) Core L-6

	Sand	Silt	clay	TOC	TN	TP	BSi	Al	Ti	Fe	Mn	Mg	Ca	Cr	Co	Cu	Pb	Cd	Ni	Zn	Ba
Sand	1.00																				
Silt	-0.46	1.00																			
clay	**-0.91**	0.05	1.00																		
TOC	**-0.75**	**0.62**	**0.55**	1.00																	
TN	-0.10	-0.47	0.33	-0.23	1.00																
TP	**-0.56**	0.49	0.40	0.48	-0.35	1.00															
BSi	**0.62**	-0.48	-0.47	**-0.54**	-0.19	-0.26	1.00														
Al	0.39	-0.27	-0.31	-0.10	-0.10	-0.47	0.06	1.00													
Ti	0.03	0.25	-0.15	0.02	-0.43	0.23	**0.56**	-0.25	1.00												
Fe	-0.38	0.18	0.35	0.37	0.01	**0.61**	-0.21	-0.32	-0.12	1.00											
Mn	0.25	-0.29	-0.15	-0.13	-0.01	0.08	0.17	0.32	-0.17	0.42	1.00										
Mg	-0.30	0.00	0.33	0.28	0.28	-0.20	**-0.56**	0.08	**-0.62**	-0.22	-0.48	1.00									
Ca	0.11	0.20	-0.22	-0.03	0.17	0.22	-0.08	-0.36	0.21	0.13	0.22	-0.42	1.00								
Cr	-0.19	0.10	0.17	0.29	-0.02	0.19	-0.41	-0.12	-0.27	0.29	0.20	0.19	0.10	1.00							
Co	-0.34	-0.29	0.52	0.17	0.21	-0.17	-0.04	0.13	-0.28	0.01	0.25	0.24	-0.33	-0.12	1.00						
Cu	0.22	0.07	-0.28	0.23	-0.01	-0.19	0.00	0.33	0.01	-0.26	-0.16	0.10	0.26	-0.41	-0.19	1.00					
Pb	**0.54**	-0.14	**-0.54**	-0.40	-0.19	-0.11	**0.57**	-0.16	0.42	0.05	0.43	**-0.78**	**0.53**	-0.24	-0.16	0.12	1.00				
Cd	-0.06	-0.04	0.09	0.27	-0.07	-0.28	-0.09	0.08	-0.37	0.06	0.00	0.26	-0.21	-0.22	**0.55**	0.34	0.12	1.00			
Ni	-0.14	-0.43	0.36	0.09	0.36	-0.32	-0.12	**0.62**	-0.49	-0.09	0.32	0.26	-0.38	-0.11	**0.72**	0.11	-0.36	0.35	1.00		
Zn	-0.34	-0.06	0.41	0.29	0.10	-0.09	-0.25	0.15	-0.37	0.20	0.35	0.13	-0.29	-0.12	**0.66**	-0.01	0.03	**0.62**	0.50	1.00	
Ba	-0.12	-0.24	0.25	-0.05	0.10	-0.21	-0.12	**0.60**	-0.13	-0.35	-0.01	0.25	-0.35	-0.26	0.48	0.02	-0.43	-0.01	**0.67**	0.10	1.00

Bold values represent correlation significant at P=<0.05, N=14

Section 4: Beryllium (Be) estimation

Besides many paleoclimatic proxies, such as sedimentological, geochemical, major and trace elements, Be concentration in lacustrine and marine sediments has emerged out as a potential tool to unravel the past environmental changes linked directly/indirectly with the solar activity. The mobility of Be from terrestrial to the oceanic domain enables its isotopes to use effectively for understanding the weathering and erosional processes. Therefore, in order to use Be concentration as environmental proxy, their spatial and temporal variations in surface and subsurface sediments are studied. Many studies using Be as a proxy from Polar Regions (Arctic, Antarctic, Greenland and Southern Ocean) and other parts of the world in international scene have been carried out. **(**Anderson et al., 1998; Christl and Strabl, 2003; Von Blanckenburg, 2006; Frank et al., 2008, 2009; Murray et al., 2010; Dreyer et al., 2010; Kretschmer et al., 2011; Pedro et al., 2011; Kim et al., 2012; Wittman et al., 2012; Simon et al., 2016, 2017, 2018). However, in the Indian context it is likely to be developed and is represented by few namely Nath et al. (2007), Khare et al. (2011), Kumar et al. (2014) and Dhal et al. (2018)**.**

3.4. A Surface sediment samples

3.4.A.a Prydz Bay (Thala Fjord), East Antarctica

Along the Prydz Bay, (Fig. 3.4.1) ^{9}Be content fluctuated in a range between 17.62 ppb at station P2 and 166.64 at station P6. Overall, ^{9}Be showed an increasing trend with increasing water depth (31-140 m) away from the coast (P1-P7) similar to that of silt and clay as finer grain size provides large surface area for the adsorption of authigenic ^{9}Be. Metals like Ti and Fe showed increasing trend away from the coast similar to that of ^{9}Be suggesting their source to be lithogenic, derived from the continent. Fe oxy-hydroxides must have regulated the distribution of authigenic ^{9}Be in the Prydz Bay as Fe oxy-hydroxides are potential scavengers of authigenic ^{9}Be (Wittman et al., 2012). Authigenic ^{9}Be isotope is derived from the catchment area by physical and mechanical weathering and delivered into the Prydz Bay through glacial processes.

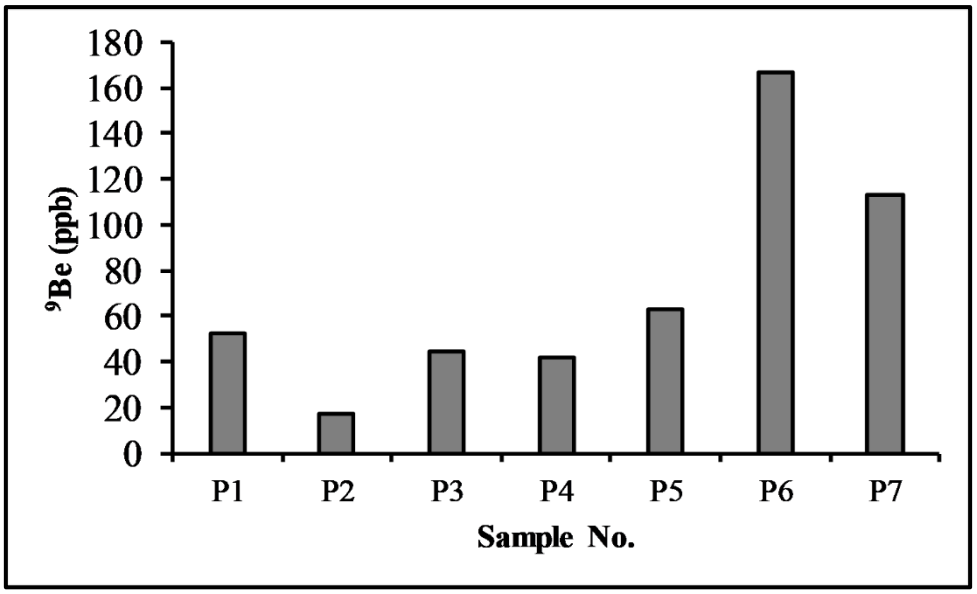

Fig. 3.4.1 Distribution of ^{9}Be isotope along the Prydz Bay.

3.4.B Sediment cores

3.4.B.a. Antarctic lakes (Larsemann Hills, East Antarctica)

^{9}Be concentration was high (average 122.91 ppb) in core L-8 and low in core L-10 (66.97 ppb). However, ^{9}Be concentration in core L-8, L-10 and L-12 is lower in all the three cores as compared to the average crustal values (~2 ppm).

In core L-8 (Fig. 3.4.2a) ^{9}Be showed a decreasing trend towards the surface similar to that of silt indicating their association with finer sediments. The vertical profile of ^{9}Be showed opposite distribution as that of sand indicating that high percentage of coarse-grained sediments have possibly diluted the concentration of ^{9}Be. Fe and Mn showed similar concentration as that of ^{9}Be from 28 cm to 12 cm indicating its association with Fe and Mn oxyhydroxides. Fe and Mn oxyhydroxides are reported (Wittmann et al., 2012) as favourable carrier for ^{9}Be in lakes.

In core L-10 (3.4.2b), ^{9}Be showed an overall similar trend to that of Al and Mn. Aluminosilicates are reported (Kaste and Baskaran, 2012) as major carriers of ^{9}Be in lake sediments and apart from primary and secondary silicates and Mn oxyhydroxides are potential scavengers of ^{9}Be in lakes.

In core L-12 (3.4.2c), ^{9}Be showed lower than the average values in the lower portion from 28 cm to 16 cm and higher than the average values in the upper portion from 12 cm to the surface. ^{9}Be showed similar trend as that of silt and clay in the upper portion from 8 cm to the surface indicating its association with finer sediments at these depth intervals. Metals like Ti and Fe showed similar trend as that of ^{9}Be indicating their similar source and Fe-oxyhydroxides are the main carriers of ^{9}Be in lake sediments.

In all the three cores, L-8 consist of high concentration of ^{9}Be possibly due to the availability of higher fine-grained sediments in this lake as compared to the other two lakes. High ^{9}Be concentration in this lake is attributed to the increase in surface area and sorption capacity with decrease in grain size. While, low concentration of ^{9}Be in core L-10 and L-12 is attributed to subsequent dilution by quartz in coarse bedload (Wittmann et al., 2012). Dissolved ^{9}Be is scavenged from the continents easily through turbid meltwater and remains in suspension with fine sediment particles and transported to the lakes depositing within the sediments. The flux of ^{9}Be isotope are constant with respect to lithogenic changes indicating nearly constant rate of denudation and transport processes.

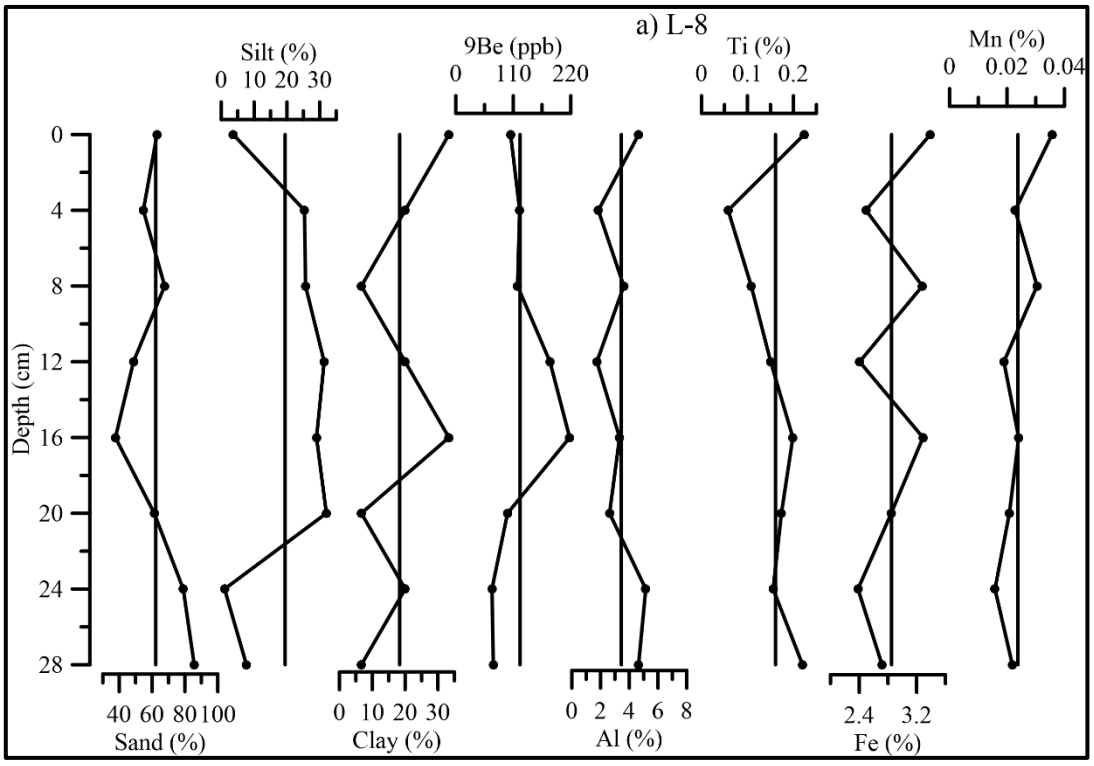

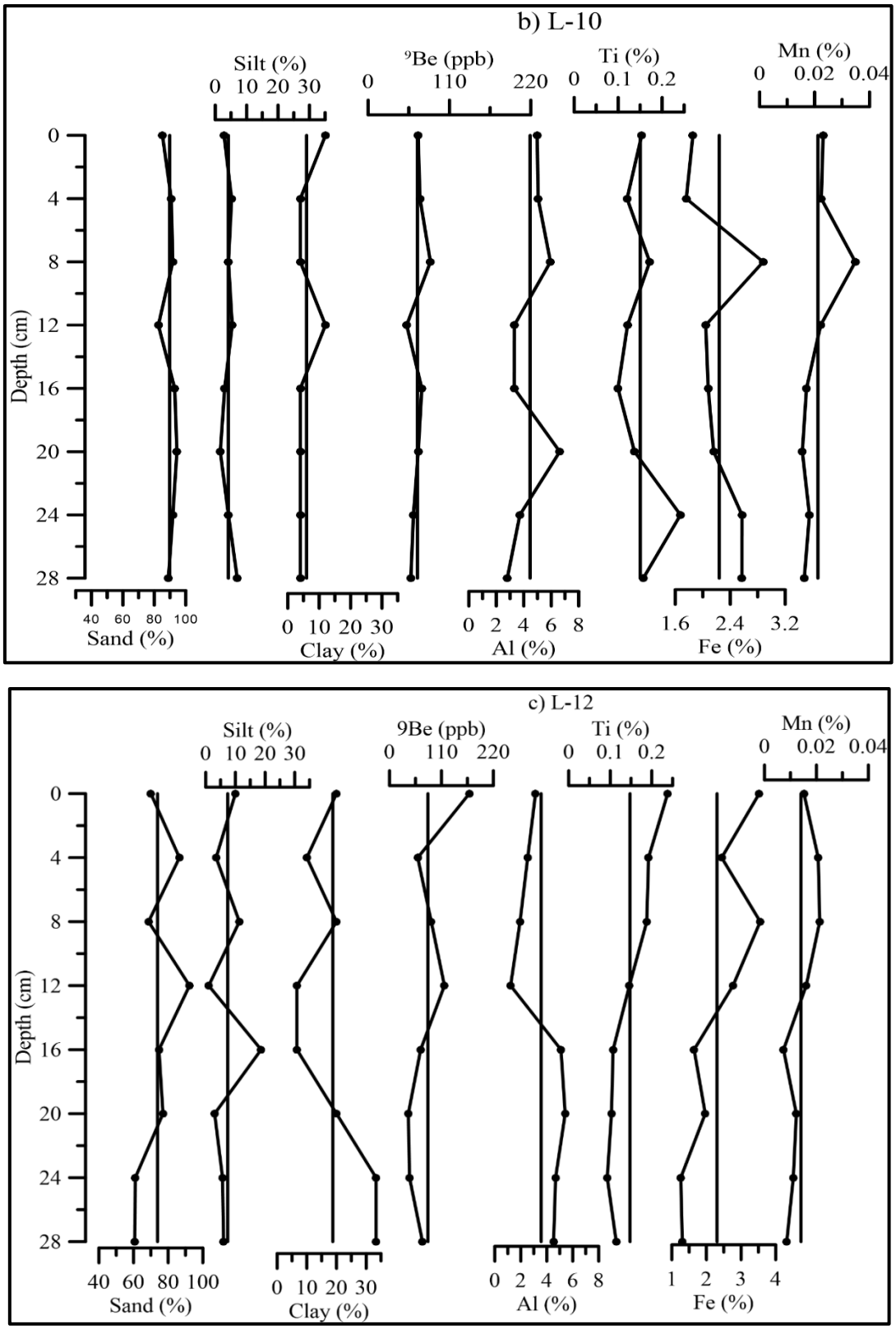

Fig.3.4.2 Distribution of ^{9}Be along with sediment components (sand, silt and clay) and major metals (Al, Ti, Fe and Mn) in a) core L-8, b) core L-10 and c) core L-12

3.4. B. b. Antarctic Lakes (Schirmacher Oasis, East Antarctica)

^{9}Be concentration was high in core L-6 (average 105.74 ppb) and low in core V-1 (average70.69 ppb). However, ^{9}Be concentration is lower in core GL-1, V-1 and L-6 as compared to the average crustal values (~2ppm).

In core GL-1 (Fig.3.4.3 a), ^{9}Be showed lower than the average values in the lower portion from 32 cm to 20 cm and higher than the average values in the upper portion from 16 cm to 4 cm followed by a decrease towards the surface similar to that of silt ^{9}Be concentration showed lower values with high concentration of sand while higher values with lower concentration of sand. This distribution is consistent with the scavenging efficiency of Be (dissolved phase) which depends on the grain size and composition of the particle available in the water column (Simon et al., 2016). Among the major metals Mn showed a similar trend as that of ^{9}Be indicating their similar source and post depositional processes. Mn oxyhydroxides are main carriers of ^{9}Be.

In core V-1 (Fig.3.4.3 b), ^{9}Be showed an overall increasing trend towards the surface with lower than the average values in the lower portion from 28 cm to 16 cm and higher than the average values in the upper portion from 12 cm to the surface similar to that of silt. Metals like Ti showed similar trend as that of ^{9}Be up to 12 cm in the lower portion suggesting their similar source.

In core L-6 (Fig.3.4.3 c), ^{9}Be showed an overall decreasing trend towards the surface similar to that of silt. Al and Ti showed similarity with that of ^{9}Be in the middle portion of the core from 40 cm to 16 cm depth indicating their lithogenic nature and similar processes have regulated the distribution of these metals at this depth.

In all the three cores, ^{9}Be concentration was found to be higher in core L-6 possibly due to the presence of high concentration of finer sediment in this core. This suggests strong association between ^{9}Be concentration and terrigenous input. Relatively lakes and Bays receive high concentration of ^{9}Be inputs than the deep

ocean basins due to their close proximity to the continents and their smaller size and shape of the lakes and Bay (Nuttin and Hillaire-Marcel, 2015).

From all the six cores studied, it is observed that silt has high scavenging efficiency of ^{9}Be as compared to the clay. Clay has tendency to form aggregates which have faster sinking rates. These aggregates provide less surface area for the adsorption of ^{9}Be suggesting high scavenging efficiency of silt as compared to the clays (Simon et al., 2016). Sand showed opposite trend to that of ^{9}Be in all the cores suggesting that the distribution of authigenic Beryllium (^{9}Be) is robustly dependent on the grain size. ^{9}Be is derived from the denudation of bedrocks at the basal interface of the glacial streams through mechanical erosion and weathering and delivered through meltwater into the lakes (Simon et al., 2016).

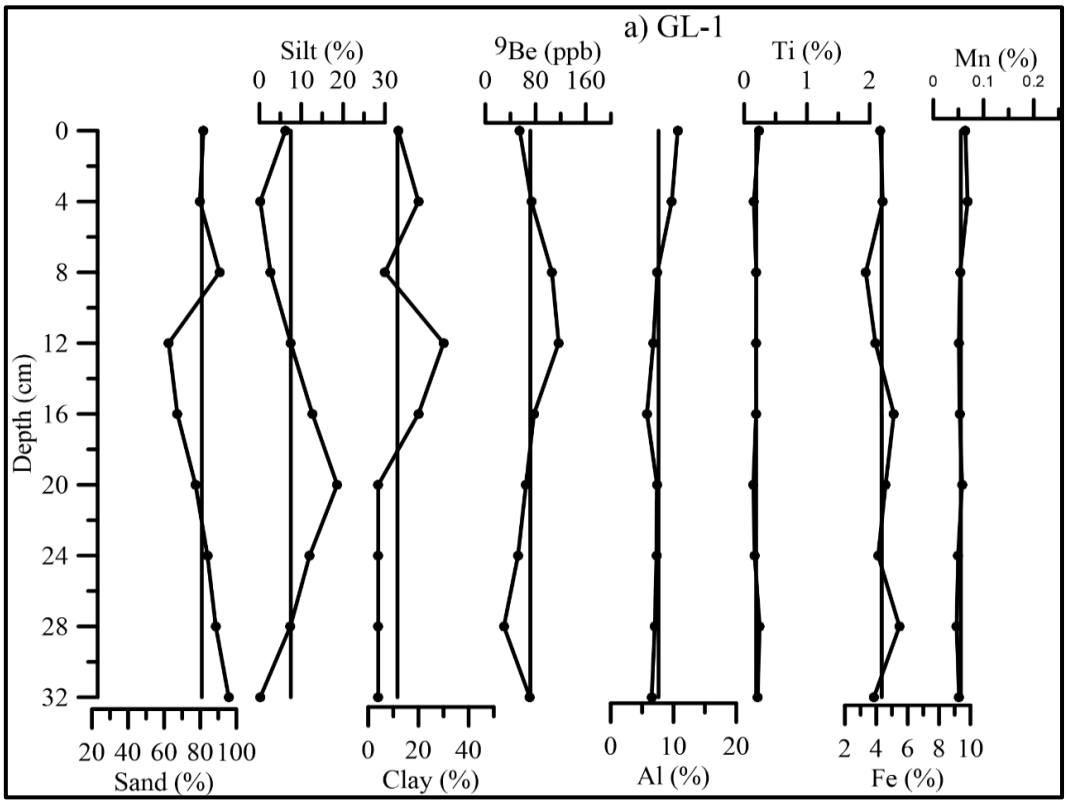

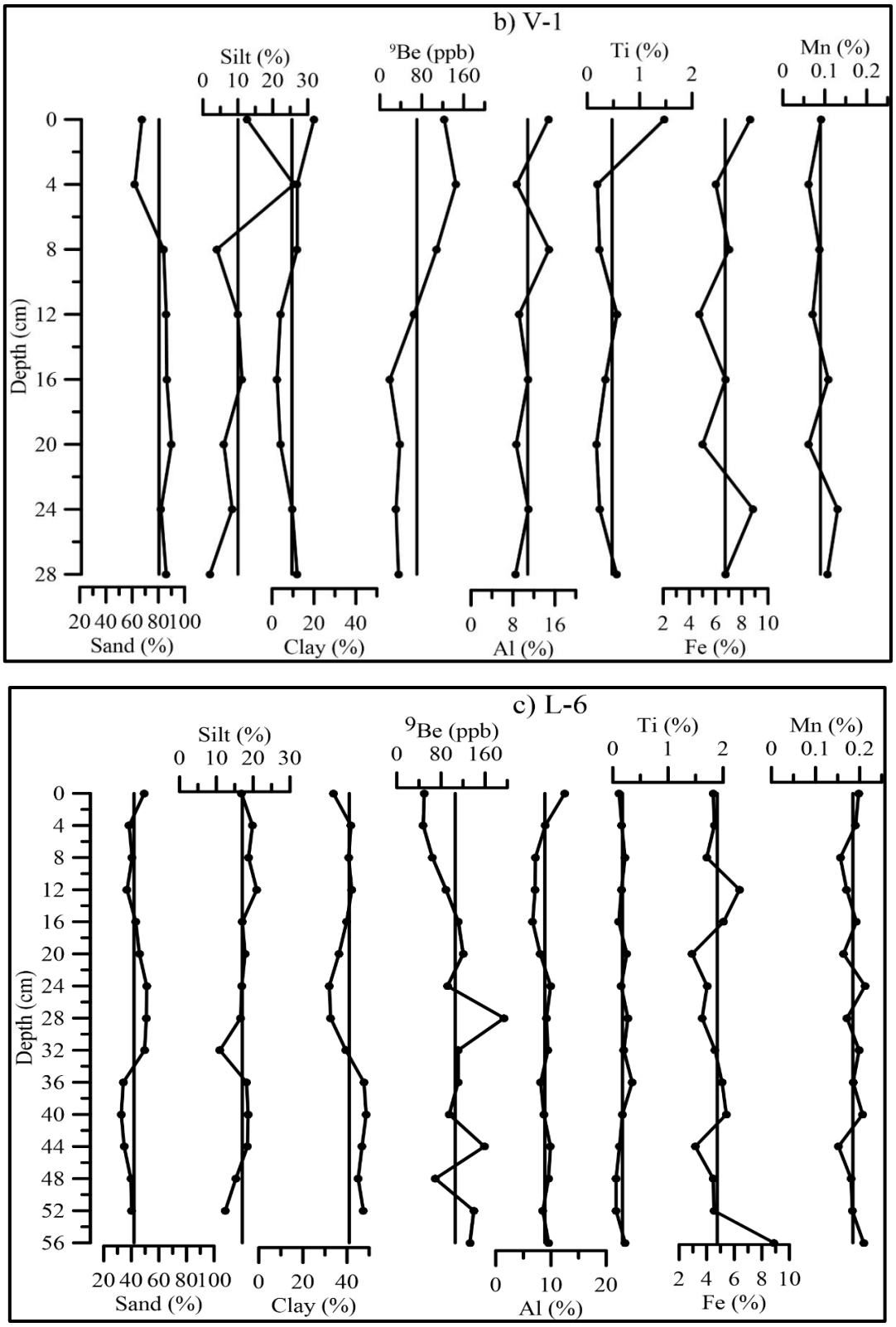

Fig.3.4.3 Distribution of ^{9}Be along with sediment components (sand, silt and clay) and major metals (Al, Ti, Fe and Mn) in a) core GL-1, b) core V-1 and c) core L-6

Polar regions are characterized by a variety of glacial landforms out of which lakes and fjords have great potential to unravel the sedimentary processes, depositional environment and change in climate. Lakes and fjords are local response systems which act as high resolution archives of local and regional change. They integrate the processes of their surrounding catchments; therefore, they are highly sensitive to the changes in landscape. Depending upon their topographic settings these lakes are classified as Proglacial lakes, landlocked lakes and epishelf lakes (Ravindra et al., 2001). Geologically, fjord is a U-shaped glacial valley and act as nexus between the terrestrial (source) and the oceanic domain (sink) providing a potential for continuous exchange of fjord and coastal waters on the adjacent continental shelf. Despite the occurrence of numerous lakes and fjords along the coastline of high latitude regions (Hjelstuen et al., 2009) and their potential to unravel the sedimentary processes and depositional environment these landforms have received considerably less attention. Although the climate change has severely impacted the terrestrial, marine and freshwater ecosystems.

Arctic and Antarctic are highly sensitive areas of capturing even the minute changes to the environment. The pristine environment of these regions is devoid of much anthropogenic input and adapted to or can tolerate persistent low temperature, freeze and thaw cycles, seasonal and interannual variations in energy and supply of nutrients. Ecosystems of polar regions are therefore a sensitive actuator to the intensity and magnitude of environmental changes and pre-requisites for environmental research. Therefore, a multiproxy approach was adopted to understand the depositional processes, occurring in lakes and fjord as these depositional environments act as sink for nutrients and metals. The present study has been carried out in lakes and fjords of Arctic and Antarctic region with following objectives:

1. To study sediment texture and understand the depositional processes.
2. To understand the past climatic changes through the study of trace elements in sediments.
3. To study spatial and temporal variations in Be concentration in sediment of higher latitude and understand the signatures of past climatic changes.

In order to achieve the following objectives, sediment samples have been collected from Arctic and Antarctic region. From the Arctic region, 13 surface sediment samples have been collected from Krossfjord and Kongsfjord along with five cores, one from the mouth of Krossfjord and remaining four from different lakes of Ny-Alesund region. From the Antarctica, 7 surface sediment samples have been collected from Thala fjord, Prydz Bay along with six cores three each from Schirmacher Oasis and Larsemann Hills. These samples were analyzed for grain size, total organic carbon, total nitrogen, total phosphorus, biogenic silica, calcium carbonate, clay minerals, bulk and speciation of metals along with the estimation of Beryllium concentration. Further, to understand the depositional environment and hydrodynamic conditions in which the sediments have been deposited, the data was plotted on a ternary diagram proposed by Shepard (1954) and Pejrup (1988) and Isocon diagram (Grant, 1986). Pearson's correlation ($p<0.05$), paired sample t-test (two-tailed), principal component analysis and factor analysis were conducted on sediment components and metals to determine the inter-relationship between metals and sediment components and to identify possible sources or sinks. Furthermore, fractionation of metals was carried out to understand the source of metals, depositional processes, occurrence, mobility and availability of metals for uptake of biota (potential bioavailability) for the fjord sediments. A synoptic view of the methodology used in the study carried out is described with the help of flowchart in figure 2.8.

Surface sediment samples from the Krossfjord and Kongsfjord, Arctic showed that among the sediment components silt is predominant along with considerable concentration of clay. Sand concentration is higher at stations near the glacier outlets. Overall, coarse-grain fraction is higher in Kongsfjord as compared to the Krossfjord as it is largely influenced by different tidewater glaciers debouching in the fjord. Less calm to less violent hydrodynamic conditions prevailed facilitating deposition of finer sediments in the fjord. Along the Prydz Bay, east Antarctica, silt is predominant among the sediment components. Overall, grain size showed decreasing trend on moving away from the coast. Finer sediments were deposited in the Prydz Bay owing to the less violent to violent hydrodynamic conditions. Sediment cores from the

mouth of the Krossfjord showed high concentration of silt suggesting deposition of finer sediments through suspension mode. High concentration of clay in the upper portion of the core collected from fjord, as compared to the lower portion suggested deposition of finer sediments through temperature-salinity stratification or aggregation of finer particles in the upper portion or hydrodynamic conditions.

Sediment cores collected from the lakes of Arctic region consist of >50% of sand in the upper portion of all the four cores (LA, L-1, L-2, L-3) which suggested the dominance of mechanical (glacial) weathering / frost weathering processes releasing coarse-grained material to the lake basin in the recent years. Along with the glacial activity, aeolian processes must have also played an important role in supplying finer sediments to the lake basin. Due to the warming conditions in the region, glaciers retreated and the area was with less ice allowing intense winds to rework the sediments (Kar et al., 2018). Silt higher than the average value is attributed to the deposition of finer sediments by snowmelt water.

Sediment cores from the lakes of Larsemann Hills and Schirmacher Oasis, Antarctic region showed sand higher than the average value with a low percentage of silt and clay in lower and upper sections of core L-8 and GL-1, a major section of core L-10 and V-1, and middle section of core L-12 and L-6. Higher sand corresponds to the glaciofluvial deposition due to the retreat of glaciers in the study area, suggesting warmer conditions in the region. The coarse-grained particles were transported from the catchment area into the lake basin by glacial meltwater during warmer conditions. Relatively, higher clay from 18 to 10 cm and upper 6 cm in core L-8, around 12 cm and upper 2 cm in core L-10, and 28 to 24 cm and from 10 cm to the surface in core L-12 indicated deposition of fine-grained sediments in the lake due to the supply of ice meltwater.

Organic components of the surface sediment samples from the Arctic region showed that TOC is increasing from the inner fjord to the outer fjord (Kr-5 to Kr-1) with exceptionally high values at one station in the inner fjord. TN showed similar increasing trend as that of TOC. TOC and TN showed a clear spatial gradient with lower values at the glacier dominated inner fjord due to the high turbidity at the fjord

head resulting in the shallow photic zone. Both the fjords showed higher C: N values in shallower regions because of the presence of high amount of terrestrial material and their association with coarse-grained sediment suggested grain size to be a dominant factor regulating the distribution of organic matter. TP varied without any particular trend. BSi showed increasing trend from inner fjord towards the outer fjord similar to that of organic carbon and finer sediment indicating high primary productivity. Overall, nutrients concentrations were found low in the inner fjord as it is in the close proximity of the glacier and glacial water is devoid of nutrients and supplies huge amount of coarser material. Along the Prydz Bay, Antarctica TOC and TN showed similar increasing trend on moving away from the coast similar to that of finer sediments indicating that most of the TN was associated with TOC and therefore it indicates the amount of organic nitrogen (Kurian et al., 2013). Overall, C/N is low in the shallower region may be because either C/N is diagenetically affected or bacterial action must have caused the dissolution of organic matter. TP varied without any particular trend. Scatter plot between TOC and TN with TP showed poor association with each other suggesting a differential pathway of phosphorus or effect of diagenesis on phosphorus.

Sediment core from the mouth of the Krossfjord showed that TOC fluctuated around the average line throughout the core. TOC showed negative peaks at depth 22 cm and 4 cm similar to that of silt and clay respectively and a positive peak at 15 cm similar to that of silt indicating that these sediment components regulated the distribution of organic matter at these depths. Further, TOC and TN showed an increasing trend from 4 cm to the surface similar to that of clay towards the surface suggesting increased primary productivity. Fluctuating trend with depth indicates changing rate of supply of organic matter through changing processes.

Sediment cores from the lakes of Arctic showed that TOC and TN were higher than the average value in the upper portion of core L-1 and L-2 suggesting high productivity due to the exposure of the lakes to the ice meltwater influx. C/N ratio varied from 15.50 to 38.32 suggesting a mixed source of organic matter, however at some intervals it showed terrestrial origin.TP showed higher values in core L-1 and L-3 similar to that of silt and sand indicating its source to be terrigenous in this core.

Further, Increase in TOC is accompanied by decrease in $CaCO_3$ in all the three cores except core L-2 suggesting that the CO_2 produced by the decomposition of organic matter reduces the pH of anoxic pore waters enough to dissolve $CaCO_3$.

Sediment cores from the Larsemann Hills, Antarctica showed that TOC and TN showed similar increasing trend towards the surface suggesting their similar source while in core L-10 and L-12 they showed different trend indicating their source to be different. C/N ratio varied from 1.22 to 4.08 suggesting the source of organic matter as autochthonous. BSi showed high concentration in the middle portion of core L-8 and upper portion of core L12 indicating high productivity at these depths. $CaCO_3$ showed decrease in concentration with increase in TOC. In Schirmacher Oasis, all the geochemical proxies like TOC, TN, TP, BSi showed an increasing trend towards the surface suggesting high productivity due to the exposure of the lakes to the ice meltwater influx.

Major and trace elements analyzed showed a considerable spatial variation from the inner fjord to the outer fjord. Major elements like Al and Ti showed a decreasing trend from the inner fjord towards the outer fjord similar to that of sand indicating their terrigenous source. Elements like Mg and Ca showed similar decreasing trend as that of Al and Ti indicating their source to be lithogenic. However, average concentration (0.34 and 0.38%) of Ti is low indicating the source of sediment to be felsic. Trace metals like Ni, Ba and Pb showed similar increasing trend as that of major metals indicating their similar source and post-depositional processes. High Ba and Pb content in the sediment supported the source of fjord sediment to be felsic as Ba and Pb are usually accommodated in rocks rich in feldspars (Prinz, 1967; Sensarma et al., 2016) such as gneisses and granites. Cadmium showed an increasing trend from the inner fjord towards the outer fjord similar to that of organic matter and finer sediments suggesting that Cd is biologically active and behaves as nutrients, therefore, its distribution is regulated by the organic matter. In addition, Cd is a redox sensitive element and may have been enriched in anoxic sediments by Cadmium sulphide precipitation (Grotti et al., 2017).

Clay minerals have also been analysed in the fjord system to understand the source and depositional processes as the mixing of different density waters in fjords affects the sedimentation process. Illite is the predominant clay mineral in the Krossfjord Kongsfjord system followed by kaolinite and chlorite. Illite showed a decreasing trend on moving away from the glacial outlets in both the fjords similar to that of sand suggesting its source to be terrigenous originated from glacial weathering of the source rocks. The bedrock north of Kongsfjorden consists of mid-Proterozoic metamorphic rocks, mainly mica-schists and phyllites which act as the major source for illite in the study area. An appreciable amount of kaolinite in this region might have been formed either in an interval of warmer and colder conditions resulting in chemical weathering of Quartzites or possibly it is of detrital nature, transported from a distant source, probably located underneath the ice (Srivastava et al., 2011). Among the clay minerals, chlorite content was low having may be due to the highly unstable nature of chlorite. The chlorite in the study area mainly comes from low-grade Proterozoic metamorphic phyllite and mica schists that surround Kongsfjord (Fendeng et al., 2018).

Speciation of metals have also been carried out in the fjord as due to the mixing of fresh glacial water and saline coastal water, a wide range of salinity exists in the fjord system which influence the deposition of metals in different phases. Therefore, to assess different chemical forms of metals in the sediment, fractionation of the metals was carried out in the five geochemical phases namely exchangeable (F1), Carbonate (F2), Fe-Mn oxide (Reducible-F3), organic matter/ sulfide bound (oxidizable-F4) and Residual (F5) for the surface samples of Krossfjord and Kongsfjord. Iron was concentrated in substantial amount in the residual fraction at all the stations along the Krossfjord and Kongsfjord. High concentration of Fe (>80%) in the residual phase indicated an input of terrigenous material from weathering of rocks available in the catchment area. In the residual fraction, Fe is immobile due to its bonding with primary and secondary minerals and therefore it is unavailable for uptake of organisms (Tessier et al., 1979). Among the bioavailable phses, Fe was concentrated in the Fe-Mn oxide phase at all the stations in both the fjords. The concentration of Fe in the organic/ sulfide bound phase is attributed to the formation of iron sulfides. It is

known that Fe prefers oxide phase in oxic conditions and sulphides in anoxic environments.

Manganese is a redox-sensitive element similar to that of Fe which exhibits active biogeochemical behavior in the aqueous environment and transforms easily from dissolved phase to the particulate phase and vice-versa due to the physicochemical changes. Residual phase consists of relatively lower concentration of Mn in the sediments of the Krossfjord (average 37.73%) and Kongsfjord (average 34.05%) and was found concentrated in the Fe-Mn oxide bound phase in both the fjords (average 42.16% in Krossfjord and 43.33% in Kongsfjord) due to the formation of oxides. Carbonate fraction is a loosely bound phase. Considerable quantity of Mn (average 10.90% in Krossfjord and 11.34% Kongsfjord) is concentrated in carbonate fraction. Similar ionic radii of Mn as that of Ca enables Mn to replace Ca in the carbonate fraction (Noronha-D' Mello and Nayak, 2015; Grotti et al., 2017). Manganese is relatively low (4.96% in Krossfjord and 5.98% in Kongsfjord) in the organic/sulfide phase due to low organic affinity of Mn (Bendell young and Harvey, 1992).

Chromium was largely associated with the residual phase in the sediments of Krossfjord (average 85.80%) and Kongsfjord (average 83.92%) as it mainly gets transported to the sediment within the residual phase (Noronha-D' Mello and Nayak, 2015). Among bioavailable phases a considerable quantity of Cr was found associated with organic/ sulfide bound fraction. because of structural and electronic incompatibilities with pyrite, Cr (III) uptake by authigenic Fe-sulfides is very limited. Therefore Cr, is preferably associated with organic matter as compared to sulfides.

Cobalt was predominantly bound to the residual fraction both in Kongsfjord (average 39.55%) and Krossfjord (average 35.05%) indicating its preferential association with silicates and aluminosilicates (Grotti et al., 2017). Higher Co concentration in Fe-Mn Oxide (average 34.00 %) fraction in the Krossfjord explains the adsorption of Co on the surface of Fe-Mn colloids as observed by Nasnodkar and Nayak (2017) in the sediments of the tropical estuaries. Fe-Mn colloids have played an important role in controlling the mobility of Co in the fjord environment due to their ability of

scavenging Co in sediments (Kaasalainen and Yli-Halla, 2003). Considerable percentage of Co was available in reducible fraction (average 33.01%) in Kongsfjord.

Average 50% of Cu was found associated with the residual fraction and the remaining 50% was found distributed in the bioavailable fractions in both the fjords indicating their availability to the sediment-associated biota. Among bioavailable phases, Cu in oxidizable (organic/sulfide) fraction was appreciable (average 27.11% in Krossfjord and 24.49% in Kongsfjord) suggesting its partial association with the refractory organic matter as humic substances or sulfides (Grotti et al., 2017).

The metal fractionation showed >80% average concentration of metals viz. Fe and Cr in the residual phase indicating their source to be lithogenic derived from the weathering of source rock while bio-available phases consist of the remaining <20%. Cu showed 50% average concentration in residual phases and remaining 50% was associated with bioavailable phases. However, Mn and Co showed <40% concentration in the residual phase and >60% concentration of these metals were distributed in the bioavailable phases suggesting their availability for uptake and accumulation in aquatic biota (Gambrell, 1994; Ladigbolu, 2014).

Along the Prydz Bay, East Antarctica, major elements like Al and Ti showed decreasing trend on moving away from the coast similar to that of sand suggesting their source to be lithogenic in nature. Elements like Fe, Mn and Mg showed similar decreasing trend as that of Al and Ti indicating their common source and post-depositional processes. Trace metals like Cu, Cd, Ni and Zn showed an increasing trend on moving away from the coast similar to that of clay, TOC, TN and TP indicating their source to be biogenic in nature and suggested that these trace metals regulated the productivity along with the nutrients in the Prydz Bay.

Sediment core from the Krossfjord, Arctic showed that in the lower zone from 22 to 15 cm elements like Al, Fe, Mn, Mg, Ca, Co, Ni, Zn and Ba showed an increasing trend similar to that of silt, TOC, TN, TP and BSi suggesting that these sediment components regulated the distribution of metals in this zone. In zone B from 14 to 8 cm except Mn and Zn, other metals showed high concentration similar to that of sand, clay and TOC suggesting their association with these sediment components. Almost

all the metals except Ti, Cr, Cu, Pb and Cd showed an increasing trend towards the surface may be due to the increase in melting, releasing metals trapped beneath the ice or may be due to the increased local erosion.

Sediment cores from lakes of the Arctic and Antarctic region (Larsemann Hills and Schirmacher Oasis) showed that the elemental concentrations have increased towards the surface suggested either increased melt water influx in recent years or diagenetic remobilisation (Volvoikar and Nayak, 2014). Earlier studies, Davis (1984); Ali and Dzomback (1996); Tessier et al. (1996) have reported that oxides (Murray,1975) or organic ligands by forming stable complexes can scavenge elements from surface water to the sediment.

Further Beryllium estimation was carried out in the Antarctic region. Surface sediment samples from the Prydz Bay showed that ^{9}Be concentration increased on moving away from the coast similar to that of silt and clay indicating that the finer sediments regulated the distribution of authigenic ^{9}Be in the Prydz Bay. Elements like Ti and Fe showed increasing trend similar to that of authigenic ^{9}Be suggesting the source of ^{9}Be to be lithogenic in nature and Fe-oxyhydroxides regulated the distribution of authigenic ^{9}Be as Fe oxyhydroxides are potential scavengers of authigenic ^{9}Be (Simons et al., 2016).

In Larsemann Hills, East Antarctica, ^{9}Be concentration showed a decreasing trend as that of silt in core L-8 indicating their similar source. Fe and Mn showed increasing trend in the lower portion up to 12 cm similar to that of authigenic ^{9}Be suggesting that Fe-Mn oxyhydroxides has controlled the distribution of ^{9}Be at these depths. In core L-10 ^{9}Be showed increasing trend towards the surface similar to that of Al and Mn suggesting that aluminosilicates along with Mn-oxyhydroxides regulated the distribution. In core L-12, ^{9}Be showed increasing trend similar to that of silt, Ti and Fe suggesting high run off of the weathering material depositing on the surface of the lake.

In Schirmacher Oasis, ^{9}Be showed decreasing trend as that of silt in the upper portion of core GL-1 and L-6 and lower and upper portion of core V-1. Elements like Ti showed lower than the average value in the lower portion in core V-1 similar to that of 9Be. In core L-6 Al and Ti showed similar trend as that of ^{9}Be from 56 cm up to 4 cm.

From all the six cores studied, it is observed that silt has high scavenging efficiency of ^{9}Be as compared to the clay. Clay has tendency to from aggregates which have faster sinking rates. These aggregates provide less surface area for the adsorption of ^{9}Be. Sand showed opposite trend to that of ^{9}Be in all the cores suggesting that the distribution of authigenic Beryllium (^{9}Be) is robustly dependent on the grain size. ^{9}Be is derived from the mechanical erosion and weathering (i.e.) denudation of bedrocks at the basal interface of the glacial streams and delivered through meltwater into the lakes (Simons et al., 2016).

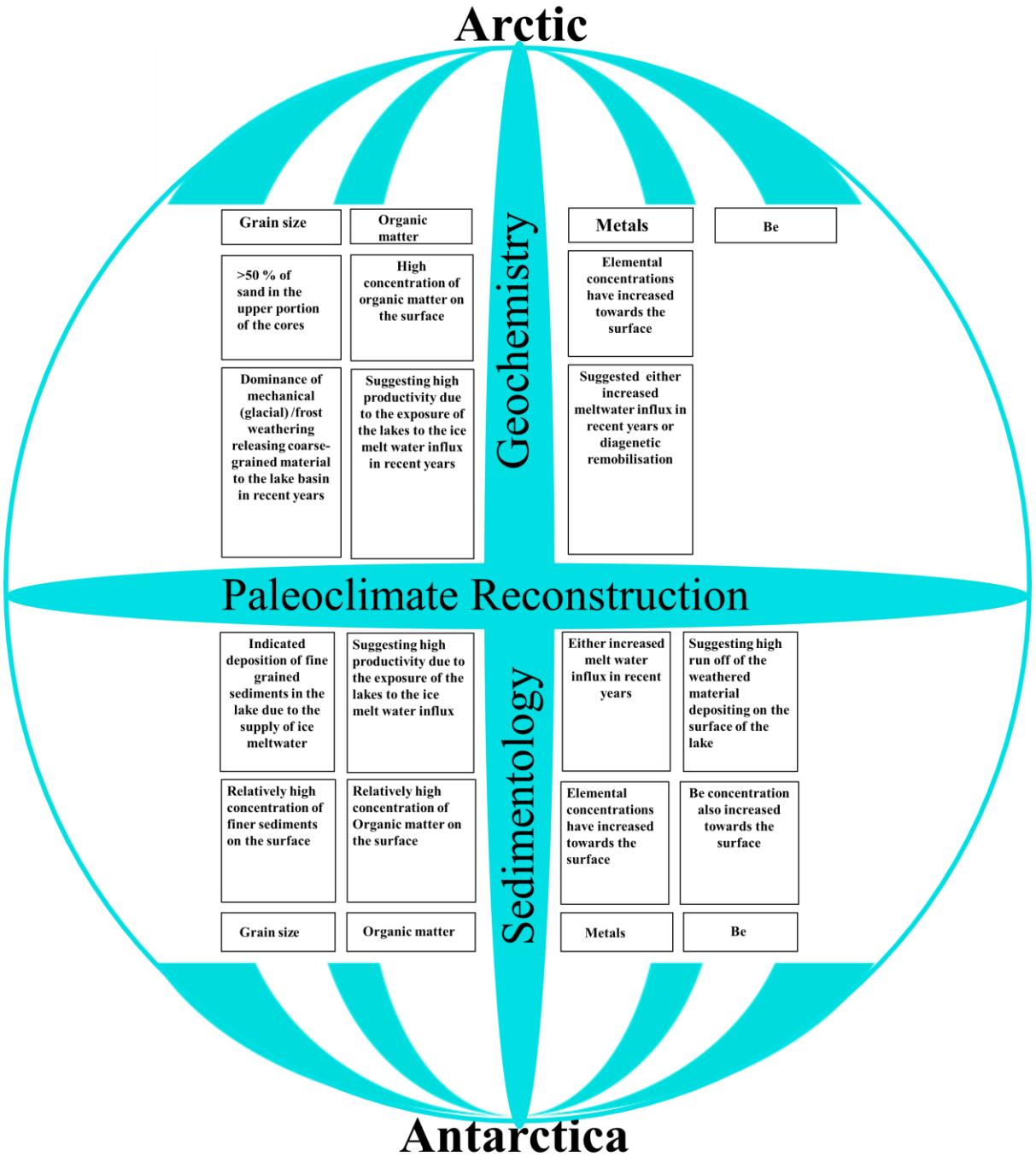

Fig.4.1 Environmental conditions with time through a comprehensive flow diagram

Algarasamy, R. and Zhang, J., 2008. Geochemical characterization of major and trace elements in coastal sediments of India. *Environmental Monitoring and Assessment*, 669–735.

Ali, M.A., Dzomback, D.A., 1996. Effects of simple organic acids on sorption of Cu^{2+} and Ca^{2+} on goethite. *Geochimica et Cosmochimica Acta*, 60: 291–304.

Alvarez-Valero, A.M., Saez, R., Perez-Lopez, R., Delgado, J. and Nieto, J.M., 2009. Evaluation of heavy metal bio-availability from Almagrera pyrite-rich tailings dam (Iberian Pyrite Belt, SW Spain) based on a sequential extraction procedure. *Journal of Geochemical Exploration*, 102: 87–94.

Anderson, R.F., Kumar, N., Mortlock, R.A., Froelich, P.N., Kubik, P., Dittrichannen, D. and Suter, M., 1998. Late-Quaternary changes in productivity of the Southern Ocean, *Journal of Marine system*. 17(1-4): 497–514.

Andrade, R.P., Michel, R.F.M., Schaefer, C.E.G.R., Simas, F.N.B. and Windmoller, C.C., 2012. Hg distribution and speciation in Antarctic soils of the Fildes and Ardley peninsulas, King George Island. *Antarctic Science*, *24*(4): 395–407.

Armstrong-Altrin, J.S., 2009. Provenance of sands from Cazones, Acapulco, and Bahia Kino beaches, Mexico. *Revista Mexicana de Ciencias Geologicas*, 26(3).

Armstrong-Altrin, J.S., Lee, Y.I., Kasper-Zubillaga, J.J. and Trejo-Ramirez, E., 2017. Mineralogy and geochemistry of sands along the Manzanillo and El Carrizal beach areas, southern Mexico: Implications for palaeoweathering, provenance, and tectonic setting. *Journal of Geology*, 52(4): 559–582.

Armstrong-Altrin, J.S., Nagarajan, R., Balaram, V. and Natalhy-Pineda, O., 2015a. Petrography and geochemistry of sands from the Chachalacas and Veracruz beach areas, Western Gulf of Mexico, Mexico: constraints on provenance and tectonic setting. *Journal of South American Earth Sciences*, 64: 199–216.

Armstrong-Altrin, J.S., Ramos-Vázquez, M.A., Zavala-Leon, A.C. and Montiel-Garcia, P.C., 2018. Provenance discrimination between Atasta and Alvarado beach sands, western Gulf of Mexico, Mexico: Constraints from detrital zircon chemistry and U–Pb geochronology. *Journal of Geology*, https://doi.org/ 10.1002/gj.3122.

Asthana, R., Shrivastava, P.K., Shrivastava, H.B., Beg, M.J. and Kumar, P., 2013. Hydrochemistry and sediment characteristics of polar periglacial lacustrine environments on Fisher Island and the Broknes Peninsula, East Antarctica. *Advances in Polar Sci*ences, *24*(4): 281–295.

Asthana, R., Shrivastava, P.K., Srivastava, H.B., Swain, A., Beg, M.J. and Dharwadkar, A., 2019. Role of lithology, weathering and precipitation on water chemistry of lakes from Larsemann Hills and Schirmacher Oasis of East Antarctica. *Advances in Polar Sciences*, 30(1): 35–51.

Beg, J., 2005. Geological Studies in the Larsemann Hills Ingrid Christensen Coast, East Antarctica, Report of Second Task Force to New Station Site, NCAOR, India.

Bejugam, P. and Nayak, G.N., 2017. Source and depositional processes of the surface sediments and their implications on productivity in recent past off Mahanadi to Pennar River mouths, western Bay of Bengal. *Paleogeography, Paleoclimatology, Paleoecology*, 483: 58–69.

Bendell-Young, L.I. and Harvey, H.H., 1992. The relative importance of manganese and iron oxides and organic matter in the sorption of trace metals by surficial lake sediments. *Geochimica et Cosmochimica Acta*, 56: 1175–1186.

Bergh, S.G., Maher, H.D. and Braathen, A., 2000. Tertiary divergent thrust directions from partitioned transpression, Brøggerhalvøya, Spitsbergen Norsk Geologisk Tidsskrift 80: 63–82.

Birnie, J., 1990. Holocene environmental change in South Georgia: evidence from lake sediments. *Journal of Quaternary Science*, 5(3): 171–187.

Biscaye, P.E., 1965. Mineralogy and sedimentation of recent deep-sea clay in the Atlantic Ocean and adjacent seas and oceans. *Geological Society of America Bulletin*, 76: 803–832.

Boger, S.D., Wilson, C.J.L. and Fanning, C.M. 2001. Early Paleozoic tectonism within the East Antarctic craton: the final suture between east and west Gondwana? *Geology*, 29: 463–466.

Bordowskiy, O.K., 1965. Sources of organic matter in marine basins. *Marine Geology*, 3: 5–31.

Bormann, P. and Fritzsche, D., 1995. In: The Schirmacher Oasis, Queen Maud Land, East Antarctica, and its Surroundings, Petermans Geographische Mitteilungen: Erganzungsheft; Nr 289. Jusus Perthes Verlag Gotha.

Boszke, L., Sobezynski, T., Glosinska, G., Kowalski, A. and Siepak, J., 2004. Distribution of mercury and other heavy metals in bottom sediments of middle Odra River (Germany / Poland). *Polish Journal of Environmental Studies*, 13(5): 495–502.

Boyle, E.A., Sclater, F.R. and Edmond, J.M., 1977. The distribution of dissolved copper in the Pacific. *Earth and Planetary Science Letters*, 37(1): 38–54.

Bradtmiller, L.I., Anderson, R.F., Fleisher, M.Q. and Burckle, L.H., 2006. Diatom productivity in the equatorial Pacific Ocean from the last glacial period to the present: A test of the silicic acid leakage hypothesis. *Palaeoceanography*, 21(4).

Bruland, K.W. and Franks, R.P., 1983. Mn, Ni, Cu, Zn and Cd in the western North Atlantic. In: Trace metals in seawater, Springer, US, pp. 395–414.

Burdige, D.J., 1993. The biogeochemistry of manganese and iron reduction in marine sediments. *Earth-Science Reviews*, 35: 249–284.

Chakraborty, P., Sarkar, A., Vudamala, K., Naik, R. and Nath, B.N., 2015. Organic matter—a key factor in controlling mercury distribution in estuarine sediment. *Marine Chemistry*, 173: 302–309.

Chamley, H., 1989. Clay Sedimentology Berlin: Springer-Verlag pp.623.

Chan, L.H., Drummond, D., Edmond, J.M. and Grant, B., 1977. On the barium data from the Atlantic GEOSECS expedition. *Deep-Sea Research*, 24(7): 613–649.

Chase, Z., Anderson, R.F., Fleisher, M.Q. and Kubik, P.W., 2003. Accumulation of biogenic and lithogenic material in the Pacific sector of the Southern Ocean during the past 40,000 years. *Deep Sea Res PT II: Topical Studies in Oceanography*, 50(3): 799–832.

Chen, H.F., Chang, Y.P., Kao, S.J., Chen, M.T., Song, S.R., Kuo, L.W., Wen, S.Y., Yang, T.N. and Lee, T.Q., 2011. Mineralogical and geochemical investigations of sediment-source region change in the Okinawa Trough during the past 100ka (IMAGES core MD012404). *Journal of Asian Earth Science*, 40(6): 1238–1249.

Chen, H.F., Song, S.R., Lee, T.Q., Lowemark, L., Chi, Z.Q., Wang, Y. and Hong, E., 2010. A multiproxy lake record from Inner Mongolia displays a late Holocene teleconnection between central Asian and North Atlantic climate. *Quaternary International*, 227: 170–183.

Chester, R. and Jickells, T.D., 2012. The Transport of Material to the Oceans: The Fluvial Pathway. In: Marine Geochemistry, New York: John Wiley & Sons.

Choudhary, S., Nayak, G.N. and Khare, N., 2018. Provenance, processes and productivity through spatial distribution of the surface sediments from Kongsfjord to Krossfjord system, Svalbard. *Journal of Indian Association of Sedimentologists*, 35(1): 47–56.

Choudhary, S., Nayak, G.N., Tiwari, A.K. and Khare, N., 2018. Source, processes and productivity from distribution of surface sediments, Prydz Bay, East Antarctica. *Polar Science, 18*: 63–71.

Choudhary, S., Nayak, G.N., Tiwari, A.K. and Khare, N., 2018. Sediment composition and its effect on the productivity in Larsemann Hills, East Antarctica. *Arabian Journal of Geosciences, 11*(15): 416.

Choudhary, S., Tiwari, A.K., Nayak, G.N. and Bejugam, P., 2018. Sedimentological and geochemical investigations to understand source of sediments and processes of recent past in Schirmacher Oasis, East Antarctica. *Polar Science, 15*: 87–98.

Christl, M. and Strobl, C., 2003. Beryllium-10 in deep-sea sediments: a tracer for the Earth's magnetic field intensity during the last 200,000 years. *Quaternary Science Review*, 22(5-7): 725–739.

Collier, R. and Edmond, J., 1984. The trace element geochemistry of marine biogenic particulate matter. *Progress in Oceanography*, 13 (2): 113–199.

Colman, S.M., Peck, J.A., Karabanov, E.B., Carter, S.J., Bradbury, J.P., King, J.W. and Williams, D.F., 1995. Continental climate response to orbital forcing from biogenic silica records in Lake Baikal. *Nature,* 378: 769–771.

Conley, D.J., 1998. An inter-laboratory comparison for the measurement of biogenic silica in sediments. *Marine Chemistry*, 63(1): 39–48.

Cottier, F., Tverberg, V., Inall, M.E., Svendsen, H., Nilsen, F. and Griffiths, C., 2005. Water mass modification in an Arctic fjord through cross-shelf exchange: the seasonal hydrography of Kongsfjorden, Svalbard. *Journal of Geophysical Research*: *Oceans*. 110: 1–18.

Cremer, H., Heiri, O., Wagner, B. and Wagner-Cremer, F., 2007. Abrupt climatic warming in East Antarctica during the early Holocene. *Quaternary Science Reviews*, 26: 2012–2018.

Cuong, D.T. and Obbard, J.P., 2006. Metal Speciation in Coastal Marine Sediments from Singapore using a Modified BCR-Sequential Extraction Procedure. Applied Geochemistry, 21(8): 1335–1346.

Dalai, T.K., Rengarajan, R. and Patel, P.P., 2004. Sediment Geochemistry of the Yamuna River system in the Himalaya: implications to weathering and transport. *Journal of Geochemistry,* 38: 441–453.

Dallman, W.K., 1999. Lithostratigrahic lexicon of Svalbard: review and recommendations for nomenclature use: Upper Paleozoic to Quaternary bedrock. Norsk Polarinstitut.

Davis, J.A., 1984. Complexation of trace metals by adsorbed natural organic matter. *Geochimica et Cosmochimica Acta*, 46: 2381–2393.

Dhal, S.P., Balakrishnan, S., Kumar, P., Singh, P., Sharan, A. and Chopra, S., 2018. $^{10}Be/^{9}Be$ ratios of Cauvery river delta sediments, southern India: implications for palaeo-denudation rates in the catchment and variation in summer monsoon rainfall during Late Quaternary. *Current Science, 115*(9): 1770.

Dirks, P.H.G.M. and Wilson, C.J.L., 1995. Crustal evolution of the East Antarctic mobile belt in Prydz Bay: continental collision at 500 Ma? *Precambrian Research*, 75: 189–207.

Doran, P.T., McKay, C.P., Clow, G.D., Dana, G.L., Fountain, A.G., Nylen, T. and Lyons, W.B., 2002. Valley floor climate observations from the McMurdo Dry Valleys, Antarctica, 1986–2000. *Journal of Geophysical Research*, 107: 4772.

Dowdeswell, J.A., Elverhøi A. and Spielhagen, R., 1998. Glaciomarine sedimentary processes on the polar north Atlantic margins. *Quaternary Science Reviews*, 17: 243–272.

Dowdeswell, J.A and Forsberg C.F., 1992**.** The size and frequency of icebergs and bergy bits derived from tidewater glaciers in Kongsfjorden, Northwest Spitsbergen. *Polar Research*, 11: 81–91.

Dreyer, B.M., Morris, J.D. and Gill, J.B., 2010. Incorporation of subducted Slab-derived sediment and fluid in Arc margins: B-Be-^{10}Be-εNd systematics of the Kurile Convergent Margin, Russia. *Journal of Petrology*, 51(8): 1761–1782.

Ehrmann, W., Setti, M. and Marinoni, L., 2005. Clay minerals in Cenozoic sediments off Cape Roberts (McMurdo Sound, Antarctica) reveal palaeoclimatic history. *Paleogeography, Palaeoclimatology, Palaeoecology*, 229(3): 187–211.

Eilertsen, H.C., Taasen, J.P. and Weslawski, J.M., 1989. Phytoplankton studies in the fjords of West Spitsbergen: physical environment and production in spring and summer. *Journal of Plankton Research, 11*(6): 1245–1260.

El Bilali, L., Rasmussen, P.E., Hall, G.E.M. and Fortin, D., 2002. Role of sediment composition in trace metal distribution in lake sediments. *Applied Geochemistry*, *17*(9): 1171-1181.

Esquevin, J., 1969. Influence de la composition chimique des illites sur leur cristallinité. *Bulletin du Centre de Recherches, Pau-SNPA*, *3*(1): 147–153.

Farias, C.O., Hamacher, C., Wagener, A.D.L.R., de Campos, R.C. and Godoy, J.M., 2007. Trace metal contamination in mangrove sediments, Guanabara Bay, Rio de Janeiro, Brazil. *Journal of Brazilian Chemical Society*, 18: 1194–1206.

Farmer, D. and Freeland, H.J. 1983. The physical oceanography of fjords. In: Angel MV, O´Brien J.J. (Eds.), *Progress in Oceanography,* 12: 147–220.

Fendeng, S., Xeufa, S., Xin, S., Xisheng, F., Yenghua, W., Zhenbo, C. and Zhengyuan, Y., 2018. Clay minerals in Arctic Kongsfjorden surface sediments and their implications on provenance and paleoenvironmental change. *Acta Oceanologia Sinica*, 37(5): 29–38.

Feng, S., Xue, Z. and Chi, W., 2008. Topographic features around Zhongshan Station, southeast of Prydz Bay. *Chinese Journal of Oceanology and Limnology*, 26(4): 469–474.

Fernandes, M.C. and Nayak, G.N., 2017. Geochemistry of mudflat and mangrove sedimentary environments, within tropical (Sharavati) estuary, Karnataka coast, India. *Journal of Indian Association of Sedimentologists*, 34(1-2): 103–119.

Filgueiras, A.V., Lavilla, I. and Bendicho, C., 2004. Evaluation of distribution, mobility and binding behaviour of heavy metals in surficial sediments of Louro River (Galicia, Spain) using chemometric analysis: a case study. *Science of the Total Environment*, 330(1-3): 115–129.

Fitzsimons, I.C.W. and Harley, S.L., 1991. Geological relationships in high-grade gneiss of the Brattstrand Bluffs coastline, Prydz Bay, East Antarctica. *Australian Journal of Earth Sciences*, 38: 497–519.

Folk, R.L.,1974. In Petrology of sedimentary rocks. Austin, Texas: Hemphill. PP. 182.

Forsberg, C.F., Florindo, F., Grutzner, J., Venuti, A. and Solheim, A., 2008. Sedimentation and aspects of glacial dynamics from physical properties, mineralogy and magnetic properties at ODP Sites 1166 and 1167, Prydz Bay, Antarctica. *Paleogeography, Paleoclimatology and Paleoecology*,260: 184 – 201.

Frank, M., Backmann, J., Jakobsson, M. and Moran, K., 2008. Beryllium isotopes in central Arctic Ocean sediments over the past 12.3 million years. *Palaeooceanography*, 23(1).

Frank, M., Porcelli D., Anderson, P., Baskaran M., Bjork, G., Kubik, P.W., Hattendorf, B. and Guenther, D., 2009.The dissolved Beryllium isotope composition of the Arctic Ocean, *Geochimica et Cosmochimica Acta*, 73: 6114–6133.

Franklin, D.C., 1997. The Sedimentology of Holocene Prydz Bay: Sedimentary Patterns and Processes. Doctoral Dissertation: University of Tasmania, Hobart.182.

Fritsen, C.H. and Priscu, J.C., 1999. Seasonal change in the optical properties of the permanent ice cover on Lake Bonney, Antarctica: consequences for lake productivity and phytoplankton dynamics. *Limnology and Oceanography*, 44(2): 47–454.

Gambrell, R.P., 1994. Trace and toxic metals in wetland - a review: *Journal of Environmental Quality*, 23: 883–891.

Gasparon, M. and Burgess, J.S., 2000. Human impacts in Antarctica: trace-element geochemistry of freshwater lakes in the Larsemann Hills, East Antarctica. *Environmental Geology*, *39*(9): 963–976.

Gasparon, M. and Matschullat, J., 2006. Trace metals in Antarctic ecosystems: results from the Larsemann Hills, East Antarctica. *Applied Geochemistry*, 21(9): 1593–1612.

Geological Survey of India, 2006. Geomorphological Map of Schirmacher Oasis, East Antarctica. Director General, Geological Survey of India. Government of India, New Delhi.

Gingele, F.X., 1996. Holocene climatic optimum in Southwest Africa—evidence from the marine clay mineral record. *Palaeogeography, Palaeoclimatology and Palaeoecology*, 122(1): 77–87.

Gobeil, C., Macdonald, R.W., Smith, J.N., 1999. Mercury profiles in sediments of the Arctic Ocean basins. *Environmental Science and Technology*, 33: 4194–4198.

Gorlich, K., Weslawski, J.M. and Zajaczkowski, M., 1987. Suspension settling effect on macrobenthos biomass distribution in the Hornsund Fjord, Spitsbergen. *Polar Research*, 5: 175–192.

Govil, P., Asthana, R., Mazumder, A. and Ravindra, R., 2012. Grain size distribution and its influence on biological productivity during Holocene in a fresh water lake in Larsemann Hills, Antarctica. *National Academy Science Letters*, 35(2): 115–119.

Govil, P., Mazumder, A., Asthana, R., Tiwari, A. and Mishra, R., 2016. Holocene climate variability from the lake sediment core in Schirmacher Oasis region, East Antarctica: Multiproxy approach. *Quaternary international*, *425*: 453–463.

Govil, P., Mazumder, A., Ram, R., Singh, D.S. and Azharuddin, S., 2018. Meltwater flux and climate change record of last 18.5 ka from Schirmacher Oasis, East Antarctica. *Polar Science*, *18*: 135–141.

Govil, P., Mazumder, A., Tiwari, A. and Kumar, S., 2011. Holocene climate variability from lake sediment core in Larsemann Hills, Antarctica. *Journal of Geological Society of India*. 78(1): 30–35.

Grant, J.A., 1986. The isocon diagram-a simple solution to Gresens' equation for metasomatic alteration. *Economic Geology*, 81: 1976–1982.

Griffin, J.J., Windom, H. and Goldberg, E.D., 1968. The distribution of clay minerals in the World Ocean. In: *Deep Sea Research in Oceanography*, Abstract,15(4): 433–459.

Griffith, T.W. and Anderson, J.B. 1989. Climatic control of sedimentation in bays and fjords of the northern Antarctic Peninsula. *Marine Geology*, 85: 181–204.

Grotti M., Soggia, F., Ardini, F., Bazzano, A., Moroni, B., Vivani, R., Cappelletti, D. and Misic, C., 2017. Trace elements in surface sediments from Kongsfjorden, Svalbard: occurrence, sources and bioavailability. *International Journal of environment and analytical chemistry*, 97(5): 401–418.

Grotti, M., Soggia, F., Iann, C., Magi, E. and Udisti, R., 2013. Bioavailability of trace elements in surface sediments from Kongsfjorden, Svalbard. *Marine Pollution Bulletin*, 77: 367–374.

Harris, P.T., Taylor, F., Pushina, Z., Leitchenkov, G., O'Brien, P.E. and Smirnov, V., 1998. Lithofacies distribution in relation to the geomorphic provinces of Prydz Bay, East Antarctica. *Antarctic Science*, 10: 227–235.

Hawes, I., 1983. Nutrients and their effects on phytoplankton populations in lakes on Signy Island, Antarctica. *Polar Biology*, 2(2): 115–126.

Hedges, J.I., Clark, W.A., Quay, P.D., Richey, J.E., Devol, A.H. and Santos, M., 1986. Compositions and fluxes of particulate organic material in the Amazon River. *Limnology and Oceanography*, *31*(4): 717–738.

Hernandez-Hinojosa, V., Montiel-Garcia, P.C., Armstrong-Altrin, J.S., Nagarajan, R. and Kasper-Zubillaga, J.J., 2018. Textural and geochemical characteristics of beach sands along the western Gulf of Mexico, Mexico. *Carpathian Journal of Earth and Environmental Science*, 13(1): 161–174.

Hjelle, A., 1993. Geology of Svalbard. Oslo: Norsk Polarinstitutt, pp.1–165.

Hjelstuen, B.O., Haflidason, H., Sejrup, H.P. and Lysa, A., 2009. Sedimentary processes and depositional environments in glaciated fjord systems—Evidence from Nordfjord, Norway. *Marine Geology*, *258*(1–4): 88–99.

Hodgson, D.A., McMinn, A., Kirkup, H., Cremer, H., Gore, D., Melles, M., Roberts, D. and Montiel, P., 2003. Colonization, succession, and extinction of marine floras during a glacial cycle: A case study from the Windmill Islands (East Antarctica) using biomarkers. *Palaeoceanography*, 18(3).

Hodgson, D.A., Noon, P.E., Vyverman, W., Bryant, C.L., Gore, D.B., Appleby, P., Gilmour, M., Verleyen, E., Sabbe, K., Jones, V.J. and Ellis-Evans, J.C., 2001. Were the Larsemann Hills ice-free through the last glacial maximum? *Antarctic Science*, 13(4): 440–454.

Hodgson, D.A., Roberts, S.J., Bentley, M.J., Carmichael, E.L., Smith, J.A., Verleyen, E., Vyverman, W., Geissler, P., Leng, M.J. and Sanderson, D.C.W., 2009a. Exploring former subglacial-hodgson lake, Antarctica. Paper II: palaeolimnology. *Quaternary Science Reviews*, 28: 2310–2325.

Hodgson, D.A., Verleyen, E., Vyverman, W., Sabbe, K., Leng, M.J., Pickering, M.D. and Keely, B.J., 2009b. A geological constraint on relative sea level in Marine Isotope Stage 3 in the Larsemann Hills, Lambert Glacier region, East Antarctica (31366–33228 calyr BP). *Quaternary Science Reviews*, 28: 2689–2696.

Hodgson, D.A., Whitehouse, P.L., De Cort, G., Berg, S., Verleyen, E., Tavernier, I., Roberts, S.J., Vyverman, W., Sabbe, K. and O'Brien, P., 2016. Rapid early Holocene sea-level rise in prydz bay, East Antarctica. *Global and Planetary Change*, 139: 128–140.

Holloway, J.M. and Dahlgren, R. A., 1999. Geologic nitrogen in terrestrial biogeochemical cycling. *Geology*, 27(6): 567–570.

Hop, H., Pearson, T., Hegseth, E.N., Kovacs, K.M., Wiencke, C., Kwasniewski, S., Eiane, K., Mehlum, F., Gulliksen, B., Wlodarska-Kowalczuk, M. and Lydersen, C., 2002. The marine ecosystem of Kongsfjorden, Svalbard. *Polar Research*, *21*(1): 167–208.

Horowitz, A.J., 1991. A primer on trace metal sediment chemistry. Chelsa MI: (Lewis publishers) 136.

Howe, J.A., Austin, W.E., Forwick, M., Paetzel, M., Harland, R. and Cage, A.G. 2010. Fjord systems and archives: a review. *Geological Society of London, Special Publications*, 344(1): 5–15.

Huang, J.P., Swain, A.K., Thacker, R.W., Ravindra, R., Andersen, D.T. and Bej, A. K., 2013. Bacterial diversity of the rock-water interface in an East Antarctic freshwater ecosystem, Lake Tawani. *Aquatic Biosystem,* 9: 1-10

Huerta-Diaz, M.A. and Morse, J.W., 1992. Pyritization of trace metals in anoxic marine sediments. *Geochimica et Cosmochimica Acta*, 56(7): 2681–2702.

Ingole, B.S. and Dhargalkar, V.K., 1998. Ecobiological assessment of a freshwater lake at Schirmacher Oasis, East Antarctica, with reference to human activities. *Current Science,* 74: 529–534.

IPCC 2014. (Pachauri, R.K., Meyer, L., Plattner, G.K. and Stocker, T.) Climate change 2014: synthesis report. *IPCC, Geneva, Switzerland.*

Isla, E., Masque, P., Palanques, A., Guillen, J., Puig, P. and Sanchez-Cabeza, J.A., 2004. Sedimentation of biogenic constitutes during the last century in western Bransfield and Gerlache Straits, Antarctica: a relation to currents, primary production and sea floor relief. *Marine Geology*, 209: 265–277.

Jarvis, I. and Jarvis, K.E., 1985. Rare-earth element geochemistry of standard sediments: a study using inductively coupled plasma spectrometry. *Chemical Geology*, 53(3–4): 335–344.

Jeelani, G. and Shah, A.Q., 2006. Geochemical characteristics of water and sediment from the Dal Lake, Kashmir Himalaya: constraints on weathering and anthropogenic activity. *Environmental Geology*, 50(1): 12–23.

Jiang, S., Liu, X., Sun, J., Yuan, L., Sun, L. and Wang, Y., 2011. A multi-proxy sediment record of late Holocene and recent climate change from a lake near Ny-Ålesund, Svalbard. *Boreas, 40*(3): 468–480.

Kaasalainen, M. and Yli-Halla, M., 2003. Use of sequential extraction to assess metal partitioning in soils. *Environmental Pollution*, 126: 225–233.

Kamatani, A. and Oku, O., 2000. Measuring biogenic silica in marine sediments. *Marine Chemistry*, 68(3): 219–229.

Kaplan, M.R., Wolfe, A.P. and Miller, G.H., 2002. Holocene environmental variability in southern Greenland inferred from lake sediments. *Quaternary Research*, 58(2): 149–159.

Kar, R., Mazumder, A., Mishra, K., Patil, S.K., Ravindra, R., Ranhotra, P.S., Govil, P., Bajpai, R. and Singh, K., 2018. Climatic history of Ny-Alesund region, Svalbard, over the last 19,000 year: Insights from quartz grain microtexture and magnetic susceptibility. *Polar Science*, *18*: 189–196.

Kaste, J.M. and Baskaran, M., 2012. Meteoric ^{7}Be and ^{10}Be as process tracers in the environment. In: *Handbook of environmental isotope geochemistry* (pp.61–85). Springer, Berlin, Heidelberg.

Khare, N., Govil, P., Kumar, P., Mazumder, A., Chopra, S., Pattanaik, J. K., Balakrishnan, S. and Roonwal, G. S., 2011. ^{10}Be as paleoclimatic tracer: initial results from south western Indian Ocean sediments. *Journal of Radioanalytical and Nuclear Chemistry*, 290(1): 197–201.

Kim, J.H., Peterse, F., Willmott, V., Kristensen, D.K., Baas, M., Schouten, S. and Sinninghe Damste, J.S., 2011. Large ancient organic matter contributions to Arctic marine sediments (Svalbard). *Limnology and Oceanography*, *56*(4): 1463–1474.

Kim, K.J., Zolitschka, B., Timothy, A.J., Ohlendorf, C., Haberzettl, T. and Matsuzaki, H., 2012. Tracing Environmental change in southern Patagonia using Beryllium isotopes, Laguna Portok, Aike, Argentina. *Quaternary Geochronology*, 9: 27–33.

Knies, J., Brookes, S. and Schubert, C.J., 2007. Re-assessing the nitrogen signal in continental margin sediments: New insights from the high northern latitudes. *Earth and Planetary Science Letters*, *253*(3-4): 471–484.

Koziorowska, K., Kuliński, K. and Pempkowiak, J., 2016. Sedimentary organic matter in two Spitsbergen fjords: terrestrial and marine contributions based on carbon and nitrogen contents and stable isotopes composition. *Continental Shelf Research*, 113: 38–46.

Koziorowska, K., Kuliński, K. and Pempkowiak, J., 2017. Distribution and origin of inorganic and organic carbon in the sediments of Kongsfjorden, Northwest Spitsbergen, European Arctic. *Continental Shelf Research*, 150: 27–35.

Kretschmer, S., Geibert, W., Rutgers, V.D., Loeff, M., Schnabel, C., Xu, S. and Mollennauer G., 2011. Fractionation of ^{230}Th, ^{231}Pa, ^{10}Be induced by particle size and composition within opal-rich sediment if the Atlantic Southern Ocean. *Geochimica et Cosmochimica Acta*, 75(22): 6971–6987.

Kumar, P., Pattanaik, J.K., Khare, N. and Balakrishnan, S., 2018. Geochemistry and provenance study of sediments from Krossfjorden and Kongsfjorden, Svalbard (Arctic Ocean). *Polar Science*, *18*: 72–82.

Kumar, P., Pattanaik, J.K., Khare, N., Chopra, S., Yadav, S., Balakrishnan, S. and Kanjilal, D., 2014. Study of 10 Be in the sediments from the Krossfjorden and Kongsfjorden Fjord System, Svalbard. *Journal of Radioanalytical and Nuclear Chemistry*, *302*(2): 903–909.

Kumar, V., Tiwari, M. and Rengarajan, R., 2018. Warming in the Arctic Captured by productivity variability at an Arctic Fjord over the past two centuries. *Plos one*, *13*(8): 201456.

Kumar, V., Tiwari, M., Nagoji, S. and Tripathi, S., 2016. Evidence of Anomalously Low δ13 C of Marine Organic Matter in an Arctic Fjord. *Scientific reports*, *6*: 36192.

Kurian, S., Nath, B.N., Kumar, N.C. and Nair, K.K.C., 2013. Geochemical and isotopic signatures of surficial sediments from the western continental shelf of India: inferring provenance, weathering, and the nature of organic matter. *Journal of Sedimentary Research*, 83(6): 427–442.

Ladigbolu, I.A., 2014. Chemical speciation and mobility of heavy metals in the sediments of selected streams in Ibadan Metropolis, Nigeria. IOSR, *Journal of Applied Chemistry*, 7(8): 21–28.

Lamb, A.L., Wilson, G.P. and Leng, M.J., 2006. A review of coastal palaeoclimate and relative sea-level reconstructions using $^{\delta 13}$C and C/N ratios in organic material. *Earth Science Reviews*, 75(1): 29–57.

Landvik, J.Y., Bondevik, S., Elverhøi, A., Fjeldskaar, W., Mangerud, J.A.N., Salvigsen, O., Siegert, M.J., Svendsen, J.I. and Vorren, T.O. 1998. The last glacial maximum of Svalbard and the Barents Sea area: ice sheet extent and configuration. *Quaternary Science Reviews*, 17(1–3): 43–75.

Lawrence, M.J.F. and Hendy, C.H., 1985. Water column and sediment characteristics of Lake Fryxell, Taylor Valley, Antarctica. *New Zealand, Journal of Geology and Geophysics*, 28(3): 543–552.

Lehman, S.J. and Forman, S.L., 1992. Late Weichselian glacier retreat in Kongsfjorden, west Spitsbergen, Svalbard. *Quaternary Research*, 37: 139–154.

Li, M., 2006. Geochronology and geochemistry of granitoids from the Prydz Belt, East Antarctica, and their tectonic implications. Ph.D. thesis, Chinese Academy of Geological Sciences, 73 [Unpublished].

Liu, B., Xu, H., Lan, J., Sheng, E., Che, S. and Zhou, X., 2014. Biogenic silica contents of Lake Qinghai sediments and its environmental significance. *Frontiers of earth science*, *8*(4): 573–581.

Liu, X.C., Jahn, B.M., Zhao, Y., Li, M., Li, H.M. and Liu, X.H., 2006. Late Pan-African granitoids from the Grove Mountains, East Antarctica: age, origin and tectonic implications. *Precambrian Research*, 145: 131–154.

Lu, Z., Cai, M., Wang, J., Yin, Z. and Yang, H., 2013. Levels and distribution of trace metals in surface sediments from Kongsfjorden, Svalbard, Norwegian Arctic. *Environmental Geochemical Health*, 35: 257–69.

Lu, Z.B. and Kang, M., 2018. Risk assessment of toxic metals in marine sediments from the Arctic Ocean using a modified BCR sequential extraction procedure. *Journal of Environmental Science and Health*, Part A, 53(3): 278–293.

Lyons, W.B., Mayewski, P.A., Donahue, P. and Cassidy, D. 1985. A preliminary study of the sedimentary history of Lake Vanda, Antarctica: Climatic implications. *New Zealand Journal of Marine and Freshwater Research*, 19: 253–260.

Mahesh, B.S., Nair, A., Warrier, A.K., Avadhani, A., Mohan, R. and Tiwari, M., 2018. Palaeolimnological records of regime shifts from marine-to-lacustrine system in a coastal Antarctic lake in response to post-glacial isostatic uplift. *Current Science*, 115(9): 1679.

Mahesh, B.S., Warrier, A.K., Mohan, R. and Tiwari, M., 2019. Impact of Antarctic climate during the Late Quaternary: Records from Zub Lake sedimentary archives from Schirmacher Hills, East Antarctica. *Palaeogeography, Palaeoclimatology, Palaeoecology*, 514: 398–406.

Mahesh, B.S., Warrier, A.K., Mohan, R., Tiwari, M., Babu, A., Chandran, A., Asthana, R., and Ravindra, R., 2015. Response of Long Lake sediments to Antarctic climate: A perspective gained from sedimentary organic geochemistry and particle size analysis. *Polar Science*, 9(4): 359–367.

Mahesh, B.S., Warrier, A.K., Mohan, R., Tiwari, M., Roy, R., Asthana, R. and Ravindra, R., 2017. Response of Sandy Lake in Schirmacher Oasis, East Antarctica to the glacial-interglacial climate shift. *Journal of Paleolimnology*, 58(3): 275–289.

Manoj, M.C. and Thamban, M., 2015. Shifting frontal regimes and its influence on bioproductivity variations during the Late Quaternary in the Indian sector of Southern Ocean. *Deep-Sea Research, Part II Topical Studies in Oceanography*, 118: 261–274.

Mantoura, R.F.C., Dickson, A. and Riley, J.P., 1978. The complexation of metals with humic materials in natural waters. *Estuarine Coastal Marine Science*, 6: 387–408.

Marchand, C., Lallier-Verges, E., Baltzer, F., Alberic, P., Cossa, D. and Baillif, P., 2006. Heavy metals distribution in mangrove sediments along the mobile coastline of French Guiana. *Marine Chemistry*, 98: 1–17.

Martínez Cortizas, A., Rozas Muñiz, I., Taboada, T., Toro, M., Granados, I., Giralt, S. and Pla-Rabés, S., 2014. Factors controlling the geochemical composition of Limnopolar Lake sediments (Byers Peninsula, Livingston Island, South Shetland Island, Antarctica during the last ca. 1600 years. *Solid Earth*, *5*(2): 651–663.

Masuda, N., Nishimura, M. and Torii, T., 1982. Distribution and Origin of some trace metals in Lake Vanda, Antarctica. *Antarctic Record, Tokyo*, 75: 25–36.

Matini, L., Moutou, J.M., Ongoka, P.R. and Tathy, J.P., 2011. Clay mineralogy and vertical distribution of lead, zinc and copper in soil profile in the vicinity of an abandoned treatment plant research. *Journal of Environmental Earth Science*, 3(2): 114–123.

Matsumoto, G.I., Honda, E., Seto, K., Tani, Y., Watanabe, T., Ohtani, S., Kashima, K., Nakamura, T. and Imura, S., 2014. Holocene paleolimnological changes of Lake Oyako-ike in the Soya Kaigan of East Antarctica. *Inland Waters*, *4*(2): 105–112.

Matsumoto, G.I., Watanuki, K., and Torii, T., 1989. Vertical distribution of organic constituents in an Antarctic lake: Lake Fryxell. *Hydrobiologia*, 172: 291–303.

Mazumder, A. and Govil, P., 2013. Signature of warmer Late Holocene around Vestfold Hills, East Antarctica. *Canadian Journal of Basic and Applied Sciences, 1*(1): 33–43.

Mazumder, A., Govil, P., Kar, R. and Gayathri, N.M., 2017. Paleoenvironments of a proglacial lake in Schirmacher Oasis, East Antarctica: Insights from quartz grain microtextures. *Polish Polar Research, 38*(1): 1–19.

McLennan, S.M., Hemming, S., McDaniel, D.K. and Hanson, G.N., 1993. Geochemical approaches to sedimentation, provenance, and tectonics. *Geological Society of America*, Special Papers, 284: 21–40.

McLennan, S.M., Taylor, S.R., Mc Culloch, M.T. and Maynard, J.B., 1990. Geochemical and Nd-Sr isotopic composition of deep-sea turbidites: crustal evolution and plate tectonic associations. *Geochimica et Cosmochimica Acta*, 54(7): 2015–2050.

Mentasti, E., Abollino, O., Aceto, M. and Sarzanini, C., 1998. Distribution and statistical correlations of major, minor and trace metals in lake environments of Antarctica. *International Journal of Environmental Analytical Chemistry*, 71: 245–255.

Meyers, P.A., 2003. Applications of organic geochemistry to paleolimnological reconstructions: a summary of examples from the Laurentian Great Lakes. *Organic Geochemistry,* 34: 261–289.

Meyers, P.A., 1997. Organic geochemical proxies of paleoceanographic, paleolimnologic, and paleoclimatic processes. *Organic geochemistry,* 27(5): 213–25.

Meyers, P.A., 1994. Preservation of elemental and isotopic source identification of sedimentary organic matter. *Chemical Geology*, 114(3-4): 289–302.

Meyers, P.A. and Ishiwatari, R., 1993. Lacustrine organic geochemistry—an overview of indicators of organic matter sources and diagenesis in lake sediments. *Organic geochemistry*, *20*(7): 867–900.

Meyers, P.A. and Teranes, J.L., 2001. Sediment organic matter. In: Tracking environmental changes using lake sediments-volume II: physical and chemical techniques. *Kluwer, Dordrecht*, 239–269.

Mohan, M., Sreelakshmi, U., Sagar, M.V., Gopikrishna, V.G., Pandit, G.G., Sahu, S.K., Tiwari, M., Ajmal, P.Y., Kannan, V.M., Shukkur, M.A. and Krishnan, K.P., 2018. Rate of sediment accumulation and historic metal contamination in a tidewater glacier fjord, Svalbard. *Marine Pollution Bulletin*, *131*: 453–459.

Morel, F.M.M., Reinfelder, J.R., Roberts, S.B., Chamberlain C.P., Lee, J.G. and Yee, D., 1994. Zinc and carbon co-limitation of marine phytoplankton. *Nature,* 369: 740–742.

Mortlock, R.A. and Froelich, P.N., 1989. A simple method for the rapid determination of biogenic opal in pelagic marine sediments. *Deep Sea Research, Part A Oceanography Research Papers*, 36(9): 1415–1426.

Muller, P.J. 1977. C/N ratios in Pacific deep-sea sediments: Effect of inorganic ammonium and organic nitrogen compounds sorbed by clays. *Geochimica et Cosmochimica Acta*, *41*(6): 765–776.

Muller, P.J. and Schneider, R., 1993. An automated leaching method for the determination of opal in sediments and particulate matter. *Deep Sea Research Part I: Oceanography Research Papers*, 40(3): 425–444.

Munoz, Y.P. and Wellner, J.S., 2016. Local controls on sediment accumulation and distribution in a fjord in the West Antarctic Peninsula: implications for paleoenvironmental interpretations. *Polar Research*, *35*(1): 25284.

Murphy, J. and Riley, J.P., 1962. A modified single solution method for the determination of phosphate in natural waters. *Analytica Chimica Acta*, *27*: 31–36.

Murray, D.S., Singer, B.S., Carlson, A.E. and Caffee, M.W., 2010. Cosmogenic age constraints on the last deglaciation in Southern Patagonia (49 - 50°S), American Geophysical Union, Fall Meeting 2010, abstract #GC21A-0859.

Murray, J.W., 1975. The interaction of metal ions at the manganese dioxide-solution interface. *Geochimica et Cosmochimica Acta*, 39: 505–520.

Murray, R.W. and Leinen, M., 1996. Scavenged excess aluminium and its relationship to bulk titanium in biogenic sediment from the central equatorial Pacific Ocean. *Geochimica et Cosmochimica Acta*, 60(20): 3869–3878.

Muzuka, A.N. and Shaghude, Y.W., 2000. Grain size distribution along the Msasani Beach, north of Dar es Salaam Harbour. *African Journal of Earth Sciences*, 30(2): 417–426.

Nasnodkar, M.R. and Nayak, G.N., 2017. Chemical speciation and bio-availability of selected trace metals in the mudflat core sediments of the tropical estuaries, India. *Environmental Earth Science*, 76(21): 727.

Nath, B.N., Aldahan, A., Possnert, G., Selvaraj, K., Mascarenhas-Pereira, M.B.L. and Chen, C.T.A., 2007. ^{10}Be variation in surficial sediments of the Central Indian Basin. *Nuclear Instruments and Methods in Physics Research Section B: Beam Interactions with Materials and Atoms*, *259*(1): 610–615.

Nazneen, S. and Raju, N.J., 2017. Distribution and sources of carbon, nitrogen, phosphorus and biogenic silica in the sediments of Chilika lagoon. *Journal of Earth System Science, 126(13).*

Nemati, K., Bakar, N.K.A., Abas, M.R. and Sobhanzadeh, E., 2011. Speciation of Heavy Metals by Modified BCR Sequential Extraction Procedure in Different Depths of Sediments from Sungai Buloh, Selangor, Malaysia. *Journal of Hazardous Material*, 192(1): 402–410.

Nilsen, F., Cottier, F., Skogseth, R. and Mattsson, S., 2008. Fjord–shelf exchanges controlled by ice and brine production: the interannual variation of Atlantic Water in Isfjorden, Svalbard. *Continental Shelf Research*, 28(14): 1838–1853.

Nioti, D., Maravelis, A., Tserolas, P. and Zelilidis, A., 2013. TOC and $CaCO_3$ content in Oligocene shelf deposits on Lemnos Island and their relation with depositional conditions. *Bulletin of Geological Society of Greece*, 47(2): 852–861.

Noronha-D' Mello, C.A. and Nayak, G.N., 2015. Geochemical characterization of mangrove sediments of the Zuari estuarine system, West coast of India. *Estuarine, Coastal Shelf Science*, 167: 313–325.

Nuttin, L. and Hillaire-Marcel, C., 2015. U-and Th-series isotopes in deep Baffin Bay sediments: tracers of detrital sources and of contrasted glacial/interglacial sedimentary processes. *Marine Geology*, 361:1-10.

Nyangababo, J.T., Henry, I. and Omutunge, E., 2005. Heavey metal contamination in plants, sediments and air precipitation of Katonga, Simiyu and Nyando wetlands of Lake Victoria Basin, East Africa. *Bulletin of Environmental Contamination and Toxicology*, 75: 189-196.

Ohmsen, G.S., Chenhall, B.E. and Jones, B.G., 1995. Trace metal distributions in two saltmarsh substrates, Illawarra region, New South Wales, Australia. *Wetlands* (Australia), 14: 1931.

Ohyama, Y., Morimoto, K. and Mochida, Y., 1992, March. Seasonal changes of nutrient concentration in Lake Ô-Ike near Syowa Station, Antarctica. In: *Proceedings National Institute of Polar Research, Symposium, Polar Biol*ogy, 5: 146–150.

Padma, S. and Periakali, P., 1999. Physico-chemical and geochemical studies in Pulicat lake, east coast of India. *Indian Journal of Geo- Marine Sciences,* 28: 434–437.

Pais, J. and Jones, J.B., 1997. The Handbook of Trace Elements. Boca Raton: CRC Press.

Passchier, S., O'Brien, P.E., Damuth, J.E., Januszczak, N., Handwerger, D.A. and Whitehead, J.M., 2003. Pliocene–Pleistocene glaciomarine sedimentation in eastern Prydz Bay and development of the Prydz trough-mouth fan, ODP Sites 1166 and 1167, East Antarctica. *Marine Geology*, 199: 279–305.

Paytan, A. and Kastner, M., 1996. Benthic Ba fluxes in the central Equatorial Pacific, implications for the oceanic Ba cycle. *Earth and Planetary Science Letters*, 142(3–4): 439–450.

Peck, J.A., Green, R.R., Shanahan, T., King, J.W., Overpeck, J.T. and Scholz, C.A., 2004. A magnetic mineral record of Late Quaternary tropical climate variability from Lake Bosumtwi, Ghana. *Palaeogeography, Palaeoclimatology, Palaeoecology, 215*(1-2): 37-57.

Pedro, J.B., Hekikila, U.E., Smith, A.M., Ommen, V.T.D. and Curran M.J., 2011. Beryllium-10 transport to Antarctica: Results from seasonally resolved observations and modelling, *Journal of Geophysical Resolution*, 116: D23120.

Pejrup, M., 1988. The triangular diagram used for classification of estuarine sediments: a new approach. In: De Boer, P.L., Van Gelder, A., Nios, S.D. (Eds.) *Tide-influenced sedimentary environments and facies* (Reidel, Dordrecht), 289–300.

Pelto, M.S., Higgins, S.M., Hughes, T.J. and Fastook, J.L., 1990. Modeling mass-balance changes during a glaciation cycle. *Annals of Glaciology*, 14: 238–241.

Phartiyal, B., 2014. Holocene paleoclimatic variation in the Schirmacher Oasis, East Antarctica: A mineral magnetic approach. *Polar Science*, *8***:** 357–369.

Phartiyal, B., Sharma, A. and Bera, S.K., 2011. Glacial lakes and geomorphological evolution of Schirmacher Oasis, east Antarctica, during late Quaternary. *Quaternary International,* 235(1): 128–136.

Prahl, F.G., Ertel, J.R., Goni, M.A., Sparrow, M.A. and Eversmeyer, B., 1994. Terrestrial organic carbon contributions to sediments on the Washington margin. *Geochimica et Cosmochimica Acta,* 58(14): 3035–3048.

Prinz, M., 1967. Geochemistry of basaltic rocks: Trace elements. *Basalts*, 1, pp.271–323.

Priscu, J.C. and Foreman, C.M., 2009. In: Likens, G.E. (Ed.), Encyclopedia of Inland Waters. Lakes of Antarctica, 2, Elsevier Press, Oxford.

Rao, V.P. and Rao, B.R., 1995. Provenance and distribution of clay minerals in the sediments of western continental shelf and slope of India. *Continental shelf research*, 15(14): 1757–1771.

Rasmussen, P.E., Villard, D.J., Gardner, H.D., Fortescue, J.A.C., Schiff, S.L. and Shilts, W.W., 1998. Mercury in lake sediments of the Precambrian Shield near Huntsville, Ontario, Canada. *Environmental Geology*, 33: 170–181.

Ravindra, R. and Laluraj, C.M., 2012, September. Cryosphere Research: Indian Perspective In: Proceedings, *Indian National Science Academy*, 78(3): 249–257

Ravindra, R., Chaturvedi, A. and Beg, M.J., 2001. Melt Water Lakes of Schirmacher Oasis - Their Genetic Aspects and Classification. In: Sahu, D.B. and Pandey, P.C. (Eds.), *Advances in Marine and Antarctic Science*, Dariyaganj, New Delhi, 301–313.

Redfield, A.C., 1934. On the proportions of organic derivatives in sea water and their relation to the composition of plankton. University press of Liverpool, Liverpool, UK, 32.

Reynolds, R.L. and King, J.W., 1995. Magnetic records of climate change. *Review of Geophysics*, 33: 101-110.

Roberts, D., Van Ommen, T.D., McMinn, A., Morgan, V. and Roberts, J.L., 2001. Late-Holocene East Antarctic climate trends from ice-core and lake-sediment proxies. *The Holocene*, 11(1): 117–120.

Rubio, B., Nombela, M.A. and Vilas, F., 2000. Geochemistry of major and trace elements of Rio de Vigo (NW) Spain: an assessment of metal pollution. *Marine Pollution Bulletin*, 40: 968–980.

Salomons, W. and Forstner, U., 1980. Trace Metal Analysis on Polluted Sediments: Part II: Evaluation of Environmental Impact. *Environmental Technology*, 1(11): 506–517.

Santos, I.R., Favaro, I.T., Schaefer, E.G.R. and Silva-Filho, E.V., 2007. Sediment Geochemistry in coastal maritime Antarctica (Admiralty Bay, King George Island): Evidence from rare earths and other elements. *Marine Chemistry*, 107: 464–474.

Saraswat, R., Roy, C., Khare, N., Saalim, S.M. and Kurtarkar, S.R., 2018. Assessing the environmental significance of benthic foraminiferal morpho-groups from the northern high latitudinal regions. *Polar Science*, 18: 28–38.

Schenau, S.J. and De Lange, G.J., 2001. Phosphorus regeneration vs. burial in sediments of the Arabian Sea. *Marine Chemistry*, 75(3): 201–217.

Schoepfer, S.D., Shen, J., Wei, H., Tyson, R.V., Ingall, E. and Algeo, T.J., 2015. Total organic carbon, organic phosphorus, and biogenic barium fluxes as proxies for paleomarine productivity. *Earth-Science Reviews*, 149: 23–52.

Schubert, C.J. and Calvert, S.E., 2001. Nitrogen and carbon isotopic composition of marine and terrestrial organic matter in Arctic Ocean sediments: implications for nutrient utilization and organic matter composition. *Deep Sea Research Part I: Oceanographic Research Papers*, 48(3): 789–810.

Sensarma, S., Chakraborty, P., Banerjee, R. and Mukhopadhyay, S., 2016. Geochemical fractionation of Ni, Cu and Pb in the deep-sea sediments from the Central Indian Ocean Basin: An insight into the mechanism of metal enrichment in sediment. *Chemie der Erde-Geochemistry*, 76(1): 39–48.

Serrano, S., Garrido, F., Campbell, C.G. and Garcia-Gonzalez, M.T., 2005. Competitive sorption of cadmium and lead in acid soils of Central Spain. *Geoderma*, 124(1): 91–104.

Shan, J., Liu, D., LiQiang, X., LiGuang, S., 2011. Potential application of biogenic silica as an indicator of paleo-primary productivity in East Antarctic lakes. *Advances in Polar Science*, 22: 131–142.

Sharma, R., Umapathy, G.R., Kumar, P., Ojha, S., Gargari, S., Joshi, R., Chopra, S. and Kanjilal, D., 2019. AMS and upcoming geochronology facility at Inter University Accelerator Centre (IUAC), New Delhi, India. *Nuclear Instruments and Methods in Physics Research Section B: Beam Interactions with Materials and Atoms*, 438: 124–130.

Shepard, F.P., 1954. Nomenclature based on sand-silt-clay ratios. *Journal of Sedimentary Research*, 24(3): 151–158.

Sheppard, D.S., Deely, J.M. and Edgerley, W.H.L. 1997. Heavy metal content of meltwaters from the Ross Dependency, Antarctica. *New Zealand Journal of Marine and Freshwater Research*, 31: 313–325

Shetye, S., Mohan, R., Shukla, S.K., Maruthadu, S. and Ravindra, R. 2011. Variability of Nonionellina labradorica Dawson in surface sediments from Kongsfjorden, West Spitsbergen. *Acta Geologica Sinica (English Edition)*, 85(3): 549–558.

Shi, Q., Leipe, T., Rueckert, P., Di, Z. and Harff, J., 2010. Geochemical sources, deposition and enrichment of heavy metals in short sediment cores from the Pearl River estuary, Southern China. *Journal of Marine Systems*, 82: 28–42.

Shimmield, G.B. and Mowbray, S.R., 1991. The inorganic geochemical record of the northwest Arabian Sea: a history of productivity variation over the last 400 k. y. from Sites 722 and 724. In: Prell, W.L. and Niitsuma, N. (Eds.), Proceedings of the Ocean Drilling Program, Scientific Results, College Station, TX (Ocean Drilling Program) pp. 409–429.

Shimmield, G.B. and Pedersen, T.F., 1990. The geochemistry of reactive trace-metals and halogens in hemipelagic continental-margin sediments. *Aquatic Science Reviews*, 3(2-3): 255–279.

Shrivastava, P.K., Asthana, R., Roy, S.K, Swain, A. K. and Dharwadkar, A., 2012. Provenance and depositional environment of epishelf lake sediment from Schirmacher Oasis, East Antarctica, *vis-a-vis* scanning electron microscopy of quartz grain, size distribution and chemical parameters. *Polar Science,* 6**:** 165–182.

Simmons Jr, G.M., Wharton Jr, R.A., McKay, C.P., Nedell, S., Clow, G., 1986. Sand/ice interactions and sediment deposition in perennially ice-covered Antarctic lakes. *Antarctic Journal of the United states*, 21(5): 217–220.

Simon, Q., Bourlès, D.L., Bassinot, F., Nomade, S., Marino, M., Ciaranfi, N., Girone, A., Maiorano, P., Thouveny, N., Choy, S. and Dewilde, F., 2017. Authigenic 10Be/9Be ratio signature of the Matuyama–Brunhes boundary in the Montalbano Jonico marine succession. *Earth and Planetary Science Letters*, 460: 255–267.

Simon, Q., Thouveny, N., Bourlès, D.L., Bassinot, F., Savranskaia, T., Valet, J.P. and ASTER Team, 2018. Increased production of cosmogenic ^{10}Be recorded in oceanic sediment sequences: Information on the age, duration, and amplitude of the geomagnetic dipole moment minimum over the Matuyama–Brunhes transition. *Earth and Planetary Science Letters*, 489: 191–202.

Simon, Q., Thouveny, N., Bourles, D.L., Nuttin, L., Hillaire-Marcel, C. and St-Onge, G., 2016. Authigenic 10Be/9Be ratios and 10Be-fluxes (230Thxs-normalized) in central Baffin Bay sediments during the last glacial cycle: Paleoenvironmental implications. *Quaternary Science Reviews*, 140:142–162.

Singh, M., Muller, G. and Singh, I., 2002. Heavey metals in freshly deposited stream sediments of rivers associated with urbanization of the Ganga Plain, India. *Water Air Soil Pollution*, 141: 35–54.

Singh, S. M., Ochyra, R., Pednekar, S.M., Asthana, R. and Ravindra, R., 2012. A Holocene moss species preserved in lake sediment core and the present moss diversity at Schirmacher Oasis, Antarctica. *Antarctic Science*, 24: 353–358.

Sinha, R. and Chatterjee, A., 2000. Thermal structure, sedimentology, and hydro-geochemistry of Lake Priyadarshini, Schirmacher Oasis, Antarctica. Sixteenth Indian Scientific Expedition to Antarctica, Department of Ocean Development, 14: 1–36.

Siraswar, R.R. and Nayak, G.N., 2012. Distribution of Sediment Components and Metals in Recent Sediments within Tidal Flats along Mandovi Estuary. *Journal of Indian Association of Sedimentologists*, 31(1&2): 33–44.

Smith, J.A., Hodgson, D.A., Bentley, M.J., Verleyen, E., Leng, M.J. and Roberts, S.J., 2006. Limnology of two Antarctic epishelf lakes and their potential to record periods of ice shelf loss. *Journal of Paleolimnology*, 35(2): 373–394.

Smith, N. and Treguer, P., 1994. Physical and chemical oceanography in the vicinity of Prydz Bay, Antarctica. Cambridge: Cambridge University Press.

Smith, N.R., Dong, Z.Q., Kerry, K.R. and Wright, S., 1984. Water masses and circulation in the region of Prydz Bay, Antarctica. *Deep-Sea Research I - Oceanography Research Papers*, 31: 1121–1147.

Spaulding, S.A., McKnight, D.M., Stoermer, E.F. and Doran, P. T., 1997. Diatoms in sediments of perennially ice-covered Lake Hoare and implications for interpreting lake history in the McMurdo Dry Valleys of Antarctica. *Journal of Paleolimnology*, 17(4): 403–420.

Spencer, K.L. and MacLeod, C.L., 2002. Distribution and partitioning of heavy metals in estuarine sediment cores and implications for the use of sediment quality standards. *Hydrology and Earth System Science*, 6: 989–998.

Srivastava, A.K., Ingle, P.S. and Khare, N., 2018. Controlling factor for nature, pattern and accumulation of the glacial sediments of Schirmacher Oasis, East Antarctica: Comments on paleoclimatic condition. *Polar Science*, *18*: 113–122.

Srivastava, A.K., Ingle, P.S., Lunge, H.S. and Khare, N., 2012. Grain size characteristics of deposits derived from different glacigenic environments of the Schirmacher Oasis, East Antarctica, *Geologos*, 18: 251–266.

Srivastava, A.K., Khare, N. and Ingle, P.S., 2011. Characterization of clay minerals in the sediments of Schirmacher Oasis, East Antarctica: their origin and climatological implications. *Current Science*, 363–372.

Srivastava, A.K. and Khare, N., 2009. Granulometric analysis of glacial sediments, Schirmacher Oasis, East Antarctica. *Journal of Geological Society of India*, 73 (5): 609-620.

Srivastava, A. K., Randive, K. R. and Khare, N. 2013. Mineralogical and geochemical studies of glacial sediments from Schirmacher Oasis, East Antarctica. *Quaternary International*, 292: 205–216.

Stein, R. 2008. Arctic Ocean Sediments: Processes, Proxies and Paleoenvironment. *Developments in Marine Geology*, 2: 205-247; 247–287.

Stein, R., Grobe, H. and Wahsner, M., 1994. Organic carbon, carbonate, and clay mineral distributions in eastern central Arctic Ocean surface sediments. *Marine Geology*, *119*(3-4): 269–285.

Stein, R. and MacDonald, R.W., 2004. In: Stein, R. and MacDonald, R.W. (Eds.) The organic carbon cycle in the Arctic Ocean, *Springer,* Berlin, 8: 315–322.

Sun, D., Bloemendal, J., Rea, D.K., Vandenberghe, J., Jiang, F., An, Z. and Su, R., 2002. Grain-size distribution functions of polymodal sediments in hydraulic and aeolian environments, and numerical partitioning of the sedimentary components. *Sedimentary geology*, 152(3–4): 263–277.

Sun, W.P., Hu, C.Y., Weng, H.X., Han, Z.B., Shen, C. and Pan, J.M., 2013. Sources and geographic heterogeneity of trace metals in the sediments of Prydz Bay, East Antarctica. *Polar Research*, 32(1): 20049.

Sunda, W.G., 2012. Feedback interactions between trace metal nutrients and phytoplankton in the ocean. *Frontiers of Microbiology*, 3.

Svendsen, H., Beszczynska-Moller, A., Hagen, J.O., Lefauconnier, B., Tverberg, V., Gerland, S., Borre Orbaek, J., Bischof, K., Papucci, C., Zajaczkowski, M. and Azzolini, R., 2002. The physical environment of Kongsfjorden–Krossfjorden, an Arctic fjord system in Svalbard. *Polar Research, 21*(1):133–166.

Takahashi, T., Broecker, W. S. and Langer, S. Redfield ratio based on chemical data from isopycnal surfaces. 1985. *Journal of Geophysical Research and Ocean*, 90: 6907–6924.

Talbot, M.R. and Johannessen, T., 1992. A high-resolution palaeoclimatic record for the last 27,500 years in tropical West Africa from the carbon and nitrogen isotopic composition of Lacustrine organic matter. *Earth and Planetary Science Letters*, 110(1): 23–37.

Tanaka, S., Inoue, T. and Huang, Z.Y., 1982. ^{10}Be and ^{10}Be/^{9}Be in near Antarctica sediment cores. *Geochemical Journal*, *16*(6): 321–325.

Tang, J. and You, Z., 1987. The combination character and formation of clay mineral in Don Juan Pond and other lakes in Antarctic. *Marine science bulletin/Haiyang Tongbao, Tianjin*, 6: 36–42.

Tatur, A., Valle, R.D., Barczuk, A. and Martinez-Macchiavello, J., 2004. Records of Holocene environmental changes in terrestrial sedimentary deposits on King George Island, Antarctica; a critical review. *Ocean Polar Research*, 26(3): 531–537.

Taylor, S.R. and McLennan, S.M., 1985. The continental crust: its composition and evolution. Blackwells Scientific, Oxford, pp. 312.

Tessier, A., Campbell, P.G. and Bisson, M., 1979. Sequential extraction procedure for the speciation of particulate trace metals. *Analytical Chemistry*, 51: 844–851.

Tessier, A., Fortin, D., Belzile, N., Devitre, R.R., Leppard and G.G., 1996. Metal sorption to diagenetic iron and manganese oxyhydroxides and associated organic matter: narrowing the gap between field and laboratory measurements. *Geochimica et Cosmochimica Acta*, 60: 387–404.

Thamban, M., Rao, V.P. and Schneider, R.R. 2002. Reconstruction of late Quaternary monsoon oscillations based on clay mineral proxies using sediment cores from the western margin of India. *Marine Geology*, 186(3): 527–539.

Tong, L., Jahn, B.M., Liu, X., Liang, X., Xu, Y.G. and Ionov, D., 2017. Ultramafic to mafic granulites from the Larsemann Hills, East Antarctica: Geochemistry and tectonic implications. *Journal of Asian Earth Sciences*, 145: 679-690.

Torres, M.E., Brumsack, H.J., Bohrmann, G. and Emeis, K.C., 1996. Barite fronts in continental margin sediments: a new look at barium remobilization in the zone of sulfate reduction and formation of heavy barites in diagenetic fronts. *Chemical Geology*, 127(1–3): 125–139.

Tribovillard, N., Bout-Roumazeilles, V., Algeo, T., Lyons, T.W., Sionneau, T., Montero-Serrano, J.C., Riboulleau, A. and Baudin, F., 2008. Paleodepositional conditions in the Orca Basin as inferred from organic matter and trace metal contents. *Marine Geology*, 254(1-2): 62–72.

Tribovillard, N., Bout-Roumazeilles, V., Riboulleau, A., Baudin, F., Danelian, T. and Riquier, L., 2011. Transfer of germanium to marine sediments: Insights from its accumulation in radiolarites and authigenic capture under reducing conditions. Some examples through geological ages. *Chemical Geology*, 282(3): 120–130.

Trusel, L.D., Powell, R.D., Cumpston, R.M. and Brigham-Grette, J., 2010. Modern glacimarine processes and potential future behaviour of Kronebreen and Kongsvegen polythermal tidewater glaciers, Kongsfjorden, Svalbard. *Fjord System and Archives*, 344: 89–102.

Turekian, K.K. and Wedepohl, K.H., 1961. Distribution of the elements in some major units of the earth's crust. *Bulletin of Geological Society of America*, 72(2): 175–192.

Van Os, B.J., Middelburg, J.J. and De Lange, G.J., 1991. Possible diagenetic mobilization of barium in sapropelic sediment from the eastern Mediterranean. *Marine Geology*, 100(1–4): 125–136.

Verleyen, E., Hodgson, D.A., Sabbe, K. and Vyverman, W., 2004. Late Quaternary deglaciation and climate history of the Larsemann Hills (East Antarctica). *Journal of Quaternary Science*, 19(4): 361–375.

Vincent, W.F., 1988. Microbial ecosystems of Antarctica. Cambridge University Press, Cambridge.

Volvoikar, S.P. and Nayak, G.N., 2014. Factors controlling the distribution of metals in intertidal mudflat sediments of Vaitarna estuary, North Maharashtra coast, India. *Arabian Journal of Geosciences*, *7*(12): 5221–5237.

Von Breymann, M.T., Emeis, K.C. and Suess, E., 1992. Water depth and diagenetic constraints on the use of barium as a palaeoproductivity indicator. *Geological Society of London, Special Publications*, 64(1): 273–284.

Wang, H., Chen, Z., Wang, K., Liu, H., Tang, Z. and Huang, Y., 2016. Characteristics of heavy minerals and grain size of surface sediments on the continental shelf of Prydz Bay: implications for sediment provenance. *Antarctic Science*, *28*(2): 103–114.

Warrier, A.K., Mahesh, B.S., Mohan, R., Shankar, R., Asthana, R. and Ravindra, R., 2014. Glacial–interglacial climatic variations at the Schirmacher Oasis, East Antarctica: The first report from environmental magnetism. *Palaeogeography, Palaeoclimatology, Palaeoecology*, 412: 249–260.

Warrier, A.K., Pednekar, H., Mahesh, B.S., Mohan, R. and Gazi, S., 2016. Sediment grain size and surface textural observations of quartz grains in late quaternary lacustrine sediments from Schirmacher Oasis, East Antarctica: Paleoenvironmental significance. *Polar Science*, *10*(1): 89–100.

Webster, J.G., Webster, K.L., Nelson, P., and Waterhouse, E., 2003. The behavior of residual contaminants at a former station site, Antarctica. *Environmental Pollution*, 123: 163–179.

Wedepohl, K.H., 1995. The composition of the continental crust. *Geochimica et Cosmochimica Acta*, 59(7): 1217–1232.

Wehrmann, L.M., Formolo, M.J., Owens, J.D., Raiswell, R., Ferdelman, T.G., Riedinger, N. and Lyons, T.W., 2014. Iron and manganese speciation and cycling in glacially influenced high-latitude fjord sediments (West

Spitsbergen, Svalbard): evidence for a benthic recycling-transport mechanism. *Geochimica et Cosmochimica Acta*, 141: 628–655.

Wharton, R.A., Lyons, W.B. and Des Marais, D.J., 1993. Stable isotopic biogeochemistry of carbon and nitrogen in a perennially ice-covered Antarctic lake. *Chemical Geology*, 107(1): 159–172.

Whitlock, C., Dean, W., Rosenbaum, J., Stevens, L., Fritz, S., Bracht, B. and Power, M., 2008. A 2650-year-long record of environmental change from northern Yellowstone National Park based on a comparison of multiple proxy data. *Quaternary International*, 188(1): 126–138.

Wilson, T., Grunow, A.M. and Hanson, R.E., 1997. Gondwana assembly: the view from southern Africa and East Gondwana. *Journal of Geodynamics*, 23: 263–286.

Windom, H.L., 1976. Lithogenous material in marine sediments. In: Riley J.P., Chester R. (Eds.), *Chemical oceanography*, (Vol. 5,) New York: Academic Press, pp.103–135.

Winkelmann, D. and Knies., J., 2005. Recent distribution and accumulation of organic carbon on the continental margin west off Spitsbergen. *Geochemistry Geophysics Geosystems*, 6: Q09012.

Włodarska-Kowalczuk, M., Szymelfenig, M. and Zajączkowski, M., 2007. Dynamic sedimentary environments of an Arctic glacier-fed river estuary (Adventfjorden, Svalbard) II:meio- and macrobenthic fauna. *Estuarine Coastal Shelf Science*, 74: 274–284.

Wronkiewicz, D.J. and Condie, K.C., 1989. Geochemistry and provenance of sediments from the Pongola supergroup, South Africa:Evidence for a 3.0-Ga old continental craton. *Geochimica et Cosmochimica Acta*, 53: 1537–1549.

Xijie, Y., Yunhai, L., Lei, Q., Aijun, W.A.N.G., Yonghang, X.U. and Jian, C.H.E.N., 2014. Source and spatial distributions of particulate organic carbon and its isotope in surface waters of Prydz Bay, Antarctica, during summer. *Advances in polar science*,25(3): 175–182.

Yang, Z., Sun, L., Zhou, X. and Wang, Y., 2018. Mid-to-late Holocene climate change record in palaeo-notch sediment from London Island, Svalbard. *Journal of Earth System Science, 127*(4): 57.

Yoon, H., Khim, B., Lee, K., Park, Y. and Yoo, K., 2006. Reconstruction of postglacial Palaeoproductivity in Long Lake, King George Island, West Antarctica. *Polish Polar Research*, 27(3): 189–206.

Yu, Y., Song, J., Li, X., Yuan, H., Li, N. and Duan, L., 2013. Environmental significance of biogenic elements in surface sediments of the Changjiang Estuary and its adjacent areas. *Journal of Environmental Sciences*, *25*(11): 2185–2195.

Zaborska, A., Pempkowiak, J., and Papucci, C., 2006. Some sediment characteristics and sedimentation rates in an Arctic fjord (Kongsfjorden, Svalbard). *Annual Environmental Protection,* 8: 79–96.

Zajączkowski, M. and Włodarska-Kowalczuk, M., 2007. Dynamic sedimentary environments of an Arctic glacier-fed river estuary (Adventfjorden, Svalbard). I. Flux, deposition, and sediment dynamics. *Estuarine, Coastal and Shelf Science, 74*(1-2): 285–296